January 2010

Dact Family Molecules In Wnt Signaling In Mouse Development

Daniel Fisher
Washington University in St. Louis

WASHINGTON UNIVERSITY IN SAINT LOUIS

Division of Biology and Biomedical Sciences

Program in Neurosciences

Dissertation Examination Committee:
Benjamin Cheyette, Chair
Eugene Johnson, Co-Chair
David Ornitz, Co-chair
Raphael Kopan
Fanxin Long
Jeanne Nerbonne
Joshua Rubin

DACT FAMILY MOLECULES IN WNT SIGNALING IN MOUSE DEVELOPMENT

By

Daniel Arthur Corpuz Fisher

A dissertation presented to the
Graduate School of Arts and Sciences
Of Washington University in
Partial fulfillment of the degree
Of Doctor of Philosophy

December 2010

Saint Louis, Missouri

ABSTRACT OF THE DISSERTATION

Dact family molecules in Wnt signaling in mouse development

by Daniel Arthur Corpuz Fisher

Doctor of Philosophy in Biology and Biomedical Sciences (Neurosciences)

Washington University in Saint Louis, 2010

Benjamin Cheyette, MD, PhD, *Assistant Professor of Psychiatry, UCSF*, Chair
Eugene Johnson, PhD, *Professor Emeritus*, Mentor of Record

The Wnt (Wingless-Integration) molecular signaling pathways are known to be integral in the embryonic patterning of multicellular animals, and are misregulated in multiple types of cancer. Wnt signaling includes multiple biochemical signaling pathways downstream of the Wnt family of secreted proteins and their receptors. Many, and possibly all, of these pathways converge on the intracellular protein Dishevelled, whose interactions appear essential in determining the cell-autonomous effects of the Wnt signal. Dact (Dapper, Antagonist of Beta Catenin Targeting) proteins were identified based on their binding to Dishevelled. There are three Dact encoding genes in mammals, and these show unique expression patterns in the development of the mouse. A mouse mutant lacking the *Dact1* gene has been constructed. Despite expression of this gene in patterns suggesting roles in somitogenesis and neuronogenesis, *Dact1* mutant mice are caudally truncated due to defective mesoderm formation in late gastrulation. *Dact1* mutant mice show reduced Wnt/β-catenin signaling. The *Dact1* mutation and the mouse planar cell polarity mutant Loop-tail rescue one another's phenotypes, showing

antagonism between Wnt/β-catenin and planar cell polarity signaling pathways at the level of Dact1.

Special thanks to,

My mentor, Dr. Benjamin Cheyette,

My thesis committee at Washington University,

All members of the Cheyette laboratory, particularly my friends and collaborators Rowena Suriben and Saul Kivimäe, and Uta Grieshammer from Gail Martin's laboratory at the University of California, San Francisco,

The members of the committee of the Medical Scientist Training Program at Washington University, who supported my work,

Brian Sullivan, whose assistance was priceless in coordinating the arrangements for the phase of my thesis work that was done at long distance from Saint Louis at the University of California, San Francisco,

Dr. Jeanne Nerbonne, whose support and guidance helped me through the greatest challenges in my graduate education and in my life during this time,

My earliest friends in laboratory science, Drs. Melanie Mark, Yuechueng Liu, and Enrique Villacrés, whose enthusiasm lit the way along the earliest steps of my path in neurologic and developmental molecular biology,

My parents and family, especially my sister, Rachel Danielle, who loved for me to read to her my neuroscience textbooks when she was four years old, sitting on my shoulders in our favorite armchair,

And especially my wife, Catherine, our son, Gabriel Keith, and our daughter, Gabriela Louise, whose love is a wonder beyond anything I can describe in words.

Note on Sources of Funding:

Work presented in my thesis was funded by NIH (NIGMS) RO1 grant to Dr. Benjamin Cheyette, by funds directed to him by the Department of Psychiatry and Stem Cell Center, University of California, San Francisco, and by the Medical Scientist Training Program grant to Washington University in Saint Louis. Previous work during my graduate studies was funded by the Medical Scientist Training Program, Washington University in Saint Louis, by Exelixis Pharmaceuticals, and by NIH (NINDS) grants to Dr. William D. Snider, formerly of Washington University in Saint Louis, and presently Director of the Neuroscience Institute at University of North Carolina, Chapel Hill.

Table of Contents:

List of Figures and Illustrations:

Chapter 1 **Page**

Chapter 2

Chapter 3 **Page**

Chapter 4

Chapter 4 illustrations and tables (continued) **Page**

Chapter 1:

Introduction to the Thesis.

1. Wnt, Dishevelled, and Dact molecules.

2. Structure and interactions of Dact proteins.

3. The Dact gene family.

4. Interactions of Dact beyond Dishevelled.

5. Wnt pathways: canonical and non-canonical.

6. Caudalogy: the study of caudal embryonic development as a model system.

7. Somitogenesis: Wnt3a powers the somite segmentation clock.

8. Dacts and Dact interactors in nervous system development.

9. In summary…

Introduction:

Wnt, Dishevelled, and Dact molecules.

The topic of histogenesis, or the formation of a tissue from precursor cells, has two primary components. One is cell fate, the determination of what the precursor cells are to become. The other is morphogenesis, in other words how, mechanistically, the cells form the structures which they are fated to compose. These processes involve continuing decision-points at the level of individual cells, which are typically mediated by the cell sensing an extracellular molecular signal, or morphogen, whose sensation is transduced by an array of intracellular signaling molecules to the machinery that can control and compose cellular structure.

The Wnt (contraction of Wingless-Integration) signaling pathways have historically been associated with histogenesis, particularly in embryonic development, as have a number of other widely studied signaling pathways downstream of extracellular morphogens: the FGF (Fibroblast Growth Factor), Hedgehog, Notch, EGF (Epidermal Growth Factor)/neuregulin, and TGFβ (Transforming Growth Factor)/BMP (Bone Morphogenic Protein) families. The extracellular Wnt ligands were originally identified from the fruit fly *Wingless* mutant, and from the Int-1 protein induced by the integration of the Mouse Mammary Tumor Virus (MMTV): in this case the cancer may be

considered a phenomenon of histogenesis gone awry (Reviews: Moon et al., 2004; Nusse, 2005).

Since these initial discoveries, it has become clear that Wnt ligands (of which there are 19 in mammals) can activate multiple intracellular signal transduction pathways with divergent effects on cells (Intro. Fig. 1). Most prominently studied among these are the "canonical" Wnt/β-catenin pathway and the Planar Cell Polarity (PCP) pathway, which has primarily been studied in the fly *Drosophila melanogaster*. The distinction between these two pathways is identified by the fly *Dsh1* mutant, which has misaligned sensory bristles and ommatidia but nonetheless has wings, while other mutations in the affected gene, *Dishevelled*, phenocopy *Wingless* (Kligensmith and Nusse, 1994). The divergence between these two pathways occurs mechanistically at the level of the Dishevelled protein (abbreviated Dvl in vertebrates and Dsh in fly). The trimodular Dishevelled protein contains a DIX (Dishevelled/Axin), a PDZ (PSD-95/Discs Large/ZO-1), and a DEP (Dishevelled/Egl-10/Pleckstrin) domain arrayed from N to C terminus. The DEP domain is essential for PCP signaling, and its loss phenocopies the *Dsh1* mutation but leaves Wnt/β-catenin signaling intact (Boutros et al., 1998). The DIX domain is instead essential for Wnt/β-catenin signaling. So Dishevelled mediates multiple signaling pathways downstream of Wnts and their Frizzled receptors, but the different domains of the protein activate different pathways.

So what determines which pathways become activated? This is presumably determined in part by which other molecules are able to bind to a Frizzled-Dishevelled

complex. Dishevelled has been shown to bind directly to Frizzled receptors via its PDZ domain (Wong et al., 2003). Researchers frequently describe Dishevelled as a "scaffolding protein", meaning that it lacks enzymatic activity and that its main function is to bind other proteins into a heteromeric multiprotein complex. This is not a passive role, though. Multiple studies have shown that both Wnt/β-catenin and PCP signaling pathways are transduced via multiprotein complexes. The scaffolding protein can be subject to enzymatic control: as an example, Dishevelled is multiply phosphorylated. Modifications to the scaffolding protein can determine which regulatory molecules are allowed to enter into the signal transducing complex, and with which partners within it they are likely to interact. The composition of the signaling complex determines the potential readout. The signal transduced within the cell is the ultimate consequence of multiprotein scaffolding.

This thesis describes a scaffolding protein family known as the Dact proteins, which were originally identified by their binding to the PDZ domain of Dishevelled from *Xenopus laevis*. Dact is an acronym for "Dapper, antagonist of β-catenin targeting" as described in the Human Genome and Mouse Genome Databases. The name originates from the study by Benjamin Cheyette, my thesis mentor, and his colleagues (Cheyette et al., 2002), which identified the *Xenopus laevis* Dishevelled-PDZ interactor as Dapper, and showed that it could block the activation of a Wnt/β-catenin sensitive reporter and of JNK (Jun kinase) by Dishevelled, when expressed in cultured cells. The name Dapper refers to the hypothesis that the protein functions as an antagonist of Dishevelled, hence the antonym. Conflicting with this hypothesis, Gloy et al. (2002) identified a very nearly

identical protein also from *Xenopus*, named Frodo, which appeared to synergize with Dishevelled when expressed in *Xenopus* embryos, in the production of supernumerary axes, a phenomenon associated with local hyperactivation of Wnt/β-catenin signaling. The name Frodo is an acronym for Functional Regulator Of Dishevelled in Ontogenesis, reflecting the hypothesis that this protein can regulate the functional roles of Dishevelled in early embryonic development (Gloy et al., 2002). This acronym is also presumably intended to evoke the eponymous fictional character created by the fantasy writer J.R.R. (John Ronald Ruel) Tolkein. These two original studies suggested fundamentally opposite functions for nearly identical molecules. Sergei Sokol and colleagues (Hikasa and Sokol, 2004) subsequently attempted to clarify this issue by comparing both Dapper and Frodo molecules directly in the assays used by Cheyette et al. (2002) and Gloy et al (2002). Impressively, they found that the two proteins behaved identically.

One significant observation in this further study by Sergei Sokol and colleagues (Hikasa and Sokol, 2004) is that low level expression of Dapper or Frodo in cultured cells enhanced activation of a Wnt/β-catenin sensitive reporter by Dishevelled, while higher level expression antagonized it. The immediate implication was that Dact proteins (homologs of Dapper and Frodo) could act either as agonists or as antagonists of Wnt/β-catenin signaling, depending on the level of Dact protein present, and perhaps on the presence of other binding partners.

A notable caveat to the studies of Cheyette et al. (2002) and Gloy et al (2002) is that both of these relied on artificial overexpression, of the Dact molecules. It is well

established that Wnt/β-catenin signaling is regulated through the formation of multiprotein complexes that either specify the proteolytic degradation of cytoplasmic β-catenin (when the Wnt-derived signal is off: the complex is in this case referred to as the "destruction complex") or else inhibit this degradation when the Wnt signal is active (Moon et al., 2004; Nusse, 2005; Macdonald et al., 2007). Cheyette et al. (2002) showed that Dapper bound to axin and GSK-3 proteins, which are present in the β-catenin destruction complex, but which also have been shown more recently to be present in another complex which promotes Wnt/β-catenin signaling, as well (Zeng et al., 2008). It is logical that a protein that normally functions as a member of a multiprotein complex could, when overexpressed, disrupt formation of the complex by binding to its interaction partners outside of the complex and preventing the normal complex formation due to stoichiometric imbalance. Alternatively, it could alter the stoichiometry of the molecules present within the complex, so that the complex acquired a different function from its physiological one in absence of overexpression. In this way, overexpression of a complex-activating molecule could have an effect similar to a dominant negative; and overexpression of an inhibitor might paradoxically lead to hyperactive signaling (especially if the complex itself functioned to inhibit the signaling pathway, as the β-catenin destruction complex does). In either case, the functional conclusions of both studies describing Dact proteins as Wnt effectors are in reality inconclusive, due to these mechanistic considerations.

Two subsequent studies, each by authors and/or colleagues of the original Dapper and Frodo publications, attempted to clarify the agonist versus antagonist dilemma for

Dact proteins. Waxman et al. (2004) identified two Dact molecules in zebrafish, *Danio rerio*. Using overexpression and siRNA morpholino interference, zebrafish *Dapper1* was associated with Wnt/β-catenin activation, while zebrafish *Dapper2* was associated with convergent extension movements, particularly in the structure of somites. Convergent extension is a phenomenon observed in the formation of the notochord, where laterally derived cells converge at the midline and intercalate to extend the structure along the rostrocaudal axis. It is affected deleteriously by mutations in genes that are homologous to those functioning in PCP in the fly (Wallingford et al., 2002; Seifert and Mlodzik, 2007). Since convergent extension is a behavior of mesenchymal cells while planar cell polarity is a phenomenon of epithelia, they cannot be considered altogether identical mechanistically. Even so, since their molecular machinery consists largely of identical components functioning similarly in both phenomena (Wallingford et al., 2002; Seifert and Mlodzik, 2007), I will refer to both phenomena under the broad topic of PCP signaling.

In contrast to previous studies, Hikasa and Sokol (2004) identified a novel interaction of *Xenopus* Frodo, in this case with the transcription factor Tcf3. Tcf3 is a member of the LEF/TCF family of transcription factors, which mediate transcriptional control subject to regulation by Wnt/β-catenin signaling. Fundamentally, TCFs are members of a transcriptional repressor complex, which is altered to generate a transcriptional activator complex upon the binding of TCF to β-catenin (Shitashige et al., 2008 for review). When a Wnt ligand activates the Fz/LRP (Frizzled/Low-density-lipoprotein-receptor-like-protein) receptor complex at the plasma membrane, Fz binding

to Dvl precipitates the breakup of the β-catenin destruction complex. Soluble β-catenin accumulates in the cytoplasm and in the nucleus, where it can bind to TCFs and thereby initiate transcription of target genes. The findings of Hikasa and Sokol (2004) suggest that Frodo (and likely other Dacts as well) could function in a parallel pathway that could effectively bypass β-catenin to activate target genes as well. The physiological consequences of this novel interaction are not clear, as it has not yet been described *in vivo*. S. Sokol and colleagues (Itoh et al., 2005) have also described a similar role for nuclear Dvl, but in tandem with β-catenin rather than independently of it.

A subsequent study showed a hypothetical model for a function of a Dact protein (in this case, human DACT1) as a Wnt signaling inhibitor (Zhang et al., 2006). This study showed that Dact expression could lead to Dvl2 degradation in cultured mammalian cells. It also relied on overexpression, however, and is therefore functionally inconclusive. More importantly, it showed the Dvl DEP domain, rather than the PDZ domain, to be necessary for Dvl2-Dact1 binding, and showed that the DEP domain bound to both the C-terminal and central regions of Dact1. The implication, since the Dishevelled DEP domain is essential for PCP signaling, is that Dact1 (and possibly other Dacts as well) is active in the regulation of PCP signaling (Chapter 4 shows that I have demonstrated this hypothesis to be correct using a genetic intercross in mice).

These studies leave the possible roles for Dact proteins in Wnt signaling to be almost any that could be hypothesized. Dact could be an activator or an inhibitor of canonical Wnt/β-catenin, it could act in parallel to β-catenin, or it could mediate or

inhibit PCP signaling. Seemingly, every door that could be opened is open, yet there must be some specificity to the function of the molecular family.

Given the widespread application of gene manipulation in mice, and the widespread interest in Wnt signaling, the discoverers of Dapper and Frodo sought to mutate the homologous genes in mice, to observe loss-of-function phenotypes. This thesis includes a substantial phenotypic analysis of one of these mouse mutants, the null mutant of mouse *Dact1*. This is described in detail in Chapter 4 of the thesis. Another engineered mutant mouse with the same gene disrupted also exists, although its phenotypes have not yet been published, and are reportedly similar to, but milder than, the phenotypic constellation of the mouse described here (S.Y. Sokol, personal communication).

Structure and interactions of Dact proteins.

While Dact molecules were originally identified by their binding to the Dvl PDZ domain, it is clear that they interact with other proteins, several of which have been identified. The primary structure of Dact molecules is suggestive of heteromer formation, as is their binding to Dvl and Wnt signaling complex molecules. The structure contains an amino terminal leucine zipper domain, a substantially conserved C terminal domain with a C-terminal PDZ-binding motif, with roughly 400 or more intervening amino acids (overall size ranges from 610 amino acids for mouse Dact3 to 838 amino

acids for zebrafish Dact2 (see Fisher et al., 2006, included in Chapter 2; also Gillhouse et al., 2004; Waxman et al., 2004; Brott and Sokol, 2005a). Among the intervening polypeptide, there are multiple amino acid stretches conserved in multiple but not all Dact homologs. Most of these sequences center on one or more serines, and are likely to be phosphorylation sites (compare sequences in Fisher et al., 2006 and those included in Brott and Sokol, 2005a). The C-terminus was determined to be necessary for Dact binding to Dvl (Cheyette et al., 2002; Gloy et al., 2002), although in at least some Dact homologs a more central region also appears to be capable of binding to Dvl, and specifically to the DEP domain of Dvl rather than the PDZ domain, which was shown to bind to the Dact C-terminus (Zhang et al., 2006). Meanwhile, the N-terminal regions was shown to be essential for binding to Tcf3 (Hikasa and Sokol, 2004). N-terminal and central regions of *Xenopus* Frodo were also shown to be necessary for binding to Dbf4 (Homolog of Dumbbell Former: Brott and Sokol, 2004b), a Wnt/β-catenin pathway inhibitor active in heart development. The mechanism of Wnt/β-catenin pathway pathway inhibition by the Dbf4-Dact1 interaction is not yet known, but the existence of this interaction is evidence that, in at least some contexts, Dact proteins can mediate Wnt/β-catenin pathway inhibition.

The Dact gene family.

The Dacts are a gene family conserved among vertebrates, although they have not yet been identified in any invertebrates. It can be speculated, therefore, that no Dact

molecule is necessary to mediate any Wnt signaling pathway conserved among animals, but rather that Dacts represent a vertebrate-specific evolutionary adaptation which modulates regulation of Wnt pathways, possibly from other previously uncharacterized inputs. The Dact family can be divided into three subfamilies, of which there is frequently only one member each in a given vertebrate genome. My collaborators, and in particular Benjamin Cheyette, my mentor, have identified three Dact paralogs present in mammals (Fisher et al., 2006). This is described in Chapter 2, along with expression patterns of the mouse homologs of these genes in embryos and in adult brains, which I am responsible for having researched. The initially described *Xenopus Dapper* and *Frodo* are both homologs of the *Dact1* subfamily. The presence of two *Xenopus Dact1* homologs is likely to result from a duplication event within the phylogenetic ancestry of *Xenopus laevis*, which is a pseudotetraploid organism. These have diverged within this particular species of frog to maintain quite different expression patterns in the embryo (compare expression data in Cheyette et al., 2002 with that in Gloy et al., 2002).

Sequence conservation among the subfamily members is quite low outside of the leucine zipper, four serine centered sequences, and the C-terminal roughly 30 amino acids. As described in Chapter 2 (and Fisher et al., 2006), the overall amino acid sequence identities among mouse Dact1, Dact2, and Dact3 proteins are from 19% to 21% for each pair. In contrast, each subfamily member is highly conserved across vertebrate species. For example, mouse and human Dact1 orthologs are 55% and 60% identical, respectively, to *Xenopus* Dapper at the amino acid level (Cheyette et al., 2002). This

suggests there will be some evolutionary conserved non-overlapping functions maintained in each of the Dact subfamilies.

In Chapter 2, I describe the developmental expression patterns of mouse *Dact1*, *Dact2*, and *Dact3* genes. These are highly distinct from one another. The adult expression patterns, although less studied, are likely also to differ substantially. There are some areas of overlap: for instance, all three genes are expressed in the gray matter of the embryonic spinal cord. In a number of tissues, only a single *Dact* family member appears to be expressed (for example, *Dact1* in the tail bud mesoderm or *Dact2* in the embryonic thymus), or one is expressed at a much higher level than the others (as in *Dact1* in the embryonic brain in neurogenic regions and developing gray matter).

Interactions of Dact beyond Dishevelled.

Dacts have been found to bind to several other proteins besides Dvls, including proteins functioning in Wnt signaling, and in other signaling pathways as well. As already described, Dact1 (*Xenopus* Frodo) can bind to Tcf and activate transcription of target genes independently of β-catenin (Hikasa and Sokol, 2004). Another interaction in a parallel and likely divergent Wnt-related signaling pathway is the interaction of Dact with p120catenin. Dact1 (*Xenopus* Frodo) was found to bind to and stabilize p120ctn in cultured cells, enhancing derepression of Kaiso target genes through upregulation of the p120ctn-Kaiso interaction (Park et al., 2006). This interaction may be relevant for the

Wnt/β-catenin signaling pathway as well as for other pathways. Like β-catenin, p120ctn is a structural protein which binds cadherins at adherens junctions (Nelson and Nusse, 2004; Reynolds and Roczniak-Ferguson, 2004). In addition, p120ctn binds to Kaiso, a transcriptional corepressor which can bind to TCF and can repress transcription at β-catenin/TCF-dependent gene promoters (Park et al., 2005). The p120ctn-Kaiso interaction is thought to sequester Kaiso in the cytoplasm, preventing its nuclear translocation and thereby preventing its repression of target gene transcription (Kim et al., 2004). Therefore stabilizing p120ctn could have substantial effects both on the expression of β-catenin/TCF-dependent target genes and on the structural modification of cells, and on intercellular interactions mediated through adhesion molecules as well. Kaiso itself is apparently dispensable in development of the mouse (Prokhortchouk et al., 2006), but that does not exclude its function being important but also redundant with other proteins.

The interactions of Dact1 homologs (in all of these studies *Xenopus* Frodo was used: Hikasa and Sokol, 2004; Brott and Sokol, 2005b; Park et al., 2006) with Tcf3 and p120ctn suggest the promotion of gene expression promoted by Wnt/β-catenin signaling. These do not represent the canonical Wnt/β-catenin signaling pathway as historically described, but may be considered as parallel pathways or parallel and divergent pathways in the sense that they promote expression of β-catenin/TCF target genes and possibly other genes that are not β-catenin/TCF targets as well. In contrast, the interaction with Dbf4 suggests inhibition of Wnt/β-catenin signaling (Brott and Sokol, 2005b). Is it possible that Dacts both promote and inhibit Wnt/β-catenin signaling at different loci

within the pathway? Such mutual agonist/antagonist roles have been described for axin and GSK-3 (Davidson et al., 2005; Zeng et al., 2005; Zeng et al., 2008). Certainly, not all the interactions of Dact proteins affecting the Wnt/β-catenin signaling pathway(s) have yet been characterized. In Chapter 4, my collaborators and I provide evidence that the primary role of Dact1 in Wnt/β-catenin signaling during caudal mesoderm development in the mouse embryo is agonistic, and furthermore that it is linked to inhibition of the PCP pathway through the interaction of Dact1 with Vangl2. While the other interactions of Dact1 so far described are amply documented, we did not identify any of them as being essential functions of Dact1 in embryonic mouse development: indeed, the entire constellation of developmental defects observed in *Dact1* null mice was rescued by the simultaneous loss of function in *Vangl2* caused by heterozygosity for the *Loop-Tail* allele (*Vangl2* $^{Lp/+}$).

An altogether distinct function of Dact proteins is the downregulation of Nodal receptors. Zebrafish Dact2 protein was shown to bind to the cytoplasmic portions of Nodal receptors Alk4 and Alk5, and to downregulate them by mediating their internalization in a manner analogous to the function of arrestins (Zhang et al., 2004). This was accompanied by the observation that *Dact2* antisense morpholinos partially rescued Nodal pathway loss-of-function mutant phenotypes, while *Dact2* overexpression exacerbated these phenotypes. This role was specific to Dact2: zebrafish Dact1 did not bind to Alk4 or Alk5. This clearly indicates a non-redundancy of functions of Dact proteins. There is no certainty, though, whether this distinct function of Dact2 is specific to the teleost lineage. So far, no study has been reported as to whether this function of

Dact2 is conserved in mammals or other vertebrate lineages, let alone whether it is shared with other Dacts in species where the potential evolutionary divergence from teleosts is substantial.

Wnt pathways: canonical and non-canonical.

The signal transduction pathways downstream of Wnt ligands have been historically divided into "canonical" and "non-canonical" pathways (reviews: Veeman et al., 2003; MacDonald et al., 2007; Semenov et al., 2003). In practice, "canonical" Wnt signaling is considered synonymous with the Wnt/β-catenin pathway, whereas "non-canonical" is alternatively applied to all other Wnt-related signaling pathways, no matter how different they are from one another, and sometimes even if their effectors and effects overlap substantially with those of the Wnt/β-catenin pathway (as is the case with both the p120-Kaiso pathway and the Dact1-Tcf3 pathway: Hikasa and Sokol, 2004; Park et al., 2005; Park et al., 2006). The widespread interest in Wnt-related signaling has led to studies describing a great multiplicity of signaling pathways downstream of Wnt ligands, some of which can be activated by non-Wnt ligands and inputs as well (MacDonald et al., 2007; Semenov et al., 2003). The historical dichotomy of "canonical" and "non-canonical" pathways is probably best replaced by description of the specific pathway(s) under study and their components. In my study of the *Dact1* null mouse, I have focused specifically on the Wnt/β-catenin pathway and the PCP pathway (and specifically a subset of PCP signaling involving *Strabismus*/*Van Gogh* homologs and a "core" complex

of PCP related proteins: for reviews see Wallingford et al., 2002; Torban et al., 2004a; Seifert and Mlodzik, 2007; Lawrence et al., 2007).

The Wnt/β-catenin pathway regulates the presence of soluble, and specifically nuclear, β-catenin. It is dependent on the interaction of the Wnt receptor Frizzled (represented by a pair of functionally redundant genes in *Drosophila melanogaster*: Bhat, 1998; Chen and Struhl, 1999 Strapps and Tomlinson, 2001;and by a multigene family in verebrates: van Amerongen,R. and Berns,A., 2006) with Dishevelled. This has been shown to be a direct interaction of Frizzled (Fz) binding to the Dsh/Dvl PDZ domain (Wong et al., 2003). Fz-Dsh/Dvl binding destabilizes the β-catenin destruction complex, whose other essential members are the scaffold proteins Axin (or its close homolog Axin2: Jho et al., 2002) and APC (or its homolog APC2: see Aoki and Taketo, 2007 for review), and the kinases Casein Kinase I (CK-I) and GSK-3 (Glycogen Synthase Kinase 3), all of which act to promote β-catenin degradation (β-catenin is a direct substrate of CK-I and GSK-3). Dact1 (*Xenopus* Dapper) was shown to coprecipitate with members of this complex (Cheyette et al., 2002). Axin and GSK-3 have also been shown to be members of a complex together with Lrp5 or Lrp6 which promotes Wnt/β-catenin signaling (Davidson et al., 2005; Zeng et al., 2005; Zeng et al., 2008): it cannot be excluded that Dacts could interact with this complex as well, or instead of, the β-catenin destruction complex. It has been established that the presence of Lrp5 or Lrp6 in a complex with Wnt, Fz, and Dsh/Dvl is essential for Wnt/β-catenin signaling, and indeed can convert the preferred signaling modality of a Wnt-Fz binding pair to Wnt/β-catenin signaling rather than other pathways (Liu et al., 2005; Mikels and Nusse, 2006). In light

of this dependence, it is not surprising that mice mutant in *Lrp5* and/or *Lrp6* (Pinson et al., 2000; Kelly et al., 2004; Kokubu et al., 2004) resemble other mouse mutants with losses of Wnt/β-catenin signaling: specifically the *Wnt3a* expression hypomorph *Vestigial tail* (*Wnt3a* $^{vt/vt}$) and its heterozygosity with a *Wnt3a* null allele (*Wnt3a* $^{vt/-}$), and, as demonstrated in Chapter 4, *Dact1* $^{-/-}$ (Greco et al., 1996; Aulehla et al., 2003; Nakaya et al., 2005). These mutant mice are all characterized by caudal truncations and caudal vertebral disorganizations at or more caudal to the lumbar vertebrae, while the more severe *Wnt3a* null mouse is truncated at the level of the upper thoracic vertebrae, leading to a "half mouse" phenotype (Takada et al., 1994), which is associated with an almost complete absence of Wnt/β-catenin dependent gene expression in the caudal mesoderm at E8 (Nakaya et al., 2005).

When describing "non-canonical" Wnt signaling pathways, it is convenient to begin with a description of the receptor complex consisting of Fz and, sometimes but not always, Lrp5 or Lrp6. The presence of Lrp5 or Lrp6, as stated, can promote Wnt/β-catenin signaling downstream of Fz at the expense of other pathways, notably PCP signaling (Liu et al., 2005; Mikels and Nusse, 2006). Fz receptors are members of the superfamily of seven transmembrane domain serpentine receptors, and as such can activate signal transduction downstream of heterotrimeric G protein activation. G protein activation is responsible for Wnt/Fz activation of adenylate cyclase, guanylate cyclase, and PKCδ in various vertebrate developmental contexts (Penzo-Mendez et al., 2003; Chen et al., 2005; Tu et al., 2007). It is not known whether in all cases Wnt/Fz activation

of G proteins depends on Dsh/Dvl, although it appears to in the case of the Wnt-cGMP-calcium pathway (Veeman et al., 2003 for review).

Among the "non-canonical" Wnt signaling pathways, the one that has been the subject of the most extensive study has been the PCP pathway. Describing a PCP "pathway" is probably in itself an oversimplification. Planar cell polarity is a problem intrinsic to the development of any anatomic structure with axial information and containing epithelia. Together with its mesenchymal cell analogs, convergent extension and directed cell migration, it encompasses many if not most of the problems of imposing axial information upon a biological structure. This extends even to the phenomena of axon guidance and polarized dendritic extension in the development of nervous systems. It is indeed impressive that specific vertebrate Wnts and their downstream PCP signaling machinery have been described as controlling examples of all of these phenomena: epithelial cell movement in gastrulation (Heisenberg et al., 2000; Wallingford et al., 2000), notochord formation (Hikasa et al., 2002), neurulation (Hikasa et al., 2002; Wang et al., 2006a; Wang et al., 2006b, Qian et al., 2007), and axon guidance (Lyuksyutova et al., 2003; Keeble et al., 2006; Tissir et al., 2006). The problem of cell polarity was perhaps most concisely described by Sydney Brenner, referring to a time before any molecular information was available on its control:

There'd be problems in the polarity of the cells. Which in my mind is still the essential problem: in the sense that cells move in one direction and not in another, grow

in one direction, or face the world from one side of themselves and not the other. How was all this polarity established? (Brenner, 2001).

Clearly, Wnts are far from the only extracellular ligands which impart directional information in vertebrate development. They are, however, clearly a significant group of these. Likewise, information about the mechanisms of Wnts imparting polarity information to cells may be relevant for identifying mechanisms of cell polarization and directional guidance by other extracellular ligands: for example the semaphorins, which I have previously studied (see Appendix: Xu et al., 2000).

The classic PCP pathway is characterized by a "core complex" of PCP-related proteins localized to the plasma membrane (Seifert and Mlodzik, 2007 for review). The activation of this complex has been shown to occur downstream of Wnt ligands and Fz receptors, and also downstream of other Wnt receptors: Ror2 (Hikasa et al., 2002) and possibly Ryk (Cheyette, 2004; Hendrickx and Leyns, 2008). The "core PCP complex" requires several of its members for stability at the plasma membrane. Two transmembrane proteins are required: the four-pass transmembrane protein known as Strabismus (Stbm) or Van Gogh (Vang) in *Drosophila*, and represented by its homologs Vangl1 and Vangl2 (also known as Ltap) in mammals; and the cadherin related seven transmembrane protein known as Flamingo or Starry night in *Drosophila* and homolgous to the Celsr family in mammals. Either or both of these proteins might function as receptors for as yet unknown ligands. Also required for the PCP complex is the intracellular protein Scribble, which binds to homologs of Stbm/Vangl and Lgl (Lethal

giant larvae: Kallay et al., 2006). Dishevelled is also required for PCP signaling and binds to the PCP complex, including direct interaction with homologs of Stbm/Vangl and Lgl (Torban et al., 2004a; Dollar et al., 2005; Vasioukhin, 2006). Specifically, the DEP and PDZ domains of Dsh/Dvl are required for PCP signaling (Wallingford and Habas, 2005).

The mechanisms of PCP signal transduction are still poorly understood, although they clearly involve the PCP core complex and activation of small GTPases of the Rac/Rho subfamily (the PCP core complex is most likely not the only input into PCP signaling: in *Drosophila*, the heterophilic binding of Fat and Dachsous proteins on adjacent cells may activate PCP independently of the Stbm/Vangl-containing core complex: Lawrence et al., 2007). PCP was originally described in *Drosophila*, and specifically in the cuticle and retina of the fly. Indeed, the names for PCP genes, *Van Gogh* and *Starry night*, refer to whorled patterns of the normally aligned cuticular hairs of the fly that resemble the spirals of light around the stars in Vincent Van Gogh's painting *The starry night*, and which are also seen in other PCP fly mutants, including *Dsh1* (Seifert and Mlodzik, 2007 for review). The mechanisms of PCP signaling in vertebrates may differ significantly from those in *Drosophila*, however. Notably, Stbm/Vangl may act antagonistically to Fz and Dsh in fly PCP (Seifert and Mlodzik, 2007), whereas in the mouse *Dvl2*, *Vangl2*, and *Wnt5a* mutants all show phenotypic synergy (Wang et al., 2006a; Qian et al., 2007).

PCP in the mouse has mostly been described in two anatomic systems: the orientation of the cochlear sensory epithelium, and neural tube closure. Another structure that is easily affected by PCP alterations in the mouse is the tail. Known mouse PCP mutants were originally described by the presence of curled tails in the heterozygotes: hence the names *Loop-Tail* and *Circletail* for semidominant point mutants in mouse *Vangl2* and *Scrb1*, respectively (Torban et al., 2004a for review). These mutations give curled tails in heterozygotes and craniorachischisis and cochlear disorganization in homozygotes. Homozygous *Loop-Tail* mutants also show defects in convergent extension associated with notochord formation (Ybot-Gonzalez et al., 2007). The mutations appear to cause their effects by disruption of the PCP core complex, mislocalization of its component proteins within the cell, and/or reduced binding of Dvl proteins to Vangl proteins (Torban et al., 2004b; Torban et al., 2007). The importance of Dishevelled in PCP is as evident in the mouse as it is in the fly: *Dvl1*/*Dvl2* double null mutants have craniorachischisis, as do *Dvl2* $^{-/-}$, *Vangl2* $^{Lp/+}$ compound mutants, showing both Dvl1 and Dvl2 act to mediate PCP signaling in concert with Vangl2 (Wang et al., 2006a). The mouse *Wnt5a* null mutant has also been shown to synergize with *Loop-Tail* heterozygosity (*Vangl2* $^{Lp/+}$) in neural tube closure, making this a prime candidate for mediating PCP signaling among Wnt ligands acting in neurulation and caudal development in the mouse (Qian et al., 2007).

Crosstalk between Wnt/β-catenin and PCP pathways: synergy or mutual inhibition?

Wnts have been categorized as “canonical” or “non-canonical” based on their ability to activate the Wnt/β-catenin pathway (Du et al., 1995; Veeman et al., 2003). Several of the “non-canonical” vertebrate Wnts have been shown to be active in mediating cell movement during gastrulation (Du et al., 1995; Heisenberg et al., 2000; Tada and Smith, 2000). These “non-canonical” Wnts have also been shown to be active in the convergent extension movements mediating notochord extension (Tada and Smith, 2000; Hikasa et al., 2002), and in neurulation (Ciruna et al., 2006; Qian et al., 2007). As described, neural tube closure is disrupted by mutations in several mouse genes that are homologous to those encoding members of the core PCP complex in the fly. Some of these same genes, particularly the mouse *Stbm/Vangl* homolog *Vangl2*, have been shown to be essential for convergent extension of the notochord (Ybot-Gonzalez et al., 2007). Therefore, vertebrate Wnts active in convergent extension and neurulation may be thought of as PCP-active Wnts.

It has since been shown that the ability to activate PCP signaling versus the Wnt/β-catenin pathway is primarily a property of the specific Wnt receptor complex activated rather than of the Wnt ligand (Liu et al., 2005; Mikels and Nusse, 2006). Nonetheless, physiologically, a Wnt can be considered PCP-active if it has been observed to act primarily through PCP or convergent extension processes in vivo. In fact, it is not clear if any of the vertebrate PCP-active Wnts actually activates the Wnt/β-catenin pathway in vivo. In contrast, there is considerable evidence that PCP-active Wnts inhibit the Wnt/β-catenin pathway in vivo, and that this is a functional effect of the PCP pathway itself.

The first evidence for PCP antagonism of the Wnt/β-catenin pathway was the observation that the "non-canonical" Wnt5a could block transcriptional activation by the "canonical" Wnt1 in *Xenopus* embryos (Torres et al., 1996). This antagonism was shown to occur upstream of GSK-3 and β-catenin, whose effects on target gene expression were not affected by Wnt5a. Since Dvls interact directly with both Fz receptors and the β-catenin destruction complex (Wong et al., 2003; Wallingford and Habas, 2005), it can be suspected that the inhibition of Wnt/β-catenin signaling by Wnt5a may be mediated at the level of Dvl. This hypothesis is also attractive because Dvls bind directly to the core PCP complex machinery.

It has since been shown that *Wnt5a* null mice actually have elevated Wnt/β-catenin signaling in the embryonic limb buds (Topol et al., 2003: phenotypes of the *Wnt5a* null mice will be described further in the next subsection). So Wnt5a clearly inhibits Wnt/β-catenin signaling physiologically in mouse development. In addition, Wnt5a was shown to reduce the stability of intracellular β-catenin, an activity dependent on APC and the ubiquitin ligase Siah2 (Topol et al., 2003). Analogously, inversin, a vertebrate homolog of the fly PCP protein Diego, was shown to facilitate degradation of Dvl (Simons et al., 2005). Inversin is a protein localized to primary cilia in vertebrate cells, and the gene encoding it is mutated in the congenital disease nephronophthisis type II, in which cysts disrupt the architecture of renal nephrons. It was also shown to act in convergent extension in *Xenopus* embryos, so it is clearly a PCP mediator in vertebrates

as is its fly homolog. Suggestively, overexpressed Dact1 protein was also shown to promote Dvl degradation (Zhang et al., 2006).

Vertebrate Stbm/Vangl homologs have also been linked to Wnt/β-catenin pathway antagonism. Park and Moon (2002) showed that a *Xenopus* Stbm/Vangl homolog could antagonize Wnt/β-catenin signaling, but this was apparently separable from its activation of PCP signaling and binding to Dvl. Stbm/Vangl proteins, like Dact proteins, contain a C-terminal PDZ binding motif that binds to the PDZ domain of Dvl. Deletion of this motif in the *Xenopus* Stbm/Vangl homolog abrogated Dvl binding and PCP activity, but not Wnt/β-catenin antagonism (Park and Moon, 2002). The *Xenopus* Stbm/Vangl homolog also activated JNK signaling, an activity associated with PCP signaling but that may be a separate downstream pathway. "Non-canonical" Wnts and Dvls activate JNK in a manner that is dependent on the Dvl DEP domain, as is PCP signaling (Wallingford and Habas, 2005). Nonetheless, it was observed that inhibitors of Rho-kinase, a downstream PCP effector, but not JNK inhibitors, promote neural tube defects in embryos heterozygous for PCP-related mutations that cause craniorachischisis when homozygous (Qian et al., 2007: Three different mouse mutants were used in this study, *Vangl2* $^{Lp/+}$ *"Loop-Tail"*, *Scrb1* $^{Crc/+}$ *"Circletail"*, and *Celsr1* $^{Crsh/+}$).

There is some evidence that there also may in some cases be synergy between Wnt/β-catenin and PCP pathways. Notably, Wnt3a, a "canonical" wnt which is important in the development of the caudal embryo, was shown to activate cell motility via Dvl2 and RhoA activation in cultured fibroblastoid cells (Endo et al., 2005).

Therefore, in some cases Wnt3a might promote PCP-type signaling in vivo as well as the Wnt/β-catenin signaling that has been well documented to be downstream of Wnt3a. Also, two downstream effectors normally associated with "non-canonical" Wnt activity, Rac1 and Jnk2, were shown to be required for Wnt3a-induced nuclear accumulation of β-catenin in a mouse bone marrow derived cell line (Wu et al., 2008). Therefore Wnt/β-catenin and PCP pathways may not always be antagonistic to one another, but may in some cases act synergistically or be outright co-dependent.

As will be described in Chapter 4, my data on *Dact1* null and *Vangl2 Loop-Tail* mutant mice is consistent with a "mutual inhibition" model for Wnt/β-catenin and PCP pathways in the caudal mouse embryo (and specifically in caudal neural plate ectoderm). While there is ample evidence that the PCP pathway may inhibit the Wnt/β-catenin pathway, it has not been established that the converse occurs. Part of the problem is that there has been little clarity as to what a PCP gain-of-function mutation would look like: mouse neurulation mutants such as *Vangl2 Loop-Tail* and *Scrb1 Circletail* are thought to be PCP loss-of-function mutations. My data suggests that the missing Wnt/β-catenin inhibition of PCP exists in vivo, and that Dact1 is an important molecule for this process. Dact1 appears to simultaneously promote Wnt/β-catenin signaling and inhibit PCP signaling. Since Dact1 is a scaffolding molecule, it can be suggested that it may bias the integration of Fz and Dvl into multiprotein complexes promoting Wnt/β-catenin signaling as opposed to complexes promoting PCP signaling.

Caudalogy: the study of caudal embryonic development as a model system.

Mutations in a multiple signaling pathways have been shown to affect the caudal development of the mouse. In the caudal mouse embryo, multiple important developmental events occur in close spatiotemporal apposition to one another. These events include primary tissue specification in the primitive streak, closure of the endoderm ventrally to form hindgut, division of mesoderm into divergently-fated cell populations along the medial-to-lateral axis, segmentation, and closure of the neuroectoderm dorsally to form the neural tube. Therefore, the mouse tail is a particularly sensitive structure in which to identify defects affecting any of these phenomena. The multiple signaling pathways that have been shown to affect caudal body extension in ways that have been identified by caudal mouse phenotypes include Wnt/β-catenin, PCP, Notch, FGF, and retinoid signaling.

In addition to tail phenotypes observed in mouse PCP mutants, caudal phenotypes have been observed in mice mutant for the genes *Wnt3a* and *Wnt5a*. While these genes are both expressed in similar patterns in the embryonic tail bud (Takada et al., 1994), the mice mutants for these genes are notably different from one another.

The *Wnt3a* hypomorphic mutant *Vestigial tail* (*Wnt3a* $^{Vt/Vt}$) is characterized by a short and sometimes curly tail (Greco et al., 1996). This mutant is allelic to the *Wnt3a* gene and shows extremely reduced expression of *Wnt3a* mRNA, although the precise mutation has never been identified. In contrast, the *Wnt3a* null mutation is embryonic lethal and causes truncation at thoracic levels, typically just below the forelimb bud: a "half a mouse" phenotype (Takada et al., 1994). Both of these mutations lead to reduced β-catenin dependent gene expression in the tail bud mesoderm (Aulehla et al., 2003; Nakaya et al., 2005). In addition, the mutant embryos exhibit multiple ectopic neural tubes caudally, a phenotype which is thought to arise from a neural tube fate being favored over a normal mesodermal fate at the primitive streak (Yoshikawa et al., 1997; Shum et al., 1999). These defects are associated with reductions in Wnt/β-catenin signaling. This was clearly demonstrated by two studies. The *Wnt3a* null phenotype is recapitulated in *Lef1/Tcf1* double null mice (Galceran et al., 1999). Therefore, the *Wnt3a* null phenotype can be attributable to transcriptional failure at Lef/Tcf sensitive promoter sites. This conclusion was also supported by a subsequent study in which a dominant β-catenin-LEF1 fusion transgene was able to rescue the *Vestigial tail* phenotypes (Galceran et al., 2001).

The caudal truncation of *Wnt3a* mutants coincides with an arrest of somitogenesis at a level corresponding to the truncation. Typically, only the first 7-10 somites are formed in *Wnt3a* null embryos (Takada et al., 1994). Instead of somites being formed more caudally, undifferentiated mesoderm accumulates caudally in *Wnt3a* null embryos (see Intro. Fig. 1). A similar but less severe caudal accumulation of mesoderm is also

observed in *Dact1* null embryos, as described in Chapter 4 (also see Intro. Fig. 2). In addition to its failure to differentiate, the caudal mesoderm of *Wnt3a* null embryos shows a complete absence of β-catenin dependent gene expression (Nakaya et al., 2005) and widespread apoptosis, which is also observed in *Vestigial tail* homozygous embryos and in wild-type embryos in which *Wnt3a* expression has been artificially reduced by treatment with exogenous retinoic acid (Shum et al., 1999).

Mice whose *Wnt3a* genotype is compound heterozygous between *Wnt3a* null and *Vestigial tail* (*Wnt3a* $^{Neo/Vt}$) show phenotypes intermediate between those of *Wnt3a* nulls and *Vestigial tail* homozygotes (Greco et al., 1996). They also show caudal vertebral disorganization similar to what is seen in *Lrp6* null mice (Pinson et al., 2000) and *Dact1* null mice (see Intro. Fig. 3 and Chapter 4). The *Wnt3a* $^{Neo/Vt}$ mice vertebral truncations are at lumbar to upper caudal levels, similar to what is observed in *Dact1* null mice (Intro Fig. 3; compare data in Chapter 4 to that in Greco et al., 1996). The *Wnt3a* $^{Neo/Vt}$ mice, however, lack the visceral and perineal phenotypes observed in *Dact1* null mice (see Chapter 4). Considering the gene expression and rescue data, the *Wnt3a* mouse phenotypes can be attributed in their entirety or nearly so to losses in the Wnt/β-catenin signaling pathway (Galceran et al., 2001; Nakaya et al., 2005). Lrp receptors are considered to be essential for Wnt/β-catenin signaling, and to specify the activation of the Wnt/β-catenin signaling pathway in preference over other potential signaling downstream of a Wnt/Fz receptor-ligand interaction (Liu et al., 2005; Mikels and Nusse, 2006). Nonetheless, the presence of curled tails in the hypomorphic *Lrp6* mouse mutant *Ringelschwanz*, which resemble the *Loop-Tail* heterozygous phenotype, suggest there

may be a downstream input into PCP signaling as well (Kokubu et al., 2004). Wnt3a and Dvl2 proteins have, in fact, been shown to mediate RhoA activation in cultured motile fibroblastoid cells (Endo et al., 2005). Therefore, an effect on PCP signaling of Wnt3a or another protein usually associated with the Wnt/β-catenin signaling pathway cannot be excluded in the analysis of mutant mouse phenotypes.

The *Wnt5a* null mouse, like *Wnt3a* mutant mice, is caudally truncated, but the resemblance ends there. *Wnt5a* null mice have truncated, stunted limbs as well as tails (Yamaguchi et al., 1999a). They also show mild reductions in cell proliferation in the embryonic tail bud, a feature apparently not shared with *Wnt3a* or *Dact1* mutants (Chapter 4). They have elevated β-catenin dependent gene expression in the limb buds (Topol et al., 2003), although this was not replicated in the tail bud (Chapter 4). *Wnt5a* null mice also develop spina bifida if they are also heterozygous for any of several mutations in mouse homologs of the Drosophila PCP core complex proteins: *Vangl2* $^{Lp/+}$ *"Loop-Tail"*, *Scrb1* $^{Crc/+}$ *"Circletail"*, and *Celsr1* $^{Crsh/+}$ (Qian et al., 2007). This establishes the *Wnt5a* null mouse as a genuine PCP pathway mouse mutant. Nonetheless, the etiology of the limb and tail truncations in the *Wnt5a* null mouse is unclear: no embryologic mechanism for the occurrence of these phenotypes has been established. Consequently, it is not known to what degree they are actually attributable to a failure in PCP signaling: this is simply the most straightforward hypothesis based on what is already known about the actions of Wnt5a.

Somitogenesis: Wnt3a powers the somite segmentation clock.

Segmentation of the vertebrate body depends on the process of somitogenesis, the sequential generation of bilaterally paired epithelial somites from undifferentiated mesoderm. Somitogenesis, like multiple other processes in embryonic development, occurs in a sequence of maturation from rostral to caudal in the vertebrate embryo. While the first three somites may develop simultaneously or nearly so from previously undifferentiated paraxial mesoderm, after this the somites develop in a rostral to caudal sequence, so each new somite is added caudally and the most caudal somites are the youngest. Somitogenesis begins at approximately day 7.5 of gestation in the mouse embryo. It continues until embryonic day 12-13: somites that form the tail are added after embryonic day 9.5, when gastrulation is completed (Goldman et al., 2000). While gastrulation is still occurring, axial and paraxial mesoderm are continuously being generated from the primitive streak. Afterwards, in a process called secondary body formation, the tail bud mesoderm is thought to develop from a structure called the chordoneural hinge at the caudal extent of the extending neural tube and notochord (Cambray and Wilson, 2002). It has been shown that the cells of the chordoneural hinge are descendants of cells in the primitive streak (Cambray and Wilson, 2007). Cells from the primitive streak and tail bud mesoderm migrate laterally to form the paraxial mesoderm, which is progressively segmented into somitomeres, of which the most rostral three are termed presomites: S-2, S-1, and S0 from caudal to rostral (Goldman et al.,

2000; Zakany et al., 2001: to make clear, S-2 and S-1 are "S minus 2" and "S minus 1", as distinct from S1 and S2, which are the two youngest somites at any given time). The somitomeres and presomites together are termed the presomitic mesoderm.

Wnt3a null mice form only the first 7-10 somites: after that, somitogenesis is arrested, and while paraxial mesoderm continues to be generated and accumulate caudally, it does not form somites and eventually experiences widespread apoptosis (Takada et al., 1994; Shum et al., 1999). The failure to generate somites may be attributable to the failure to express three bHLH transcription factors known as mesoderm inducers: *Brachyury (T), Tbx6* and *pMesogenin1* (Yamaguchi et al., 1999b; Wittler et al., 2007). *Tbx6* null mice have irregular shaped somites and multiple caudal neural tubes as do *Wnt3a* nulls (Chapman and Papaioannou, 1998). *T* mutant mice range from the heterozygous hypomorph *No tail*, to nulls lacking notochords and all but the rostralmost somites (Herrmann, 1990; Yamaguchi et al., 1999b). *T* expression in the mouse embryo begins before *Wnt3a* expression, but *Wnt3a* is required to maintain it (Yamaguchi et al., 1999b). *pMesogenin1* null mice fail to generate paraxial mesoderm caudally, and lack all vertebrae below cervical levels (Yoon and Wold, 2000; Yoon et al., 2000). The *Wnt3a* null phenotype has been described as a gastrulation phenotype: however, considering the accumulation of undifferentiated paraxial mesoderm in *Wnt3a* null embryos, the *Wnt3a* null mouse clearly has a failure of paraxial mesoderm differentiation as well as defective gastrulation and neurulation control (Yoshikawa et al., 1997). The fact that mesoderm is formed in *Wnt3a* null embryos, but altogether lacks β-catenin dependent transcription,

implies a failure of mesoderm fate downstream of β-catenin induced genes (Nakaya et al., 2005).

The sequence of somitogenesis is regulated by the somite segmentation clock and the somite segmentation cycle. The somite segmentation clock determines that during a given time interval, a single bilateral pair of somites is separated from the rostral presomitic mesoderm (PSM). For each turn of the cycle, a presomite S0 separates from the PSM and becomes a nascent somite, S1; while presomite S-1 becomes the new S0, and presomite S-2 becomes the new S-1, a process associated with cyclic expression of the transcription factors *HoxD1* in S-1 and *Mesp2* in S-2 (Zakany et al., 2001).

Prior to any identification of the molecular components of the somite segmentation clock, the theoretical "clock and wavefront" model of somitogenesis had been proposed to explain how the repeated structure of a new pair of somites could be produced within a repeated, precise time interval (Cooke and Zeeman, 1976). According to the "clock and wavefront" model, a molecular oscillator, the clock, exists which can regenerate its own oscillation at a regular time interval within a tissue. Meanwhile, the wavefront is produced by a spatial gradient of a substance which regulates the amplitude of the clock oscillations (Cooke and Zeeman, 1976; Forsberg et al., 1998; Dubrulle et al., 2001; Aulehla et al., 2003).

The "clock and wavefront" model was substantially validated by studies following the initial publication of the theory (Cooke and Zeeman, 1976), which identified some of the molecules that constituted the "clock" and "wavefront" components. The molecular basis for the somite segmentation cycle has been suggested by the observation that multiple genes are expressed cyclically in distinct patterns, termed "phase patterns", during each turn of the somite segmentation cycle (Forsberg et al., 1998; Dubrulle et al., 2001; Zakany et al., 2001; Aulehla et al., 2003; Dale et al., 2003; Dequeant et al., 2006; Suriben et al., 2006: also see Chapter 3). Some of these cyclic genes are likely to be molecular components of the clock oscillator itself, while others are likely to be downstream morphogenic factors whose expression is regulated by the cyclic clock oscillation (Aulehla et al.,2008).

The genes originally described as exhibiting cyclic expression patterns in somite segmentation were effectors and downstream targets of the Notch pathway: for example, the glycosyltransferase *Lunatic fringe* (Dale et al., 2003). Wnts became implicated in somite segmentation when the intracellular Wnt/β-catenin antagonist *Axin2* was observed to be expressed cyclically in somitogenesis (Aulehla et al., 2003). This is dependent on Wnt3a expression: *Axin2* and *Lunatic fringe* expression were both abolished in the tail bud of *Vestigial tail* homozygous embryos. Transgenic overexpression of *Axin2* ablated *Lunatic fringe* expression as well, suggesting that cyclic expression of Wnt effectors regulated the cyclic expression of Notch effectors, and that all was dependent on the presence of Wnt3a. The authors of this study proposed a version of the "clock and wavefront" model of somitogenesis, whereby Notch and Wnt effector expression, and

indeed, active Notch and Wnt/β-catenin signaling, oscillated in opposite phases within the PSM. Once sufficient distance from the highest level *Wnt3a* expression in the caudal tail bud was achieved, the oscillations would be dampened (in the rostral PSM) to an extent that would signal separation of the new somite from the PSM (Aulehla et al., 2003). The "wavefront" in this rendition of the "clock and wavefront" model would be provided by a caudal-to-rostral decrementing gradient of Wnt3a protein in the PSM.

The molecular identities of the clock and wavefront were substantially validated by later studies. Wnt and Notch effectors do indeed cycle in the PSM, predominantly in clusters of opposite cycling phase (Dequeant et al., 2006). Wnt signaling has also been shown to activate Notch effector expression through the action of Tbx6 (Galceran et al., 2004; Hofmann et al., 2004). Olivier Pourquie and his colleagues have defined a hierarchy of signaling pathways in the embryonic tail bud and PSM, whereby FGF signaling is essential for *Wnt3a* expression, which in turn is necessary for Notch effector expression (Wahl et al., 2007). There are some caveats to the model, however. It is not clear whether Wnt/β-catenin signaling actually cycles in the PSM: from the expression of the Wnt/β-catenin sensitive BATGal reporter, there are not obviously cyclic patterns of Wnt/β-catenin target gene expression (Aulehla et al., 2008; and Chapter 4). Furthermore, transgenic expression of constitutively active mutant β-catenin in the tail bud did not disrupt the clock or the cyclic expression of Wnt or Notch effectors (Aulehla et al., 2008). It did, however, completely abolish somitogenesis, creating an expanded domain of paraxial mesoderm, which is remarkably similar morphologically to what is seen in *Wnt3a* null embryos. Therefore, although Wnt/β-catenin signaling regulation is not

intrinsic in the clock mechanism, the gradient of Wnt/β-catenin signaling is essential for somitogenesis.

I initially observed cycle phase-like expression patterns of *Dact1* expression in the PSM, which I confirmed to be cyclic expression in phase with *Axin2*, along with my collaborator Rowena Suriben (Chapter 3, Suriben et al., 2006). Neither *Dact2* nor *Dact3* was observed to be expressed in the PSM (Chapter 2, Fisher et al., 2006). This led to the suspicion that Dact1 played an important role in somitogenesis. When *Dact1* null mice where observed to be caudally truncated, sometimes exhibiting caudal vertebral disorganization, it seemed natural to hypothesize that this was due to a failure in somitogenesis. This hypothesis is probably refuted by the rescue of the *Dact1* null mouse phenotypes by the heterozygous *Vangl2 Loop-Tail* allele (Chapter 4). Since *Vangl2* is expressed in ectoderm (neural tube, neural plate, and primitive streak ectoderm) rather than in mesoderm, the *Dact1* null mouse phenotypes probably originate in the ectoderm rather than the mesoderm. At this time, the *Dact1* null mouse phenotypes seem most likely to originate from a failure in gastrulation at the caudal primitive streak. Whether they are attributable to excess PCP signaling or to reduced Wnt/β-catenin signaling as well is yet to be determined. I favor the hypothesis that *Dact1* null mouse phenotypes arise from a simultaneous reduction in Wnt/β-catenin signaling as well as exaggerated Dvl/PCP signaling, due to the resemblance of *Dact1* skeletal phenotypes to *Lrp6* null and *Wnt3a* $^{Neo/Vt}$ phenotypes, which clearly are "canonical" Wnt signaling failures.

A role for Dact1 in somitogenesis is not excluded, however, especially since the PSM and nascent somites are the most prominent loci of *Dact1* expression in E8-E10 mouse embryos (see expression data in Chapters 2-4, especially Fisher et al., 2006). The cyclic expression of *Dact1* could be an evolutionary relic: however, what of that of a large multiplicity of Wnt effectors in the PSM (Dequeant et al., 2006)? Is the cyclic expression of the entire "Wnt cluster" (Dequeant et al., 2006) to be presumed an evolutionary relic in its entirety? If so, the "Wnt cluster" of cycling genes might play a more prominent role in regulating somitogenesis in another animal at significant evolutionary distance from the mouse. It would be interesting to see if the transgenic hyperactivation of Wnt/β-catenin signaling would have the same effects in zebrafish, for example, as in the mouse. Alternatively, there may be substantial functional redundancies among these genes in somitogenesis. In the case of *Dact1*, this redundancy would have to be with a non-Dact molecule, since neither *Dact2* nor *Dact3* is expressed in E9 mouse PSM (Fisher et al., 2006). It is notable that neither *Axin2* nor *Naked1*/*Naked2* null mice exhibit defects in somitogenesis, although these mice exhibit similar defects in calvarial ossification (Yu et al., 2005; Zhang et al., 2007). *Naked1*, although a Wnt/β-catenin inhibitor, actually is expressed in the "Notch cluster", unlike *Axin2* (Ishikawa et al., 2005).

In contrast, mice lacking *Sfrp1* and *Sfrp2*, which encode soluble competitive inhibitors of Wnt/Fz binding, show disorganization of somites and their derivatives in the thoracic region (Satoh et al., 2006). This phenotype resembles the classic somite cycling phenotypes seen in mutations of Notch pathway genes, such as null mutants for the Notch

glycosyltransferase *Lunatic fringe* (Evrard et al., 1998; Zhang and Gridley, 1998). These phenotypes are characterized by disorganization in the patterning of the vertebrae and ribs. Similar defects are also seen in *Dvl2* null mice (Hamblet et al., 2002), although at a lower frequency than what is seen in most Notch pathway mutants; and I have observed vertebral defects on occasion in *Dact1* null neonates as well (Intro. Fig. 2). Furthermore, rib defects similar to those seen in *Dvl2* null mice (Hamblet et al., 2002), are also seen in *Vangl2 Loop-Tail* homozygotes (Greene et al., 1998): thus there may be a contribution to somite patterning of PCP signaling from *Vangl2*. This is highly speculative at this point: the mechanism by which *Vangl2 Loop-Tail* homozygotes develop defects in somatic derivatives remains entirely undescribed. If it is through a defect in PCP signaling, however, this might explain the resemblance between the defects in *Dvl2* null mice (Hamblet et al., 2002) and *Vangl2 Loop-Tail* homozygotes (Greene et al., 1998), since both of these mouse mutants have been shown to have defects in cochlear PCP signaling (Montcouquiol et al., 2003, 2006;Wang et al., 2006a).

Addition of *Sfrp5* (null allele) or *Vangl2 Loop-Tail* heterozygosity to the *Sfrp1* and *Sfrp2* mutant combination leads to a caudal truncation which resembles that seen in *Wnt3a* nulls or in *Dact1* nulls with a heterozygous *Wnt3a* null allele (Takada et al., 1994; Satoh et al., 2008, compare with data in Chapter 4). The *Sfrp* double or triple mutant combinations indeed synergize with *Dkk1* null homozygosity in the disorganization of somites (Satoh et al., 2008). They also synergize with *Vangl2 Loop-Tail* heterozygosity in neural tube closure and convergent extension of the notochord (Satoh et al., 2008; Compare with Wang et al., 2006a and Ybot-Gonzalez et al., 2007 for notochord defects

in *Dvl1/Dvl2* double homozygotes and *Vangl2 Loop-Tail* homozygotes, respectively). Synergy of *Sfrp* mutant phenotypes with mutations in both *Dkk1* and *Vangl2* is not surprising: since Sfrps are competitive inhibitors of Wnt/Fz binding, they should affect both "canonical" and "non-canonical" downstream signaling (the *Dkk1* mutation should be specific for signaling downstream of Lrps, since it inhibits their binding to the Wnt/Fz complex). More interestingly, Sfrp losses give somite cycling defects resembling those induced by transgenic expression of constitutively active mutant β-catenin in the tail bud, showing a consistent result for hyperactivation of Wnt/β-catenin signaling in somitogenesis (Aulehla et al., 2007; Satoh et al., 2008). Since Sfrp losses also synergize with the *Vangl2 Loop-Tail* mutation, this provides further suggestion that Wnt/β-catenin signaling and PCP signaling are antagonistic to one another in the embryonic mouse tail bud.

It is unfair to assume that multiple Wnt signaling activators and inhibitors were recruited into somitogenesis because of the importance of Wnt signaling there: this would be a teleological interpretation of evolution, and, in any case, there is only one *Wnt3a* gene upon which somitogenesis clearly depends. Nonetheless, while the fundamental role(s) of Wnt signaling in somitogenesis remain yet to be elucidated, the importance of this pathway is indubitable based on both gain-of-function and loss-of-function mouse mutants.

Dacts and Dact interactors in nervous system development.

Why study mice? Most basic developmental biology and physiology questions can be more efficiently addressed in a fast-reproducing animal like *Drosophila melanogaster*, or an organism so small it can be mapped down to the level of individual stereotyped cells, like *Caenorhabditis elegans*, the nematode worm. In contemplating the wonderful book *The mind of a worm* (White et al., 1986), which describes the anatomy of every individual neuron in *Caenorhabditis elegans*, I have been struck by the relatively astonishing difficulty of studying as complicated a structure as the mouse brain, where there are hundreds or thousands of neurons of each type, yet each develops individually according to its individual interactions with other cells and with extracellular molecules, in ways that may be substantially governed by chance. The answer, presumably, is that a mouse has a brain that is structurally similar to the human brain, and quite likely a mind that is functionally similar as well. Of course the same is true of other organs besides the brain (teleosts have no lungs, birds have no IgG, and so on), and it is of high medical importance to use a research animal that is molecularly similar to the human.

A notable observation concerning the *Dact* gene family is that, from multi-tissue Northern blots, it is evident that all three *Dacts* are highly expressed in the brain relative to most other tissues of the adult mouse (Chapter 2; Fisher et al., 2006). This expression is predominantly neuronal. All three *Dact* genes are also expressed in the embryonic nervous system, although with distinct expression patterns and levels. Given the data

from the *Dact1* null embryo suggesting that a crucial function for Dact1 is to promote Wnt/β-catenin signaling, it seems likely that this will prove to be a role for Dact1 in the developing and mature brain as well. Using Wnt/β-catenin reporter mice, it has been shown that Wnt/β-catenin dependent transcription is widespread in embryonic and adult brains, including many neuron-rich regions of the adult brain (Maretto et al., 2003).

Wnts and their downstream signaling machinery have been shown to have multiple roles in nervous system development, as has been particularly evident from studies of mutant mice. Historically, the first designed Wnt null mouse, of Wnt1, had deletions of the midbrain and cerebellum (McMahon and Bradley, 1990; McMahon et al., 1992). *Dact* genes are not expressed in the CNS (except at its caudalmost extent) until neuronogenesis (Chapter 2; Fisher et al., 2006).

For the purposes of this thesis, I will use consistently the term "neuronogenesis" to refer specifically to the generation of postmitotic neurons from precursor cells. This is used here instead of the broader term "neurogenesis", which is often used as a synonym for "neuronogenesis", but which can also mean the development of committed neural tissue within an organism, including the precursor cells that are the ancestors of future neurons and glia ("gliogenesis" denotes the differentiation of neural precursor cells into glia, and is a term analogous to "neuronogenesis" for neurons). This distinction in nomenclature is also evident in the use of the terms "neurogenic genes" and "neurogenic tissues", to refer to genes and tissues that define *the embryonic precursors of the future nervous system*.

Neuronogenesis is the earliest event in CNS development, besides neural tube closure, in which *Dact* genes are likely to be active. Embryos of mice expressing *LacZ* under a Lef/Tcf inducible promoter (BATGal) show canonical Wnt signaling in apical forebrain neuroepithelium, cortical plate, and other sites of neuronogenesis (Maretto et al., 2003). I have observed *Dact1* mRNA expression in a striated columnar pattern in forebrain neuroepithelia at E13-E14, and in cells seemingly emerging from these neuroepithelia to populate the striatum and cortical plate, where *Dact1* expression is even more prominent (Fisher et al, 2006 and Chapter 2). *Dact3* is also expressed at a lower level in these regions, although apparently without the striations observed for *Dact1*. Wnt signaling in neuronogenesis has been studied in CNS neuroepithelia, but with somewhat equivocal results. Expression of stabilized β-catenin in neuroepithelia causes hyperproliferation of neuronal precursors without preventing their eventual neuronal maturation (Chenn and Walsh, 2002, 2003; Zechner et al., 2003): admissibly, this may be considered non-physiological. Analogously, ablation of *β-catenin* was shown to reduce neuroepithelial proliferation (Zechner et al., 2003). Another study concludes oppositely that Wnt7a or stabilized β-catenin can inhibit proliferation and promote neuronal differentiation of neuroepithelial precursors in vitro via expression of neurogenin 1 (Hirabayashi et al., 2004). In vivo, ablation of the *Lrp6* gene encoding a canonical Wnt coreceptor led to mild thinning of the mouse cerebral cortex (Zhou et al., 2006: the mild phenotype may be due to partial redundancy with the alternative coreceptor Lrp5). Evidently, the functions of Wnt signaling in neuroepithelia and the maturation of their cells into neurons or glia are still unclear. Additionally, ectopically expressed *Wnt1* can

produce neocortical heterotopias (Ligon et al., 2003) and midbrain hypertrophy due to hyperproliferation (Panhuysen et al., 2004).

Dact1 null mice lack any gross neuroanatomic phenotypes: although a slight but statistically significant enlargement of the midbrain was observed in neonates, the statistical range of *Dact1* nulls overlapped over 50% with that of wild-type littermates, so the effect may be too small to be studied realistically (Jun Hoshino, unpublished observation communicated to myself and B. Cheyette). Furthermore, *Dact1*/*Dact3* double nulls apparently also lack any gross neuroanatomic phenotypes (Saul Kivimäe, unpublished observation communicated to myself and B. Cheyette). Indeed, *Dact1*/*Dact3* double nulls born so far appear to lack any gross anatomic phenotypes beyond those observed in *Dact1* null mice. Since *Dact2* is minimally expressed in the embryonic brain (unlike the embryonic spinal cord, which expresses all three *Dact* genes at high levels: Fisher et al., 2006, Chapter 2), it is unlikely that Dacts play a major role in neuronogenesis. It is also implicit that Dacts are not fundamentally required for Wnt signaling in mammals, which is not surprising given their likely non-existence in most invertebrates. The implication is that Dacts are probably functionally modulators of signaling pathways rather than crucial effectors.

Intuitively, it might seem that the apparent expression of *Dact1* in migrating embryonic neurons (Fisher et al., 2006; Chapter 2, additional data) is at odds with its hypothesized function of promoting Wnt/β-catenin signaling at the expense of PCP signaling in the tail bud (Chapter 4). If Wnt/β-catenin signaling is associated with

proliferation in neuroepithelia, as it is in many other tissues, while PCP signaling regulates the machinery of cell migration, it would seem intuitive that the newly postmitotic neurons migrating out of neuroepithelia would be downregulating Wnt/β-catenin signaling and upregulating PCP signaling. The most straightforward explanation for this dilemma would be that one of these two hypotheses is fundamentally wrong. I think it is particularly likely that the role of Dact1, and maybe of other Dacts as well, as a switch between signaling pathways is in fact context-dependent. Dacts, after all, are not enzymes but adaptors in protein-protein binding. It may be that if a given balance of binding partners is present, the combination with Dact promotes Wnt/β-catenin signaling at the expense of PCP, while perhaps in a different signaling milieu, the reverse occurs. Some evidence supporting this idea comes from a study of Dact3 in colonic epithelium, where it functions as a Wnt/β-catenin antagonist, and consequently a tumor suppressor (Jiang et al., 2008). The likely answer to the agonist/antagonist dilemma that pervades the literature on Dacts is: both, either, or sometimes one and sometimes the other. The absence of a general rule on Dact function may become evident from further study of Dact mutant brains.

Finally, it is worth noting that the field of Wnt signaling in neurobiology is in its beginnings, and novel pathways downstream of Wnts in neurons are likely to be described. In particular, Wnt/β-catenin signaling is likely to have very different consequences in the distal processes of a neuron as compared to the soma, since effects on transcription will not be the major output of signaling at long distances from the nucleus. Patricia Salinas and colleagues have proposed "a divergent canonical Wnt

pathway" which acts via β-catenin in neuronal processes (thus conserving the upstream machinery of "canonical" Wnt/β-catenin signaling), but which primarily affects the cytoskeleton, and particularly microtubules (Fradkin et al., 2005; Salinas, 2007). In this pathway, Dvls can act to stabilize microtubules, and APC, in its capacity as a microtubule plus-end binding protein, can "capture" microtubules to the cortical actin cytoskeleton, thus stabilizing microtubules, growth cones, and branching processes (Krylova et al., 2000; Zhou et al., 2004; Rosso et al., 2005). With respect to the possible actions of Wnt signaling on growth cone function, it has been observed that cultured hippocampal neurons from *Dact1* null neonates tend to exhibit a constitutively collapsed growth cone morphology (N. Okerlund and B.N. Cheyette, unpublished observation). This may be related to effects of Dact1 on p120-catenin (Park et al., 2006), or on Rac family small GTPases via the PCP pathway, since these have been observed to affect growth cone morphology and dynamics (Jin and Strittmatter, 1997; Lehmann et al., 1999; Fournier et al., 2003). Wnts have been shown to be essential for stabilizing synapses at the *Drosophila* neuromuscular junction (Packard et al., 2002), and in the murine cerebellum (Hall et al., 2000). They have also been shown to be axon guidance cues for a large number of neurons in the vertebrate CNS (see Fradkin et al., 2005 for review), and axonal and dendritic branching factors in the vertebrate CNS as well (Krylova et al., 2000; Rosso et al., 2005). Clearly, the roles of Wnt signaling in determining neuronal morphology and dynamics are myriad. It seems almost certain that Dact proteins, which can act in the selection of which downstream pathways are activated, will prove to affect neuroanatomic development. All or nearly all developing neurons in the mouse embryo seem to express at least one of the *Dact* family genes (Fisher et al., 2006; Chapter 2).

In summary…

I began working in the Cheyette laboratory at a time when the *Dact* gene family had been initially characterized in *Xenopus laevis*, but little was known about its expression or functions in the mouse, which is the preferred mammal for genetic manipulation. Benjamin Cheyette, my mentor, had constructed a *Dact1* null allele, and this was being introduced into mice. I characterized the expression of the *Dact* gene family in mouse embryonic development by in situ hybridization, the results of which are described in Chapters 2 and 3. Expression patterns for *Dact1* suggested potential roles in neuronogenesis (Fisher et al., 2006, Chapter 2) and somitogenesis (Suriben et al., 2006, Chapter 3). The *Dact1* null mice were immediately identifiable from among their littermates by their short, kinked, curly, or absent tails (Intro. Fig. 2). These were, at first glance, similar to mice with loss-of-function mutations in "canonical" Wnt/β-catenin signaling (van Amerongen and Berns, 2006 for review; also see Intro. Fig. 3). Particularly, they resembled the *Wnt3a* expression hypomorph *Vestigial tail* (Greco et al., 1996). Study of *Dact1* null embryos showed reduced "canonical" Wnt/β-catenin signaling and phenotypic synergy with a heterozygous *Wnt3a* null allele (Chapter 4). My initial hypothesis was that the caudal truncation defect in *Dact1* null mice was due to a failure in somitogenesis. This was particularly suggested by data showing that *Dact1* mRNA expression was oscillatory in the somite segmentation cycle (Suriben et al., 2006,

Chapter 3), and that cyclic oscillatory expression of other genes in somitogenesis depends on Wnt3a (Aulehla et al., 2003; further analysis provided in Aulehla et al., 2007). Somite organization defects in *Dact1* null mice are sometimes visible just rostral to the level of the truncation, but more rostral to that they are very rare (Intro. Fig. 3). In contrast, roughly 15% of *Dact1* null mice born exhibit spina bifida, suggesting an effect on the PCP pathway. To test this, I crossed *Dact1* null mice with *Vangl2 Loop-Tail* mutant mice, which is a standard test for synergy in the PCP pathway of mutant mice (Lu et al., 2004; Wang et al., 2006a; Qian et al., 2007; Satoh et al., 2008). In contrast to the expected synergy of the *Dact1* null and *Vangl2 Loop-Tail* mutations, I found mutual rescue between the homozygous *Dact1* null, characterized by caudal truncation, and the heterozygous *Loop-Tail* mutant, characterized by a curly tail: the compound mutant was, most often, a normal mouse (Chapter 4). This revealed mutual antagonism between the PCP and Wnt/β-catenin pathways in mouse gastrulation and neurulation, at the level of an interaction between Dact1 and Vangl2 proteins. Likewise, it provided evidence that Dact1 functions as a PCP antagonist as well as a Wnt/β-catenin agonist in the caudal mouse embryo.

I hypothesize that Dact1 acts to bias the multiprotein complexes downstream of Wnt/Fz interaction to favor Wnt/β-catenin signaling at the expense of PCP signaling. Future studies will presumably test this hypothesis, and also examine its applicability to other tissues and cell types other than the caudal ectoderm of the mouse embryo, which is the site of the interaction I have observed. It will be interesting to learn, in the future, if Dact proteins are generally PCP antagonists as well as Wnt/β-catenin agonists, or

whether their functions in these pathways are more variable and context-dependent. There are likely to be many ramifications in developmental biology, neurobiology, oncology, and possibly other fields of medical biology as well. While I have only identified a single inter-pathway interaction at the level of a single molecule, Dact1, I hope that this will be of assistance to future studies that can ultimately become of practical value to medical science.

Introductory Figures and Legends:

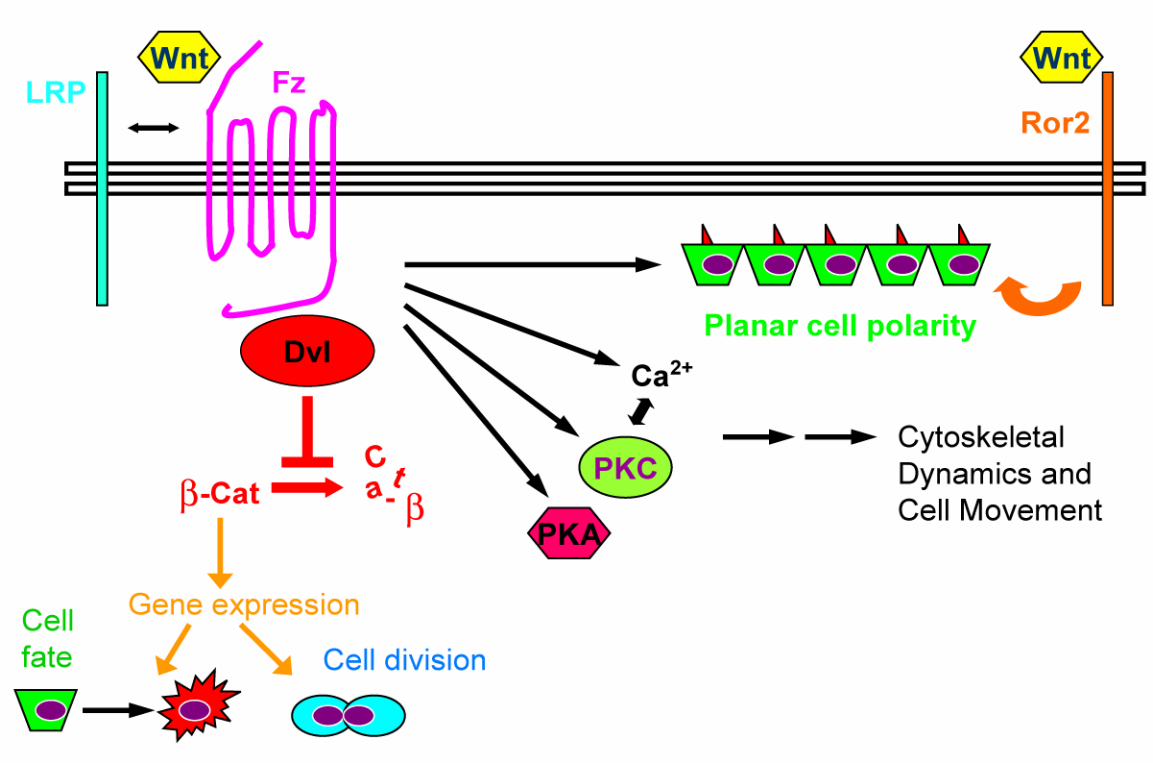

Intro. Figure 1: Cartoon depiction of Wnt signaling pathways. Wnt ligands bind to Frizzled (Fz) receptors (upper left), in a complex that may also include an Lrp5 or Lrp6 protein (LRP). Lrp proteins are single pass transmembrane proteins, while Fz proteins are members of the seven transmembrane serpentine receptor superfamily. The C-terminal cytoplasmic tail of Wnt-activated Fz binds to Dishevelled (Dvl), an interaction which is essential for the activation of several downstream signal transduction pathways. These include the "canonical" Wnt/β-catenin pathway, in which Dvl inhibits the degradation of cytoplasmic β-catenin (shown in red; this pathway is dependent on Lrp in the complex with Wnt, Fz, and Dvl). Soluble β-catenin can activate gene expression within the nucleus, which is associated with the promotion of cell division or cell fate changes. Other signaling modalities that can be activated by a complex of Wnt, Fz, and

Dvl, include activation of PKA or PKC, release of intracellular calcium, and the planar cell polarity (PCP) pathway, which affects cytoskeletal organization and cell movement, and orients cells within polarized epithelia (a row of cells in an epithelium are depicted with their primary cilia, represented by red triangles on the apical side of each cell, oriented in a uniform direction). The PCP pathway can also be activated by Wnt binding to the receptor Ror2 (upper right).

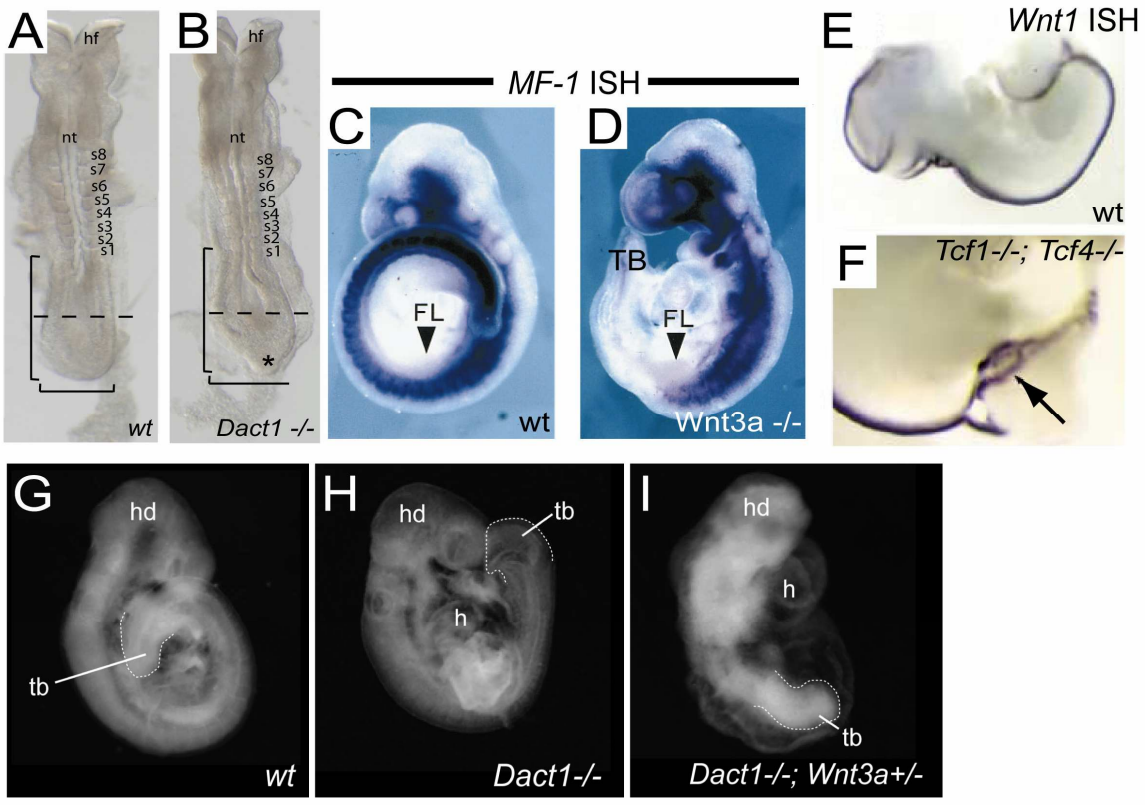

Intro. Figure 2: Comparison of *Dact1* null embryonic morphology with mutants in *Wnt3a* and its downstream effectors. A and B, also shown in Chapter 4, Figure 3: embryonic day eight (E8.0) embryos matched at the eight somite stage. A, Wild-type. B, *Dact1* null. A caudal accumulation of mesenchymal tissue (asterisk) is observed in the *Dact1* null embryo but not the wild-type. C and D, Images of E9.5 embryos reproduced from Yoshikawa et al. (1997). Embryos are labeled by in situ hybridization (ISH) for the mesoderm marker MF-1. C, Wild-type. D, *Wnt3a* null embryo. The *Wnt3a* null embryo does not show MF-1 expression caudal to the forelimb bud (FL, arrowhead). Nonetheless, it shows an extended caudal tail bud (TB), which lacks MF-1 expression. E and F, E9.5 *Tcf1/Tcf4* double null embryos labeled by ISH for *Wnt1*, which is expressed in the dorsal neural tube. The images are reproduced from Gregorieff et al. (2004).

Caudally, the embryos show forked, duplicated, and convoluted neural tubes (arrow in F, close-up). This phenotype is also observed in *Wnt3a* mutant embryos but not in *Dact1* nulls. G-I, Morphology of E9.5 embryos from genetic crosses of *Dact1* and *Wnt3a* null alleles. G, Wild-type embryo. H, *Dact1* null embryo showing a slightly ventrally curled tail bud morphology (tb). I, *Dact1* null homozygous, *Wnt3a* null heterozygous embryo. The tail bud (tb) is very short and lacks visible internal architecture, similar to what is observed in the *Wnt3a* null embryo (D). The head (hd) also appears reduced.

Intro. Figure 3.

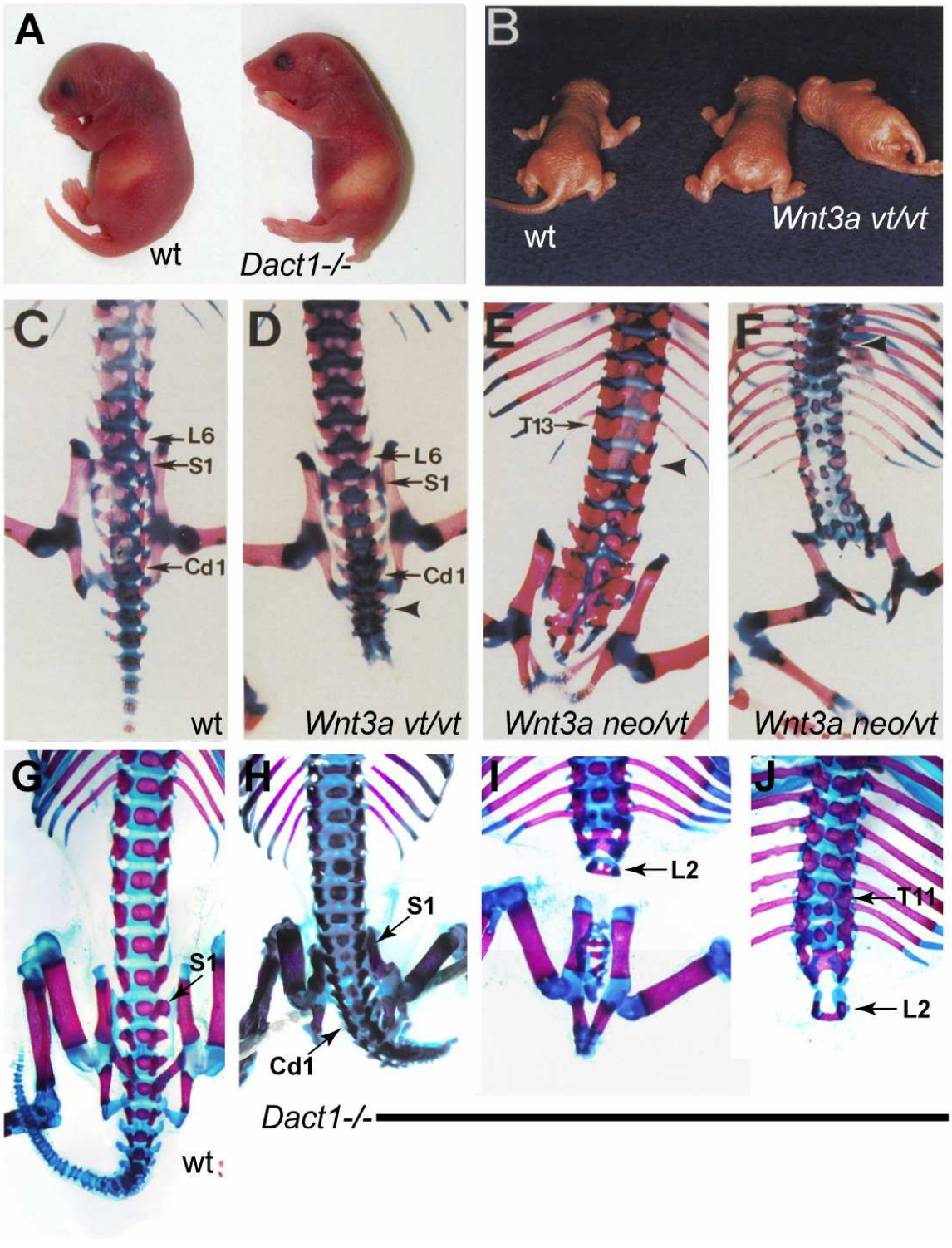

Intro. Figure 3: Comparison of skeletal phenotypes of *Dact1* null neonates with *Wnt3a* mutants. A, Wild-type (left) and *Dact1* null (right) neonatal littermates. The *Dact1* null (right) neonate has a short, crooked tail. B, Wild-type (left) and *Vestigial tail* (*Wnt3a* $^{vt/vt}$, right) neonates. *Vestigial tail* (*Wnt3a* $^{vt/vt}$) neonates have short or absent tails. C-F, Skeletal phenotypes in the lumbar to caudal region of neonatal mice. C, Wild-type. D, *Vestigial tail* (*Wnt3a* $^{vt/vt}$). E and F, Compound heterozygotes of *Vestigial tail* (*Wnt3a* ^{vt}) and *Wnt3a* null (*Wnt3a* ^{neo}) alleles, (*Wnt3a* $^{neo/vt}$). The compound heterozygous neonates (E, F) show spinal truncation at sacral levels and disorganization of lumbosacral vertebrae (F). Images B-F have been reproduced from Greco et al. (1996). G, Skeleton of a wild-type neonate from a *Dact1* null heterozygous intercross. H-J, Skeletal phenotypes of varying severity seen in *Dact1* null neonates. H, Short tail. I, Disorganized lumbosacral vertebrae and no tail. J, *Dact1* null neonate truncated at L2. Vertebrae are disorganized from T11 to the truncation.

Reference List for the Introduction

Aoki,K. and Taketo,M.M. (2007). Adenomatous polyposis coli (APC): a multi-functional tumor suppressor gene. Journal of Cell Science *120*, 3327-3335.

Aulehla,A., Wehrle,C., Brand-Saberi,B., Kemler,R., Gossler,A., Kanzler,B., and Herrmann,B.G. (2003). Wnt3A plays a major role in the segmentation clock controlling somitogenesis. Developmental Cell *4*, 395-406.

Aulehla,A., Wiegraebe,W., Baubet,V., Wahl,M.B., Deng,C., Taketo,M., Lewandoski,M., and Pourquie,O. (2008). A beta-catenin gradient links the clock and wavefront systems in mouse embryo segmentation. Nat. Cell Biol. *10*, 186-193.

Bhat,K.M. (1998). Frizzled and frizzled 2 play a partially redundant role in wingless signaling and have similar requirements to wingless in neurogenesis. Cell *95*, 1027-1036.

Boutros,M., Paricio,N., Strutt,D.I., and Mlodzik,M. (1998). Dishevelled activates JNK and discriminates between JNK pathways in planar polarity and wingless signaling. Cell *94*, 109-118.

Brenner,S. (2001). My Life in Science. Biomed Central, London.

Brott,B.K. and Sokol,S.Y. (2005a). Frodo proteins: modulators of Wnt signaling in vertebrate development. Differentiation *73*, 323-329.

Brott,B.K. and Sokol,S.Y. (2005b). A vertebrate homolog of the cell cycle regulator Dbf4 is an inhibitor of Wnt signaling required for heart development. Developmental Cell *8*, 703-715.

Cambray,N. and Wilson,V. (2002). Axial progenitors with extensive potency are localised to the mouse chordoneural hinge. Development *129*, 4855-4866.

Cambray,N. and Wilson,V. (2007). Two distinct sources for a population of maturing axial progenitors. Development *134*, 2829-2840.

Chapman,D.L. and Papaioannou,V.E. (1998). Three neural tubes in mouse embryos with mutations in the T-box gene Tbx6. Nature *391*, 695-697.

Chen,C.M. and Struhl,G. (1999). Wingless transduction by the Frizzled and Frizzled2 proteins of Drosophila. Development *126,* 5441-5452.

Chen,A.E., Ginty,D.D., and Fan,C.M. (2005). Protein kinase A signalling via CREB controls myogenesis induced by Wnt proteins. Nature *433*, 317-322.

Chenn,A. and Walsh,C.A. (2002). Regulation of cerebral cortical size by control of cell cycle exit in neural precursors. Science *297*, 365-369.

Chenn,A. and Walsh,C.A. (2003). Increased neuronal production, enlarged forebrains and cytoarchitectural distortions in beta-catenin overexpressing transgenic mice. Cereb. Cortex *13*, 599-606.

Cheyette,B.N. (2004). Ryk: another heretical Wnt receptor defies the canon. Sci. STKE. *2004*, e54.

Cheyette,B.N.R., Waxman,J.S., Miller,J.R., Takemaru,K.I., Sheldahl,L.C., Khlebtsova,N., Fox,E.P., Earnest,T., and Moon,R.T. (2002). Dapper, a Dishevelled-associated antagonist of beta-catenin and JNK signaling, is required for notochord formation. Developmental Cell *2*, 449-461.

Ciruna,B., Jenny,A., Lee,D., Mlodzik,M., and Schier,A.F. (2006). Planar cell polarity signalling couples cell division and morphogenesis during neurulation. Nature *439*, 220-224.

Cooke,J., and Zeeman,E.C. (1976). A clock and wavefront model for control of the number of repeated structures during animal morphogenesis. J. Theoretical Biol. *58,* 455-476.

Dale,J.K., Maroto,M., Dequeant,M.L., Malapert,P., McGrew,M., and Pourquie,O. (2003). Periodic Notch inhibition by lunatic fringe underlies the chick segmentation clock. Nature *421*, 275-278.

Davidson,G., Wu,W., Shen,J.L., Bilic,J., Fenger,U., Stannek,P., Glinka,A., and Niehrs,C. (2005). Casein kinase 1 gamma couples Wnt receptor activation to cytoplasmic signal transduction. Nature *438*, 867-872.

Dequeant,M.L., Glynn,E., Gaudenz,K., Wahl,M., Chen,J., Mushegian,A., and Pourquie,O. (2006). A complex oscillating network of signaling genes underlies the mouse segmentation clock. Science *314*, 1595-1598.

Dollar,G.L., Weber,U., Mlodzik,M., and Sokol,S.Y. (2005). Regulation of Lethal giant larvae by Dishevelled. Nature *437*, 1376-1380.

Du,S.J., Purcell,S.M., Christian,J.L., Mcgrew,L.L., and Moon,R.T. (1995). Identification of Distinct Classes and Functional Domains of Wnts Through Expression of Wild-Type and Chimeric Proteins in Xenopus Embryos. Molecular and Cellular Biology *15*, 2625-2634.

Dubrulle, J., McGrew,M.J., and Pourquie,O. (2001). FGF signaling controls somite boundary position and regulates segmentation clock control of spatiotemporal Hox gene expression. Cell *106,* 219-232.

Endo,Y., Wolf,V., Muraiso,K., Kamijo,K., Soon,L., Uren,A., Barshishat-Kupper,M., and Rubin,J.S. (2005). Wnt-3a-dependent cell motility involves RhoA activation and is specifically regulated by dishevelled-2. Journal of Biological Chemistry *280*, 777-786.

Evrard,Y.A., Lun,Y., Aulehla,A., Gan,L., and Johnson,R.L. (1998). Lunatic fringe is an essential mediator of somite segmentation and patterning. Nature *394*, 377-381.

Fisher,D.A., Kivimae,S., Hoshino,J., Suriben,R., Martin,P.M., Baxter,N., and Cheyette,B.N.R. (2006). Three Dact gene family members are expressed during embryonic development and in the adult brains of mice. Developmental Dynamics *235*, 2620-2630.

Forsberg,H., Crozet,F., and Brown,N.A. (1998). Waves of mouse Lunatic fringe expression, in four-hour cycles at two-hour intervals, precede somite boundary formation. Curr. Biol. *8,* 1027-1030.

Fournier,A.E., Takizawa,B.T., and Strittmatter,S.M. (2003). Rho kinase inhibition enhances axonal regeneration in the injured CNS. Journal of Neuroscience *23*, 1416-1423.

Fradkin,L.G., Garriga,G., Salinas,P.C., Thomas,J.B., Yu,X., and Zou,Y.M. (2005). Wnt signaling in neural circuit development. Journal of Neuroscience *25*, 10376-10378.

Galceran,J., Farinas,I., Depew,M.J., Clevers,H., and Grosschedl,R. (1999). Wnt3a(-/-)-like phenotype and limb deficiency in Lef1(-/-)Tcf1(-/-) mice. Genes & Development *13*, 709-717.

Galceran,J., Hsu,S.C., and Grosschedl,R. (2001). Rescue of a Wnt mutation by an activated form of LEF-1: Regulation of maintenance but not initiation of Brachyury expression. Proceedings of the National Academy of Sciences of the United States of America *98*, 8668-8673.

Galceran,J., Sustmann,C., Hsu,S.C., Folberth,S., and Grosschedl,R. (2004). LEF1-mediated regulation of Delta-like1 links Wnt and Notch signaling in somitogenesis. Genes & Development *18*, 2718-2723.

Gillhouse,M., Nyholm,M.W., Hikasa,H., Sokol,S.Y., and Grinblat,Y. (2004). Two Frodo/Dapper homologs are expressed in the developing brain and mesoderm of zebrafish. Developmental Dynamics *230*, 403-409.

Gloy,J., Hikasa,H., and Sokol,S.Y. (2002). Frodo interacts with Dishevelled to transduce Wnt signals. Nature Cell Biology *4*, 351-357.

Goldman,D.C., Martin,G.R., and Tam,P.P.L. (2000). Fate and function of the ventral ectodermal ridge during mouse tail development. Development *127*, 2113-2123.

Greco,T.L., Takada,S., Newhouse,M.M., McMahon,T.A., McMahon,A.P., and Camper,S.A. (1996). Analysis of the vestigial tail mutation demonstrates that Wnt-3a gene dosage regulates mouse axial development. Genes & Development *10*, 313-324.

Greene,N.D.E., Gerrelli,D., Van Straaten,H.M.W., and Copp,A.J. Abnormalities of floor plate, notochord and somite differentiation in the loop-tail (Lp) mouse: a model of severe neural tube defects. Mechanisms of Development *73*, 59-72.

Gregorieff,A., Grosschedl,R., and Clevers,H. (2004). Hindgut defects and transformation of the gastrointestinal tract in Tcf4(-/-)/Tcf1(-/-) embryos. Embo Journal *23*, 1825-1833.

Hall,A.C., Lucas,F.R., and Salinas,P.C. (2000). Axonal remodeling and synaptic differentiation in the cerebellum is regulated by WNT-7a signaling. Cell *100*, 525-535.

Hamblet,N.S., Lijam,N., Ruiz-Lozano,P., Wang,J.B., Yang,Y.S., Luo,Z.G., Mei,L., Chien,K.R., Sussman,D.J., and Wynshaw-Boris,A. (2002). Dishevelled 2 is essential for cardiac outflow tract development, somite segmentation and neural tube closure. Development *129*, 5827-5838.

Heisenberg,C.P., Tada,M., Rauch,G.J., Saude,L., Concha,M.L., Geisler,R., Stemple,D.L., Smith,J.C., and Wilson,S.W. (2000). Silberblick/Wnt11 mediates convergent extension movements during zebrafish gastrulation. Nature *405*, 76-81.

Hendrickx,M. and Leyns,L. (2008). Non-conventional Frizzled ligands and Wnt receptors. Dev. Growth Differ. *50*, 229-243.

Herrmann,B.G., Labeit,S., Poustka,A., King,T.R., and Lehrach,H. (1990). Cloning of the T-Gene Required in Mesoderm Formation in the Mouse. Nature *343*, 617-622.

Hikasa,H., Shibata,M., Hiratani,I., and Taira,M. (2002). The Xenopus receptor tyrosine kinase Xror2 modulates morphogenetic movements of the axial mesoderm and neuroectoderm via Wnt signaling. Development *129*, 5227-5239.

Hikasa,H. and Sokol,S.Y. (2004). The involvement of Frodo in TCF-dependent signaling and neural tissue development. Development *131*, 4725-4734.

Hirabayashi,Y., Itoh,Y., Tabata,H., Nakajima,K., Akiyama,T., Masuyama,N., and Gotoh,Y. (2004). The Wnt/beta-catenin pathway directs neuronal differentiation of cortical neural precursor cells. Development *131*, 2791-2801.

Hofmann,M., Schuster-Gossler,K., Watabe-Rudolph,M., Aulehla,A., Herrmann,B.G., and Gossler,A. (2004). WNT signaling, in synergy with T/TBX6, controls Notch signaling by regulating Dll1 expression in the presomitic mesoderm of mouse embryos. Genes & Development *18*, 2712-2717.

Ishikawa,A., Kitajima,S., Takahashi,Y., Kokubo,H., Kanno,J., Inoue,T., and Saga,Y. (2004). Mouse Nkd1, a Wnt antagonist, exhibits oscillatory gene expression in the PSM under the control of Notch signaling. Mechanisms of Development *121*, 1443-1453.

Itoh,K., Brott,B., Ratcliffe,M., and Sokol,S. (2002). Nuclear localization of disheveled is required for Wnt/beta-catenin signal transduction. Developmental Biology *247*, 522.

Jho,E.H., Zhang,T., Domon,C., Joo,C.K., Freund,J.N., and Costantini,F. (2002). Wnt/beta-catenin/Tcf signaling induces the transcription of Axin2, a negative regulator of the signaling pathway. Molecular and Cellular Biology *22*, 1172-1183.

Jiang,X., Tan,J., Li,J., Kivimäe,S., Yang,.X., Zhuang,L., Lee,P.L., Chan,M.T., Stanton,L.W., Liu,E.T., Cheyette,B.N.R., and Yu,Q. (2008). DACT3 is an epigenetic regulator of Wnt/beta-catenin signaling in colorectal cancer and is a therapeutic target of histone modifications. Cancer Cell. *13(6),* 529-541.

Jin,Z. and Strittmatter,S.M. (1997). Rac1 mediates collapsin-1-induced growth cone collapse. J. Neurosci. *17*, 6256-6263.

Kallay,L.M., McNickle,A., Brennwald,P.J., Hubbard,A.L., and Braiterman,L.T. (2006). Scribble associates with two polarity proteins, Lgl2 and Vangl2, via distinct molecular domains. Journal of Cellular Biochemistry *99*, 647-664.

Keeble,T.R., Halford,M.M., Seaman,C., Kee,N., Macheda,M., Anderson,R.B., Stacker,S.A., and Cooper,H.M. (2006). The Wnt receptor Ryk is required for Wnt5a-mediated axon guidance on the contralateral side of the corpus callosum. Journal of Neuroscience *26*, 5840-5848.

Kelly,O.G., Pinson,K.I., and Skarnes,W.C. (2004). The Wnt co-receptors Lrp5 and Lrp6 are essential for gastrulation in mice. Development *131*, 2803-2815.

Kim,S., Park,J., Spring,C.M., Sater,A.K., Ji,H., Otchere,A.A., Daniel,J.M., and Mccrea,P.D. (2004). Non-canonical Wnt signals are modulated by the Kaiso transcriptional repressor and p120-catenin. Molecular Biology of the Cell *15*, 360A.

Klingensmith,J., Nusse,R., and Perrimon,N. (1994). The Drosophila Segment Polarity Gene Dishevelled Encodes A Novel Protein Required for Response to the Wingless Signal. Genes & Development *8*, 118-130.

Kokubu,C., Heinzmann,U., Kokubu,T., Sakai,N., Kubota,T., Kawai,M., Wahl,M.B., Galceran,J., Grosschedl,R., Ozono,K., and Imai,K. (2004). Skeletal defects in ringelschwanz mutant mice reveal that Lrp6 is required for proper somitogenesis and osteogenesis. Development *131*, 5469-5480.

Krylova,O., Herreros,J., Cleverley,K.E., Ehler,E., Henriquez,J.P., Hughes,S.M., and Salinas,P.C. (2002). WNT-3, expressed by motoneurons, regulates terminal arborization of neurotrophin-3-responsive spinal sensory neurons. Neuron *35*, 1043-1056.

Lawrence,P.A., Struhl,G., and Casal,J. (2007). Planar cell polarity: one or two pathways? Nature Reviews Genetics *8*, 555-563.

Lehmann,M., Fournier,A., Selles-Navarro,I., Dergham,P., Sebok,A., Leclerc,N., Tigyi,G., and McKerracher,L. (1999). Inactivation of Rho signaling pathway promotes CNS axon regeneration. Journal of Neuroscience *19*, 7537-7547.

Ligon,K.L., Echelard,Y., Assimacopoulos,S., Danielian,P.S., Kaing,S., Grove,E.A., McMahon,A.P., and Rowitch,D.H. (2003). Loss of Emx2 function leads to ectopic expression of Wnt1 in the developing telencephalon and cortical dysplasia. Development *130*, 2275-2287.

Liu,G.Z., Bafico,A., and Aaronson,S.A. (2005). The mechanism of endogenous receptor activation functionally distinguishes prototype canonical and noncanonical Wnts. Molecular and Cellular Biology *25*, 3475-3482.

Lu,X., Borchers,A.G., Jolicoeur,C., Rayburn,H., Baker,J.C., and Tessier-Lavigne,M. (2004). PTK7/CCK-4 is a novel regulator of planar cell polarity in vertebrates. Nature *430*, 93-98.

Lyuksyutova,A.I., Lu,C.C., Milanesio,N., King,L.A., Guo,N.N., Wang,Y.S., Nathans,J., Tessier-Lavigne,M., and Zou,Y.M. (2003). Anterior-posterior guidance of commissural Axons by Wnt-frizzled signaling. Science *302*, 1984-1988.

Macdonald,B.T., Semenov,M.V., and He,X. (2007). SnapShot: Wnt/beta-catenin signaling.
Cell *131(6),* 1204.

Maretto,S., Cordenonsi,M., Dupont,S., Braghetta,P., Broccoli,V., Hassan,A.B., Volpin,D., Bressan,G.M., and Piccolo,S. (2003). Mapping Wnt/beta-catenin signaling

during mouse development and in colorectal tumors. Proceedings of the National Academy of Sciences of the United States of America *100*, 3299-3304.

McMahon,A.P. and Bradley,A. (1990). The Wnt-1 (int-1) proto-oncogene is required for development of a large region of the mouse brain. Cell *62*, 1073-1085.

McMahon,A.P., Joyner,A.L., Bradley,A., and McMahon,J.A. (1992). The midbrain-hindbrain phenotype of Wnt-1-/Wnt-1- mice results from stepwise deletion of engrailed-expressing cells by 9.5 days postcoitum. Cell *69*, 581-595.

Mikels,A.J. and Nusse,R. (2006). Purified Wnt5a protein activates or inhibits β-catenin-TCF signaling depending on receptor context. PLoS Biology *4 (4),* 570-582.

Montcouquiol,M., Rachel,R.A., Lanford,P.J., Copeland,N.G., Jenkins,N.A., and Kelley,M.W. (2003). Identification of Vangl2 and Scrb1 as planar polarity genes in mammals. Nature *423*, 173-177.

Montcouquiol,M., Sans,N., Huss,D., Kach,J., Dickman,J.D., Forge,A., Rachel,R.A., Copeland,N.G., Jenkins,N.A., Bogani,D., Murdoch,J., Warchol,M.E., Wenthold,R.J., and Kelley,M.W. (2006). Asymmetric localization of Vangl2 and Fz3 indicate novel mechanisms for planar cell polarity in mammals. Journal of Neuroscience *26*, 5265-5275.

Moon,R.T., Kohn,A.D., De Ferrari,G.V., and Kaykas,A. (2004). WNT and beta-catenin signalling: Diseases and therapies. Nature Reviews Genetics *5*, 689-699.

Nakaya,M.A., Biris,K., Tsukiyama,T., Jaime,S., Rawls,J.A., and Yamaguchi,T.P. (2005). Wnt3a links left-right determination with segmentation and anteroposterior axis elongation. Development *132*, 5425-5436.

Nelson,W.J. and Nusse,R. (2004). Convergence of Wnt, beta-catenin, and cadherin pathways. Science *303*, 1483-1487.

Nusse,R. (2005). Wnt signaling in disease and in development. Cell Research *15*, 28-32.

Packard,M., Koo,E.S., Gorczyca,M., Sharpe,J., Cumberledge,S., and Budnik,V. (2002). The drosophila wnt, wingless, provides an essential signal for pre- and postsynaptic differentiation. Cell *111*, 319-330.

Panhuysen,M., Weisenhorn,D.M.V., Blanquet,V., Brodski,C., Heinzmann,U., Beisker,W., and Wurst,W. (2004). Effects of Wnt1 signaling on proliferation in the developing mid-/hindbrain region. Molecular and Cellular Neuroscience *26*, 101-111.

Park,J.I., Kim,S.W., Lyons,J.P., Ji,H., Nguyen,T.T., Cho,K.C., Barton,M.C., Deroo,T., Vleminckx,K., and McCrea,P.D. (2005). Kaiso/p120-catenin and TCF/beta-catenin complexes coordinately regulate canonical Wnt gene targets. Developmental Cell *8*, 843-854.

Park,J.I., Ji,H., Jun,S., Gu,D.M., Hikasa,H., Li,L., Sokol,S.Y., and McCrea,P.D. (2006). Frodo links dishevelled to the p120-catenin/Kaiso pathway: Distinct catenin subfamilies promote Wnt signals. Developmental Cell *11*, 683-695.

Park,M. and Moon,R.T. (2002). The planar cell-polarity gene stbm regulates cell behaviour and cell fate in vertebrate embryos. Nature Cell Biology *4*, 20-25.

Penzo-Mendez,A., Umbhauer,M., Djiane,A., Boucaut,J.C., and Riou,J.F. (2003). Activation of G beta gamma signaling downstream of Wnt-11/Xfz7 regulates Cdc42 activity during Xenopus gastrulation. Developmental Biology *257*, 302-314.

Pinson,K.I., Brennan,J., Monkley,S., Avery,B.J., and Skarnes,W.C. (2000). An LDL-receptor-related protein mediates Wnt signalling in mice. Nature *407*, 535-538.

Prokhortchouk,A., Sansom,O., Selfridge,J., Caballero,I.M., Salozhin,S., Aithozhina,D., Cerchietti,L., Meng,F.G., Augenlicht,L.H., Mariadason,J.M., Hendrich,B., Melnick,A., Prokhortchouk,E., Clarke,A., and Bird,A. (2006). Kaiso-deficient mice show resistance to intestinal cancer. Molecular and Cellular Biology *26*, 199-208.

Qian,D., Jones,C., Rzadzinska,A., Mark,S., Zhang,X.H., Steel,K.P., Dai,X., and Chen,P. (2007). Wnt5a functions in planar cell polarity regulation in mice. Developmental Biology *306*, 121-133.

Reynolds,A.B. and Roczniak-Ferguson,A. (2004). Emerging roles for p120-catenin in cell adhesion and cancer. Oncogene *23*, 7947-7956.

Rosso,S.B., Sussman,D., Wynshaw-Boris,A., and Salinas,P.C. (2005). Wnt signaling through Dishevelled, Rac and JNK regulates dendritic development. Nature Neuroscience *8*, 34-42.

Salinas,P.C. (2007). Modulation of the microtubule cytoskeleton: a role for a divergent canonical Wnt pathway. Trends in Cell Biology *17*, 333-342.

Satoh,W., Gotoh,T., Tsunematsu,Y., Aizawa,S., and Shimono,A. (2006). Sfrp1 and Sfrp2 regulate anteroposterior axis elongation and somite segmentation during mouse embryogenesis. Development *133*, 989-999.

Satoh,W., Matsuyama,M., Takemura,H., Aizawa,S., and Shimono,A. (2008). Sfrp1, Sfrp2, and Sfrp5 regulate the Wnt/beta-catenin and the planar cell polarity pathways during early trunk formation in mouse. Genesis *46*, 92-103.

Semenov,M.V., Habas,R., Macdonald,B.T., and He,X. (2007). SnapShot: Noncanonical Wnt Signaling Pathways. Cell *131(7),* 1378.

Seifert,J.R.K. and Mlodzik,M. (2007). Frizzled/PCP signalling: a conserved mechanism regulating cell polarity and directed motility. Nature Reviews Genetics *8*, 126-138.

Shitashige,M., Hirohashi,S., and Yamada,T. (2008). Wnt signaling inside the nucleus. Cancer Science *99*, 631-637.

Shum,A.S.W., Poon,L.L.M., Tang,W.W.T., Koide,T., Chan,B.W.H., Leung,Y.C.G., Shiroishi,T., and Copp,A.J. (1999). Retinoic acid induces down-regulation of Wnt-3a, apoptosis and diversion of tail bud cells to a neural fate in the mouse embryo. Mechanisms of Development *84*, 17-30.

Simons,M., Gloy,J., Ganner,A., Bullerkotte,A., Bashkurov,M., Kronig,C., Schermer,B., Benzing,T., Cabello,O.A., Jenny,A., Mlodzik,M., Polok,B., Driever,W., Obara,T., and Walz,G. (2005). Inversin, the gene product mutated in nephronophthisis type II, functions as a molecular switch between Wnt signaling pathways. Nature Genetics *37*, 537-543.

Strapps,W.R., and Tomlinson,A. (2001). Transducing properties of Drosophila Frizzled proteins. Development *128,* 4829-4835.

Suriben,R., Fisher,D.A., and Cheyette,B.N.R. (2006). Dact1 presomitic mesoderm expression oscillates in phase with Axin2 in the somitogenesis clock of mice. Developmental Dynamics *235*, 3177-3183.

Tada,M. and Smith,J.C. (2000). Xwnt11 is a target of Xenopus Brachyury: regulation of gastrulation movements via Dishevelled, but not through the canonical Wnt pathway. Development *127*, 2227-2238.

Takada,S., Stark,K.L., Shea,M.J., Vassileva,G., Mcmahon,J.A., and McMahon,A.P. (1994). Wnt-3A Regulates Somite and Tailbud Formation in the Mouse Embryo. Genes & Development *8*, 174-189.

Tissir,F., Bar,I., Jossin,Y., De Backer,O., and Goffinet,A.M. (2006). Protocadherin Celsr3 is crucial in axonal tract development (vol 8, pg 451, 2005). Nature Neuroscience *9*, 147.

Topol,L., Jiang,X.Y., Choi,H., Garrett-Beal,L., Carolan,P.J., and Yang,Y.Z. (2003). Wnt-5a inhibits the canonical Wnt pathway by promoting GSK-3-independent beta-catenin degradation. Journal of Cell Biology *162*, 899-908.

Torban,E., Kor,C., and Gros,P. (2004). Van Gogh-like2 (Strabismus) and its role in planar cell polarity and convergent extension in vertebrates. Trends in Genetics *20*, 570-577.

Torban,E., Wang,H.J., Groulx,N., and Gros,P. (2004). Independent mutations in mouse Vangl2 that cause neural tube defects in looptail mice impair interaction with members of the Dishevelled family. Journal of Biological Chemistry *279*, 52703-52713.

Torban,E., Wang,H.J., Patenaude,A.M., Riccomagno,M., Daniels,E., Epstein,D., and Gros,P. (2007). Tissue, cellular and sub-cellular localization of the Vangl2 protein during embryonic development: Effect of the Lp mutation. Gene Expression Patterns *7*, 346-354.

Torres,M.A., YangSnyder,J.A., Purcell,S.M., DeMarais,A.A., Mcgrew,L.L., and Moon,R.T. (1996). Activities of the Wnt-1 class of secreted signaling factors are antagonized by the Wnt-5A class and by a dominant negative cadherin in early Xenopus development. Journal of Cell Biology *133*, 1123-1137.

Tu,X.L., Joeng,K.S., Nakayama,K.I., Nakayama,K., Rajagopal,J., Carroll,T.J., McMahon,A.P., and Long,F.X. (2007). Noncanonical Wnt signaling through G protein-linked PKC delta activation promotes bone formation. Developmental Cell *12*, 113-127.

van Amerongen,R. and Berns,A. (2006). Knockout mouse models to study Wnt signal transduction. Trends Genet. *22*, 678-689.

Vasioukhin,V. (2006). Lethal giant puzzle of Lgl. Developmental Neuroscience *28*, 13-24.

Veeman,M.T., Axelrod,J.D., and Moon,R.T. (2003). A second canon: Functions and mechanisms of beta-catenin-independent wnt signaling. Developmental Cell *5*, 367-377.

Wahl,M.B., Deng,C., Lewandoski,M., and Pourquie,O. (2007). FGF signaling acts upstream of the NOTCH and WNT signaling pathways to control segmentation clock oscillations in mouse somitogenesis. Development *134*, 4033-4041.

Wallingford,J.B., Rowning,B.A., Vogeli,K.M., Rothbacher,U., Fraser,S.E., and Harland,R.M. (2000). Dishevelled controls cell polarity during Xenopus gastrulation. Nature *405*, 81-85.

Wallingford,J.B., Fraser,S.E., and Harland,R.M. (2002). Convergent extension: The molecular control of polarized cell movement during embryonic development. Developmental Cell *2*, 695-706.

Wallingford,J.B. and Habas,R. (2005). The developmental biology of Dishevelled: an enilgmatic protein governing cell fate and cell polarity. Development *132*, 4421-4436.

Wang,J.B., Hamblet,N.S., Mark,S., Dickinson,M.E., Brinkman,B.C., Segil,N., Fraser,S.E., Chen,P., Wallingford,J.B., and Wynshaw-Boris,A. (2006a). Dishevelled genes mediate a conserved mammalian PCP pathway to regulate convergent extension during neurulation. Development *133*, 1767-1778.

Wang,Y.H., Guo,N.N., and Nathans,J. (2006b). The role of frizzled3 and frizzled6 in neural tube closure and in the planar polarity of inner-ear sensory hair cells. Journal of Neuroscience *26*, 2147-2156.

Waxman,J.S., Hocking,A.M., Stoick,C.L., and Moon,R.T. (2004). Zebrafish Dapper1 and Dapper2 play distinct roles in Wnt-mediated developmental processes. Development *131*, 5909-5921.

White,J.G., Southgate,E., Thomson,J.N., and Brenner,S. (1986). The Structure of the Nervous-System of the Nematode Caenorhabditis-Elegans (The Mind of a Worm). Philosophical Transactions of the Royal Society of London Series B-Biological Sciences *314*, 1-340.

Wilkinson,D.G., Bhatt,S., and Herrmann,B.G. (1990). Expression Pattern of the Mouse T-Gene and Its Role in Mesoderm Formation. Nature *343*, 657-659.

Wittler,L., Shin,E.H., Grote,P., Kispert,A., Beckers,A., Gossler,A., Werber,M., and Herrmann,B.G. (2007). Expression of Msgn1 in the presomitic mesoderm is controlled by synergism of WNT signalling and Tbx6. Embo Reports *8*, 784-789.

Wong,H.C., Bourdelas,A., Krauss,A., Lee,H.J., Shao,Y.M., Wu,D.Q., Mlodzik,M., Shi,D.L., and Zheng,J. (2003). Direct binding of the PDZ domain of Dishevelled to a conserved internal sequence in the C-terminal region of frizzled. Molecular Cell *12*, 1251-1260.

Wu,X.M., Tu,X.L., Joeng,K.S., Hilton,M.J., Williams,D.A., and Long,F.X. (2008). Rac1 activation controls nuclear localization of beta-catenin during canonical Wnt signaling. Cell *133*, 340-353.

Xu,X.M., Fisher,D.A., Zhou,L.J., White,F.A., Ng,S., Snider,W.D., and Luo,Y.L. (2000). The transmembrane protein semaphorin 6A repels embryonic sympathetic axons. Journal of Neuroscience *20*, 2638-2648.

Yamaguchi,T.P., Bradley,A., McMahon,A.P., and Jones,S. (1999a). A Wnt5a pathway underlies outgrowth of multiple structures in the vertebrate embryo. Development *126*, 1211-1223.

Yamaguchi,T.P., Takada,S., Yoshikawa,Y., Wu,N.Y., and McMahon,A.P. (1999b). T (Brachyury) is a direct target of Wnt3a during paraxial mesoderm specification. Genes & Development *13*, 3185-3190.

Ybot-Gonzalez,P., Savery,D., Gerrelli,D., Signore,M., Mitchell,C.E., Faux,C.H., Greene,N.D.E., and Copp,A.J. (2007). Convergent extension, planar-cell-polarity signalling and initiation of mouse neural tube closure. Development *134*, 789-799.

Yoon,J.K., Moon,R.T., and Wold,B. (2000). The bHLH class protein pMesogenin1 can specify paraxial mesoderm phenotypes. Developmental Biology *222*, 376-391.

Yoon,J.K. and Wold,B. (2000). The bHLH regulator pMesogenin1 is required for maturation and segmentation of paraxial mesoderm. Genes & Development *14*, 3204-3214.

Yoshikawa,Y., Fujimori,T., McMahon,A.P., and Takada,S. (1997). Evidence that absence of Wnt-3a signaling promotes neuralization instead of paraxial mesoderm development in the mouse. Developmental Biology *183*, 234-242.

Yu,H.M.I., Jerchow,B., Sheu,T.J., Liu,B., Costantini,F., Puzas,J.E., Birchmeier,W., and Hsu,W. (2005). The role of Axin2 in calvarial morphogenesis and craniosynostosis. Development *132*, 1995-2005.

Zakany,J., Kmita,M., Alarcon,P., de la Pompa,J.L., and Duboule,D. (2001). Localized and transient transcription of Hox genes suggests a link between patterning and the segmentation clock. Cell *106*, 207-217.

Zechner,D., Fujita,Y., Hulsken,J., Muller,T., Walther,I., Taketo,M.M., Crenshaw,E.B., Birchmeier,W., and Birchmeier,C. (2003). beta-catenin signals regulate cell growth and the balance between progenitor cell expansion and differentiation in the nervous system. Developmental Biology *258*, 406-418.

Zeng,X., Tamai,K., Doble,B., Li,S.T., Huang,H., Habas,R., Okamura,H., Woodgett,J., and He,X. (2005). A dual-kinase mechanism for Wnt co-receptor phosphorylation and activation. Nature *438*, 873-877.

Zeng,X., Huang,H., Tamai,K., Zhang,X.J., Harada,Y., Yokota,C., Almeida,K., Wang,J., Doble,B., Woodgett,J., Wynshaw-Boris,A., Hsieh,J.C., and He,X. (2008). Initiation of Wnt signaling: control of Wnt coreceptor Lrp6 phosphorylation/activation via frizzled, dishevelled and axin functions. Development *135*, 367-375.

Zhang,L., Gao,X., Wen,J., Ning,Y.H., and Chen,Y.G. (2006). Dapper 1 antagonizes Wnt signaling by promoting dishevelled degradation. Journal of Biological Chemistry *281*, 8607-8612.

Zhang,L.X., Zhou,H., Su,Y., Sun,Z.H., Zhang,H.W., Zhang,L., Zhang,Y., Ning,Y.H., Chen,Y.G., and Meng,A.M. (2004). Zebrafish Dpr2 inhibits mesoderm induction by promoting degradation of nodal receptors. Science *306*, 114-117.

Zhang,N.A. and Gridley,T. (1998). Defects in somite formation in lunatic fringe deficient mice. Nature *394*, 374-377.

Zhang,S., Cagatay,T., Amanai,M., Zhang,M., Kline,J., Castrillon,D.H., Ashfaq,R., Oz,O.K., and Wharton,K.A. (2007). Viable mice with compound mutations in the Wnt/Dvl pathway antagonists nkd1 and nkd2. Molecular and Cellular Biology *27*, 4454-4464.

Zhou,C.J., Borello,U., Rubenstein,J.L.R., and Pleasure,S.J. (2006). Neuronal production and precursor proliferation defects in the neocortex of mice with loss of function in the canonical Wnt signaling pathway. Neuroscience *142*, 1119-1131.

Chapter 2:

Characterization of the *Dact* Gene Family in Mouse Development.

Chapter 2:

This chapter includes the published manuscript, *Three Dact Gene Family Members are Expressed During Embryonic Development and in the Adult Brains of Mice,* by Daniel A. Fisher, Saul Kivimäe, Jun Hoshino, Rowena Suriben, Pierre-Marie Martin, Nichol Baxter, and Benjamin N.R. Cheyette. This was published in Developmental Dynamics as Fisher et al., 2006 *Dev. Dynamics 235*, 2620-2630. I have included all supplemental data along with the full publication, and also four figures of additional data, with legends, that are not part of the publication. My contribution to this chapter consists of the design for probe constructs for mouse *Dact1, Dact2, and Dact3*, and in situ hybridizations using these probes, at all ages of mouse development described. Other contributions were work of the other authors. Some of the published in situ hybridization images were the work of N. Baxter under my supervision. All work was carried out in the laboratory of Benjamin Cheyette. The data in the four Additional Data figures are entirely my own.

Three Dact Gene Family Members are Expressed During Embryonic Development and in the Adult Brains of Mice

Daniel A Fisher, Saul Kivimäe, Jun Hoshino, Rowena Suriben, Pierre-Marie Martin, Nichol Baxter, Benjamin NR Cheyette

Department of Psychiatry & Graduate Programs in Developmental Biology and Neuroscience, University of California, San Francisco, 94143-2611

Correspondence:

Benjamin NR Cheyette

bc@lppi.ucsf.edu

415.476.7826

Running Title: Mouse Dact Gene Family Expression

Key Words: mouse, Dpr, Frodo, Thyex, Dact, Wnt, Dvl, expression, embryo, brain

Supported by:

NIH: MH01750 K08; NARSAD Young Investigator Award; NAAR award #551.

Abstract

Members of the Dact protein family were initially identified through binding to Dishevelled (Dvl), a cytoplasmic protein central to Wnt signaling. During mouse development, *Dact1* is detected in the presomitic mesoderm and somites during segmentation, in the limb bud mesenchyme and other mesoderm-derived tissues, and in the central nervous system (CNS). *Dact2* expression is most prominent during organogenesis of the thymus, kidneys, and salivary glands, with much lower levels in the somites and in the developing CNS. *Dact3*, not previously described in any organism, is expressed in the ventral region of maturing somites, limb bud and branchial arch mesenchyme, and in the embryonic CNS; of the three paralogs it is the most highly expressed in the adult cerebral cortex. These data are consistent with studies in other vertebrates showing that *Dact* paralogs have distinct signaling and developmental roles, and suggest they may differentially contribute to postnatal brain physiology.

Introduction

Signaling downstream of secreted Wnt ligands is a conserved process in multicellular animals that plays important roles during development and, when misregulated, contributes to cancer and other diseases (Polakis, 2000; Moon et al., 2002). In mammals many Wnt signaling components are expressed in the postnatal brain, where manipulations of their activity can lead to effects on behavior (Madsen et al., 2003; Beaulieu et al., 2004; Kaidanovich-Beilin et al., 2004; O'Brien et al., 2004; Shimogori et al., 2004). Although more than one molecular cascade has been identified downstream of Wnt receptors, all such cascades involve a cytoplasmic scaffold protein called Dishevelled (Dvl in mammals) (Veeman et al., 2003; Wharton, Jr., 2003). Because of its central role in Wnt signal transduction, efforts have been made to identify the direct binding partners of Dvl. One such protein, which binds to the Dvl PDZ domain via a conserved C-terminal PDZ-binding motif (Cheyette et al., 2002), has alternately been named Dapper (Dpr), Frodo/Frd, THYEX3, HNG3, MTNG3, and Dact in various organisms (Cheyette et al., 2002; Gloy et al., 2002; Gillhouse et al., 2004; Yau et al., 2004; Zhang et al., 2004; Hunter et al., 2005; Katoh, 2005). For simplicity, hereafter we use the symbol "*Dact"* assigned by the Human Genome Organization Nomenclature Committee and the Mouse Genome Informatics website for all members of this gene family. Interestingly, despite the importance of Wnt signaling during invertebrate development, we have been unable to identify *Dact* orthologs in the completely sequenced genomes of the invertebrates *Drosophila melanogaster* and *Caenorhabditis elegans,* nor in that of the simple chordate, *Ciona intestinalis* (data not shown).

The function of Dact proteins in signal regulation remains ambiguous, with some studies indicating they act positively in Wnt signal transduction (Gloy et al., 2002; Waxman et al., 2004), and others indicating an inhibitory function (Cheyette et al., 2002; Wong et al., 2003; Yau et al., 2004; Brott and Sokol, 2005a; Zhang et al., 2006). Previous research in zebrafish has shown that two members of the Dact family have distinct effects on Wnt signaling, with Dact1 having a greater impact on ß-catenin-dependent signaling, and Dact2 having a greater impact on a ß-catenin-independent process called planar cell polarity/convergent-extension signaling (Waxman et al., 2004). Furthermore, in zebrafish and when overexpressed in mammalian cells, Dact2 but not Dact1 can inhibit Nodal signaling by promoting the endocytic degradation of Type I TGFß receptors (Zhang et al., 2004). Taken together, the evidence suggests that different Dact paralogs have distinct signaling activities, and that even a single Dact protein may have more than one role that can vary under changing cellular conditions (Hikasa and Sokol, 2004; Brott and Sokol, 2005b).

Because of this gene family's manifold yet conserved functions in vertebrate signal transduction, we have cloned cDNAs corresponding to the full-length coding regions of all three mouse *Dact* homologs, and have characterized their developmental and adult expression patterns.

Results and Discussion

Identification of a Three-Member *Dact* Gene Family

Using the previously described *Dact* sequences from frogs and fish, we scanned the mouse genome and expressed sequence tag (EST) databases for similar sequences,

and then cloned full-length cDNAs by RT-PCR (Fig. 1A). Based on sequence similarity, *Dact1,* which maps to mouse chromosome 12D1, is the closest mammalian homolog to the *Dpr* and *Frodo* sequences identified in *Xenopus*, and corresponds to the mammalian *Dpr1* and *Frd1* genes reported in the literature (Cheyette et al., 2002; Katoh and Katoh, 2003; Yau et al., 2004; Zhang et al., 2004; Brott and Sokol, 2005; Hunter et al., 2005). *Dact2*, which is most closely related to the *frd2*/*dpr2* sequences identified in zebrafish (Gillhouse et al., 2004; Waxman et al., 2004), maps to mouse chromosome 17A2. *Dact3*, which has not previously been described, maps to mouse chromosome 7A2.

Dact3 is a bone fide member of the *Dact* gene family (Fig.1A-C). Upon alignment at the amino acid sequence level, mouse Dact3 is approximately 27% similar to Dact1 and 24% similar to Dact2 (compared to 26% similarity between Dact1 and Dact2, Fig. 1B). In and around a conserved leucine zipper domain, Dact1 and Dact2 are more closely similar to each other than to Dact3. However, at the C-terminus Dact1 and Dact3 are more closely related (compare PDZ-binding domains in Fig. 1A).

The predicted amino acid sequence for the Dact3 protein is approximately 20% shorter than either Dact1 or Dact2 (610 amino acids for Dact3 *vs*. 778 amino acids for Dact1 and 757 amino acids for Dact2). There is an open reading frame that continues upstream to an ATG located at position -156 in the genomic locus of *Dact3*, which if transcribed and translated could therefore theoretically add 52 amino acids to the amino terminus of the Dact3 polypeptide. We have excluded this upstream sequence as a part of the *Dact3* transcript produced in newborn forebrain by using 5' RACE to determine the start of transcription (see Methods for details). A highly conserved ortholog of *Dact3* is identifiable in the human genome and EST databases. The human *DACT3* gene maps to

chromosome 19q13.32 and is predicted to encode a protein 85% identical to mouse Dact3 (Fig. 1C, Supplemental Fig. S1). A similar *Dact3* gene distinct from *Dact1* and *Dact2* is also identifiable in the zebrafish and pufferfish genomic and EST public sequence databases (data not shown).

The 5' region of each of the mouse *Dact* genes is extremely GC-rich, and the intron-exon structure is also conserved, consisting of three small 5' coding exons which together encode a short 5' UTR and the amino-terminus of the polypeptide, and a larger fourth exon containing approximately 2/3 of the translated sequence plus a longer 3' UTR (data not shown). To summarize, we have identified three paralogous *Dact* genes in mouse, one of which (*Dact3*) is entirely novel. Overall homology relationships between the principal members of the proposed *Dact* gene family are diagrammed schematically in Fig. 1C.

Developmental and Tissue-Specific Expression

Using Northern blots we have profiled the expression of each *Dact* gene across embryonic stages and adult tissues. This has been complemented by Quantitative PCR (Q-PCR) to more accurately compare relative mRNA levels between the three genes. Over the course of embryogenesis, the *Dact* genes have quite different temporal patterns of expression. From embryonic day (E) 4.5-8.5 there is only weak expression of these genes, some of which may occur in maternal and extra-embryonic tissues (Fig. 1D). In the embryo proper, *Dact1* expression increases dramatically from E9.5-10.5, peaks between E11.5-13.5, then diminishes slowly thereafter. In contrast, *Dact2* expression is very low overall for most of embryogenesis (Fig. 1D middle blot). *Dact3* expression is

initially low, peaks at E10.5, then declines again (Fig. 1D bottom blot). Because both *Dact1* and *Dact3* levels decline while *Dact2* remains relatively constant overall, all three genes are expressed at roughly comparable levels at E18.5, three days prior to birth (Fig. 1D, G).

Using similar methodology, the three *Dact* genes show quite different adult tissue expression patterns. In the adult, *Dact1* is present primarily in the brain, lung, and uterus, with significantly weaker expression in other tissues (Fig. 1E). *Dact2* is present in the brain and uterus, but is also quite notable in the kidneys, small intestines, thymus, and testes (Fig. 1E, H, I). The adult distribution of *Dact3* is most restricted: it is present in the uterus (Fig. 1E, I), and is the principally-expressed Dact family member in the adult brain (Fig. 1E, H).

In summary, the three *Dact* genes are broadly expressed during mouse embryogenesis and in adult tissues, and yet have distinct temporal and tissue-specific signatures. This is consistent with these molecules playing separable roles during development and in adult tissue physiology. To further clarify these differences, we have performed mRNA in situ hybridization analysis in whole mounts (WISH) and sections (ISH) during embryonic development and in the adult brain.

Embryonic Expression of the *Dact* gene family through Segmentation Stages

As expression of all three family members is low at early embryonic stages, and as the expression of *Dact1* has been described up to E8.5-9, we have focused our attention primarily on later developmental stages. Consistent with a prior report (Hunter et al., 2005), at E7.5 our *Dact1*-specific probe detects expression primarily in the

mesoderm and at very low levels in the neurectoderm (Dr. Uta Grieshammer and BNRC, data not shown). In the E9.0 embryo, *Dact1* expression is highest in the septum transversum, cranial mesenchyme, the caudal presomitic mesoderm (PSM), and in the somites that derive from it (Hunter et al., 2005), as well as in the wall of Rathke's pouch, the dorsal aorta, the aortic sac, and the branchial arch arteries (Fig. 2A). Within the PSM, a band of low *Dact1* is apparent between high expressing zones in the caudal PSM and the newly forming somite at the rostral edge (Fig. 2A). *Dact1* exhibits a strong caudal to rostral gradient that inversely correlates with the developmental age of somites: highest expression in the most recently formed (*i.e.* caudal) somite, and diminishing expression in more mature (*i.e.* rostral) somites. Within individual somites *Dact1* shows a progressively restricted spatial pattern. In younger (caudal) somites, *Dact1* is preferentially expressed ventromedially along the rostral-caudal extent and along both the rostral and caudal somite walls (Fig. 2A, I). As the somite matures, *Dact1* expression decreases rostrally, such that its localization becomes progressively restricted to the ventromedial and caudal domains (Fig. 2A inset). By section ISH, *Dact1* expression is also prominent in the nephrogenic cords, the ventral mesentery and the mesenchymal outer walls of the foregut, the dorsal aorta, and its main branches (Fig. 2G).

Dact2 is detectable only at very low levels in the E9.0 embryo by mRNA in situ techniques (Fig. 2B), though it is fairly widely distributed. At this stage, low *Dact2* expression is appreciable in the retina, otic vesicle, ventral mesentery of the foregut, the umbilical veins, dorsal neural tube, and in a gradient in the somites with highest levels in the caudal (youngest) somites much like *Dact1* (Figure 2B and insets). Unlike *Dact1*, *Dact2* is not detected within the caudal PSM at this stage (Fig. 2B). Compared to *Dact1*,

Dact2 also shows a significantly different domain of expression within each somite. Whereas *Dact1* is most highly expressed ventromedially, *Dact2* is more highly expressed dorsolaterally. Furthermore, unlike *Dact1* which becomes more *caudally* restricted, *Dact2* becomes progressively more *rostrally* restricted (Fig. 2B left inset). As a consequence, the two paralogs occupy complementary intrasomitic distributions as somites mature.

At E9.0, *Dact3* mRNA is found in a tissue distribution distinct from the other two *Dact* genes (Fig. 2C). Like *Dact1*, *Dact3* is expressed in craniofacial mesenchyme, but it is more prominent in the branchial arch mesenchyme, the aortic sac, and the aortic arches (Fig. 2C, P) where *Dact1* expression is comparatively lower. Also different from *Dact1*, *Dact3* is not expressed in the PSM, nor is it present in a caudal-rostral gradient among developing somites like both *Dact1* and *Dact2*. Instead, *Dact3* is expressed in the ventral domain of more mature somites, located centrally along the rostral-caudal axis (Fig. 2C, Q).

At E10.5, high *Dact1* expression continues in the PSM and caudal somites (Fig. 2D, L, compare to 2A). *Dact1* is also present at low levels in other tailbud tissues, such as the ventral mesoderm of the tail bud (Fig. 2D). More anteriorly, *Dact1* at this stage is present in the forelimb and hindlimb buds, where it is expressed in mesoderm in a proximal (low)-apical (high) gradient (Fig. 2D, J). It continues to be expressed significantly in mesenchyme surrounding foregut derivatives such as the left and right main bronchi, as well as in the sclerotome derived from the ventral somite (Fig. 2J), but comparatively is only weakly detectable in the branchial arch mesenchyme (data not

shown). At this stage, it first starts to be expressed in post-mitotic neurons, chiefly evident in the differentiating motor pools of the ventral spinal cord (Fig. 2J).

Consistent with the Northern and Q-PCR data, at E10.5 *Dact2* is only weakly detectable by mRNA in situ hybridization and appears to be more restricted in its tissue distribution than at E9.0. The main loci of expression at this time are in the otic vesicle and in the caudal-most somites where the strongest signal is in the most-recently formed somite and a diminishing signal is in the next two youngest somites (Fig. 2E, inset E). In contrast, *Dact3* at this stage is very prominent throughout the branchial arch mesenchyme, limb bud mesenchyme, as well as continued expression in maturing somites (Fig. 2F, Q, R, S).

Taken together, the expression of *Dact* family members at embryonic stages through E10.5 suggests overlapping roles especially during mesoderm and neural crest development. At E9.0, *Dact1* and *Dact3* overlap in the facial mesoderm and septum transversum, where they may play either complementary or redundant roles. The exclusive expression of *Dact1* in the PSM suggests a more unique function in that tissue during segmentation. The robust expression of *Dact3* in the branchial arches, facial mesenchyme, and ventral somites is consistent with this gene being important in the migration or differentiation of neural crest cells and of mesoderm-derived mesenchyme. The expression pattern of *Dact1* at early stages has been proposed to indicate a role in mesenchymal to epithelial transitions (Hunter et al., 2005). A comprehensive view based on the embryonic expression patterns of all three *Dact* genes suggests involvement in a subset of signaling events, including those that control morphogenesis but extending to the regulation of cellular differentiation and tissue patterning.

The distinct domains of *Dact* gene expression within developing somites correlate with domains of signaling activity that pattern this tissue. Sonic hedgehog (Shh) secreted from the notochord and floor plate is an important ventromedial somite patterning signal, whereas TGFßs and Wnts play a similar role dorsolaterally (Lee et al., 2000; Christ et al., 2004). Given that *Dact1* and *Dact3* are primarily restricted to the ventromedial domain, and that *Dact2* is concentrated dorsally and laterally, these signaling cascades could differentially regulate *Dact* expression. Simultaneously, based on their known functions Dact proteins are likely to be involved in the intracellular modulation of the signaling cascades that pattern these tissues. The ventromedial expression of *Dact1* and *Dact3* is consistent with a role in signaling within the presumptive sclerotome, which produces the cartilage and vertebral bodies making up the axial skeleton (Christ et al., 2004). The complementary expression of *Dact2* dorsolaterally is consistent with a signaling role in the presumptive dermomyotome, which at later stages gives rise to the dermis as well as the deep back and intercostal musculature (Borycki et al., 1999; Wagner et al., 2000).

Prenatal Expression of Dact genes in the Developing Central Nervous System

After E10.5, expression of *Dact1* and *Dact3* becomes concentrated in the developing CNS. In situ hybridization of sagittally-sectioned embryos at E14.5 shows that *Dact1* and *Dact3* RNA are broadly expressed in the brain and spinal cord, (Fig. 3A, C). By contrast, *Dact2*, although also expressed in the developing CNS, is clearly present at higher levels in several non-neuronal tissues, particularly the developing kidneys, salivary glands, and thymus (Fig. 3B, K-N).

In the developing brain, *Dact1* is expressed in some progenitor zones. In the ventricular zone of the cerebral cortex at E14.5, it is expressed in a ventral (high)-dorsal (low) gradient (Fig. 3D). There is high expression in the ventricular zone of the basal ganglia anlagen (lateral and medial ganglionic eminences) (Fig. 3D); here, *Dact1* expression labels radially aligned clusters of cells (Fig. 3D, G). *Dact1* also shows differential regional expression in postmitotic neurons. For instance, within the cerebral cortex (Fig. 3D), *Dact1* is expressed in the cortical plate in a rostroventral (low)-caudodorsal (high) gradient, which is complementary to the gradient in the underlying ventricular zone. *Dact3* is also concentrated in the cortical plate zone at this stage (Fig. 3F). By contrast, using a carefully-validated probe to avoid cross-detection of the two more heavily expressed paralogs (see Methods), *Dact2* message is detectable only very weakly in either the proliferative zones or post-mitotic domains of the forebrain (Fig. 3E).

Since *Dact1* is regionally expressed in the CNS at this stage of development, we have conducted a more thorough analysis of its distribution in developing nervous tissue. At the level of the developing midbrain (Fig. 3H), *Dact1* message is notable dorsally in the tectum, in postmitotic neurons of the ventral midbrain, as well as in some nuclei of the developing hypothalamus. Moving more caudally within the CNS, *Dact1* is also found in cerebellar precursors near the midbrain-hindbrain junction, as well as in the rhombic lip region and in the pons (Fig. 3A, I). In the spinal cord, *Dact1* is detected in primary sensory neurons of the developing dorsal horns, and in neurons of the motor pools located ventrally (Fig. 3J).

Postnatal Expression of the *Dact* genes in the Central Nervous System

In sharp contrast to the embryonic period, *Dact1* is the most weakly expressed of the gene family in the adult brain (*cf.* Fig. 1E, H). Nonetheless, *Dact1* message can be detected in many postnatal neuronal populations, and it is differentially expressed in neuronal sub-types (Fig. 3O). For example in the adult cerebellum, although *Dact1* is present at relatively high levels in the granule cell layer, it is not detectable in most Purkinje cells (Fig. 3O, inset). This pattern of expression in the adult cerebellum is complementary to *Dact2* and *Dact3*, both of which are detected more strongly in the Purkinje cell layer (Fig. 3P, Q insets). Elsewhere in the brain, all three *Dact* genes are co-expressed in the hippocampus. In the dorsal forebrain *Dact1* and *Dact3* are expressed throughout all layers of the cerebral cortex, *Dact2* is preferentially expressed in more superficial layers (Fig. 3P, compare to Fig. 3O, Q). Given prior studies showing that changes in Wnt signaling components can alter complex behaviors (Madsen et al., 2003; Beaulieu et al., 2004; Long et al., 2004; Kaidanovich-Beilin et al., 2004; O'Brien et al., 2004), the regional adult brain expression patterns of *Dact* family members suggest different roles in brain function.

Implications for signaling

Sequence similarities and differences among the three mouse *Dact* genes, together with prior studies focused on *Dact1* and *Dact2* in other organisms (Waxman et al., 2004; Zhang et al., 2004; Zhang et al., 2006), suggest that each *Dact* paralog has both conserved and divergent functions in signal transduction. The tissue distribution of the three murine genes during embryogenesis is consistent with roles in a subset of

developmental events downstream of Wnt signaling, as well as perhaps in other types of signaling as has been suggested for *Dact2* in modulating TGFß receptors (Zhang et al., 2004). The postnatal expression of the mouse *Dact* genes points to important functions in several adult organs including the CNS, uterus, testes, thymus, and kidneys. Ongoing work in our lab will explore the molecular and cellular roles of these signal scaffold molecules during development, and especially in the postnatal CNS.

Methods

5' RACE to determine transcriptional start of *Dact3*.

5'RACE was carried out using an RNA ligation-mediated protocol to ensure capture of the 5'end of the mRNA. FirstChoice RLM-RACE kit (Ambion, Austin TX) was used according to the manufacturer's protocol with the addition of Thermo-X RT polymerase (Invitrogen, Carlsbad, CA). The RT reaction was performed at 62ºC for 2 h with reverse primer: 5'CAGGCGTCCATAGGAGCCAGATCCGGAG3' on total RNA extracted from mouse strain C57Bl/6 neonatal forebrain. Dissected brain was frozen on dry ice and RNA isolated with RNeasy kit (Invitrogen) using the manufacturer's animal tissue protocol. RT products were amplified with the 5'RACE outer primer provided by the manufacturer and gene-specific reverse primer: 5'GTGGTGAATCTGGGCCTCCAGTAGAACTG3' using Pfx DNA polymerase (Invitrogen, Carlsbad, CA). Purified PCR products were treated with Taq polymerase in the presence of 2mM dATP and cloned into pCR-4 TOPO vector (Invitrogen Carlsbad, CA). 12 RACE clones were sequenced to determine the mRNA start site. Relative to the

proposed translational start, the distribution of transcriptional start sites was: 1 clone of each: positions –120, -111, -104, -77, -47, +11; 2 clones of each: -115, -110, -56.

Consistent with the proposed translational start site for *Dact3* based on 5'RACE, the sequence surrounding this codon corresponds to the Kozak consensus site (Kozak, 1987) at 8 out of 10 residues (gccgcagccATGa). This methionine is also conserved in the predicted sequence of human *DACT3*, and aligns well with the starts of the two other Dact family members (Fig. 1A).

Cloning of Mouse *Dact* Genes

The cloning of mouse *Dact1* (*Dpr1*) has previously been described (Cheyette et al., 2002). The full-length clones of mouse *Dact2* and *Dact3* were obtained by RT-PCR from adult cerebral cortex and neonatal forebrain respectively (see above for mRNA extraction). RT reactions were performed using Thermoscript (*Dact2*) and Thermo-X RT (*Dact3*) polymerases (Invitrogen, Carlsbad, CA) according to the manufacturer's instructions for GC-rich templates, and the following gene-specific primers:

gene	RT primer
Dact2	5'AGCGCAATAGCAAGGTTGATAC3'
Dact3	5'ATTAACTGCAGTGAAGTTCAAGCCCATCCCGCCCCAAC3'

RT product was amplified by PCR with Pfu (Stratagene, La Jolla, CA) and Pfx (Invitrogen, Carlsbad, CA) polymerases for *Dact2* and *Dact3* respectively, using a forward primer specific for the 5'UTR of each gene and a reverse primer specific for the 3'UTR internal to the first-strand synthesis primer. Amplified cDNAs were isolated and subcloned using standard molecular biology techniques, and confirmed by sequencing with both vector-based and gene-specific primers.

Accession Numbers and Sequence Comparisons

The GenBank accession number for mouse *Dact1* (*Dpr1*) has previously been reported (Cheyette et al., 2002) and is AF488775. For the mouse *Dact2* (*Dpr2*) and *Dact3* sequences whose cloning is described here, accession numbers are AY297430 and DQ832319 respectively. Chromosomal positions were determined using the June 2006 update of the Ensembl Genome Browser (v 39).

Protein sequences were compared with VectorNTI Advance v. 9.1 (Invitrogen, Carlsbad, CA) AlignX software using an amino acid identity matrix. In the phylogenetic tree shown (Fig. 1C), distance from a node along the horizontal axis indicates sequence divergence. Distance from a node along the vertical axis is arbitrary and has been manually enhanced to emphasize family subgroupings (*i.e. Dact1 vs. Dact2 vs. Dact3* subfamilies).

Northern Blotting

DNA probes were labeled by incorporation of ^{32}P-labeled dCTP. Mouse embryonic multi-stage and postnatal multi-tissue Northern blots (Seegene, Seoul S. Korea) containing 20 μg total RNA per lane were hybridized according to the manufacturer's instructions and the following stringencies and times: hybridization overnight at 55^{O}C in Ultrahyb buffer (Ambion, Austin TX), wash 3 X 15 minutes in 0.2x SSC, 0.5% SDS at 60 ^{O}C. Exposure to film was overnight (15 hours) at -80 ^{O}C with two intensification screens. Two different probes were used to validate each gene pattern, and a pair of fresh blots (1 embryonic and 1 adult multi-tissue) was used for the initial

characterization of each gene. Probes used for data shown (numbers relative to translational start): *Dact1* 613-1377; *Dact2* 586-1769; *Dact3* 853-1673.

Quantitative Reverse-Transcriptase PCR (Q-PCR)

For preparation of template, 2 μg total RNA was isolated from the experimental tissue indicated, taken from CD1 outbred mice (Charles River Laboratories, Wilmington MA), DNaseI-treated (Roche, Indianapolis IN), and reverse-transcribed (25°C x 10 min, 42°C x 50 min, 72°C x 10 min) using random primers and Superscript II (Invitrogen, Carlsbad, CA). Q-PCR primers for *Dact1*, *Dact2*, and *Dact3* have been designed using PrimerExpress (Applied Biosystems, Foster City, CA) and validated to ensure: 1) amplification of a single product and 2) appropriate efficiency of amplification. The linear plot of cycle number determined at threshold (C_T) *vs*. cDNA concentration (log ng) gives a linear slope of -3.3±0.1 for the housekeeping gene (mouse cyclophilin) and for *Dact1, Dact2*, and *Dact3*. Furthermore, a no-template control was conducted in each trial to ensure that the primers did not dimerize, and that amplified DNA is not the result of contamination. Steady-state mRNA was measured using an ABI 7300 quantitative real time PCR thermal cycler and standard conditions [1 cycle x (2 min @ 50°C, 10 min @ 95°C), then 40 cycles x (15 sec @ 95°C, 1 min @ 60°C)]. Sybr green (Applied Biosystems, Foster City, CA) was utilized to detect the PCR product in real-time, and a standard dissociation curve was generated. Mouse cyclophilin (NM 011149) was employed as an internal control for standardizing the measurements between reactions. Experimental PCR products were subcloned and sequenced to verify their identity. Data from each experiment (n=3 for 2 independent tissue samples in each case) was calculated

using the ΔΔCt method (Livak and Schmittgen, 2001). The following primer pairs were used:

gene	*forward*	*reverse*
Cyclophilin	5'TGGAGAGCACCAAGACAGACA3'	5'TGCCGGAGTCGACAATGAT3'
Dact1	5'TCAGGGTTTTATGAGCTGAGT3'	5'GAACACGGAGTTGGAGGAGTTA3'
Dact2	5'GGCTGACGGGCATGTTC3'	5'CCCCACGTCAGCTGGAA3'
Dact3	5'AGGCTTCTATGAAGACCCCAGTT3'	5'AGATCCGGAGAAGCCACTGT3'

Probes for mRNA in situ Hybridization

Riboprobes were labeled by incorporation of digoxigenin-labeled UTP (DIG RNA Labeling Mix, Roche Applied Science, Indianapolis IN). Sense controls were performed in parallel and compared in each case to confirm the specificity of the expression patterns shown (Supplemental Fig. S3). The validity of tissue expression observed for each gene was further confirmed by the observation of identical expression patterns using multiple non-overlapping antisense probes derived from the same cDNA. Probes used (nt numbers relative to translational start):

gene	probe for data shown (nt)	pattern validated with probe (nt)
Dact1	1250-1601	316-692
Dact2	1639-1963	610-1080
Dact3	239-607	813-1153, 1162-1641, 1643-1910

mRNA in situ Hybridization: Tissue Preparation

Embryos were fixed by immersion, neonatal and postnatal animals by perfusion, with 4% paraformaldehyde in PBS. Embryos or tissue (*e.g.* brains) were dehydrated in sequential concentrations of ethanol and stored in 100% ethanol at -20°C. Prior to experimental use, tissue was rehydrated sequentially from ethanol into PBS containing 0.1% Tween-20.

mRNA in situ Hybridization: Thick sections

Embryos/tissues were embedded in gelatin/albumin gel polymerized with glutaraldehyde. Gel solution was 30% ovalbumin (w/v), 0.5% gelatin in 0.1M sodium acetate, pH 6.5, filtered. Gel was polymerized by addition of 2.5% glutaraldehyde, and solidified by storing overnight with embedded tissue at 4°C. Embedded tissue was sectioned to 100 μm thickness on a Leica VT1000S fluid immersion vibratome.

mRNA in situ Hybridization: Hybridization and Development

Embryos or thick sections were collected in PBT (PBS containing 0.1% Tween-20), and treated with 3% H_2O_2 (for whole mounts) or 6% H_2O_2 (for sections, including adult brain sections) in PBT for 1 h. Embryos/sections were washed sequentially in 3 X 5 min PBT, 5 min 10ug/mL proteinase K in PBT, 5 min 2mg/mL glycine in PBT, 2 X 5 min PBT, 20 min 4% paraformaldehyde, 0.2% glutaraldehyde in PBT, 3 X5 min PBT. Tissue was prehybridized for 2 h in hybridization solution at 70°C, followed by hybridization overnight in fresh hybridization solution containing 0.5 μg/ml digoxigenin labeled RNA probe. Hybridization solution was 50% formamide, 5X SSC pH4.5 (pH 7.0 for adult brain sections), 1% SDS, 50ug/mL yeast tRNA, 50ug/mL heparin. Stringency washes were used to remove unbound probe. These consisted of 2 X 30 min in 50% formamide, 4X SSC, 1% SDS at 70ºC, followed by 2 X 30 min in 50% formamide, 2X SSC, 1% SDS at 70ºC.

Following hybridization, tissue was washed with MABT (0.1M maleic acid buffer pH 7.5 with 0.1% Tween-20) for 2 X 10 min at room temperature. Tissue was labeled with 1:4000 anti-digoxigenin (Roche, Indianapolis, IN) overnight at 4°C. Blocking for 2

h and immunolabeling were performed in 10% heat inactivated sheep serum, 2% BM blocking reagent (Roche, Indianapolis, IN), in MABT. Following antibody incubation, tissues were washed 5 X 30 min with MABT at room temperature.

For development reactions, tissue was washed 3 X 10 min in NTMT (0.1 M Tris pH 9.5, 0.1 M NaCl, 0.05 M $MgCl_2$, 0.1% Tween-20), and incubated in dark in NBT/BCIP (Bio-Rad) in NTMT. Incubation times were variable depending on when clear development was visible, but usually 4-6 h at room temperature for embryos, and 10-14 h for adult brain sections.

Acknowledgments

BNRC thanks Dr. Randall Moon and Dr. John Rubenstein for mentoring related to this project. Dr. Uta Grieshammer has shared unpublished information regarding expression of the *Dact* genes prior to E8.0. Eric P. Fox, Francesca Mueller, and Edwina Wilcox provided technical assistance during early stages of project development. Dr. Deborah Kurrasch gave helpful advice regarding Q-PCR. Dr. Samuel Pleasure, Dr. Rubenstein, and Dr. Grieshammer provided useful comments on the text. This work was supported by NIH MH01750 K08; a NARSAD Young Investigator Award; and NAAR award #551, all to BNRC; as well as by several intramural awards from the University of California, San Francisco including the UCSF Center for Neurobiology and Psychiatry.

Figure 1: Dact gene family molecular data.

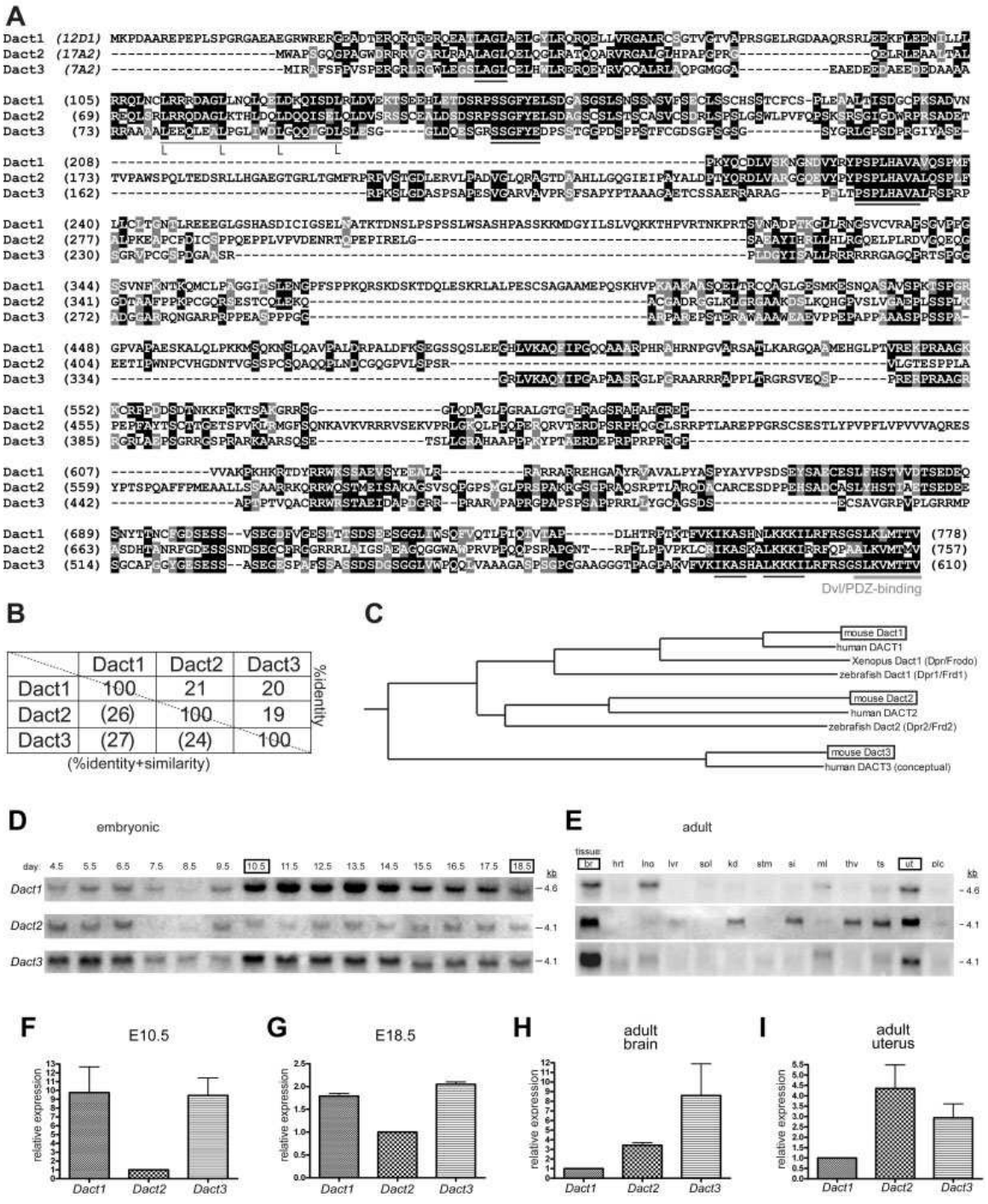

Fig. 1. Dact gene family molecular data. **A.** Alignment of primary protein sequences, mouse Dact1, Dact2, Dact3. Chromosomal positions are shown in the first line. Black

blocks indicate identity; grey indicates similarity. Blocks of four or more amino acids conserved in all three paralogs are underlined in black. The coiled-coil domain (with four absolutely conserved leucines indicated) and the Dvl/PDZ-binding domain (Cheyette et al, 2002) are underlined in grey. **B.** Table showing percentage conservation in the primary protein sequences, aligned as in **A**. Numbers to the top right indicate % identity; numbers (in parentheses) to the bottom left indicate % identity plus highly similar residues. **C.** Deduced phylogenetic relationships between the Dact proteins described in this paper and those previously described. The three mouse cDNAs whose coding sequences have been cloned in their entirety are boxed. The originally-described *Dpr* and *Frodo* genes are both homologs of *Dact1*, corresponding to a recent duplication event in the *Xenopus* lineage (not shown). The human DACT3 sequence is a predicted cDNA based on public database information (see text and also Fig. S1). **D, E.** Northern blots. *Note:* Different blots were probed for each gene, loading controls are provided in Fig. S2. **D.** Embryonic stages. Samples from the first three days post-coitus (E4.5-6.5) include both extra-embryonic and maternal uterine tissue, while the next three (E7.5-9.5) are the embryo plus extra-embryonic membranes. E10.5-18.5 correspond to embryonic tissues only. **E.** Adult tissues: (br) brain, (hrt) heart, (lng) lung, (lvr) liver, (spl) spleen, (kd) kidney, (stm) stomach, (si) small intestine, (ml) striated muscle, (thy) thymus, (ts) testis, (ut) non-pregnant uterus, (plc) placenta. **F-I.** Q-PCR showing relative expression of *Dact1 vs. Dact 2 vs. Dact3* at selected developmental stages and adult tissues. **F.** E10.5 **G.** E18.5 **H.** adult (8 week postnatal) brain, **I**. adult (8 week postnatal; non-pregnant) uterus. *Note:* Y-axis scale changes from F-I; units denote *relative* expression within each sample, absolute levels are not measured by this technique.

Figure 2. Developmental expression of mouse *Dact* genes, E9.0-E10.5.

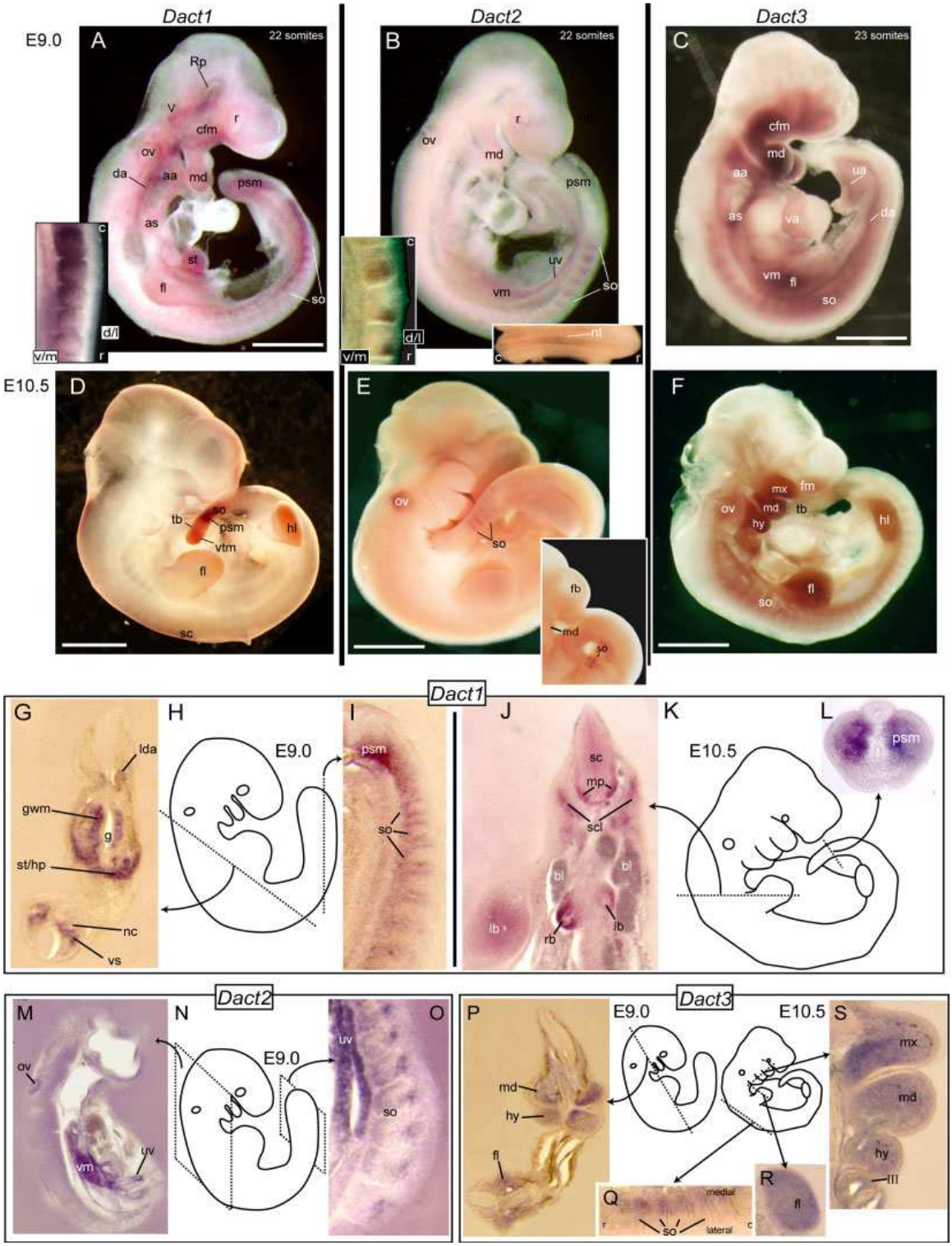

Fig. 2. Developmental expression of *Dact* genes. **A-C.** WISH at E9.0. **A**. *Dact1*-specific probe. Expression is most prominent in presomitic mesoderm (psm), somites (so), septum transversum (st), craniofacial mesenchyme (cfm), and the ganglion of cranial nerve V (V), and is also present in the retina (r), around Rathke's pouch (Rp), the otic vesicle epithelium (ov), the mandibular arch (md), aortic sac (as), aortic arches (aa), and dorsal aorta (da), and in the forelimb bud (fl). Inset (lateral aspect): *Dact1* becomes polarized ventromedially (v/m) and caudally (c) as somites mature. **B.** *Dact2*-specific probe. Only weak expression is detectable: in caudal somites (so), umbilical veins (uv), ventral mesentery of the foregut (vm), otic vescicle (ov), mandibular arch (md), and retina (r). Left inset (lateral aspect): *Dact2* becomes polarized dorsolaterally (d/l) and rostrally (r) in the caudal somites. Right inset (dorsal aspect): *Dact2* is expressed in the dorsal neural tube caudally. **C.** *Dact3*-specific probe. Expression in the craniofacial mesenchyme (cfm), mandibular arch mesenchyme (md), aortic sac (as), aortic arches (aa), and dorsal aorta (especially caudally; da), umbilical artery (ua), vitelline artery (va), ventral mesentery of the foregut (vm), forelimb bud (fl), and ventrally in mature somites (so). **D-F.** WISH at E10.5. **D.** *Dact1*-specific probe. Expression in the presomitic mesoderm (PSM), caudal somites (so), more weakly in the ventral mesoderm of the tail bud (tb; vtm), limb buds (fl, hl), as well as the ventral spinal cord (sc). **E.** *Dact2*-specific probe. Expression is detected in the otic vesicle plus the rostral portion of the most recently formed somites (so). Inset: another example of caudal somite expression plus no expression detected in the forebrain (fb) or mandibular arch (md; obscured in **E**). **F.** *Dact3*-specific probe. Expression in facial mesenchyme (fm), branchial arch mesenchyme: (mx) maxillary, (md) mandibular, (hy) hyoid, limb buds (fl, hl), as well as ventral somites (so). **G-S**. Dact family member ISH on representative

sections from E9-E10.5. **G.** At E9.0 *Dact1* is detected in the ventral somite (vs), nephrogenic cords (nc), septum transversum and hepatic primordium (st/hp), and the gut wall mesenchyme (gwm). **H.** Schematic showing approximate level and orientation of sections in **G**, **I. I.** At E9.0 *Dact1* is expressed in the PSM, in the ventral domains of somites, and along the rostral and caudal somite walls. **J.** At E10.5 *Dact1* is detected in the limb bud mesoderm (lb), outer walls of the right and left main bronchi (rb, lb), sclerotome (scl), and the motor pools of the spinal cord (mp, sc). **K.** Schematic showing approximate level and orientation of sections in **J**, **L. L.** At E10.5 and earlier *Dact1* is highly expressed in the PSM and caudal somites. **M.** At E9.0 *Dact2* is detected in the otic vesicle (ov), ventral mesentery of the foregut (vm), and umbilical veins (uv). **N.** Schematic showing approximate levels and orientation of sections in **M** and **O**. **O.** *Dact2* is detected in the umbilical veins (uv) and within somites (so) rostrally and dorsally. **P.** At E9.0 *Dact3* is detected throughout mesenchyme, including that of the limb buds such as the forelimb (fl), as well as the hyoid (hy) and mandibular (md) branchial arches, in a section corresponding to the plane shown in the schema at right. **Q-S.** E10.5 ISH on sections corresponding to the planes shown in the accompanying diagram. **Q.** Expression ventrally in maturing somites. **R.** Expression in forelimb mesoderm (fl). **S.** Expression in branchial arch mesenchyme: (mx) maxillary, (md) mandibular, (hy) hyoid, (III) third. Other abbreviations: (lda) left dorsal aorta, (bl) blood. Scale bars: **A-C** 0.5 mm; **D-F** 1.0 mm.

Figure 3. Expression of *Dact* genes at E14.5 and in adult brain.

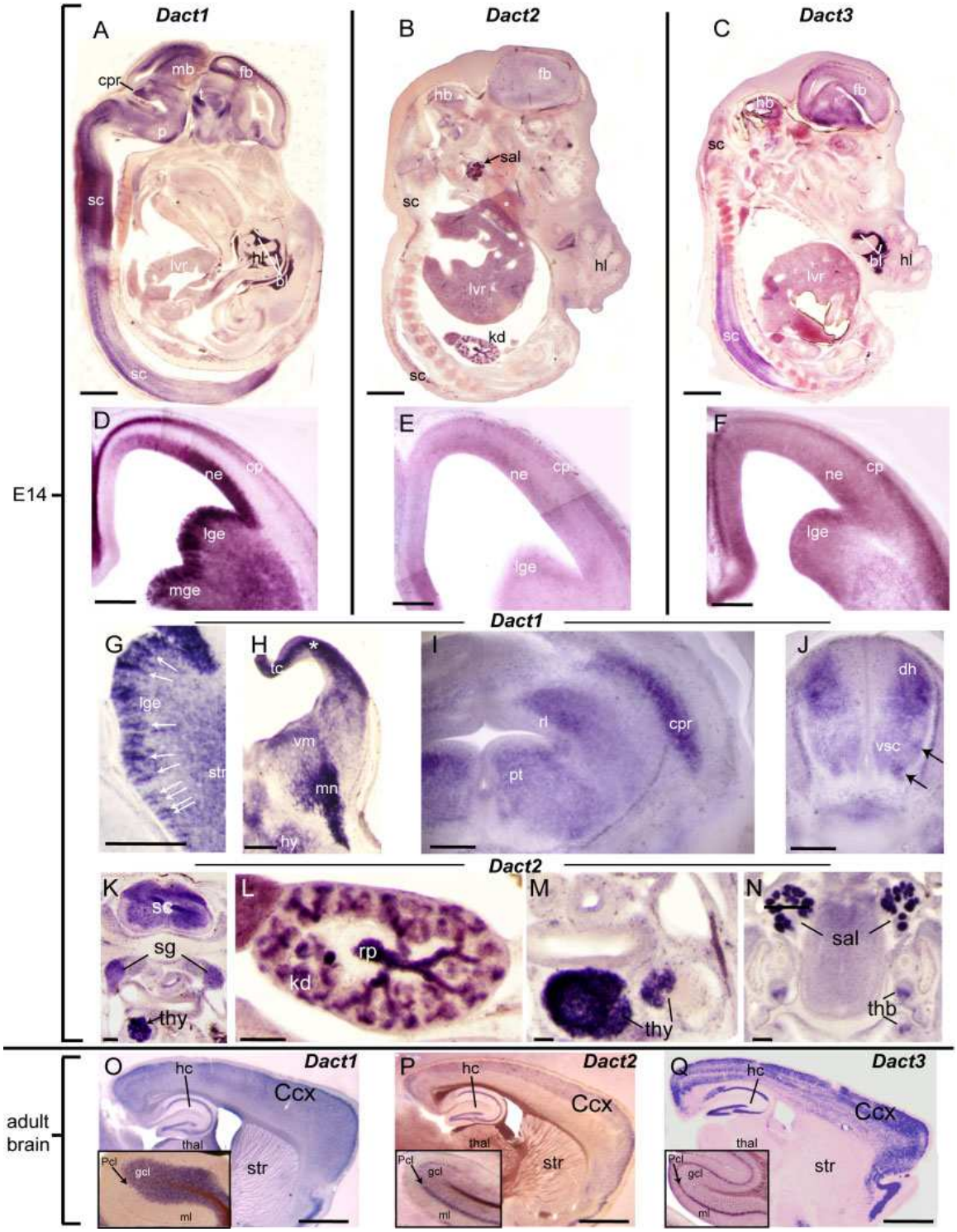

Fig. 3. Expression of *Dact* genes at E14.5 and in adult brain. **A-C.** Sagittal sections of whole embryos at E14.5 stained by in situ hybridization with probes for *Dact1* (**A**), *Dact2* (**B**), and *Dact3* (**C**). *Dact1* and *Dact3* are most prominent in the developing CNS, *Dact2* has domains of higher expression in the developing salivary glands (sal) and kidneys (kd). **D-F.** Horizontal sections of forebrain at E14.5 stained with probes for *Dact1* (**D**), *Dact2* (**E**), and *Dact3* (**F**). **G.** Close-up of horizontal section through the ventricular proliferative zone at the level of the lateral ganglionic eminence, showing *Dact1* expression in radially-arranged cell clusters (arrows). **H-J.** Horizontal sections at progressively more caudal planes of the E14.5 CNS showing *Dact1* expression in many populations of differentiating neurons. **H.** Midbrain. **I.** Midbrain-hindbrain junction and pons. **J.** Spinal cord. Abbreviations: (tc) tectum/dorsal midbrain, (vm) ventral midbrain, (mn) migrating neurons of the ventral midbrain, (hy) hypothalamic nuclei, (pt) pontine tegmentum, (rl) rhombic lip of the fourth ventricle, (cpr) cerebellar precursors, (dh) developing dorsal horn of the spinal cord. Arrows: neurons in the motor pools of the ventral spinal cord (vsc). **K-N.** Sections showing *Dact2* expression in E14.5 tissues. **K**. Horizontal section through spinal cord (sc) and sympathetic ganglia (sg). Compare to higher level of expression in the nearby edge of the developing thymus (thy). **L**. Section of developing kidney showing high levels of expression in the collecting system and renal pelvis (rp). **M**. Section through the main lobe of the thymus (thy). **N**. Section of the oral cavity showing expression in the developing salivary glands (sal) as well as weaker expression in the toothbuds (thb). **O-Q.** Sagittal sections of adult brains stained with in situ hybridization probes for *Dact1* (**N**), *Dact2* (**O**), and *Dact3* (**P**). All three genes are expressed in the hippocampus (hc), in different patterns in the cerebral cortex (Ccx) and other structures of the forebrain (see text). Insets:

Expression in the adult cerebellum. *Dact1* (inset O) is specifically expressed in the granule cell layer (gcl), whereas both *Dact2* (inset P) and *Dact3* (inset Q) are expressed significantly in the Purkinje cell layer (Pcl). Sense and no probe controls provided in Fig. S3. Other abbreviations: (fb) forebrain, (mb) midbrain, (hb) hindbrain, (thal) adult thalamus, (str) striatum, (t) thalamic eminence, (p) pons, (lvr) liver, (hl) hindlimb, (cp) cortical plate zone, (ne) neuroepithelium, (lge) lateral ganglionic eminence, (mge) medial ganglionic eminence, (ml) molecular layer of the cerebellum, (bl) extravasated blood, (*) folded tissue. Scale bars: A-C 1 mm; D-N 0.2 mm; O-Q 2 mm.

Supplemental Figures:

Fig. S1. Predicted human DACT3 sequence (*H.s.* Dact3) compared to translation of cloned mouse *Dact3* cDNA (*M.m.* Dact3). Chromosomal positions are shown in the first line. Black blocks indicate identity; grey indicates similarity. The human sequence is based on publicly-available human cDNA fragments (*e.g.* GenBank CV029753, BG715516, BF515069, BF115250, BM468105, etc), previously identified 5'truncated cDNAs (*e.g.* BC016161), and human genomic sequence corresponding to chromosome 19q13.32. Genscan also identifies this as a transcribed locus based on genomic sequence-level criteria.

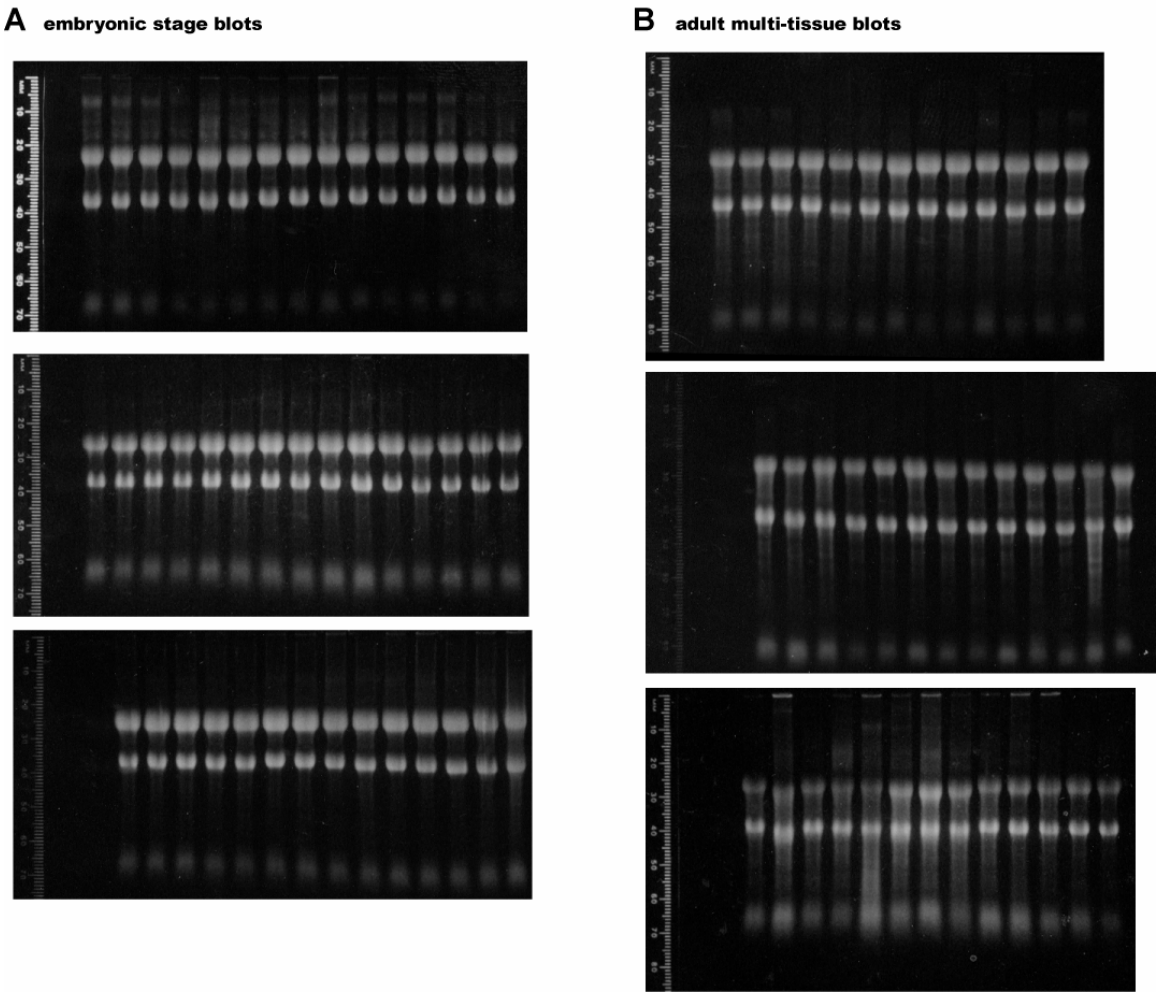

Fig. S2. Ethidium bromide stained gels corresponding to all Northern blots shown in Fig. 1D, E, demonstrating similar levels of 18S and 28S ribosomal RNA in each lane as a loading control. A total of 6 (3 pairs of embryonic (**A**) and adult (**B**) blots) were used to generate data in Fig 1: one pair of fresh blots for each *Dact* gene. Expression data was cross-validated by sequentially stripping and re-testing each blot pair with the other 2 probes.

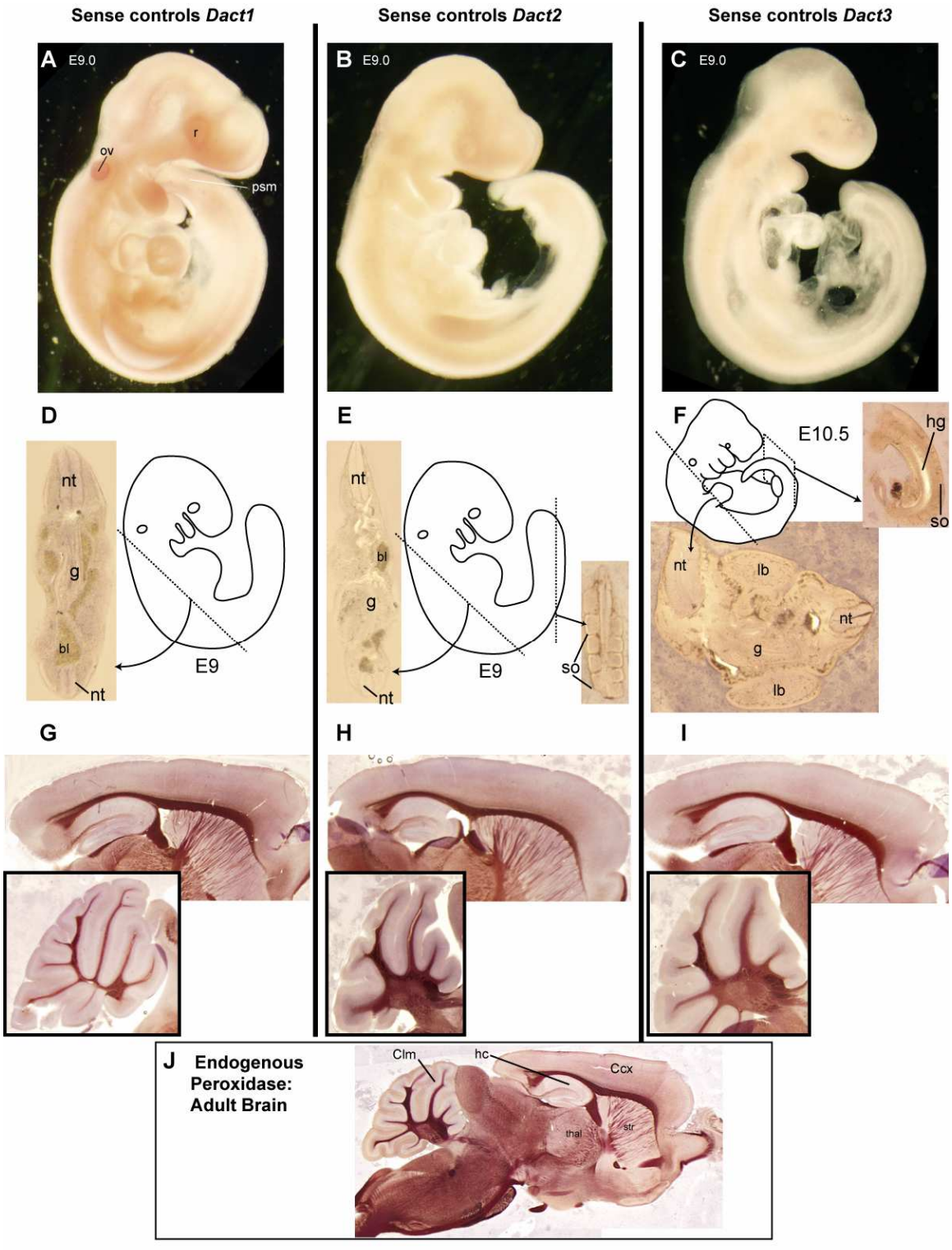
Sense controls *Dact1*
Sense controls *Dact2*
Sense controls *Dact3*
A E9.0
ov
r
psm
B E9.0
C E9.0
D
nt
g
bl
nt
E9
E
nt
bl
g
nt
E9
so
F
E10.5
hg
so
nt
lb
nt
g
lb
G
H
I
J Endogenous Peroxidase: Adult Brain
Clm
hc
Ccx
thal
str

Fig. S3. In situ hybridization controls using reverse complementary (sense) probes corresponding to the cDNAs, hybridization, and development conditions used in Figs. 2 and 3. **A-C**.WISH at E 9.0: (**A**) *Dact1*. (**B**) *Dact2*. (**C**) *Dact3*. Aside from very weak staining of the retina and otic vesicle with the sense probe for *Dact1*, essentially no signal comparable to the antisense staining is seen with any of the sense controls. Note the absence of PSM, somite, septum transversum, and major arterial staining with the *Dact1* sense probe. *Abbreviations:* (r) retina, (ov) otic vesicle, (psm) presomitic mesoderm. **D-F.** ISH on representative sections at E9.0 and E10.5 using sense probes: (**D**) *Dact1*. (**E**) *Dact2*. (**F**) *Dact3*. No specific signal is detected. **G-I.** ISH on adult brain sections, forebrain and cerebellum (insets): (**G**) *Dact1*. (**H**) *Dact2*. (**I**) *Dact3*. No signals comparable to the cortical, hippocampal, or cerebellar staining in Fig. 3**O-Q** is observed. **J.** No-probe control for adult brain section ISH, showing background levels of endogenous peroxidase activity under conditions used to generate adult brain expression data shown in Fig. 3**O-Q** and Fig. S3**G-I** . Note absence of staining in cortical structures including the cerebellum (Clm), hippocampus (hc), and cerebral cortex (Ccx). Brownish peroxidase stain is apparent in the striatum (str) and thalamus (thal).

References

Beaulieu, J.M., Sotnikova, T.D., Yao, W.D., Kockeritz, L., Woodgett, J.R., Gainetdinov, R.R., and Caron, M.G. 2004. Lithium antagonizes dopamine-dependent behaviors mediated by an AKT/glycogen synthase kinase 3 signaling cascade. Proc. Natl. Acad. Sci. U. S. A 101: 5099-5104.

Borycki, A.G., Brunk, B., Tajbakhsh, S., Buckingham, M., Chiang, C., and Emerson, C.P., Jr. 1999. Sonic hedgehog controls epaxial muscle determination through Myf5 activation. Development 126: 4053-4063.

Brott, B.K. and Sokol, S.Y. 2005a. A vertebrate homolog of the cell cycle regulator Dbf4 is an inhibitor of Wnt signaling required for heart development. Dev. Cell 8: 703-715.

Brott, B.K. and Sokol, S.Y. 2005b. Frodo proteins: modulators of Wnt signaling in vertebrate development. Differentiation 73: 323-329.

Cheyette, B.N.R., Waxman, J.S., Miller, J.R., Takemaru, K., Sheldahl, L.C., Khlebtsova, N., Fox, E.P., Earnest, T., and Moon, R.T. 2002. Dapper, a Dishevelled-associated antagonist of beta-catenin and JNK signaling, is required for notochord formation. Dev. Cell 2: 449-461.

Christ, B., Huang, R., and Scaal, M. 2004. Formation and differentiation of the avian sclerotome. Anatomy and Embryology 208: 333-350.

Gillhouse, M., Nyholm, M.W., Hikasa, H., Sokol, S.Y., and Grinblat, Y. 2004. Two Frodo/Dapper homologs are expressed in the developing brain and mesoderm of zebrafish. Developmental Dynamics 230: 403-409.

Gloy, J., Hikasa, H., and Sokol, S.Y. 2002. Frodo interacts with Dishevelled to transduce Wnt signals. Nat. Cell Biol. 4: 351-357.

Hikasa, H. and Sokol, S.Y. 2004. The involvement of Frodo in TCF-dependent signaling and neural tissue development. Development 131: 4725-4734.

Hunter, N.L., Hikasa, H., Dymecki, S.M., and Sokol, S.Y. 2005. Vertebrate homologues of Frodo are dynamically expressed during embryonic development in tissues undergoing extensive morphogenetic movements. Dev. Dyn. 235: 279-284.

Kaidanovich-Beilin, O., Milman, A., Weizman, A., Pick, C.G., and Eldar-Finkelman, H. 2004. Rapid antidepressive-like activity of specific glycogen synthase kinase-3 inhibitor and its effect on beta-catenin in mouse hippocampus. Biological Psychiatry 55: 781-784.

Katoh, M. and Katoh, M. 2003. Identification and characterization of human DAPPER1 and DAPPER2 genes in silico. Int. J. Oncol. 22: 907-913.

Katoh, M. 2005. Identification and characterization of rat Dact1 and Dact2 genes in silico. International Journal of Molecular Medicine 15: 1045-1049.

Kozak, M. 1987. At least six nucleotides preceding the AUG initiator codon enhance translation in mammalian cells. J. Mol. Biol. 196: 947-950.

Lee, C.S., Buttitta, L.A., May, N.R., Kispert, A., and Fan, C.M. 2000. SHH-N upregulates Sfrp2 to mediate its competitive interaction with WNT1 and WNT4 in the somitic mesoderm. Development 127: 109-118.

Livak, K.J. and Schmittgen, T.D. 2001. Analysis of relative gene expression data using real-time quantitative PCR and the 2(-Delta Delta C(T)) Method. Methods 25: 402-408.

Long, J.M., LaPorte, P., Paylor, R., and Wynshaw-Boris, A. 2004. Expanded characterization of the social interaction abnormalities in mice lacking Dvl1. Genes Brain Behav. 3: 51-62.

Madsen, T.M., Newton, S.S., Eaton, M.E., Russell, D.S., and Duman, R.S. 2003. Chronic electroconvulsive seizure up-regulates beta-catenin expression in rat hippocampus: Role in adult neurogenesis. Biological Psychiatry 54: 1006-1014.

Moon, R.T., Bowerman, B., Boutros, M., and Perrimon, N. 2002. The promise and perils of Wnt signaling through beta-catenin. Science 296: 1644-1646.

O'Brien, W.T., Harper, A.D., Jove, F., Woodgett, J.R., Maretto, S., Piccolo, S., and Klein, P.S. 2004. Glycogen synthase kinase-3beta haploinsufficiency mimics the behavioral and molecular effects of lithium. J. Neurosci. 24: 6791-6798.

Polakis, P. 2000. Wnt signaling and cancer. Genes Dev. 14: 1837-1851.

Shimogori, T., VanSant, J., Paik, E., and Grove, E.A. 2004. Members of the Wnt, Fz, and Frp gene families expressed in postnatal mouse cerebral cortex. Journal of Comparative Neurology 473: 496-510.

Veeman, M.T., Axelrod, J.D., and Moon, R.T. 2003. A second canon: Functions and mechanisms of beta-catenin-independent wnt signaling. Developmental Cell 5: 367-377.

Wagner, J., Schmidt, C., Nikowits, W., and Christ, B. 2000. Compartmentalization of the somite and myogenesis in chick embryos are influenced by Wnt expression. Developmental Biology 228: 86-94.

Waxman, J.S., Hocking, A.M., Stoick, C.L., and Moon, R.T. 2004. Zebrafish Dapper1 and Dapper2 play distinct roles in Wnt-mediated developmental processes. Development 131: 5909-5921.

Wharton, K.A., Jr. 2003. Runnin' with the Dvl: proteins that associate with Dsh/Dvl and their significance to Wnt signal transduction. Dev. Biol. 253: 1-17.

Wong, H.C., Bourdelas, A., Krauss, A., Lee, H.J., Shao, Y., Wu, D., Mlodzik, M., Shi, D.L., and Zheng, J. 2003. Direct binding of the PDZ domain of Dishevelled to a conserved internal sequence in the C-terminal region of Frizzled. Mol. Cell 12: 1251-1260.

Yau, T.O., Chan, C.Y., Chan, K.L., Lee, M.F., Wong, C.M., Fan, S.T., and Ng, I.O. 2004. HDPR1, a novel inhibitor of the WNT/beta-catenin signaling, is frequently downregulated in hepatocellular carcinoma: involvement of methylation-mediated gene silencing. Oncogene 24: 1607-1614.

Zhang, L., Gao, X., Wen, J., Ning, Y., and Chen, Y.G. 2006. Dapper 1 antagonizes Wnt signaling by promoting dishevelled degradation. J. Biol. Chem. 281: 8607-8612.

Zhang, L., Zhou, H., Su, Y., Sun, Z., Zhang, H., Zhang, L., Zhang, Y., Ning, Y., Chen, Y.G., and Meng, A. 2004. Zebrafish Dpr2 inhibits mesoderm induction by promoting degradation of nodal receptors. Science 306: 114-117.

Chapter 1, Additional Data:

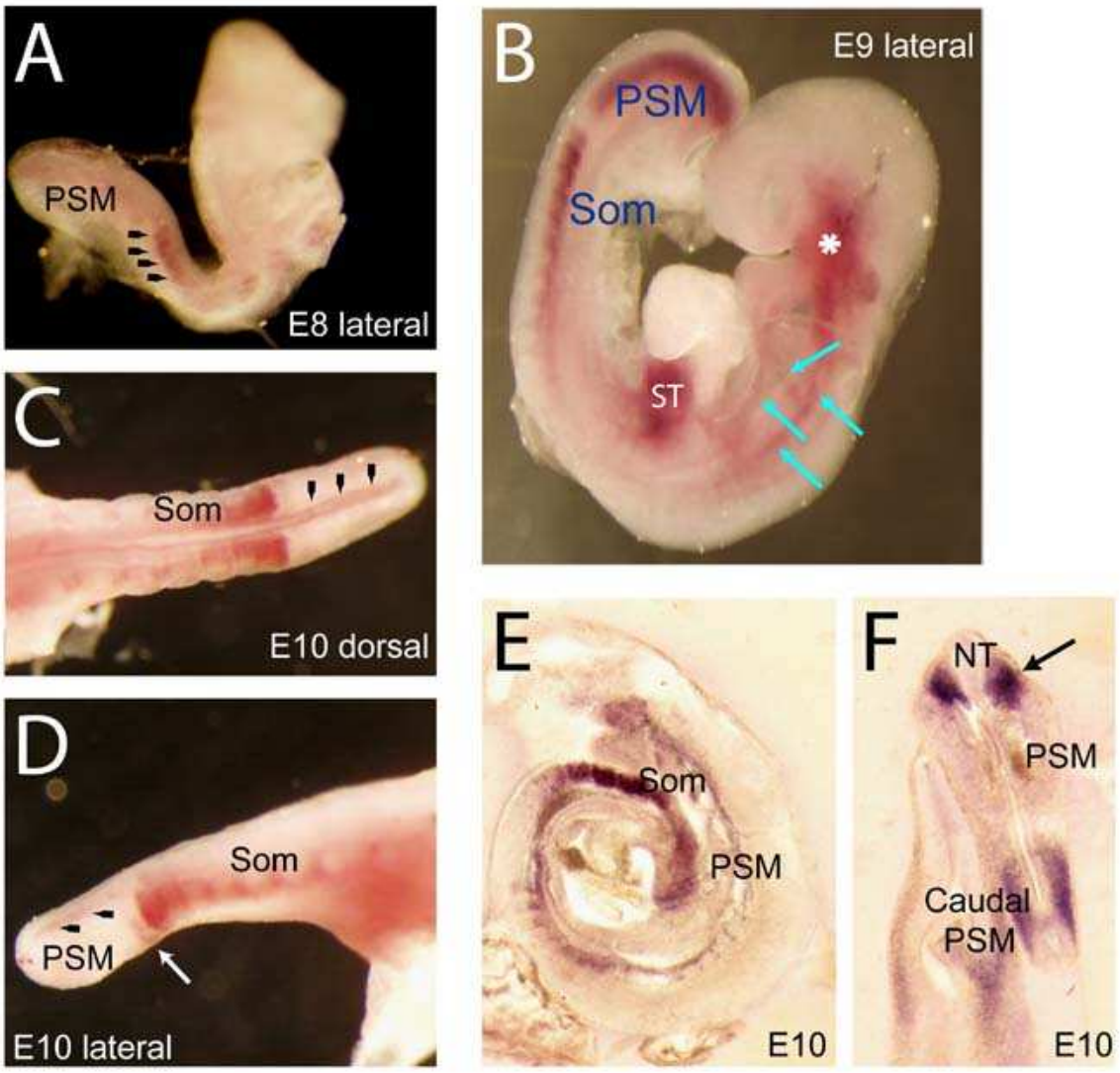

Chapter 1, Additonal Data Fig. 1: Expression of *Dact1* from E8-10 in caudal somites and presomitic mesoderm.

A, at E8 of gestation, *Dact1* expression is observed in the nascent caudal somites (arrowheads show expression in the four caudalmost somites: fewer than 10 somites are present at this unturned embryo stage from E8.0 to E8.5). A lower level of expression is present in the presomitic mesoderm (PSM).

B, at E9, *Dact1* expression is evident in the PSM and caudal somites (Som), where it is visible in a decrementing caudal-to-rostral gradient (signal is visible in 8 caudal somites in this particular embryo, as well as a band in the rostralmost portion of the PSM, and a broader segment of the caudal PSM and tail bud: this expression pattern is described in detail in Chapter 3). *Dact1* mRNA is also expressed in the septum transversum (ST, the future diaphragm), several components of the developing vasculature (arrows), and an accumulation of tissue cranially (*) which is likely to be neural crest derived tissue which will form branchial arch mesenchyme, based on comparison with *Dact1* in situ hybridization of sectioned E9 and E10 embryos.

C and D, dorsal and lateral (respectively) views of a caudal portion of an E10 embryo, labeled for *Dact1* mRNA. *Dact1* expression is weak in the PSM, but is present in the caudalmost somites, where the expression is seen to decrement sharply in the rostral direction from the caudalmost (newest) somite. Expression is also visible in the caudalmost extent of the neural tube (arrowheads) and in a sharp band near the rostral extent of the PSM (arrow).

E and F, lateral (E) and transverse (F) sections of the caudal regions of an E10 embryo, labeled for *Dact1* mRNA.

E, *Dact1* expression is visible in the caudal somites (Som) and throughout the PSM.

F, *Dact1* mRNA appears to be present in a banded expression pattern in the PSM. The strongest sites of expression visible are the caudal PSM and a region (arrow) which may be a new somite emerging from the rostral PSM.

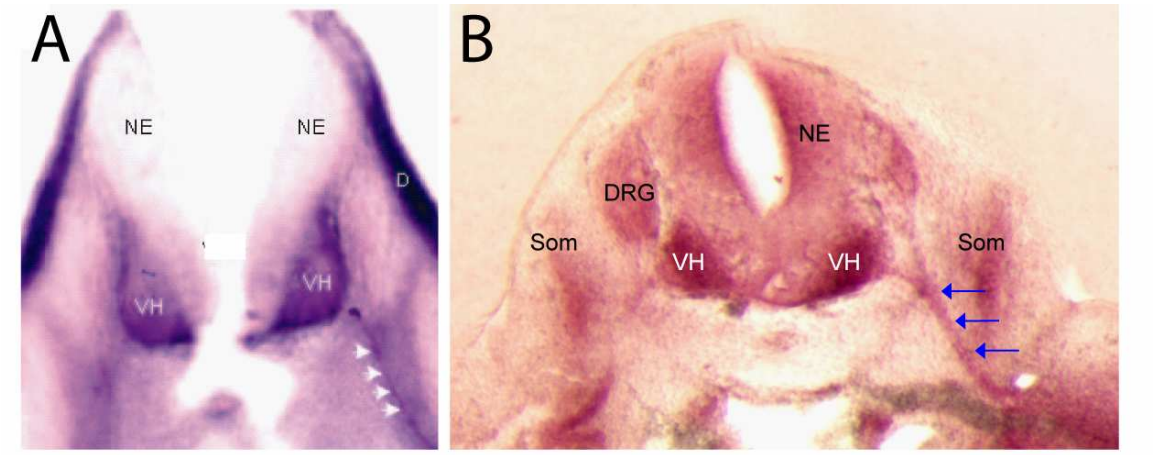

Additional Data, Figure 2: *Dact1* mRNA expression in E10 spinal cord and targeting to peripheral axons. Horizontal 100μm thick sections of E10 embryos at upper thoracic levels, roughly corresponding to the forelimb bud and rostral mediastinum.

A, *Dact1* mRNA expression is visible in the vental horn (VH) of the spinal cord, where postmitotic motor neurons are located, but not in the neuroepithelium (NE), which consists of premitotic neuronal precursors and newly postmitotic migratory neurons. *Dact1* mRNA expression signal is also seen in the peripheral nerve (white arrowheads), which, at this stage, consists entirely of axons, predominantly of motor neurons. This indicates that *Dact1* mRNA is axonally transported in developing motor axons.

B, *Dact1* mRNA expression signal is strongest in the ventral horn (VH), but is also evident in the spinal cord neuroepithelium (NE), the developing somite (Som), and the dorsal root ganglia (DRG), which at this stage of development consist predominantly of premitotic neuronal precursors and a smaller population of newly postmitotic sensory neurons. *Dact1* mRNA expression signal is also evident in the peripheral nerve (arrows), which contains axons extending from the VH (motor axons) and DRG (peripheral sensory axons): this is consistent with axonal targeting of *Dact1* mRNA .

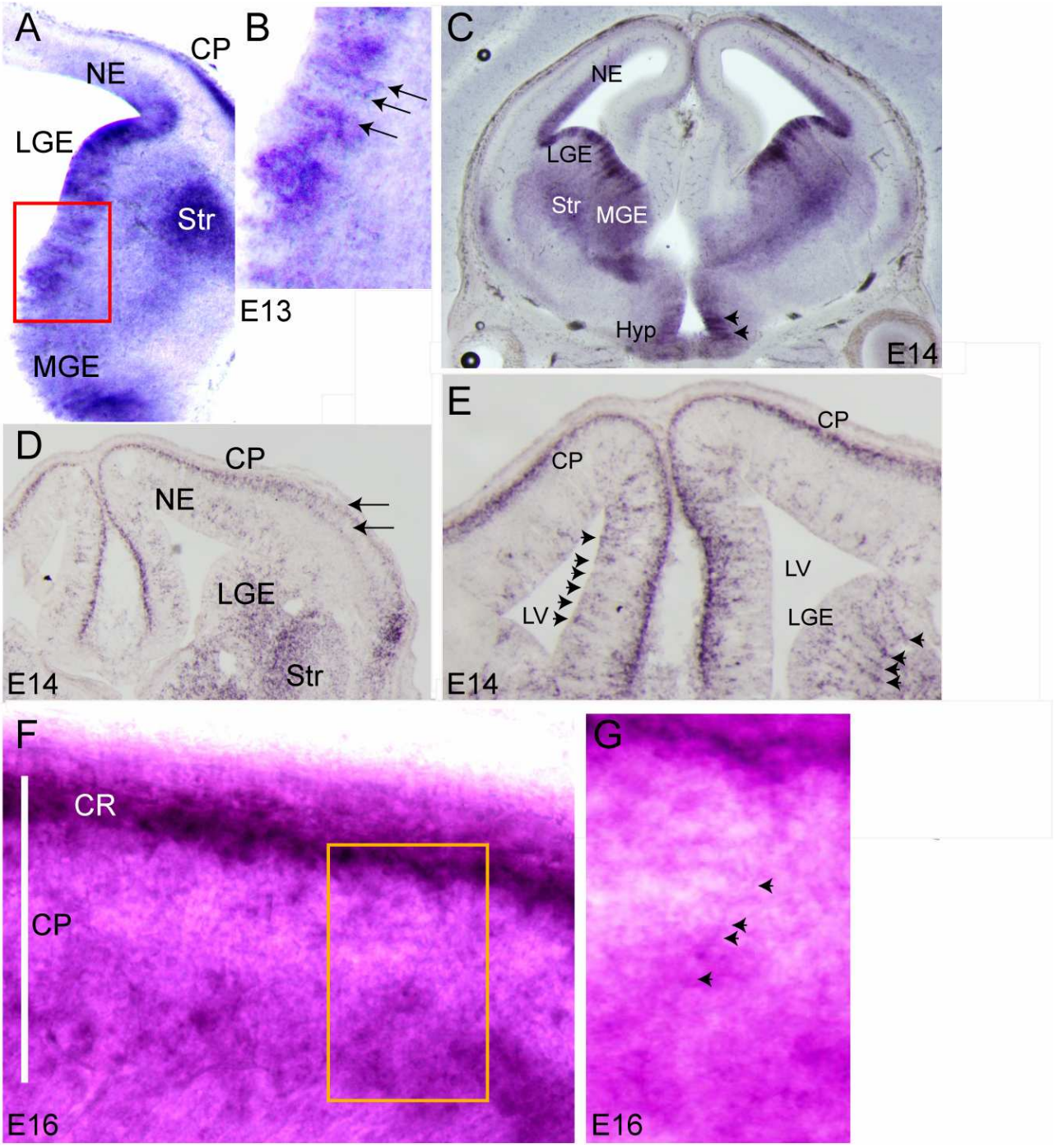

Additional Data, Figure 3: *Dact1* mRNA expression in mouse brain, E13-E16.

Additional Data, Figure 3: *Dact1* mRNA expression in mouse brain, E13-E16.

A, E13 forebrain, coronal section, 100μm thickness. The area in the red box is shown enlarged in B, Closeup of E13 forebrain neuroepithelium. *Dact1* mRNA expression is observed in the neuroepithelia of the lateral ganglionic eminence (LGE) and medial ganglionic eminence (MGE), as well as the nascent cortical plate (CP) and the anlage of the striatum (Str). Neuroepithelial *Dact1* mRNA expression is visible in radial columnar striations (arrows in B). C, Coronal section of E14 forebrain, 100μm thickness. *Dact1* expression in the neuroepithelium (NE) surrounding the lateral ventricle increases ventrally relative to dorsally. Columnar striations are seen in the neuroepithelia of the LGE, MGE, and hypothalamus (Hyp). The striations evidently extend into streams of cells, probably migrating into the striatum (Str). D and E, 20μm thick coronal cryosections of E14 forebrain. Arrows in D denote expression in the cortical plate (CP), which separates into two distinct layers ventrolaterally. Arrowheads in E label columns of *Dact1* expressing cells in the neuroepithelia surrounding the lateral ventricle (LV), notably in the LGE. F and G, 100μm thick sections through E16 cerebral cortex. G is a closeup of the boxed area in F. The white column in F labels the thickness of the cortical plate (CP). *Dact1* expression is most prominent in the Cajal-Retzius cell layer, CR, and in the deeper layers of the cortical plate. G shows a cortical pyramidal neuron with *Dact1* mRNA label extending into its axon and apical dendrite (arrowheads).

Additional Data, Figure 4: *Dact* family gene expression in P3 and P5 cerebellum.

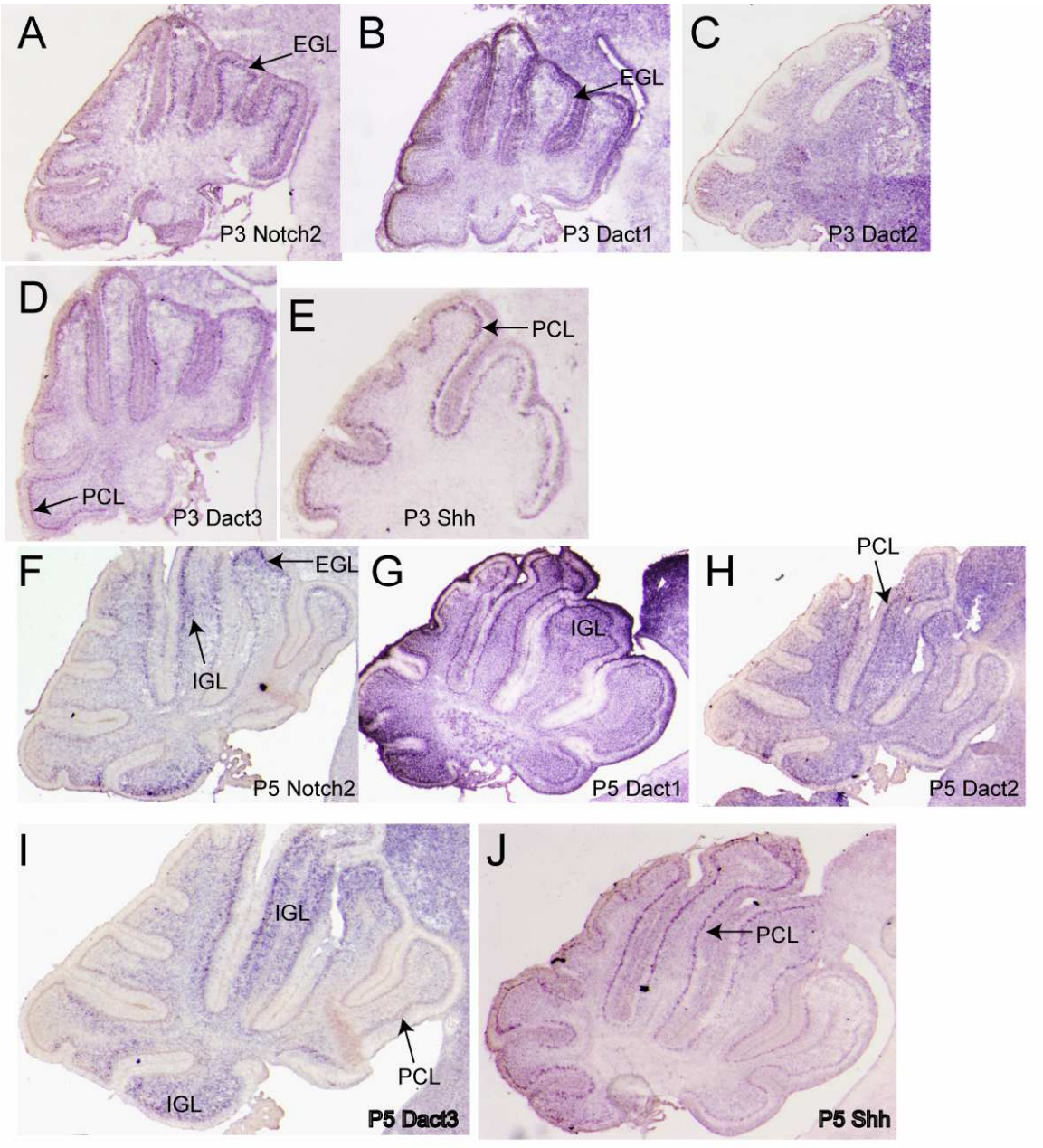

Additional Data, Figure 4: *Dact* expression in P3 and P5 cerebellum. A-E, P3 cerebellum. F-J, P5 cerebellum. All sections are sagittal, 20μm thick. A, F: *Notch2* is a label for the granule cell lineage, predominantly in the external granular layer (EGL) at P3, and extending into the nascent internal granular layer (IGL, F) at P5. B, G: *Dact1* expression resembles *Notch2* expression. C, H: *Dact2* is expressed throughout cellular regions of the cerebellum (likely in glia), with expression in the Purkinje cell layer (PCL) becoming evident as well at P5. D, I: *Dact3* is expressed in the PCL at P3, and becomes evident in the IGL as well at P5. E, J: *Sonic hedgehog (Shh)* is a specific marker for the Purkinje cell lineage at P3 and P5.

Chapter 3:

Dact1 Expression in Somitogenesis.

Chapter 3: Dact1 Expression in Somitogenesis.

This chapter is a description of *Dact1* gene expression in the somitogenesis clock of embryonic mice. I initially characterized the *Dact1* mRNA expression as showing variable patterns in the presomitic mesoderm (PSM), resembling the cycling phase patterns of cyclically expressed genes in the somite segmentation cycle. Together with Rowena Suriben, who was a rotation student in the Cheyette Laboratory at the time, I was able to show that *Dact1* cycles in the presomitic mesoderm, in phase with *Axin2*, which is both an effector and a target of Wnt/β-catenin signaling. Rowena performed all the hemisections for this study, while I performed all other single WISH experiments (Whole-mount In Situ Hybridization). Both Rowena and I contributed double WISH experiments, shown in Fig. 2, and we are indebted to Jozka Zakany and Marie Kmita of the University of Geneva for their invaluable advice on performing this protocol. This work has been published as Suriben,R., Fisher,D.A., and Cheyette,B.N.R. (2006). **Dact1 presomitic mesoderm expression oscillates in phase with Axin2 in the somitogenesis clock of mice.** *Developmental Dynamics 235*, 3177-3183. This publication subsumes the remainder of this chapter.

***Dact1* Presomitic Mesoderm Expression Oscillates in phase with *Axin2* in the Somitogenesis Clock of Mice**

Rowena Suriben,* Daniel A Fisher,* Benjamin NR Cheyette†

Department of Psychiatry & Graduate Programs in Developmental Biology and Neuroscience, University of California, San Francisco, 94143-2611

*Contributed equally

†Correspondence:

Benjamin NR Cheyette

bc@lppi.ucsf.edu

415.476.7826

Running Title: *Dact1* Expression Cycles during Somitogenesis

Key Words: somitogenesis, mouse, Dact, Dpr, Frodo, Wnt, Presomitic Mesoderm

Supported by: The University of California, San Francisco.

Abstract

During segmentation (somitogenesis) in vertebrate embryos, somites form in a rostral to caudal sequence according to a species-specific rhythm, called the somitogenesis clock. The expression of genes participating in somitogenesis oscillates in the presomitic mesoderm (PSM) in time with this clock. We previously reported that the *Dact1* gene (aka *Dpr1*/*Frd1*/*ThyEx3*), which encodes a Dishevelled-binding intracellular regulator of Wnt signaling, is prominently expressed in the PSM as well as in a caudal-rostral gradient across the somites of mouse embryos. This observation led us to examine whether *Dact1* expression oscillates in the PSM. We have found that *Dact1* PSM expression does indeed oscillate in time with the somitogenesis clock. Consistent with its known signaling functions and with the "clock and wavefront" model of signal regulation during somitogenesis, the oscillation of *Dact1* occurs in phase with the Wnt signaling component *Axin2*, and out of phase with the Notch signaling component *Lfng*.

Introduction

Vertebrates are segmented organisms whose vertebrae, ribs, muscles, and dermis innervated by each spinal nerve are embryonically derived from packets of mesoderm called somites. Bilateral pairs of somites bud in a rostral to caudal sequence from the presomitic mesoderm (PSM), which is formed from mesoderm arising initially by gastrulation at the primitive streak, and at late stages in the tail bud. The time interval between the budding of each new pair of somites varies according to the animal species and has been termed the somitogenesis clock. For example, in mouse embryos the somitogenesis clock takes approximately 2 hours to complete a full cycle, that is the time between the generation of successive somites (Forsberg et al., 1998; Iulianella et al., 2003; Giudicelli and Lewis, 2004).

Expression of the Notch signaling inhibitor *Lunatic fringe* (*Lfng*) as well as that of several other Notch signaling molecules and target genes cycles rhythmically in the PSM (McGrew et al., 1998; Forsberg et al., 1998; Aulehla and Johnson, 1999; Bessho et al., 2001; Pourquié, 2003a). Levels of *Axin2*, a cytoplasmic inhibitor of the Wnt/ß-catenin pathway, also cycle in the PSM, but out of phase with *Lfng* (Aulehla et al., 2003). This observation of reciprocal expression cycling between *Lfng* and *Axin2*, in combination with phenotypes in Notch and Wnt loss and gain of function experiments (Greco et al., 1996; Evrard et al., 1998; Zhang and Gridley, 1998; Hamblet et al., 2002; Serth et al., 2003; Dale et al., 2003) supports a "clock and wavefront" model of somitogenesis (Cooke and Zeeman, 1976) in which Notch and Wnt signaling alternate in the PSM via delayed negative feedback (Pourquié, 2003a; Aulehla and Herrmann, 2004). According to this model, as presomitic cells mature and migrate rostrally within the PSM they

experience alternating cycles of high Notch and Wnt signal transduction, while a gradient of Wnt3a originating caudally from the tail bud establishes the "determination front": the point at which the most anterior "presomite" pinches off from the PSM to form a new somite (Aulehla et al., 2003; Pourquié, 2003a). The complementary cyclical expression patterns of Wnt signaling inhibitors (*i.e.* Axin2) and Notch signaling inhibitors (*i.e.* Lfng) has led to the hypothesis that oscillations in levels of such inhibitors creates an offset between peaks in Wnt and Notch signal transduction in PSM cells, via signal pathway cross-talk at the level of the Dishevelled (Dvl) protein, combined with delayed negative feedback (Aulehla et al., 2003).

We previously compared embryonic expression levels and patterns of the three murine members of the Dact (Dpr/Frd) gene family, which encode conserved Dvl-binding regulators of Wnt signaling (Fisher et al., 2006). Compared to its paralogs, *Dact1* is uniquely expressed at high levels in the PSM. This led us to examine whether *Dact1* exhibits cycles of expression in the PSM, and if so, whether such cycles of *Dact1* occur in phase with the somitogenesis cycling of the Wnt signaling inhibitor *Axin2*, or instead with the Notch signaling inhibitor, *Lfng*.

Results and Discussion

Dact1 expression in the PSM is dynamic and consistent with somitogenesis cycling

We performed whole-mount in situ hybridization (WISH) using a *Dact1* specific probe on embryonic day (E) 9.0-9.5 mouse embryos and examined the distribution of *Dact1* in the PSM to determine whether patterns observed were consistent with cyclical gene expression. In over 100 embryos examined by this technique, we have observed a

range of *Dact1* expression in the caudal PSM that can be organized into 3 apparent phases by analogy with the phase patterns of *Axin2* which the *Dact1* patterns most closely resemble (Pourquié and Tam, 2001, Aulehla et al., 2003). In a representative sample taken from 4 complete litters in the CD1 outbred mouse strain (38 embryos) numbers observed in each of these phases correspond to expected ratios based on previous descriptions of genes undergoing somitogenesis cycling (Aulehla et al., 2003; Dale et al., 2003) (Table 1).

Table 1. *Dact1* PSM expression at E9.5:

	Phase 1 pattern	Phase 2 pattern	Phase 3 pattern
number of embryos	20	9	9
approximate ratio	2	1	1

The phases of *Dact1* expression that we observe in the PSM can be arranged into a cyclical pattern that coincides with the formation of new somites (Fig 1). In all phases, expression is pronounced in the s0 presomite (those cells at the rostral tip of the PSM that will pinch off to form the next somite). In Phase 1, *Dact1* expression also extends from the caudal tip of the PSM rostrally up to the position of the s-1 presomite (the next somite to form after s0), where its expression is low (Fig 1A, B). In Phase 2, expression of *Dact1* commences in the s-1 presomite, and the caudal expression of *Dact1* recedes, such that the band of low expression moves to the s-2 somite (Fig 1C, D). At the juncture between Phase 2 and Phase 3, the s0 presomite pinches off from the rostral PSM to become the new s1 somite. At this point the former s-3 becomes the new s-2, the former s-2 becomes s-1, and the former s-1 becomes s0 (Fig 1E, H). In Phase 3, expression is strong in s0 but weak throughout the rest of the PSM (Fig 1F). Expression in the caudal

PSM then resumes, bringing the PSM back into Phase 1 and completing the cycle (Fig 1H).

Dact1 cycling in the PSM occurs in phase with *Axin2* and out of phase with *Lfng*

To establish that *Dact1* is indeed cycling in the PSM with the somitogenesis clock, as well as to compare its pattern of cycling to that of previously described cycling genes in the Notch and Wnt signaling pathways, we performed Double-WISH for *Dact1* and either *Lfng* or *Axin2* on E9.5 embryos (Fig 2A, B). As expected, the expression patterns of all three genes varied from embryo to embryo depending on the phase of the somitogenesis clock. The spatial domains of *Dact1* and *Axin2* expression in the PSM overlap and correspond to the same phase, suggesting that these genes cycle together in PSM cells. The degree of spatial overlap in the caudal PSM is especially evident when both genes are in Phase 1 (Fig 2A). In contrast, in any given embryo the *Dact1* and *Lfng* patterns correspond to different phases of their cycle, such that their spatial distribution in the caudal PSM is most frequently complementary (*e.g.* Fig 2B, compare with Aulehla et al Fig 2G and Dale et al., 2003; by convention, *Lfng* phases are written in Roman numerals; *Axin2* and *Dact1* phases in Arabic numerals.) These results are entirely consistent with a prior study demonstrating that *Lfng* and *Axin2* have reciprocal cycles of expression in the PSM (Aulehla et al., 2003), and show that the cycling of *Dact1* in the caudal PSM coincides with that of *Axin2*.

To confirm this result, we also performed WISH for *Dact1* versus either *Lfng* or *Axin2* on paired (L-R) sagittal hemisections from single E9.5 embryos. This is informative because maturation of both sides of a normal vertebrate embryo is tightly

coordinated; the PSM on each side proceeds through the somitogenesis cycle in synchrony with its bilaterally-symmetrical partner (Aulehla et al., 2003; Pourquié, 2003b; Vermot and Pourquié, 2005; Saude et al., 2005). Each embryo was scored for its phase of the somitogenesis cycle based on the *Axin2* or *Lfng* WISH pattern from the PSM on one side, and this was compared to the phase of *Dact1* WISH observed on its other side. Consistent with the Double-WISH data, *Lfng* and *Dact1* expression from left and right halves of the same embryo correspond to different phases (*e.g.* Fig 2C *vs.* C'). Taken together and with previously reported results, our data indicate that when *Dact1* expression in the caudal PSM peaks (Phase 1), *Lfng* expression in the caudal PSM is lowest (Phase III), and that when *Dact1* expression is regressing in the caudal PSM (Phase 2), *Lfng* expression is increasing and moving rostrally (Phase I) (Dale et al, 2003). In contrast, although the spatial patterns of *Dact1* and *Axin2* are distinct in many locations including the neural tube (where *Axin2* is far more prominent) and newly formed somites (where *Dact1* is far more prominent), these genes are expressed in overlapping domains in the rostral presomites and in the caudal PSM. Using the hemisection technique, a range of E9.5 embryos spanning the somitogenesis clock show similar patterns of expression for *Dact1* and *Axin2* in their left and right PSM, especially caudally (Fig 2D). Taken together and with previously reported results, these data indicate that *Axin2* expression and *Dact1* expression wax and wane together in the caudal PSM throughout the somitogenesis cycle.

That said, although the expression of *Dact1* overlaps with that of *Axin2* in the PSM, it is worth noting that there are potentially important differences as well. For example, whereas *Axin2* is always expressed in a tightly restricted domain at the caudal

edge of the s0 presomite, *Dact1* is more uniformly expressed throughout this presomite (Fig. 1A-F, 2A,D-F). In Phase 1 when *Axin2* is expressed strongly in the s-2 presomite (and further caudally), *Dact1* is more weakly expressed at this level of the PSM (Fig. 2D). In Phase 2 when *Axin2* is expressed most strikingly in the s-1 presomite, *Dact1* expression is still low there compared to s0 (Fig 1C, 2E). Finally, in Phase 3, when *Axin2* is expressed in a broad band in the PSM caudal to s-1, *Dact1* levels are very low throughout this domain (Fig. 1F, 2F).

Implications for Dact1 function in Somitogenesis

We have discovered that *Dact1* expression cycles in the PSM during segmentation stages in the mouse. Furthermore, we have shown that unlike *Nkd1* (Ishikawa et al., 2004), which encodes another protein that binds to Dvl (Rousset et al., 2001), *Dact1* gene expression in the PSM cycles in phase with *Axin2*, which itself is transcribed downstream of Wnt/ß-catenin signaling (Jho et al., 2002). These results suggest that like *Axin2*, the expression of *Dact1* in PSM cells is positively regulated by cyclical waves of Wnt/ß-catenin signaling. β-catenin-dependent *Axin2* expression in the PSM is regulated via conserved TCF/LEF sites located within its promoter and first intron (Jho et al., 2002), as is the expression of the Notch ligand *Dll1* (Galceran et al., 2004). We have identified twelve potential TCF/LEF binding sites in the 5 kb promoter region and the first intron of the mouse *Dact1* gene, many of which are conserved in the human *DACT1* locus (Supplemental Fig S1). The presence of these conserved TCF/LEF binding sites in the *Dact1* and *Axin2* genomic regions, together with the synchronous oscillation of these genes in the caudal PSM, suggests the possibility that other Wnt/ß-

catenin-responsive genes regulated by TCF/LEF transcription factors might undergo somitogenesis cycling in phase with *Dact1* and *Axin2*.

Observations that the Wnt inhibitor *Axin2* cycles out of phase with Notch signaling molecules in the PSM, combined with prior evidence that the Wnt signal transducer Dvl can inhibit Notch signaling in some contexts (Axelrod et al., 1996), has led to a model for the somitogenesis clock involving negative feedback between these two signaling pathways (Aulehla et al., 2003; Pourquié, 2003a; Aulehla and Herrmann, 2004). This model proposes that when Wnt signaling is high in PSM cells, one activity of the Dvl protein is to repress simultaneous Notch signaling, whereas Axin2 serves in a delayed feedback loop to cyclically inhibit Wnt signal transduction and disinhibit Notch signal transduction.

In the context of this molecular model, Dact1, which has been characterized as a Wnt/ß-catenin antagonist (Cheyette et al., 2002; Wong et al., 2003; Kakinuma et al., 2004; Brott and Sokol, 2005; Zhang et al., 2006) might cooperate with Axin2 as both a target and an inhibitor of Wnt/ß-catenin signaling. Such functional redundancy between the Dact1 and Axin2 proteins in the PSM could explain why mutations in *Axin2* alone do not cause defects in somitogenesis (Yu et al., 2005). However, insertion of Dact1 alongside Axin2 as part of the clock and wavefront model of somitogenesis is speculative because the function of Dact proteins in Wnt/ß-catenin signal regulation is not securely established: some studies have indicated that Dact proteins act positively in Wnt/ß-catenin signaling (Gloy et al., 2002; Hikasa and Sokol, 2004; Waxman et al., 2004). Moreover, Dact proteins also regulate non-ß-catenin-dependent forms of Wnt signaling (Cheyette et al., 2002; Hikasa and Sokol, 2004; Waxman et al., 2004), which may

contribute to morphogenetic movements such as those necessary for PSM cell migration and to the mesenchymal-epithelial transition in the s0 presomite as it becomes the new s1 somite (Duband et al., 1987; Nakaya et al., 2004; Hunter et al., 2005). Further elucidation of the role of *Dact1* in these and other embryonic processes will be aided by phenotypic analysis and signaling assays in targeted mutant mouse lines.

Methods

Probes for Whole mount mRNA in situ Hybridization (WISH)

Riboprobes were labeled by incorporation of digoxigenin-labeled UTP (DIG RNA Labeling Mix, Roche Applied Science, Indianapolis IN). Sense controls (for *Dact1*) were the same as previously reported (Fisher et al., 2006). Multiple antisense probes were used to validate expression of *Dact1*, and phasic patterns of expression in the PSM were observed with all of them:

gene	probe	nt (numbered from translation start)
Dact1	"A"	316-692 (Fisher et al., 2006)
Dact1	"B"	1250-1473 (not previously reported)
Dact1	"C"	1250-1601 (Fisher et al., 2006)
Axin2	-	1-2397 (Jho et al., 2002)
Lfng	-	273-1030 (Cohen et al., 1997)

WISH Tissue Preparation and Hybridization

Embryos were fixed by immersion in 4% paraformaldehyde in PBS, then dehydrated in sequential concentrations of ethanol and stored in 100% ethanol at -20°C. Prior to experimental use, tissue was rehydrated sequentially from ethanol into PBS containing 0.1% Tween-20. Embryos were treated with 3% H_2O_2 in PBT for 1 hr, then washed sequentially in: 3 X 5 min PBT, 5 min 10μg/ml proteinase K in PBT, 5 min 2mg/ml

glycine in PBT, 2 X 5 min PBT, 20 min 4% paraformaldehyde + 0.2% glutaraldehyde in PBT, 3 X 5 min PBT. Tissue was prehybridized for 2 hrs in hybridization solution at 70°C, followed by hybridization overnight in fresh hybridization solution containing 0.5 µg/ml digoxigenin labeled RNA probe. Hybridization solution was 50% formamide, 5X SSC pH4.5, 1% SDS, 50μg/ml yeast tRNA, 50μg/ml heparin. Stringency washes were used to remove unbound probe. These consisted of 2 X 30 min in 50% formamide, 4X SSC, 1% SDS at 70ºC, followed by 2 X 30 min in 50% formamide, 2X SSC, 1% SDS at 70ºC.

Antibody labeling and Colorimetric Development (Single-WISH)

Following hybridization, tissue was washed with MABT (0.1M maleic acid buffer pH 7.5 with 0.1% Tween-20) for 2 X 10 min at room temperature. Tissue was labeled with alkaline phosphatase (AP) conjugated 1:4000 anti-digoxigenin (Roche Applied Science) overnight at 4°C. Blocking for 2 hrs and immunolabeling were performed in 10% heat inactivated sheep serum, 2% BM blocking reagent (Roche Applied Science), in MABT. Following antibody incubation, tissues were washed 5 X 30 min with MABT at room temperature.

For development reactions, tissue was washed 3 X 10 min in NTMT (0.1 M Tris pH 9.5, 0.1 M NaCl, 0.05 M $MgCl_2$, 0.1% Tween-20), and incubated in the dark in NBT/BCIP (Bio-Rad) in NTMT. Incubation times were variable depending on when clear development was visible, but usually 4-6 hrs at room temperature (RT).

Hemisection WISH

For hemisection experiments, embryos were collected and fixed as for single WISH. Following rehydration individual embryos were bisected sagittally in PBS using etched tungsten micro-needles (Fine Science Tools Inc, North Vancouver, Canada). The halves of each embryo were moved to histology baskets (15mm Netwell Insert, Corning Co., Corning NY) and were fixed overnight in 4% paraformaldehyde, then washed 3 X 10 min PBS. Baskets were kept in adjacent wells and treated as a pair for all subsequent hybridization, incubation, and development steps. Antibody labeling and colorimetric development were as described for single-WISH and double-WISH.

Double-WISH

Dact1/Axin2: Initial stages of double-WISH were identical to single-WISH until the hybridization step. For double-WISH hybridization, embryos were incubated in hybridization solution (as in single WISH) containing two probes: digoxigenin-labeled *Dact1* and fluorescein-labeled *Axin2*. Fluorescein labeling of RNA used the same procedure as digoxigenin labeling, but with fluorescein RNA labeling mix (Roche Applied Science) instead of digoxigenin labeling mix. Following hybridization, embryos underwent stringency washes, blocking, and immunolabeling with anti-digoxigenin Fab fragments (Roche Applied Science) at 1:4000 dilution (as in single WISH). After 5 x 30 min washes in MABT, double labeled embryos were incubated for development in 0.1M Tris pH8.2, 0.1% Tween-20 for 3 x 10 min, followed by incubation in the same buffer containing 6 µl/ml each of Vector Blue reagents 1, 2 and 3 (Vector Laboratories,

Burlingame CA) to detect *Dact1* signal. *Dact1* signal incubation proceeded for approximately 4 hrs in the dark at RT. Once a desired intensity of color development was achieved, embryos were post-fixed for 1 hr at RT in 4% paraformaldehyde in PBS. Following post-fixing, residual AP was inactivated by incubation for 1 hr at 65ºC in PBS, followed by 15 min in 0.1M glycine pH2.2, 0.1% Tween-20 at RT. Following AP inactivation, blocking and immunostaining steps were repeated using 1:4000 AP-conjugated anti-fluorescein Fab (Roche Applied Science). MABT washes and development proceeded as previously, but using Vector Red reagents 1, 2 and 3 at 6μl/ml (Vector Laboratories) for detection of fluorescein-labeled *Axin2*. Development time was approximately 5 hrs at RT for *Axin2*. Embryos were post-fixed for 1 hr at RT in 4% paraformaldehyde in PBS prior to photography.

Dact1/Lfng: Double-WISH was identical to *Dact1/Axin2* except for the following changes and substitutions. *Lfng* probe was digoxigenin-labeled and *Dact1* probe was fluorescein-labeled. *Lfng* signal was developed first, by washing 3 X 10 min in NTMT and then incubation in the dark in 75ul INT/BCIP (Roche Applied Sciences)/10 ml NTMT. First post-fixing, AP inactivation, *Dact1* signal development, and second post-fixing were as described above.

Imaging

Samples were photographed at 5.6x magnification on an Olympus SZX7 microscope equipped with an Olympus DP70 digital camera.

Acknowledgments

We thank Dr. Marie Kmita and Dr. Joska Zakany (University of Geneva, Switzerland) for advice on performing double-WISH, and members of the Cheyette laboratory for helpful discussions. This work was solely supported by intramural funds from the University of California, San Francisco, including the UCSF Innovations in Basic Science Award, the Academic Senate Committee on Research, the Research Evaluation Allocation Committee, and the Center for Neurobiology and Psychiatry.

Figure 1. ***Dact1*** **expression patterns in the PSM at E9.5**

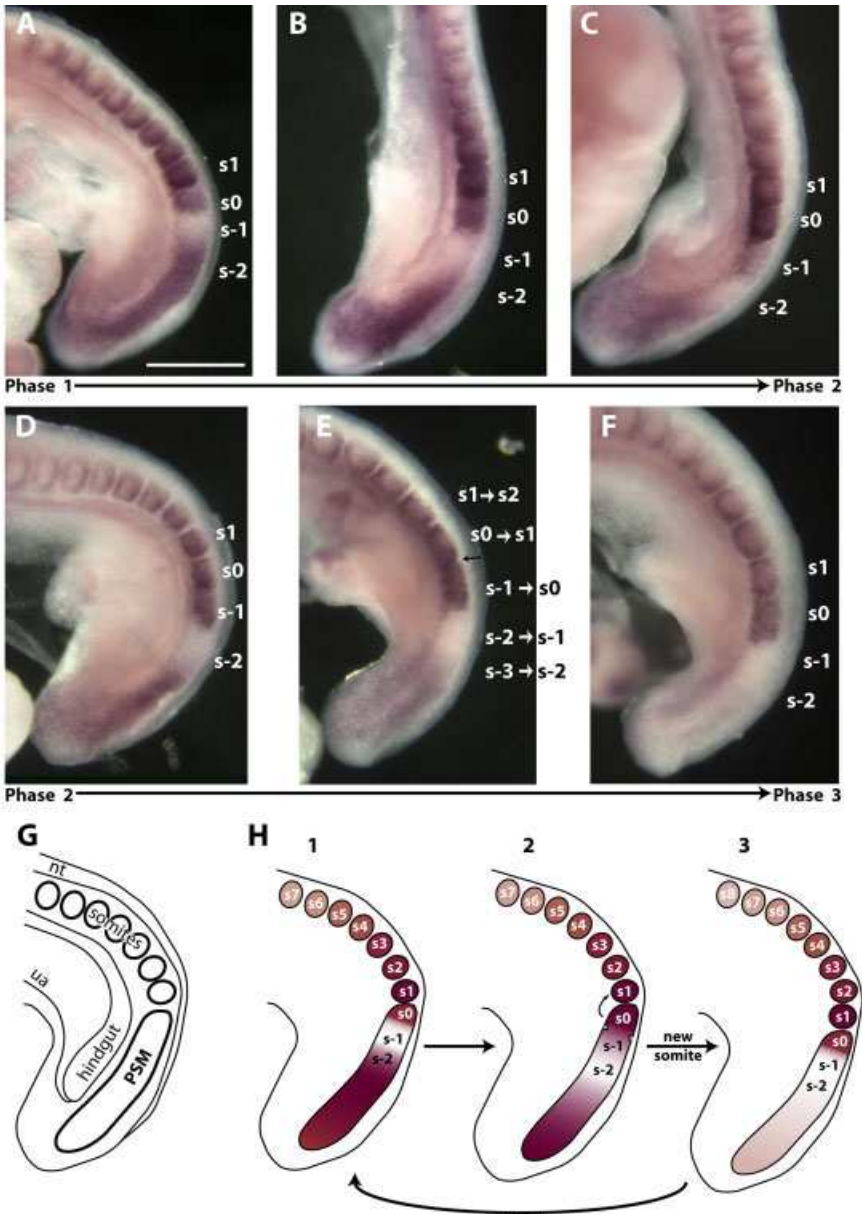

Fig. 1. *Dact1* expression patterns in the PSM at E9.5 (littermates). **A-B.** Phase 1: *Dact1* is prominent in the presomite s0 as well as caudally in the PSM up to the position of the s-1 presomite, where expression is low. **C-D.** Phase 2: *Dact1* begins to be expressed in s-1, and the band of low expression shifts caudally to s-2. **E.** Transition Phase2-Phase 3: As a new somite boundary forms (black arrow) to separate the former s0 from the PSM,

the next *Dact1* expressing presomite (former s-1) becomes the new s0 presomite. Similarly, the former s-2 presomite becomes the new s-1 presomite, and the former s-3 presomite becomes s-2. **F.** Phase 3: *Dact1* expression diminishes throughout the PSM except for in s0. **G.** Diagram of the lateral aspect of the E9.5 tail bud as shown in A-F, with orientation of the PSM and somites relative to other visible structures. Abbreviations: (nt) neural tube, (ua) umbilical artery. **H.** Cartoon of proposed PSM cycling of *Dact1* expression and its relationship to new somite formation. Scale bar in A = 0.5 mm, magnification equivalent for all photomicrographs.

Figure 2. ***Dact1*** **cycles in phase with** ***Axin2*** **but out of phase with** ***Lfng*****.**

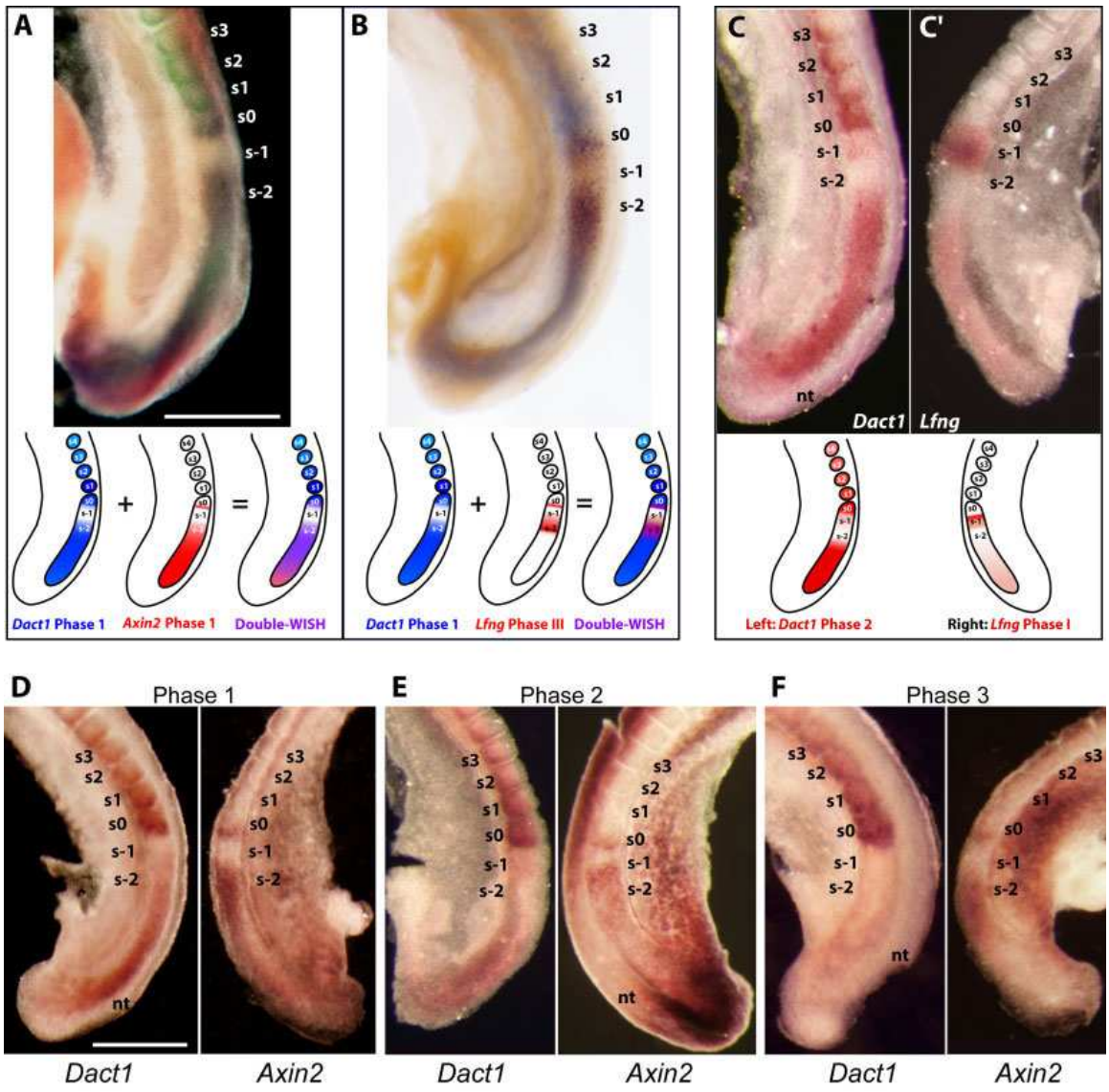

Fig. 2. *Dact1* cycles in phase with *Axin2* but out of phase with *Lfng* **A-B.** Double-WISH for *Dact1* and *Axin2* (A) or *Lfng* (B) ; top: photomicrograph, bottom: explanatory diagram. A. *Dact1* (blue) + *Axin2* (red). Expression in the PSM closely coincides except in the rostral part of s0 (where *Dact1* is exclusively expressed). Both are in a Phase 1 pattern. B. *Dact1* (blue) + *Lfng* (red). Expression overlaps at the caudal boundaries of the s0 and s-1 presomites and in s-2. *Dact1* is strongly expressed in the caudal PSM, where *Lfng* is not

detected. The *Dact1* pattern corresponds to Phase 1 whereas the *Lfng* pattern corresponds to Phase III [Compare to Figure 2G in (Aulehla et al., 2003)]. **C, C'.** Hemisection WISH comparing *Dact1* to *Lfng* on left-right halves of a single embryo; top: photomicrograph, bottom: explanatory diagram. C. *Dact1* (left side). Phase 2, characterized by onset of weak expression in s-1 and recession of caudal PSM staining such that expression is undetectable at the s-2 position (see also Fig 1C,H). C'. *Lfng* (right side). Phase I, characterized by expression in s-1 plus weak expression caudally in the PSM (Dale et al, 2003). *n.b.*: For hemisection experiments, only one side (the left side in this case) includes the neural tube (nt) which does not express *Dact1*, but does express *Axin2* (below). **D-F.** Hemisection WISH series comparing *Dact1* to *Axin2* on the left *vs*. right sides of single embryos. **D.** Phase 1; **E.** Phase 2; **F.** Phase 3. Although *Dact1* and *Axin2* have distinct presomitic distributions in each phase (see text), throughout the somitogenesis clock *Axin2* expression (right) overlaps with *Dact1* (left) caudally in the PSM and in the s0 presomite. Scale bars = 0.5 mm; magnification equivalent in A-C', and in D-F.

Supplemental Figure 1

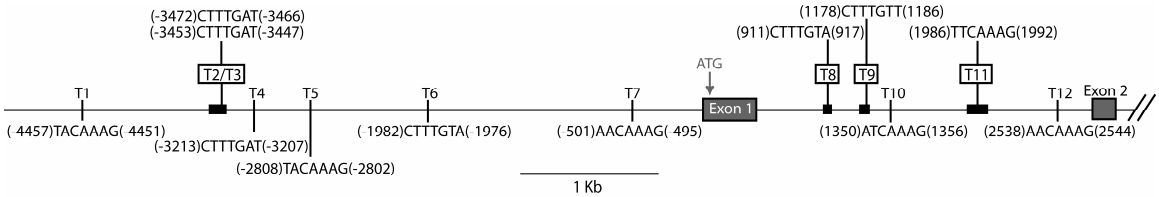

Fig. S1. TCF/LEF binding site consensus map of the mouse *Dact1* promoter region plus intron 1 (to scale). In the 5 kb region upstream of the transcriptional start (position 1: 62 bp 5' of ATG), there are 7 elements (T1-T7) matching the TCF/LEF binding site consensus [(A/T)(A/T)CAAAG or reverse complement] (van de Wetering et al., 1997; Roose and Clevers, 1999; Jho et al., 2002). Another 5 sites (T8-T12) are present in intron 1. Five of the sites (T2, T3, T8, T9, and T11; boxed) occur in the same position in the human *DACT1* locus where they are 100% identical to the mouse sites. Each of these conserved sites is nested within longer stretches of conserved sequence (filled black boxes = mouse:human sequences >90% identical over >50 bp surrounding a TCF/LEF binding site). Other conserved regions are not shown.

References

Aulehla, A. and Herrmann, B.G. (2004). Segmentation in vertebrates: clock and gradient finally joined. Genes Dev. *18*, 2060-2067.

Aulehla, A. and Johnson, R.L. (1999). Dynamic expression of lunatic fringe suggests a link between notch signaling and an autonomous cellular oscillator driving somite segmentation. Dev. Biol. *207*, 49-61.

Aulehla, A., Wehrle, C., Brand-Saberi, B., Kemler, R., Gossler, A., Kanzler, B., and Herrmann, B.G. (2003). Wnt3a plays a major role in the segmentation clock controlling somitogenesis. Dev. Cell *4*, 395-406.

Axelrod, J.D., Matsuno, K., Artavaris-Tsakonas, S., and Perrimon, N. (1996). Interaction between Wingless and Notch signaling pathways mediated by dishevelled. Science *271*, 1826-1832.

Bessho, Y., Sakata, R., Komatsu, S., Shiota, K., Yamada, S., and Kageyama, R. (2001). Dynamic expression and essential functions of Hes7 in somite segmentation. Genes Dev. *15*, 2642-2647.

Brott, B.K. and Sokol, S.Y. (2005). A vertebrate homolog of the cell cycle regulator Dbf4 is an inhibitor of Wnt signaling required for heart development. Dev. Cell *8*, 703-715.

Cheyette, B.N.R., Waxman, J.S., Miller, J.R., Takemaru, K., Sheldahl, L.C., Khlebtsova, N., Fox, E.P., Earnest, T., and Moon, R.T. (2002). Dapper, a Dishevelled-associated

antagonist of beta-catenin and JNK signaling, is required for notochord formation. Dev. Cell *2*, 449-461.

Cohen, B., Bashirullah, A., Dagnino, L., Campbell, C., Fisher, W.W., Leow, C.C., Whiting, E., Ryan, D., Zinyk, D., Boulianne, G., Hui, C.C., Gallie, B., Phillips, R.A., Lipshitz, H.D., and Egan, S.E. (1997). Fringe boundaries coincide with Notch-dependent patterning centres in mammals and alter Notch-dependent development in Drosophila. Nat. Genet. *16*, 283-288.

Cooke, J. and Zeeman, E.C. (1976). A clock and wavefront model for control of the number of repeated structures during animal morphogenesis. J. Theor. Biol. *58*, 455-476.

Dale, J.K., Maroto, M., Dequeant, M.L., Malapert, P., McGrew, M., and Pourquié, O. (2003). Periodic notch inhibition by lunatic fringe underlies the chick segmentation clock. Nature *421*, 275-278.

Duband, J.L., Dufour, S., Hatta, K., Takeichi, M., Edelman, G.M., and Thiery, J.P. (1987). Adhesion molecules during somitogenesis in the avian embryo. J. Cell Biol. *104*, 1361-1374.

Evrard, Y.A., Lun, Y., Aulehla, A., Gan, L., and Johnson, R.L. (1998). lunatic fringe is an essential mediator of somite segmentation and patterning. Nature *394*, 377-381.

Fisher, D.A., Kivimae, S., Hoshino, J., Suriben, R., Martin, P.-M., Baxter, N., and Cheyette, B.N.R. (2006). Three Dact Gene Family Members are Expressed During Embryonic Development and in the Adult Brains of Mice. Dev. Dyn, *235,* 2620-2630.

Forsberg, H., Crozet, F., and Brown, N.A. (1998). Waves of mouse Lunatic fringe expression, in four-hour cycles at two-hour intervals, precede somite boundary formation. Curr. Biol. *8*, 1027-1030.

Galceran, J., Sustmann, C., Hsu, S.C., Folberth, S., and Grosschedl, R. (2004). LEF1-mediated regulation of Delta-like1 links Wnt and Notch signaling in somitogenesis. Genes Dev. *18*, 2718-2723.

Giudicelli, F. and Lewis, J. (2004). The vertebrate segmentation clock. Current Opinion in Genetics & Development *14*, 407-414.

Gloy, J., Hikasa, H., and Sokol, S.Y. (2002). Frodo interacts with Dishevelled to transduce Wnt signals. Nat. Cell Biol. *4*, 351-357.

Greco, T.L., Takada, S., Newhouse, M.M., McMahon, T.A., McMahon, A.P., and Camper, S.A. (1996). Analysis of the vestigial tail mutation demonstrates that Wnt-3a gene dosage regulates mouse axial development. Genes & Development *10*, 313-324.

Hamblet, N.S., Lijam, N., Ruiz-Lozano, P., Wang, J., Yang, Y., Luo, Z., Mei, L., Chien, K.R., Sussman, D.J., and Wynshaw-Boris, A. (2002). Dishevelled 2 is essential for cardiac outflow tract development, somite segmentation and neural tube closure. Development *129*, 5827-5838.

Hikasa, H. and Sokol, S.Y. (2004). The involvement of Frodo in TCF-dependent signaling and neural tissue development. Development *131*, 4725-4734.

Hunter, N.L., Hikasa, H., Dymecki, S.M., and Sokol, S.Y. (2005). Vertebrate homologues of Frodo are dynamically expressed during embryonic development in tissues undergoing extensive morphogenetic movements. Dev. Dyn. *235*, 279-284.

Ishikawa, A., Kitajima, S., Takahashi, Y., Kokubo, H., Kanno, J., Inoue, T., and Saga, Y. (2004). Mouse Nkd1, a Wnt antagonist, exhibits oscillatory gene expression in the PSM under the control of Notch signaling. Mech. Dev. *121*, 1443-1453.

Iulianella, A., Melton, K.R., and Trainor, P.A. (2003). Somitogenesis: breaking new boundaries. Neuron *40*, 11-14.

Jho, E.H., Zhang, T., Domon, C., Joo, C.K., Freund, J.N., and Costantini, F. (2002). Wnt/beta-catenin/Tcf signaling induces the transcription of Axin2, a negative regulator of the signaling pathway. Molecular and Cellular Biology *22*, 1172-1183.

Kakinuma, Y., Saito, F., Osawa, S., Miura, M. (2004). A mechanism of impaired mobility of oligodendrocyte progenitor cells by tenascin C through modification of wnt signaling. FEBS letters *568,* 60-64.

McGrew, M.J., Dale, J.K., Fraboulet, S., and Pourquié, O. (1998). The lunatic fringe gene is a target of the molecular clock linked to somite segmentation in avian embryos. Curr. Biol. *8*, 979-982.

Nakaya, Y., Kuroda, S., Katagiri, Y.T., Kaibuchi, K., and Takahashi, Y. (2004). Mesenchymal-epithelial transition during somitic segmentation is regulated by differential roles of Cdc42 and Rac1. Dev. Cell *7*, 425-438.

Pourquié, O. (2003a). The segmentation clock: converting embryonic time into spatial pattern. Science *301*, 328-330.

Pourquié, O. (2003b). Vertebrate somitogenesis: a novel paradigm for animal segmentation? Int J Dev Biol. *47,* 597-603.

Pourquié, O. and Tam, P.P. (2001). A nomenclature for prospective somites and phases of cyclic gene expression in the presomitic mesoderm. Dev. Cell *1*, 619-620.

Roose, J. and Clevers, H. (1999). TCF transcription factors: molecular switches in carcinogenesis. Biochimica et Biophysica Acta-Reviews on Cancer *1424*, M23-M37.

Rousset, R., Mack, J.A., Wharton, K.A., Axelrod, J.D., Cadigan, K.M., Fish, M.P., Nusse, R., and Scott, M.P. (2001). Naked cuticle targets dishevelled to antagonize Wnt signal transduction. Genes Dev. *15*, 658-671.

Saude, L., Lourenco, R., Goncalves, A., and Palmeirim, I. (2005). terra is a left-right asymmetry gene required for left-right synchronization of the segmentation clock. Nat. Cell Biol. *7*, 918-920.

Serth, K., Schuster-Gossler, K., Cordes, R., and Gossler, A. (2003). Transcriptional oscillation of lunatic fringe is essential for somitogenesis. Genes Dev. *17*, 912-925.

van de Wetering, M., Cavallo, R., Dooijes, D., van Beest, M., van Es, J., Loureiro, J., Ypma, A., Hursh, D., Jones, T., Bejsovec, A., Peifer, M., Mortin, M., and Clevers, H. (1997). Armadillo coactivates transcription driven by the product of the *Drosophila* segment polarity gene dTCF. Cell *88*, 789-799.

Vermot, J. and Pourquié, O. (2005). Retinoic acid coordinates somitogenesis and left-right patterning in vertebrate embryos. Nature *435*, 215-220.

Waxman, J.S., Hocking, A.M., Stoick, C.L., and Moon, R.T. (2004). Zebrafish Dapper1 and Dapper2 play distinct roles in Wnt-mediated developmental processes. Development *131*, 5909-5921.

Wong, H.C., Bourdelas, A., Krauss, A., Lee, H.J., Shao, Y., Wu, D., Mlodzik, M., Shi, D.L., and Zheng, J. (2003). Direct binding of the PDZ domain of Dishevelled to a conserved internal sequence in the C-terminal region of Frizzled. Mol. Cell *12*, 1251-1260.

Yu, H.M., Jerchow, B., Sheu, T.J., Liu, B., Costantini, F., Puzas, J.E., Birchmeier, W., and Hsu, W. (2005). The role of Axin2 in calvarial morphogenesis and craniosynostosis. Development *132*, 1995-2005.

Zhang, L., Gao, X., Wen, J., Ning, Y., and Chen, Y.G. (2006). Dapper 1 antagonizes Wnt signaling by promoting dishevelled degradation. J. Biol. Chem. *281*, 8607-8612.

Zhang, N.A. and Gridley, T. (1998). Defects in somite formation in lunatic fringe deficient mice. Nature *394*, 374-377.

Chapter 4:

Characterization of *Dact1* Null Mice:

Phenotypes, Embryology,

and Signaling.

Chapter 4: Characterization of *Dact1* Null Mice: Phenotypes, Embryology,and Signaling.

This chapter describes the *Dact1* null mice and their phenotypes. *Dact1* null mice were originally designed by Benjamin Cheyette, at the time in the laboratory of Randall T. Moon, at the University of Washington, Seattle. The mice have been bred and analyzed in the Cheyette Laboratory at UCSF. This has been a multi-person, collaborative project, although I have been a participant in it since before the first *Dact1* null mice were born. This work has been submitted for peer-reviewed publication as the following manuscript: *Dact1 balances Wnt/ß-catenin versus planar cell polarity pathways during caudal development* by Rowena Suriben, Daniel A. Fisher, Saul Kivimäe, Uta Grieshammer, Randall T. Moon, and Benjamin N. R. Cheyette. As the title suggests, this manuscript describes mutual antagonism between the Wnt/β-catenin and planar cell polarity (PCP) pathways in the early mouse embryo. The respective contributions of the individual authors are listed at the end of the manuscript, following the acknowledgements. Unlike the preceding chapters, in this chapter, the references are included before the figures. I have included several Supplementary Figures and Tables, which have been submitted as Supplementary Material, but which are integral pieces of the data, or of its description, and hence are included. I have also appended four figures and one table of additional data at the end of this chapter. This additional data was not included in the manuscript (it includes negative and ambiguous results), but nonetheless represents relevant work on my part in the analysis of the *Dact1* null mouse. The results of this study, and of my previous studies, are further discussed in Chapter 5, the Discussion and Conclusions section.

Dact1 balances Wnt/ß-catenin versus planar cell polarity pathways during caudal development

Rowena Suriben[1,2*], Daniel A Fisher[1*], Saul Kivimäe[1*], Uta Grieshammer[3†], Randall T. Moon[4], Benjamin N.R. Cheyette[1,2]

[1]Department of Psychiatry, University of California San Francisco, 1550 4th St, San Francisco, CA, 94158, USA

[2]Graduate Program in Developmental Biology, University of California San Francisco, 1550 4th St, San Francisco, CA, 94158, USA

[3]Department of Anatomy, University of California San Francisco, 1550 4th St, San Francisco, CA, 94158, USA

[4]Howard Hughes Medical Institute and Department of Pharmacology, University of Washington, Seattle WA, 95195, USA

*These authors contributed equally to this work.

†Present address: California Institute for Regenerative Medicine, 210 King Street, San Francisco, CA 94107, USA

Correspondence should be addressed to B.N.R.C. (benjamin.cheyette@ucsf.edu).

Key Words: Dact (Dapper, Frodo), Vangl, Wnt, PCP, primitive streak, sirenomelia, cloacal exstrophy, caudal regression, lower mesodermal defects sequence

The mechanisms by which multiple signaling pathways orchestrate development in the posterior embryo is poorly understood, though the Dishevelled (Dvl) protein, acting in both the Wnt/ß-catenin and Planar Cell Polarity (PCP) pathways, has been implicated. Here we show that a key component of this orchestration is the Dvl-binding protein Dact1 (Dapper/Frodo). Mice with genetically-engineered mutations at the *Dact1* locus have decreases in Wnt/ß-catenin signaling during development and display complex caudal malformations that phenocopy a common spectrum of human birth defects. Surprisingly, mutations in *Dact1* rescue the semidominant *Loop-Tail* mutation in the *Vangl2* gene, which encodes a Dvl-binding transmembrane protein central to the PCP pathway. We show that these two Dvl-binding proteins also bind each other and are coexpressed in ectoderm of the primitive streak region during development. Together, these findings reveal that Dact1 acts to promote the Wnt/ß-catenin pathway and to restrain the PCP pathway in the primitive streak ectoderm, a tissue undergoing both germ-layer specification and convergent-extension movements. Thus, Dact1 is a critical cell-autonomous modulator that helps integrate competing signals and responses during embryonic morphogenesis.

During vertebrate development, tissue formation and patterning occur in a rostral to caudal sequence such that developmental events in the posterior embryo follow those in more anterior regions.[1] Consequently, while more advanced development is proceeding anteriorly, several critical early developmental processes continue at the posterior tip of the embryo. These events include primary tissue specification in the primitive streak, closure of the endoderm ventrally to form hindgut, division of mesoderm into divergently-fated cell populations along the medial-to-lateral axis, segmentation, and closure of the neuroectoderm dorsally to form the neural tube.

Among many mouse mutations that disrupt posterior embryonic events are several that affect Wnt signaling.[2-7]

Wnt signaling refers to a group of intercellular communication pathways that are conserved in multicellular animals and are important during development and in disease. The Wnt/ß-catenin signaling pathway, which influences cell proliferation and fate in many tissues, regulates the phosphorylation of ß-catenin by the kinase Gsk3. This determines the amount of free ß-catenin available in the nucleus to turn on gene expression cooperatively with the LEF/TCF family of transcription factors.[8] A key component of this pathway is Dvl, a cytoplasmic scaffold protein that helps determine the preferred binding partners and substrate of Gsk3, operating downstream of a transmembrane receptor complex composed of members of the Low-Density-Lipoprotein (LRP) and Frizzled (Fz) families.[9] There are alternate Wnt pathways that do not involve ß-catenin, but that generally do also involve Dvl. One such pathway, homologous to the PCP pathway in *Drosophila*, utilizes a distinct set of proteins that includes the transmembrane protein Vangl2, a homolog of the *Drosophila* Van Gogh/Strabismus protein.[10,11] In vertebrates this pathway contributes to convergent-extension movements involved in tissue morphogenesis.

Multiple Wnt pathways are important for caudal morphogenesis. Mouse embryos with mutations in *Wnt3a,* a Wnt/ß-catenin pathway activator, display caudal truncations due to defects in the primitive streak, where Wnt/ß-catenin signaling is necessary for mesoderm specification.[2,3,12] Mice with mutations in *Wnt5a*, which predominantly activates ß-catenin-independent signaling,[13,14] have caudal truncations associated with diminished cell proliferation.[4] Mutations of several genes in either the *Vangl* or *Dvl* families lead to caudal malformations and neural tube defects downstream of disruptions in convergent-extension movements.[5-7,15,16]

Dact (Dapper/Frodo) proteins bind to Dvl and have been reported to modulate multiple signaling pathways, but up to now the contribution of an endogenous Dact family member to signaling in mammalian development has not been investigated.[17-23]

RESULTS

A spectrum of caudal birth defects in *Dact1* mutant mice

We have genetically engineered an allelic series at the mouse *Dact1* locus including two phenotypically-indistinguishable *null* alleles (Supplementary Fig. 1, Supplementary Table 1 online). This study was conducted with one of these null alleles backcrossed to isogenicity in the C57BL/6 mouse strain; homozygotes for the $Dact1^{neo\Delta}$ allele are hereafter referred to as *Dact1* mutants.

Dact1 mutants are present at near Mendelian ratios at birth (Supplementary Table 2 online), but most (90%) are immediately distinguishable from littermates by virtue of a caudal truncation phenotype (Fig. 1a wild type *vs*. b mutant; Supplementary Table 3 online). Skeletal analysis reveals vertebral defects that are most commonly (80%) restricted to the tail segments of mutant animals (Fig. 1c,f wild type *vs*. d,g mutant). A smaller percentage (20%) have truncations extending into sacral and lumbar regions accompanied by variable malformations of the pelvis and hindlimbs that rarely include sirenomelia (hindlimb fusion) (Fig. 1e,h,i). Within this smaller subclass of severely truncated mutants, 80% also have caudal spina bifida (Fig. 1j). There is little evidence of segmentation defects anterior to the level of truncation: vertebrae located just a few segments rostrally are typically of normal morphology even in severely affected animals (Fig. 1d,e,g,h).

With rare exceptions *Dact1* mutant neonates die within a day of birth. Affected neonates have no anus, urinary outlet, nor external genitalia (Fig. 2a wild type *vs*. b mutant). Internally, the vast majority have blind-ended colons (Fig. 2c wild type *vs*. d mutant) and no bladder (Fig. 2e wild type *vs*. f mutant, Supplementary Table 4 online). Ureters are present but connect at the midline or fuse with the reproductive ducts, while the kidneys invariably show signs of hydronephrosis (Fig. 2f), indicating that they produced urine during development that was unable to escape through the malformed outflow tract. The kidneys also display variable developmental malformations ranging from fusion at the midline to complete agenesis (Fig. 2f, Supplementary Table 5 online). In marked contrast to the rest of the genitourinary system, gonads of mutant animals are generally present and grossly normal (Fig. 2f). Rare mutants that survive past the first day of life are usually sick, infertile, or both. These problems are attributable to genitourinary and digestive tract abnormalities that are detectable upon laparotomy (Fig. 2g,h).

Mutants have morphogenetic defects at the primitive streak

The earliest histologically detectable defects in *Dact1* mutant embryos occur around embryonic day (E) 7.5-8.0 when the embryo has 8 somites or less. At this stage, unstained mutant and wild type embryos are indistinguishable anteriorly, but misshapen posteriorly in the primitive streak region. Viewed from the dorsal aspect, the wild type posterior embryo at this stage has a rounded contour (Fig. 3a). In contrast, in *Dact1* mutants it resembles a spade, widening in the middle before tapering to a pointed tip (Fig. 3b). All three germ layers (ectoderm, mesoderm, and endoderm) are present in the caudal embryo (Fig. 3c wild type *vs*. d mutant) although the gross morphology of the primitive streak region is altered. Upon cross section, the most notable morphological changes are apical-basal thinning and lateral broadening of the ectoderm.

However, even in severely affected embryos the ectoderm and underlying mesenchyme of the primitive streak region are remarkably similar to wild type for such parameters as cellularity, cell proliferation, and cell death (Supplementary Fig. 2 online).

To examine developmental sequelae of these early morphogenetic defects in the primitive streak region, we performed whole-mount mRNA in situ hybridization (WISH) on *Dact1* mutants at these and slightly later stages using a marker (*Uncx4.1*) for the segmented paraxial mesoderm (somites) simultaneously with a marker (*Shh*) for the axial mesoderm (notochord) and posterior endoderm (hindgut).[24,25] The caudal-most somite served to gauge extension of the nearby notochord and hindgut. At the 9 somite stage, caudal extension of the notochord is reduced in mutant embryos when compared to wild type embryos at the same stage (Fig. 3e wild type *vs*. f mutant). Furthermore, in wild type embryos the hindgut diverticulum extends caudally beyond the notochord, whereas in *Dact1* mutants these two structures extend to approximately the same level. In their place the caudal embryo is comprised ventrally of mesenchymal tissue (Fig. 3f,h asterisks) that labels with the paraxial mesoderm marker *Dll1* (Fig. 2g wild type *vs*. h mutant). Unlike the truncated axial mesoderm and endoderm, the ectoderm extends normally to the posterior tip of the mutant embryo, even at later stages where the ventral defects are more severe (arrows in Fig. 3g wild type *vs*. h mutant).

These embryological studies demonstrate that in *Dact1* mutant embryos morphogenesis in the primitive streak region is defective. Specifically, while the major germ layers are present in approximately correct ratios and relative positions, the axial mesoderm and endoderm do not extend fully caudally, whereas the paraxial mesoderm and ectoderm extend to the tip of the embryo but are architecturally abnormal. In particular, the thinning and lateral widening of the

ectoderm is reminiscent of defects observed in mutants for the PCP pathway, in which convergent-extension movements in this tissue are disrupted.[7,16]

Dact1 promotes Wnt/ß-catenin signal transduction

Given overlapping caudal phenotypes resulting from mutations in *Wnt3a*[2] and *Wnt5a*,[4] we asked whether *Dact1* genetically interacts with these genes. We reasoned that since heterozygotes for either the *Wnt3a* null allele or the *Wnt5a* null allele are phenotypically normal, a strong exacerbation of the *Dact1* mutant phenotype due to heterozygosity at either of these loci would provide evidence that the corresponding molecules cooperate in a common signaling cascade. Consistent with this hypothesis, there was a large increase in embryonic lethality associated with severe posterior phenotypes in *Dact1* mutants heterozygous for *Wnt3a* (Fig. 4a, Supplementary Fig. 3 online), but no such increase in *Dact1* mutants heterozygous for *Wnt5a* (Fig. 4b). Since the Wnt3a ligand but not the endogenous Wnt5a ligand signals preferentially through ß-catenin,[13,26] this suggested that Dact1, directly or indirectly, contributes to Wnt/ß-catenin signal transduction in the caudal mouse embryo.

We confirmed this by directly measuring Wnt/ß-catenin signaling in *Dact1* mutants. Since our embryological studies show that the primary developmental defect in *Dact1* mutants occurs in the posterior embryo by E8.0, we measured output of the pathway in this anatomical region by taking advantage of a transgenic reporter mouse line (*BAT-gal*) in which the *LacZ* gene is under the control of Wnt/ß-catenin-responsive TCF-optimal promoters.[27] We crossed *BAT-gal* into the *Dact1* mutant mouse line and quantified transcription of *LacZ* mRNA through Quantitative Reverse-Transcriptase PCR (QPCR). We found that *LacZ* mRNA levels are decreased by approximately 40% in *Dact1* mutant caudal embryos at both E8.0 as well as at E9.0 (Fig. 4c,d).

This is similar to a ~50% reduction in the *LacZ* mRNA observed using the same technique at E9.0 in homozygous *Wnt3a* null mutants (Fig. 4e). Conversely, homozygous *Wnt5a* null mutants do not show decreases using the same *BAT-gal* read-out (Fig. 4f). We also used WISH to visually assess transcriptional activity of the *BAT-gal* reporter. At E9.5 when this tissue is easily assayed in whole mounts, *LacZ* WISH revealed reductions in *BAT-gal* reporter activity in the mutant tail bud (Fig. 4g,i wild type *vs*. h,j,k mutant).

Finally, we corroborated results obtained with the *BAT-gal* reporter by using ELISA and Western blotting to directly measure levels of activated (*i.e*. non-membrane associated) ß-catenin in the posterior tissues of *Dact1* mutant embryos at E9.0. Because of the small volume of tissues involved, ß-catenin ELISA was performed using pooled homogenates from three embryos per sample. Consistent with the *BAT-gal* reporter assays, we found an approximately 40% decrease in levels of non-membrane-associated ß-catenin by this method (Fig. 4l). Western blot of embryonic lysates using anti-dephospho-ß-catenin (ABC) antibody further corroborated this result (Fig. 4m,n).[28,29] In contrast, in these same samples we did not observe reductions in the p120catenin or Dvl2 proteins (Supplementary Fig. 4 online), whose levels have been reported to be regulated by Dact proteins in other experimental contexts.[19,23]

Mutual antagonism between Dact1 and Vangl2

Mutations in *Vangl2*, such as the semi-dominant *Loop-Tail* allele ($Vangl2^{Lp}$), produce neural tube and caudal truncation phenotypes, and genetic synergy with $Vangl2^{Lp}$ is evidence for participation in the PCP pathway.[7] We accordingly asked whether the *Dact1* mutation genetically interacts with $Vangl2^{Lp}$. Given their overlapping phenotypes both embryologically and at birth,[16,30,31] we anticipated that mice homozygous for the *Dact1* mutation and

heterozygous for *Vangl2*^{Lp} would display severe defects in convergent-extension movements and neural tube closure, characteristic of strong disruptions in the PCP pathway.

To our surprise, mutations in *Dact1* and *Vangl2* strongly and mutually rescue one another, such that nearly all *Dact1* mutant mice that are heterozygous for *Vangl2*^{Lp} display neither the *Dact1* recessive nor the *Vangl2*^{Lp} semidominant phenotypes. In fact, 90% of *Dact1*$^{-/-}$; *Vangl2*$^{Lp/+}$ mice have long straight tails, no neural tube defects, normal genitourinary and digestive systems, and are in every other respect indistinguishable from wild type animals, while the remaining 10% have only a *Loop-Tail* phenotype but no *Dact1* phenotype (Fig. 5a-f). Although this genetic interaction certainly supports the hypothesis that Dact1 and Vangl2 participate in a common pathway, it suggests that despite apparent phenotypic overlap, they play mutually antagonistic roles in this pathway.

A prerequisite for this hypothesis to be correct is that the two proteins, both of which are thought to act cell autonomously, must be expressed together in the region where their phenotypes originate. By prior report, both Dact1 and Vangl2 are expressed in the posterior neuroectoderm,[30,32] which is contiguous with ectoderm of the primitive streak region.[1] Using combined WISH and immunohistological staining techniques we showed that these genes are in fact coexpressed in ectoderm of the primitive streak region at this stage (Fig. 6a-h).

Having shown that the Dact1 and Vangl2 gene-products are present together in the same cells of the posterior embryo, we next investigated biochemical mechanisms that might explain their remarkable genetic interaction. The extreme robustness of this genetic interaction suggested to us the possibility that the corresponding proteins might be direct binding partners. We tested this hypothesis through co-immunoprecipitation studies similar to those previously used to confirm binding between Dact and Dvl family members,[18] and Dvl and Vangl family members.[33] In side-

by-side assays, recombinantly expressed mouse Dact1 and Vangl2 co-immunoprecipitate (Fig. 6i), and indeed do so to a similar order of magnitude as Dvl2 and Vangl2 (Fig. 6j), or Dact1 and Dvl2 (Fig. 6k).

DISCUSSION

We report here the first study of *Dact1* loss-of-function in a genetic model system. The novel molecular and functional interaction between Dact1 and Vangl2 that we have discovered creates an opportunity to further elucidate signaling mechanisms downstream of Vangl2, an important yet poorly understood transmembrane protein. The morphogenetic phenotype we observe in the primitive streak region, while resembling that caused by PCP pathway reduction, might equally reflect PCP pathway hyperactivity which has also been shown to disrupt convergent-extension movements.[34-37] We have also shown that loss of endogenous Dact1 decreases Wnt/ß-catenin signaling read-outs in this region of the embryo.[20,21] We accordingly propose that in ectoderm of the primitive streak region, intracellular Dact1 interacts with the Vangl2 and Dvl proteins to antagonize the PCP pathway, while simultaneously promoting the Wnt/ß-catenin pathway (Fig. 7a-d).

This model supposes that the reductions we observe in Wnt/ß-catenin signaling in *Dact1* mutant embryos are mediated by inhibitory cross-talk from the PCP pathway, perhaps via competition by Vangl2 for Dvl. This is supported by evidence that the PCP pathway inhibits the Wnt/ß-catenin pathway.[38] and provides the most parsimonious model consistent with data from the present study. Nonetheless, our data do not allow us to exclude an alternate model in which Dact1 plays a separate role in the Wnt/ß-catenin pathway. While more complex, this alternate model is plausible as previous work has shown that Dact family members can also bind to

Wnt/ß-catenin pathway components including the GSK3 kinase and members of the TCF transcription factor family.[18,21] To this extent the Dact1 scaffold protein may truly be said to take part in "a balancing act" by playing complementary roles in both pathways.

Our data *do* allow us to state that the remarkable reciprocal rescue observed between the *Vangl2* and *Dact1* mutations does not simply reflect a general phenomenon of reciprocal inhibition between the PCP and Wnt/ß-catenin pathways in the posterior embryo. Importantly, such reciprocal rescue is not observed when similarly severe mutations in *Wnt3a* (*i.e*. $Wnt3a^{vt/vt}$) are combined with $Vangl2^{Lp/+}$, which instead behave additively (Supplementary Fig. 5 online). Taken together, the genetic and biochemical data strongly support that Dact1 plays a unique role in antagonizing PCP signaling downstream of Vangl2, while balancing this pathway against Wnt/ß-catenin activity in the primitive streak region.

Several key observations in this study were obtained through the purely genetic approach of crossing phenotypically similar but otherwise unrelated mutants and carefully studying outcomes in the progeny. The success of this approach in this case may reflect a unique feature of this embryonic region in vertebrates. The posterior tip of the vertebrate embryo is a confined anatomical structure where several crucial developmental events converge in space and time. This is reflected by the large number of signaling and patterning genes that are simultaneously expressed in this region.[39] This suggests that in order for proper caudal development to proceed, tissue responses to these competing signaling pathways must be tightly choreographed. We propose that one element of this choreography occurs within signal-receiving cells that have intrinsic mechanisms to ensure that they respond appropriately to competing signals driving different developmental processes. In the case of the primitive streak ectoderm, a crucial balance must be struck between mesoderm formation driven by Wnt/ß-catenin signaling[3] and

convergent-extension movements driven by the PCP pathway.[7] Consistent with this model, ectopic neural tubes do not form in *Dact1* mutants as is found in *Wnt3a* mutants with similar overall reductions in Wnt/ß-catenin signaling. This difference may reflect the role of Dact1 in balancing multiple pathways instead of promoting a single pathway, as is expected for Wnt3a.

The broad phenotypic spectrum we observe among genetically identical (isogenic) *Dact1* mutant mice is strikingly reminiscent of a similarly broad spectrum of posterior birth defects that afflict human beings.[40] Etiologies proposed to explain all or part of this human birth defect spectrum have included vascular-steal,[41] persistence and exstrophy of the embryonic cloaca,[42] and defects in formation of the posterior mesoderm.[43] Our findings in *Dact1* mutant mice provide support for a common etiology tied to morphogenetic movements and tissue specification at the primitive streak. They accordingly suggest that causes of these malformations might include mutations or environmental insults that alter the expression or function of *DACT1* and other genes orchestrating signaling in this region of the embryo. The strong functional association between *Dact1, Dvl* and *Vangl2*, all of which are mechanistically linked to neural tube defects as well as to other developmental processes,[30,31,33] further indicates the overall importance of this emerging molecular pathway in the pathogenesis of birth defects.

Methods

Targeting Construct

Approximately 7 kb of *Dact1* genomic DNA from the 129/Sv mouse strain was inserted into pGKneoF2L2DTA2[44] to create the *Dact1* targeting vector (Supplementary Fig. 1 online). Correct targeting through homologous recombination in ES cells was confirmed by Southern blot. Mice

carrying the targeted allele were created using standard embryo manipulation and chimera breeding techniques. An allelic series at the *Dact1* locus was created genetically as described[45] by crossing to the *EIIa::Cre* (The Jackson Laboratory, Bar Harbor, ME) and FLPe transgenic mouse strains in order to excise loxP-flanked and FRT-flanked sequences respectively. Genotyping was performed by genomic PCR using allele-specific primers.

Antibody generation

The Dact1 antibody was created by injecting rabbits with a recombinantly expressed and purified GST-fusion to mouse Dact1 residues 1-328, followed by affinity purification.

General Microscopy and Imaging

As described.[46,47]

Skeleton Preparation

As described.[48]

Whole Mount mRNA in situ Hybridization

As described[47] using previously established probes[24,25,30,46,49] plus *LacZ* nucleotides 576-939.

Tissue Quantification

To measure cell density, 20um serial vibratome sections were collected from the posterior tip of each embryo forward to the level of the notochord in wild type and mutant embryos, stained using phalloidin and Hoescht 33258 (Invitrogen), and then visualized on a Nikon C1si Spectral

Confocal microscope. A single confocal plane from each 20μm section was used for counting to avoid double counting of cells. Total ectoderm and mesenchyme area (in pixels) was measured using ImageJ software (NIH) and the total number of nuclei in that area was also counted. Ectoderm and mesenchyme density was calculated by dividing the total number of nuclei by the total area in AP-matched sections for every sample (n= 2 embryos for each genotype, 5 sections per embryo), and then graphed as the average cell density across sections from the same genotype.

To measure proliferation and apoptosis, embryos were sectioned and stained for phalloidin, Hoescht 33258, and phospho-histone-H3 (Millipore) or active caspase-3 (BD Biosciences), respectively. Sectioning, imaging, and quantification techniques were as described above and graphed as the average percent across all sections from the same genotype.

To measure mesoderm volume, WISH against paraxial mesoderm marker *Dll1* was used to specifically visualize posterior mesoderm in wild type and mutant embryos at 6 somite stage. The dorsal surface area (DSA), lateral surface area (LSA) and anterior-posterior length (APL) of *Dll1* expression was measured directly in pixels from digital micrographs using ImageJ software. The following approximations were then used: DSA ≈ right-left width · APL (XY); LSA.≈ A-P length · dorsal-ventral depth (YZ). Mesoderm volume was then calculated according to the formula: V= XYZ; where V≈ (DSA· LSA)/APL = (XY·YZ)/Y= XYZ

BAT-gal Quantitative RT-PCR

As described[46] with the following modifications: Samples were embryonic tissue posterior to the last-formed somite. 0.5-1μg of total RNA was used for cDNA synthesis. Primers for LacZ were: 5'gctggagtgcgatcttcct3' and 5'cgtgcatctgccagtttga3'.

ß-catenin ELISA

Samples were collected by dividing embryos at the level of the newest intersomitic boundary. Caudal samples were removed in a drop of phosphate-buffered saline and frozen individually on dry ice, then stored at -80℃. Corresponding rostral samples were genotyped by PCR. Samples were thawed on ice in 40uL of hypotonic lysis buffer[50] plus protease inhibitors ("Complete"; Roche), homogenized, then 10uL of 1.25M sucrose, 5mM EDTA added to stabilize protein. Trios of samples were pooled by genotype, then centrifuged at 20,000 X g for 1 hour at 4℃. Supernatants were incubated with 5% concanavilin-A-sepharose (Sigma-Aldrich) for 15 min at 4℃ to extract any membrane residua; whereas pellets were resuspended in RIPA buffer plus protease inhibitors. ELISA was performed using the Total β-catenin Enzyme Immunometric Assay Kit (Assay Designs) according to manufacturer's instructions. Percent soluble β-catenin was calculated as 100% X [soluble β-catenin]/([membrane β-catenin] + [soluble β-catenin]).

Western blot and Co-immunoprecipitations

As described;[18] mouse cDNAs obtained commercially or by RT-PCR from wild type mouse total RNA. Commercial antibodies (sources): Activated ß-Catenin "ABC" (Millipore), Vangl2, HA, FLAG (Santa Cruz Biotech), Dvl2 (Cell Signaling Technology), p120catenin (Transduction Laboratories), α-tubulin (Sigma-Aldrich).

Statistical Analyses

Quantitative results were analyzed using Prism (Graphpad) and analyzed for significance by non-parametric (Mann-Whitney) unpaired two-tailed t-test, except for the ß-catenin ELISA, which

was analyzed by a parametric unpaired two-tailed t-test because each data-point represents pooled data and can therefore be expected to conform to a normal distribution.

Acknowledgments

Eric P. Fox provided technical expertise synthesizing the *Dact1* targeting construct, starting from the pGKneoF2L2DTA2 vector donated by Philippe Soriano. ES cell manipulation and chimera production were accomplished at the University of Washington Transgenic Facility. Francesca Mueller, Edwina Wilcox, and Nichol Baxter assisted with mouse husbandry. Kurt Thorn of the UCSF Nikon Imaging Center provided advice related to confocal microscopy. Susan Dymecki provided the FLPe transgenic mouse line, Andrew McMahon and Terry Yamaguchi the *Wnt3a* and *Wnt5a* mutant lines, and Stefano Piccolo the BAT-gal line. Thomas Gridley provided probes for *Uncx4.1* and *Dll1*. Mireille Montcouquiol provided the Vangl2 antibody used for tissue co-localization. Takashi Mikawa, Samuel Pleasure, and Jeremy Reiter provided helpful comments on the manuscript. Supported by grants to BNRC including NIH MH01750 K08, NIH R01HD055300, a NARSAD Young Investigator Award, the Hellman Family Award for Early Career Faculty, the UCSF Innovations in Basic Science Award, the UCSF Academic Senate Committee on Research Award, the UCSF Research Evaluation Allocation Committee Award, and the UCSF Center for Neurobiology and Psychiatry. R.S. is a recipient of a predoctoral fellowship from the California Institute of Regenerative Medicine. D.A.F. has received funding from the Washington University in Saint Louis MSTP.

Author Contributions

R.S. contributed all embryological histology (except BAT-gal WISH), Dact1/Wnt genetic analyses, BAT-gal Q-RTPCR, and Dact1/Vangl2 embryonic co-localization. D.A.F. contributed neonatal skeletal analyses, BAT-gal WISH, ß-catenin ELISA, and Vangl2 genetic analyses. S.K. contributed all biochemistry (except ß-catenin ELISA), including antigen synthesis, antibody characterization, Western blots, and co-immunoprecipitations. U.G. contributed neonatal urogenital and digestive tract analyses. The *Dact1* targeting construct was designed by B.N.R.C. while in the laboratory of R.T.M. The research of R.S., D.A.F., and S.K. was performed in the laboratory of B.N.R.C., who supervised the project and wrote the text with input and feedback from all co-authors.

References:

1. Le Douarin, N.M., Teillet, M.A. & Catala, M. Neurulation in amniote vertebrates: a novel view deduced from the use of quail-chick chimeras. *Int J Dev Biol* **42**, 909-16 (1998).
2. Takada, S. et al. Wnt-3a regulates somite and tailbud formation in the mouse embryo. *Genes Dev* **8**, 174-89 (1994).
3. Yoshikawa, Y., Fujimori, T., McMahon, A.P. & Takada, S. Evidence that absence of Wnt-3a signaling promotes neuralization instead of paraxial mesoderm development in the mouse. *Dev Biol* **183**, 234-42 (1997).
4. Yamaguchi, T.P., Bradley, A., McMahon, A.P. & Jones, S. A Wnt5a pathway underlies outgrowth of multiple structures in the vertebrate embryo. *Development* **126**, 1211-1223 (1999).
5. Torban, E. et al. Genetic interaction between members of the Vangl family causes neural tube defects in mice. *Proc Natl Acad Sci U S A* **105**, 3449-54 (2008).

6. Hamblet, N.S. et al. Dishevelled 2 is essential for cardiac outflow tract development, somite segmentation and neural tube closure. *Development* **129**, 5827-5838 (2002).

7. Wang, J. et al. Dishevelled genes mediate a conserved mammalian PCP pathway to regulate convergent extension during neurulation. *Development* **133**, 1767-78 (2006).

8. Huang, H. & He, X. Wnt/beta-catenin signaling: new (and old) players and new insights. *Curr Opin Cell Biol* (2008).

9. Wharton, K.A., Jr. Runnin' with the Dvl: proteins that associate with Dsh/Dvl and their significance to Wnt signal transduction. *Dev.Biol.* **253**, 1-17 (2003).

10. Fanto, M. & McNeill, H. Planar polarity from flies to vertebrates. *J Cell Sci* **117**, 527-33 (2004).

11. Veeman, M.T., Axelrod, J.D. & Moon, R.T. A second canon: Functions and mechanisms of beta-catenin-independent wnt signaling. *Developmental Cell* **5**, 367-377 (2003).

12. Greco, T.L. et al. Analysis of the vestigial tail mutation demonstrates that Wnt-3a gene dosage regulates mouse axial development. *Genes Dev* **10**, 313-24 (1996).

13. Liu, G., Bafico, A. & Aaronson, S.A. The mechanism of endogenous receptor activation functionally distinguishes prototype canonical and noncanonical Wnts. *Mol.Cell Biol.* **25**, 3475-3482 (2005).

14. Keeble, T.R. et al. The Wnt Receptor Ryk Is Required for Wnt5a-Mediated Axon Guidance on the Contralateral Side of the Corpus Callosum. *J.Neurosci.* **26**, 5840-5848 (2006).

15. Torban, E., Kor, C. & Gros, P. Van Gogh-like2 (Strabismus) and its role in planar cell polarity and convergent extension in vertebrates. *Trends Genet* **20**, 570-7 (2004).

16. Smith, L.J. & Stein, K.F. Axial elongation in the mouse and its retardation in homozygous looptail mice. *J Embryol Exp Morphol* **10**, 73-87 (1962).

17. Gloy, J., Hikasa, H. & Sokol, S.Y. Frodo interacts with Dishevelled to transduce Wnt signals. *Nat.Cell Biol.* **4**, 351-357 (2002).

18. Cheyette, B.N.R. et al. Dapper, a Dishevelled-associated antagonist of beta-catenin and JNK signaling, is required for notochord formation. *Dev.Cell* **2**, 449-461 (2002).

19. Zhang, L., Gao, X., Wen, J., Ning, Y. & Chen, Y.G. Dapper 1 antagonizes Wnt signaling by promoting dishevelled degradation. *J.Biol.Chem.* **281**, 8607-8612 (2006).

20. Waxman, J.S., Hocking, A.M., Stoick, C.L. & Moon, R.T. Zebrafish Dapper1 and Dapper2 play distinct roles in Wnt-mediated developmental processes. *Development* **131**, 5909-5921 (2004).

21. Hikasa, H. & Sokol, S.Y. The involvement of Frodo in TCF-dependent signaling and neural tissue development. *Development* **131**, 4725-4734 (2004).

22. Zhang, L. et al. Zebrafish Dpr2 inhibits mesoderm induction by promoting degradation of nodal receptors. *Science* **306**, 114-117 (2004).

23. Park, J.I. et al. Frodo Links Dishevelled to the p120-Catenin/Kaiso Pathway: Distinct Catenin Subfamilies Promote Wnt Signals. *Dev.Cell* **11**, 683-695 (2006).

24. Zhang, N. & Gridley, T. Defects in somite formation in lunatic fringe-deficient mice. *Nature* **394**, 374-7 (1998).

25. Echelard, Y. et al. Sonic hedgehog, a member of a family of putative signaling molecules, is implicated in the regulation of CNS polarity. *Cell* **75**, 1417-1430 (1993).

26. Topol, L. et al. Wnt-5a inhibits the canonical Wnt pathway by promoting GSK-3-independent {beta}-catenin degradation. *J.Cell Biol.* **162**, 899-908 (2003).

27. Maretto, S. et al. Mapping Wnt/beta-catenin signaling during mouse development and in colorectal tumors. *Proceedings of the National Academy of Sciences of the United States of America* **100**, 3299-3304 (2003).

28. van Noort, M., Weerkamp, F., Clevers, H.C. & Staal, F.J. Wnt signaling and phosphorylation status of beta-catenin: importance of the correct antibody tools. *Blood* **110**, 2778-9 (2007).

29. Staal, F.J., Noort Mv, M., Strous, G.J. & Clevers, H.C. Wnt signals are transmitted through N-terminally dephosphorylated beta-catenin. *EMBO Rep* **3**, 63-8 (2002).

30. Kibar, Z. et al. Ltap, a mammalian homolog of Drosophila Strabismus/Van Gogh, is altered in the mouse neural tube mutant Loop-tail. *Nat Genet* **28**, 251-5 (2001).

31. Murdoch, J.N., Doudney, K., Paternotte, C., Copp, A.J. & Stanier, P. Severe neural tube defects in the loop-tail mouse result from mutation of Lpp1, a novel gene involved in floor plate specification. *Hum Mol Genet* **10**, 2593-601 (2001).

32. Hunter, N., Hikasa, H., Dymecki, S. & Sokol, S. Vertebrate homologues of Frodo are dynamically expressed during embryonic development in tissues undergoing extensive morphogenetic movements. *Dev Dyn* **235**, 279-84 (2006).

33. Torban, E., Wang, H.J., Groulx, N. & Gros, P. Independent mutations in mouse Vangl2 that cause neural tube defects in looptail mice impair interaction with members of the Dishevelled family. *J Biol Chem* **279**, 52703-13 (2004).

34. Park, E., Kim, G.H., Choi, S.C. & Han, J.K. Role of PKA as a negative regulator of PCP signaling pathway during Xenopus gastrulation movements. *Dev Biol* **292**, 344-57 (2006).

35. Veeman, M.T., Slusarski, D.C., Kaykas, A., Louie, S.H. & Moon, R.T. Zebrafish prickle, a modulator of noncanonical Wnt/Fz signaling, regulates gastrulation movements. *Curr Biol* **13**, 680-5 (2003).

36. Takeuchi, M. et al. The prickle-related gene in vertebrates is essential for gastrulation cell movements. *Curr Biol* **13**, 674-9 (2003).

37. Yan, D. et al. Cell autonomous regulation of multiple Dishevelled-dependent pathways by mammalian Nkd. *Proc Natl Acad Sci U S A* **98**, 3802-7 (2001).

38. Park, M. & Moon, R.T. The planar cell-polarity gene stbm regulates cell behaviour and cell fate in vertebrate embryos. *Nat Cell Biol* **4**, 20-5 (2002).

39. Gofflot, F., Hall, M. & Morriss-Kay, G.M. Genetic patterning of the developing mouse tail at the time of posterior neuropore closure. *Dev Dyn* **210**, 431-45 (1997).

40. Pauli, R.M. Lower mesodermal defects: a common cause of fetal and early neonatal death. *Am J Med Genet* **50**, 154-72 (1994).

41. Stevenson, R.E. et al. Vascular steal: the pathogenetic mechanism producing sirenomelia and associated defects of the viscera and soft tissues. *Pediatrics* **78**, 451-7 (1986).

42. Manzoni, G.A., Ransley, P.G. & Hurwitz, R.S. Cloacal exstrophy and cloacal exstrophy variants: a proposed system of classification. *J Urol* **138**, 1065-8 (1987).

43. Duesterhoeft, S.M., Ernst, L.M., Siebert, J.R. & Kapur, R.P. Five cases of caudal regression with an aberrant abdominal umbilical artery: Further support for a caudal regression-sirenomelia spectrum. *Am J Med Genet A* **143**, 3175-84 (2007).

44. Hoch, R.V. & Soriano, P. Context-specific requirements for Fgfr1 signaling through Frs2 and Frs3 during mouse development. *Development* **133**, 663-73 (2006).

45. Rodriguez, C.I. et al. High-efficiency deleter mice show that FLPe is an alternative to Cre-loxP. *Nat.Genet.* **25**, 139-140 (2000).

46. Fisher, D.A. et al. Three Dact Gene Family Members are Expressed During Embryonic Development and in the Adult Brains of Mice. *Dev.Dyn.* **235**, 2620-2630 (2006).

47. Suriben, R., Fisher, D.A. & Cheyette, B.N. Dact1 presomitic mesoderm expression oscillates in phase with Axin2 in the somitogenesis clock of mice. *Dev Dyn* **235**, 3177-83 (2006).

48. Wallin, J. et al. The role of Pax-1 in axial skeleton development. *Development* **120**, 1109-21 (1994).

49. Bettenhausen, B., Hrabe de Angelis, M., Simon, D., Guenet, J.L. & Gossler, A. Transient and restricted expression during mouse embryogenesis of Dll1, a murine gene closely related to Drosophila Delta. *Development* **121**, 2407-18 (1995).

50. Mikels, A.J. & Nusse, R. Purified Wnt5a protein activates or inhibits beta-catenin-TCF signaling depending on receptor context. *PLoS.Biol.* **4**, e115 (2006).

Figures:

Figure 1

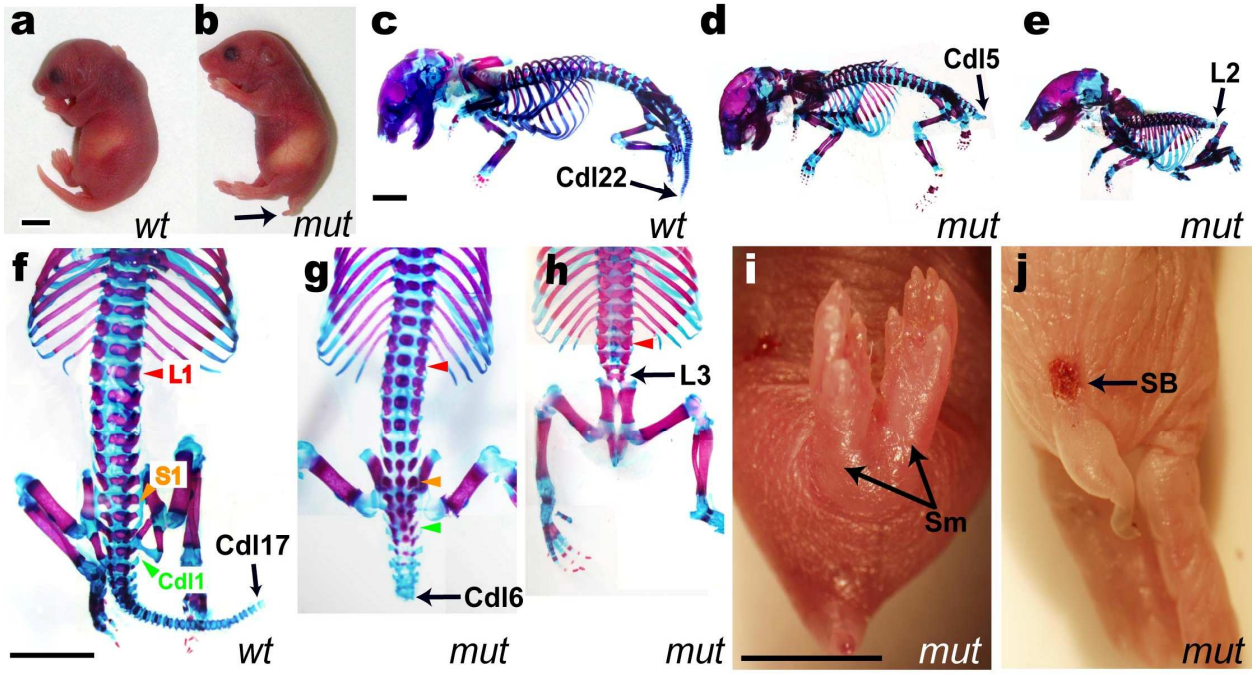

Figure 1 Caudal segmental defects in *Dact1* mutant newborns. wt, wild type; mut, *Dact1* mutant. **a,b**, outward appearance; arrow, short tail. **c-h,** skeletons; arrows indicate the identity of the terminal ossified vertebra, colored arrowheads in **f-h** indicate the position of normal segmental levels: red, lumbar-1 (L1); yellow, sacral-1 (S1); green, caudal-1 (Cdl1). **i,** Sirenomelia (Sm). **j,** Spina bifida (SB). Scale bars: 5mm

Figure 2

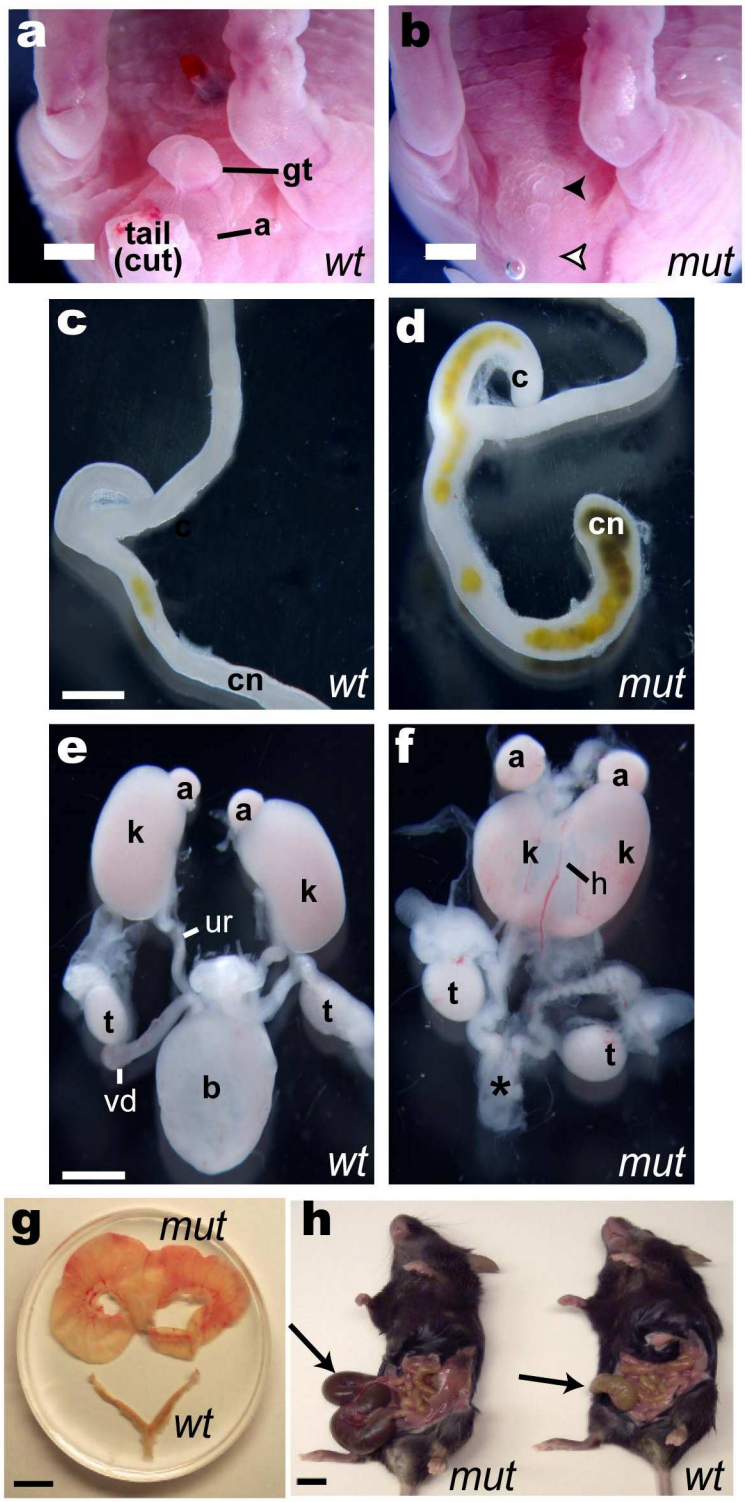
a
gt
tail
(cut)
a
wt
b
mut
c
c
cn
wt
d
c
cn
mut
e
a
a
k
k
ur
t
t
vd
b
wt
f
a
a
k
k
h
t
t
*
mut
g
mut
wt
h
mut
wt

Figure 2 Urogenital and distal digestive tract phenotypes in *Dact1* mutants. a,b, genital tubercle (gt) and anus (a) are missing in mutants (filled arrowhead, empty arrowhead), along with the tail. **c,d,** mutants have a blind-ended colon (cn), and lack a bladder (b vs. *). They have malformed hydronephrotic (h) kidneys (k, fused in this specimen), and misconnected ureters (ur, connected to the vas deferens (vd) in this male). Other abbreviations: (a) adrenal, (c) cecum, (t) testis. Scale bars: **a-f** 5mm, **g,h** 0.5mm

Figure 3

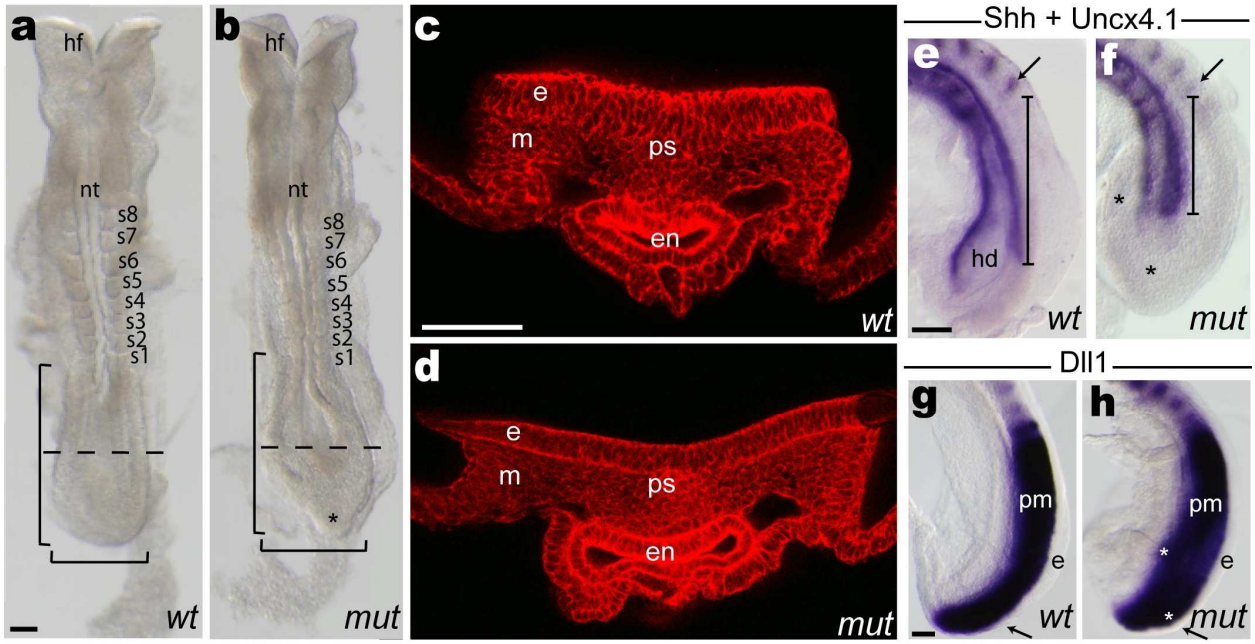

Figure 3 Embryonic phenotypes. a,b, Mutant embryos appear normal except for their posterior contour (brackets), dotted line = plane for c,d. **c,d,** Phalloidin-stained section through posterior embryo: all germ layers are present, but ectoderm (e) is thin and broad. **e,f,** *Shh/Uncx4.1* WISH: notochord (bracket) and hindgut diverticulum (hd) are short, replaced caudally by mesenchyme (asterisks in **b,f,h**). Arrow = caudal-most somite. **g,h,** *Dll1* WISH: paraxial mesoderm (pm) and ectoderm (e) length are normal. Other abbreviations (also for Fig. 5): (hf) head-folds, (nt) neural tube, (s1-s8) somites, (en) endoderm, (m) mesoderm, (ps) primitive streak. Scale bars = 0.1mm.

Figure 4

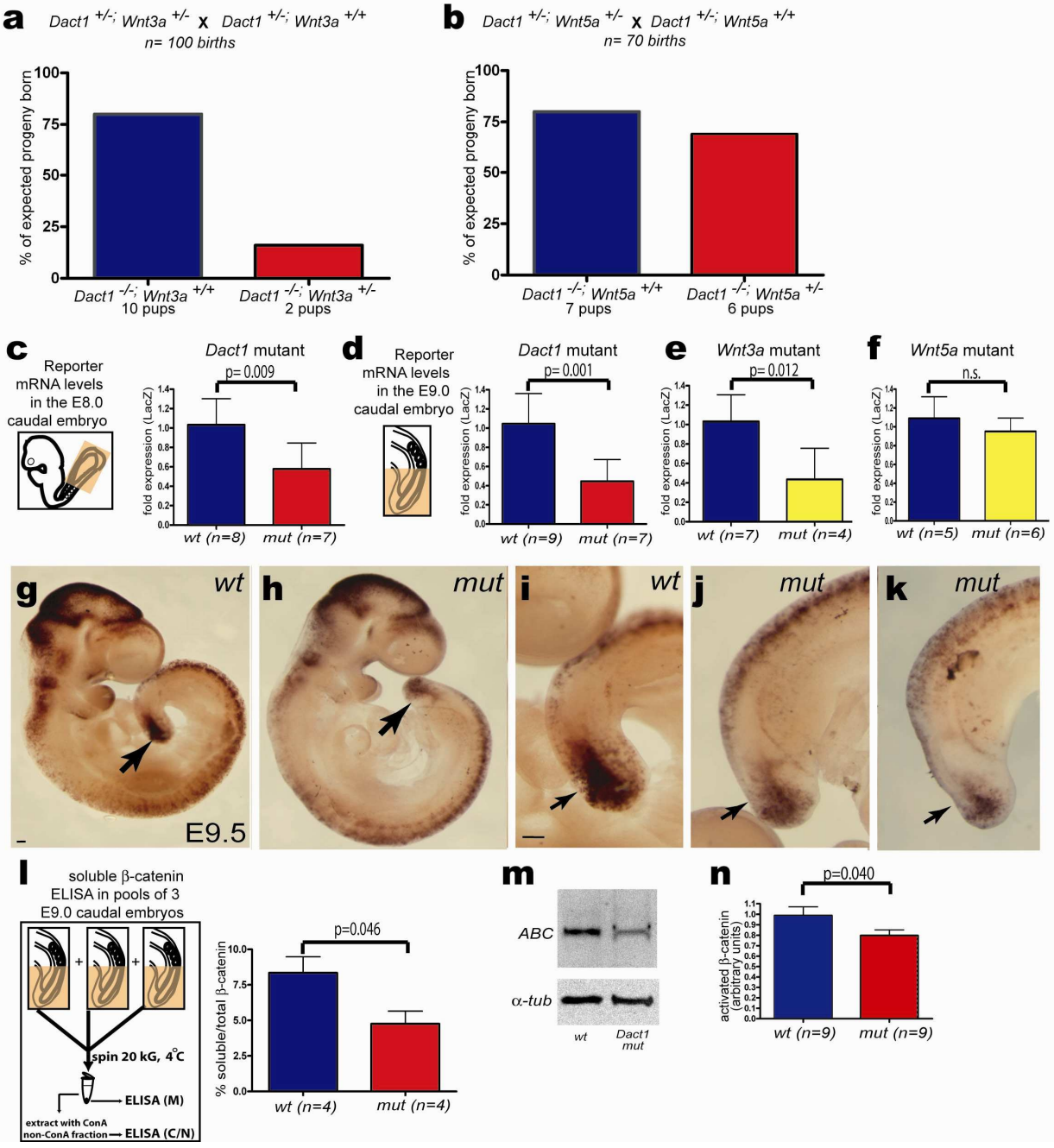
a
Dact1 +/-; Wnt3a +/- x Dact1 +/-; Wnt3a +/+
n= 100 births
% of expected progeny born
Dact1 -/-; Wnt3a +/+ 10 pups
Dact1 -/-; Wnt3a +/- 2 pups
b
Dact1 +/-; Wnt5a +/- x Dact1 +/-; Wnt5a +/+
n= 70 births
Dact1 -/-; Wnt5a +/+ 7 pups
Dact1 -/-; Wnt5a +/- 6 pups
c
Reporter mRNA levels in the E8.0 caudal embryo
Dact1 mutant
p= 0.009
fold expression (LacZ)
wt (n=8)
mut (n=7)
d
Reporter mRNA levels in the E9.0 caudal embryo
Dact1 mutant
p= 0.001
wt (n=9)
mut (n=7)
e
Wnt3a mutant
p= 0.012
wt (n=7)
mut (n=4)
f
Wnt5a mutant
n.s.
wt (n=5)
mut (n=6)
g wt
h mut
i wt
j mut
k mut
E9.5
l
soluble β-catenin ELISA in pools of 3 E9.0 caudal embryos
spin 20 kG, 4°C
ELISA (M)
extract with ConA
non-ConA fraction
ELISA (C/N)
p=0.046
% soluble/total β-catenin
wt (n=4)
mut (n=4)
m
ABC
α-tub
wt
Dact1 mut
n
p=0.040
activated β-catenin (arbitrary units)
wt (n=9)
mut (n=9)

Figure 4 Decreases in Wnt/ß-catenin pathway. **a,** *Dact*$^{-/-}$*; Wnt3a*$^{-/+}$ combination mutants die before birth; **b,** *Dact*$^{-/-}$*; Wnt5a*$^{-/+}$ mutants don't. **c-f:** QPCR of BAT-gal reporter transcript in transgenic embryos; insets: schematic of assay samples used. **c,d,** *Dact1* mutants at E8.0 (**c**), and E9.0 (**d**). **e,** *Wnt3a* mutants; **f**, *Wnt5a* mutants at E9.0. **g-k,** BAT-gal reporter WISH is reduced in E9.5 mutant tail buds (arrows) (**g,h**) whole embryo, (**i-k**) tail bud. **l,** ß-catenin ELISA on E9.0 embryos; inset: assay procedure. **m**. Western blot of activated ß-catenin in E9.0 posterior embryos. **n,** Quantification**.** Error bars = standard deviation; Scale bars = 0.1mm.

Figure 5

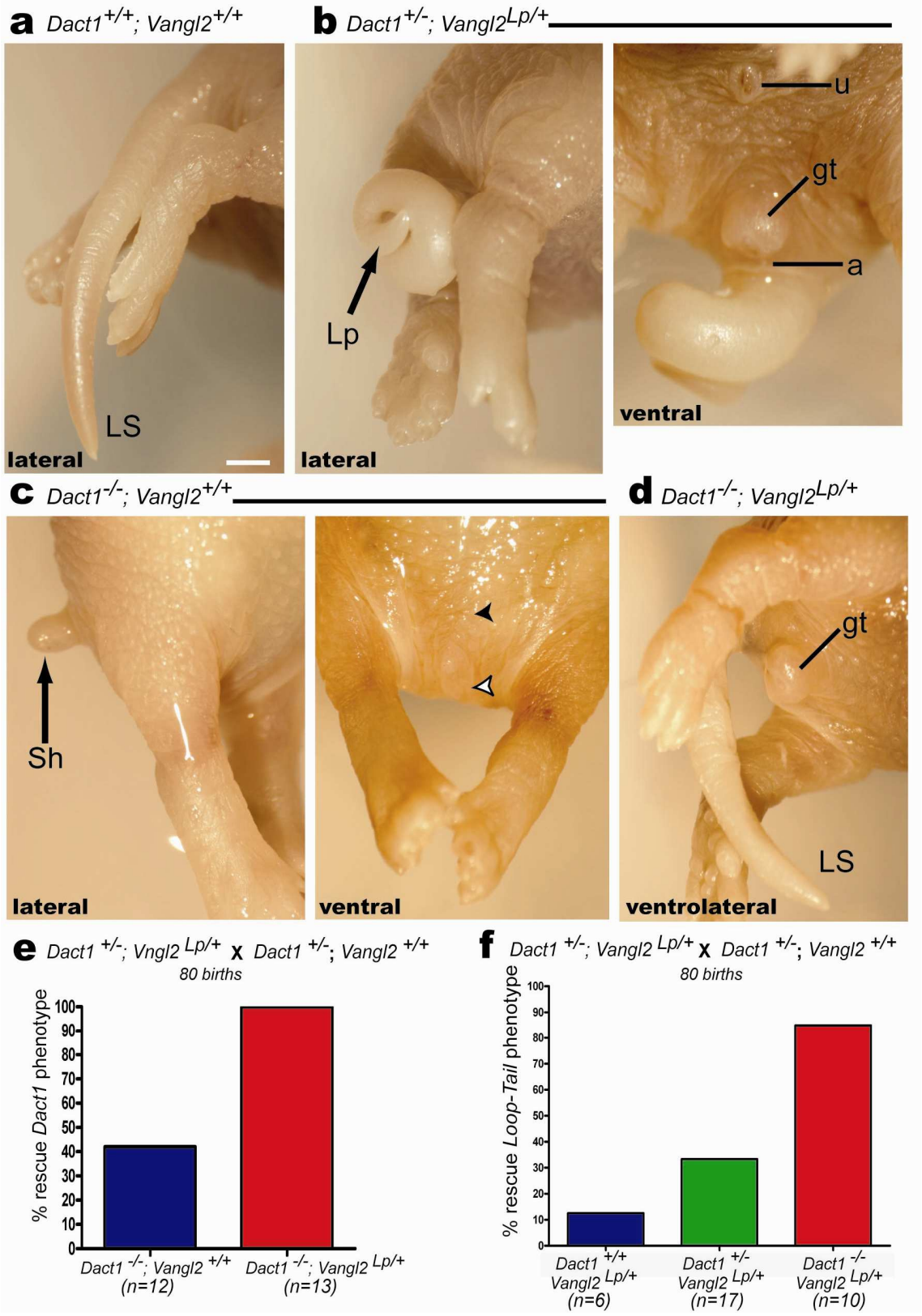
a Dact1+/+; Vangl2+/+
b Dact1+/-; Vangl2Lp/+
LS
lateral
Lp
lateral
u
gt
a
ventral
c Dact1-/-; Vangl2+/+
d Dact1-/-; Vangl2Lp/+
Sh
lateral
ventral
gt
LS
ventrolateral
e Dact1 +/-; Vngl2 Lp/+ x Dact1 +/-; Vangl2 +/+
80 births
% rescue Dact1 phenotype
100
90
80
70
60
50
40
30
20
10
0
Dact1 -/-; Vangl2 +/+ (n=12)
Dact1 -/-; Vangl2 Lp/+ (n=13)
f Dact1 +/-; Vangl2 Lp/+ x Dact1 +/-; Vangl2 +/+
80 births
% rescue Loop-Tail phenotype
100
90
80
70
60
50
40
30
20
10
0
Dact1 +/+ Vangl2 Lp/+ (n=6)
Dact1 +/- Vangl2 Lp/+ (n=17)
Dact1 -/- Vangl2 Lp/+ (n=10)

Figure 5 Dact1 and Vangl2 are mutually antagonistic. a-d, Caudal phenotypes of littermates from a *Dact1*/*Vangl2* mutant intercross. **a,** *Dact1*$^{+/+}$, *Vangl2*$^{+/+}$ neonate (wild type) has a long straight tail (LS). **b**, *Dact1*$^{+/-}$, *Vangl2* $^{Lp/+}$ neonate (trans-heterozygous) has the curled tail (Lp) characteristic of the semidominant *Loop-Tail* phenotype, while the genital tubercle (gt) and anus (a) are normal (as expected for a *Dact1* heterozygote). **c**, *Dact1*$^{-/-}$, *Vangl2*$^{+/+}$ neonate (*i.e*. *Dact1* mutant) has the shortened tail (Sh), missing genital tubercle (filled arrowhead) and missing anus (empty arrowhead) typical of *Dact1* mutants in other genetic backgrounds. **d**, *Dact1*$^{-/-}$, *Vangl2*$^{Lp/+}$ double-mutant neonate (*i.e*. *Dact1* mutant combined with the normally semi-dominant *Loop-Tail* allele) has a normal genital tubercle (gt), a long straight tail (LS). **e,f**, Quantification. **e**, *Vangl2*^{Lp} completely rescues the *Dact1*$^{-/-}$ phenotype. **f,** *Dact1*$^{-/-}$ rescues the *Vangl2*^{Lp} phenotype 90% of the time, with intermediate rescue by *Dact1* heterozygosity (middle bar). Other abbreviations: (u) umbilicus. Scale bar: 1 mm.

Figure 6

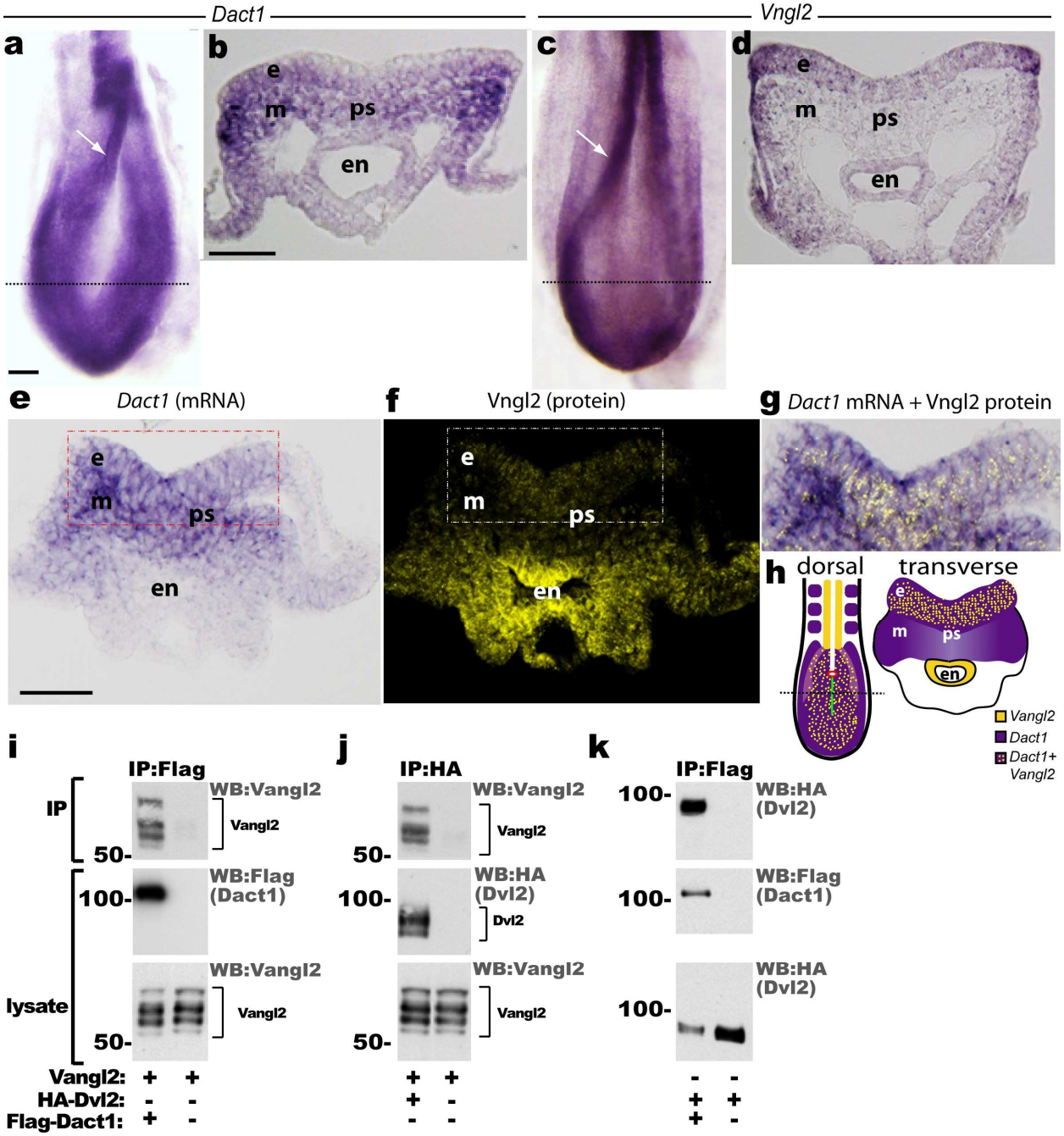
Dact1
Vngl2
a
b
c
d
e
m
ps
en
e Dact1 (mRNA)
f Vngl2 (protein)
g Dact1 mRNA + Vngl2 protein
h
dorsal
transverse
Vangl2
Dact1
Dact1+ Vangl2
i
IP:Flag
IP
WB:Vangl2
Vangl2
50-
WB:Flag (Dact1)
100-
lysate
Vangl2: + +
HA-Dvl2: - -
Flag-Dact1: + -
j
IP:HA
WB:HA (Dvl2)
Dvl2
k
100-
WB:Flag (Dact1)

Figure 6 Dact1 and Vangl2 are coexpressed in ectoderm of primitive streak region. **a,b,** *Dact1* WISH dorsal (**a**), section (**b**). **c,d**, Vangl2 WISH dorsal (**c**), section (**d**). Arrow, neural fold; dotted line, approximate level of sections in **b** & **d**. **e-h,** Combination *Dact1* WISH/Vangl2 immunohistology. **e,** *Dact1*. **f,** Vangl2. **g** overlay. **h,** schematic. **i-k**, Mouse Dact1, Vangl2, and Dvl2 bind with similar affinities when co-expressed as pairs in human embryonic kidney cells. **i,** Flag-tagged Dact1 co-immunoprecipitates Vangl2. **j,** HA-tagged Dvl2 co-immunoprecipitates Vangl2. **k**, Flag-Dact1 co-immunoprecipitates HA-Dvl2. Scale bars = 0.1 mm.

Figure 7

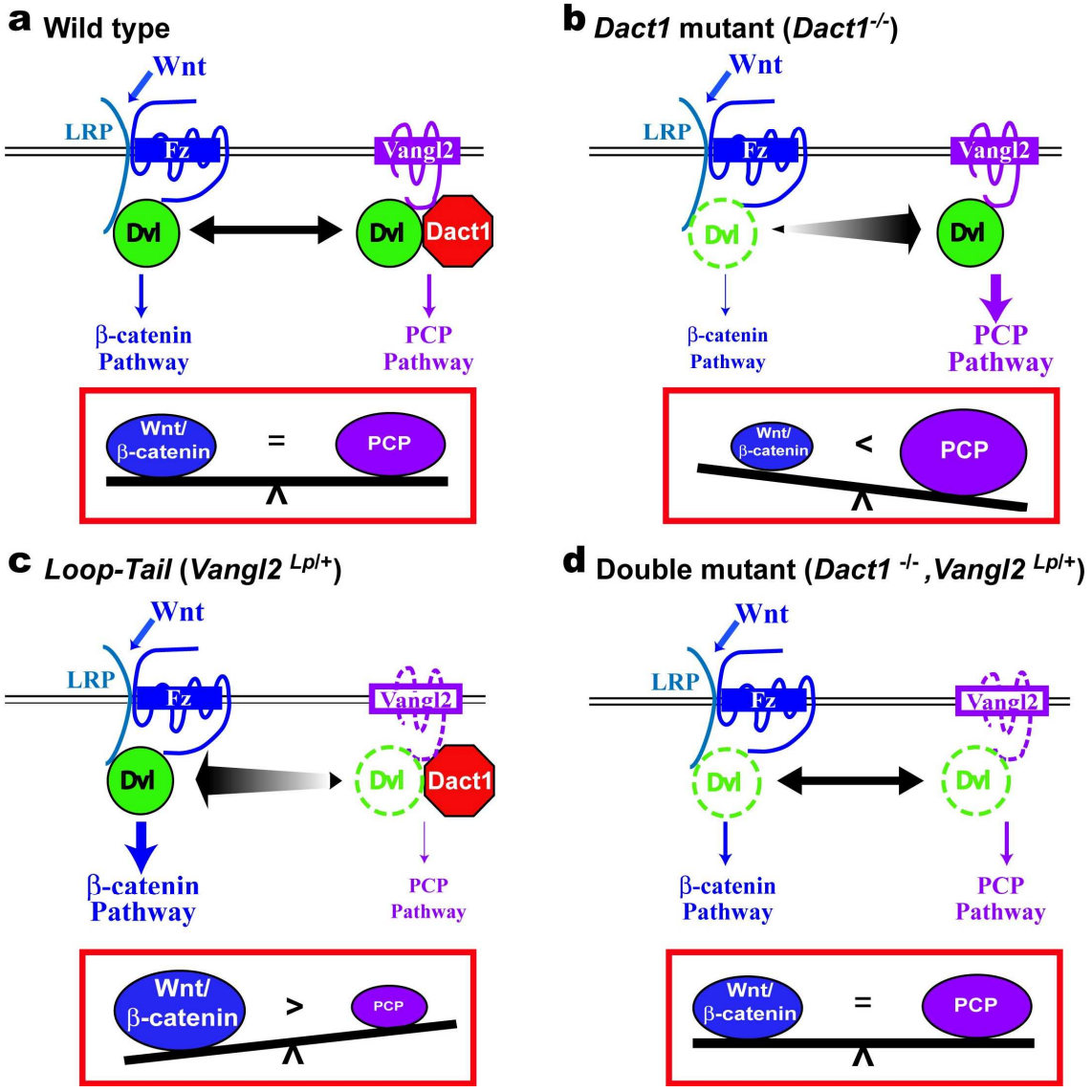

Figure 7 Model of Dact1 function in ectoderm of the primitive streak region. a, in wild type, complexes between Dvl, Dact1, and transmembrane receptors maintain balance between the Wnt/ß-catenin and PCP signaling pathways. **b,** In *Dact1* mutants, this balance is upset in favour of PCP signaling downstream of Vangl2/Dvl. **c,** In semi-dominant *Vangl2* mutants such as *Loop-Tail*, abnormal Vangl2 receptors diminish Dvl-binding and PCP downstream signaling, thereby favouring the Wnt/ß-catenin pathway. **d,** Double mutants restore an essential balance between these pathways, allowing development to proceed normally.

Supplementary Data for Chapter 4:

Supplementary data for manuscript,

Dact1 balances Wnt/ß-catenin versus planar cell polarity pathways during caudal development

Rowena Suriben[1,2*], Daniel A Fisher[1*], Saul Kivimäe[1*], Uta Grieshammer[3†], Randall T. Moon[4], Benjamin N.R. Cheyette[1,2]

Supplementary Figure 1 Gene targeting of the *Dact1* locus in mice.

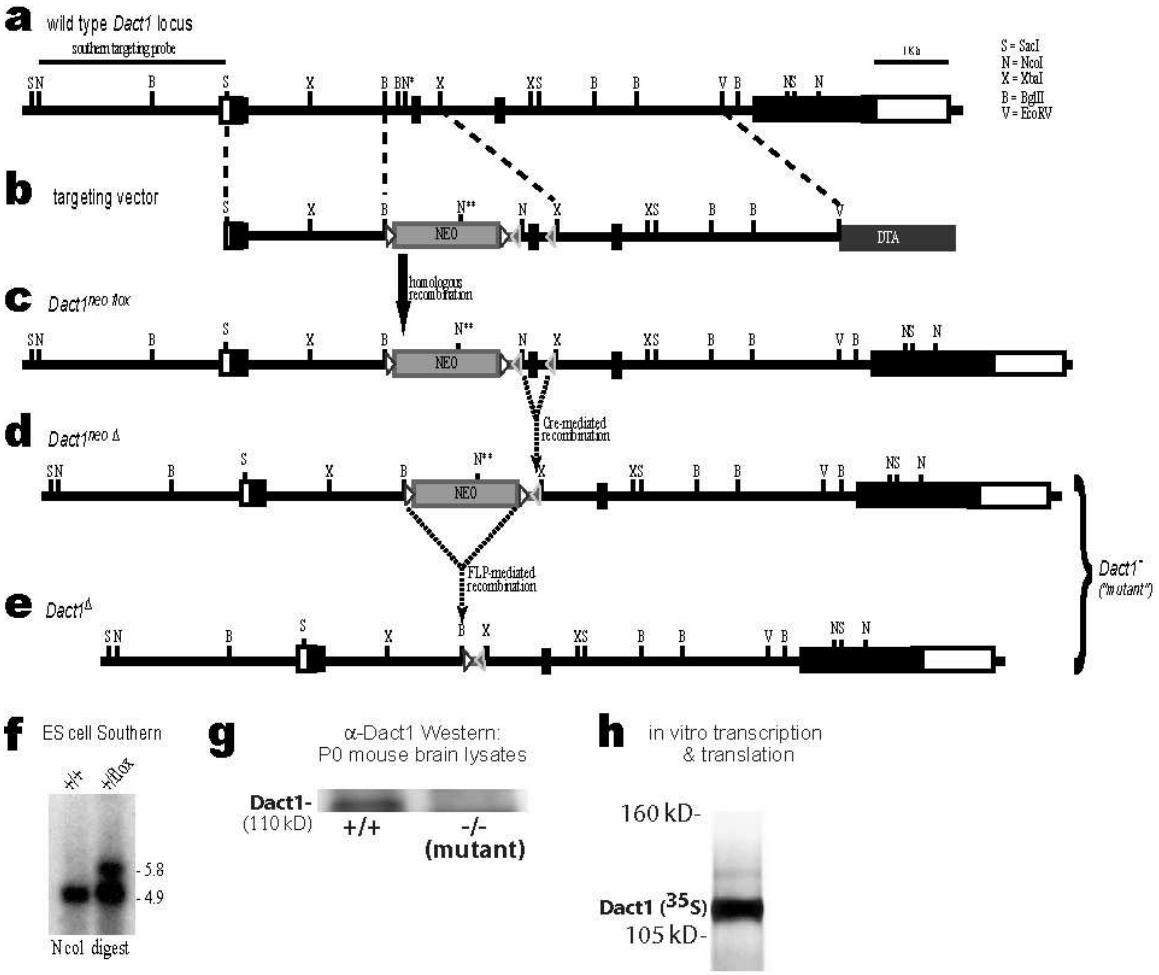

Supplementary Figure 1 Gene targeting of the *Dact1* locus in mice. a-c, Schematic representations of *Dact1* wild type locus and targeting intermediates. **a,** wild type allele. **b,** targeting vector. **c,** $Dact1^{neo\ flox}$ homologously recombined allele. Boxes represent exons: filled are coding; open are non-coding. Dashed lines denote regions in which homologous recombination occurred. Filled triangles represent *loxP* sites; open triangles, *frt* sites. **d,e,** The phenotypically-identical *Dact1* null (-) alleles $Dact1^{neo\ \Delta}$ and $Dact1^{\Delta}$, following excision by the Cre and Flp recombinases, respectively. **f,** Southern genotyping of targeted ES cells. The positions of relevant probes and restriction sites are indicated in **a-e**. **g,** Western blot of neonatal mouse lysate using antibody against mouse Dact1 (see **Methods**). A band at 110 kD, the same size as recombinantly-expressed Dact1, disappears in the homozygous mutant. **h,i,** Sizing of the mouse Dact1 protein by in vitro translation and radioactive labelling of a full-length *Dact1* cDNA (**h**), *cf*. Western blot of Flag-tagged Dact1 (**Fig. 6i,k**).

Supplementary Table 1 Evidence for *nulls*

Type of Data	Evidence that *Dact1*$^{neo\,\Delta}$ and *Dact1*$^{\Delta}$ are *null* alleles
Molecular	Exon 2 has been excised in these alleles. Exon 2 = 44 ⅔ codons. Any residual splicing between exons 1 & 3 will lead to premature frame shift (at codon 109) and stop (4 codons beyond). Any resulting truncated protein will also lack the conserved leucine zipper encoded within exon 2 (codons 109-152).
Biochemical	Western blot with purified anti-Dact1 antiserum shows specific loss of a 110 kD band corresponding to the size of *in vitro* translated and/or recombinantly expressed Dact1 protein (Fig. 5k,m, Supplementary Fig. 1g,h).
Genetic	Production of an allelic series at the *Dact1* locus: *Dact1*$^{wild\ type}$ = *Dact1*^{flox} > *Dact1*$^{neo\ flox}$ (hypomorph) >> *Dact1*$^{\Delta}$ = *Dact1*$^{neo\,\Delta}$. The last 2 alleles in the series demonstrate that excision of exon 2 completely abrogates gene function; additional disruption of the locus by the *frt-neo* cassette has no further phenotypic consequences in the context of exon 2 excision (the same cassette *does* have an effect in the *Dact1*^{flox} allele).

Supplementary Table 2 Mutants are born at near Mendelian ratios

Neonates (N10 backcross to C57Bl/6; n=9 litters)

Genotype	*Dact1*$^{+/+}$	*Dact1*$^{+/-}$	*Dact1*$^{-/-}$
Expected	25%	50%	25%
Observed	25% (n=23)	54% (n=50)	21% (n=19)

Supplementary Table 3 Mutant phenotype spectrum (C57Bl/6 isogenic strain)

Increasing phenotypic severity (total n = 30) →		
no truncation	truncation	
3 (10%)	27 (90%)	
	tail truncation only	lumbar/sacral/ pelvic truncation
	22 (81%)	5 (19%)

Hindlimb phenotypes (N = 5)			Neural tube phenotypes (N = 5)	
body truncation + normal hindlimbs	asymmetric hindlimbs	sirenomelia	closed neural tube	spina bifida
3 (60%)	1 (20%)	1 (20%)	1 (20%)	4 (80%)

Supplementary Table 4 Mutant urogenital/digestive tract phenotypes (n = 18)

Phenotype	Genital tubercle missing (no external genitalia)	Colon ends at bladder	Bladder missing; colon ends blindly	Total with genital/ bladder/ hindgut phenotype
number (%)	18 (100%)	3 (17%)	15 (83%)	18 (100%)

Supplementary Table 5 Mutant kidney malformations (n = 23)

Phenotype*	"horseshoe" kidney (fused at midline)	unilateral (single) kidney	No kidneys	Total with gross kidney malformation or absence
number (%)	16 (70%)	3 (13%)	2 (9%)	21 (91%)

*100% of kidneys are hydronephrotic, presumed secondary to impaired urinary outflow (Supplementary Table 4)

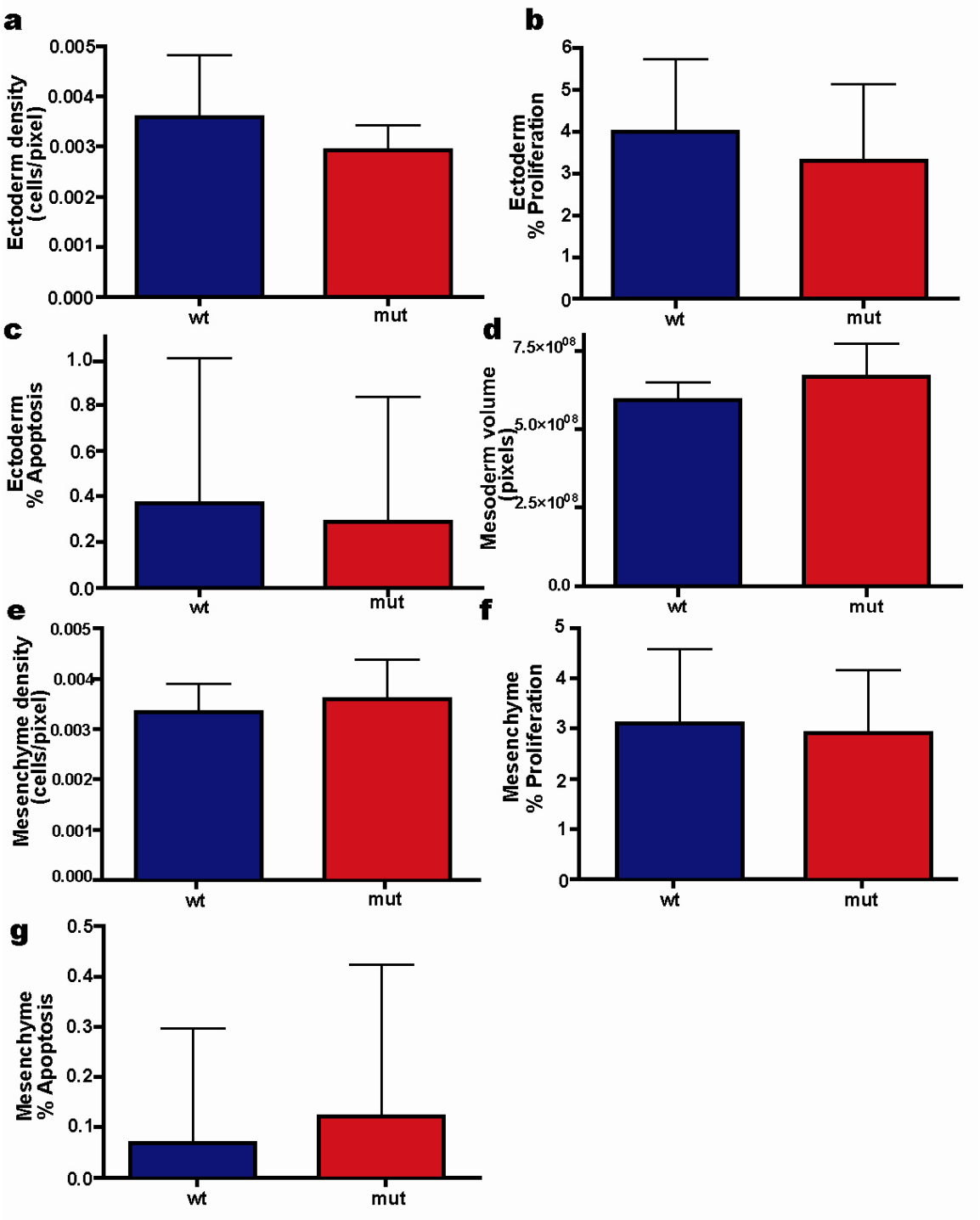

Supplementary Figure 2 Tissue parameters in the primitive streak region. Ectoderm measurements for cell density (**a**), percent of cells undergoing proliferation (**b**) and apoptosis (**c**). Mesenchyme measurements for volume (**d**), cell density (**e**), percent of cells undergoing proliferation (**f**) and apoptosis (**g**). Measurements are from wild type (blue) and mutant (red) embryos at embryonic day 8.0 (6-7 somites). See **Methods**.

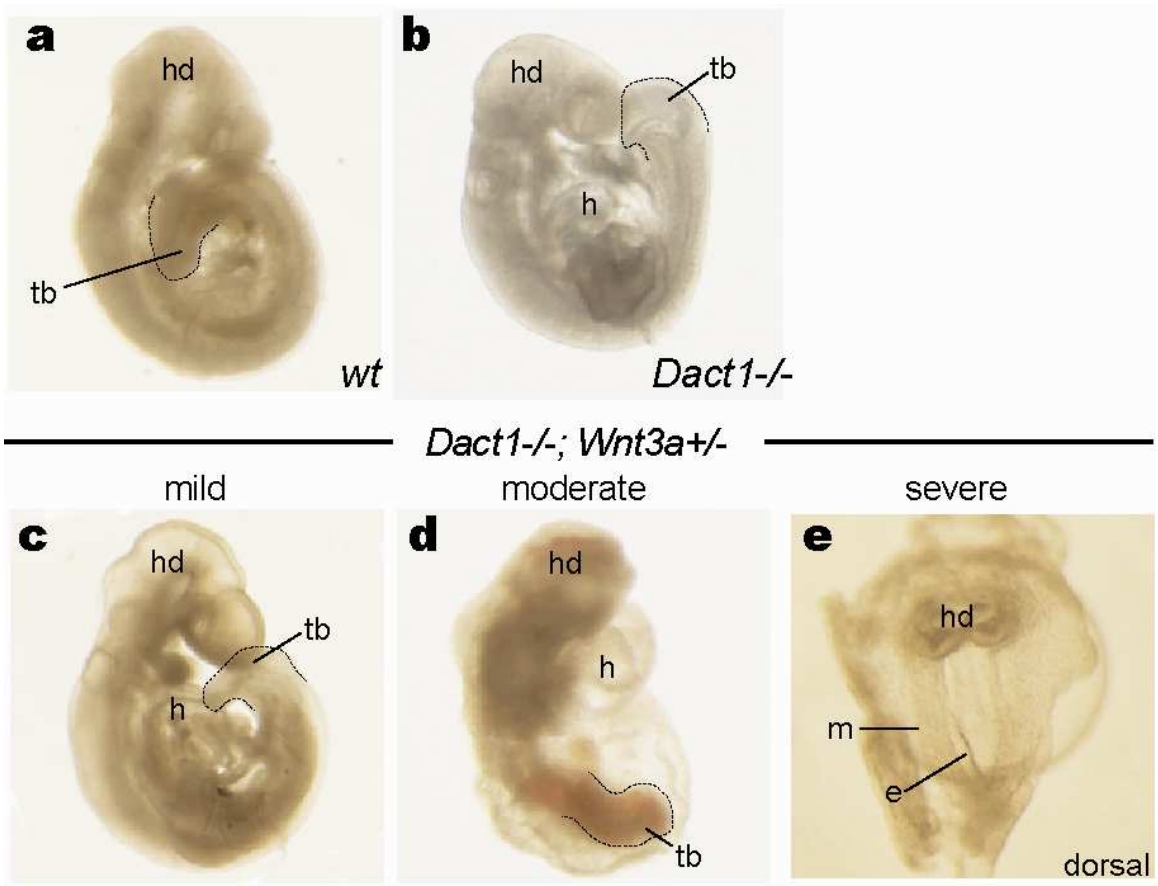

Supplementary Figure 3 Caudal phenotypes of E9.0 embryos from *Dact1*/*Wnt3a* intercross. **a,** *Dact1*$^{+/+}$, *Wnt3a*$^{+/+}$ (wild type) E9.0 embryo with normal tail bud (tb). Dashed line corresponds to contour of tail bud in this and subsequent panels. **b,** Typical *Dact1*$^{-/-}$ E9.0 embryo with abnormal tail bud contour. **c-e,** range of phenotypes observed in *Dact1*$^{-/-}$*; Wnt3a*$^{+/-}$ E9.0 embryos. **c,** Mild phenotype shows disorganized tail bud mesenchyme, more severe than in *Dact1*$^{-/-}$ alone. **d,** Moderate phenotype shows growth arrest and blood pooling in a highly disorganized tail bud. **e,** Severe phenotype shows arrest at late gastrulation stage, lacking somites and failing to turn. Other abbreviations: hd= head, h=heart, m=mesoderm, e=ectoderm

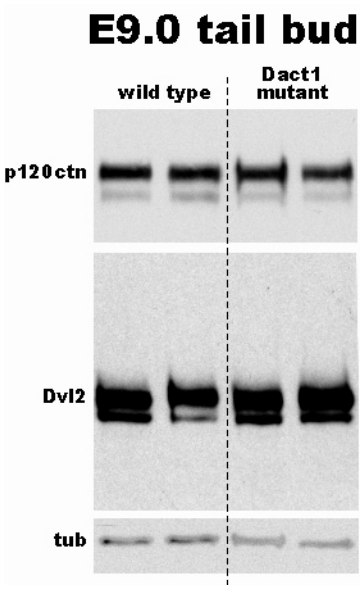

Supplementary Figure 4 Dvl2 and p120catenin levels in the posterior mutant embryo. Western blots of E9.0 posterior embryo lysates (left 2 lanes: wild type, *vs*. right 2 lanes: mutant) performed as in Figure 4m, but using antibodies to detect p120catenin (top) and Dvl2 (middle), both normalized against tubulin (bottom). There is no evidence of changes in levels of these proteins in mutant samples from the posterior embryo.

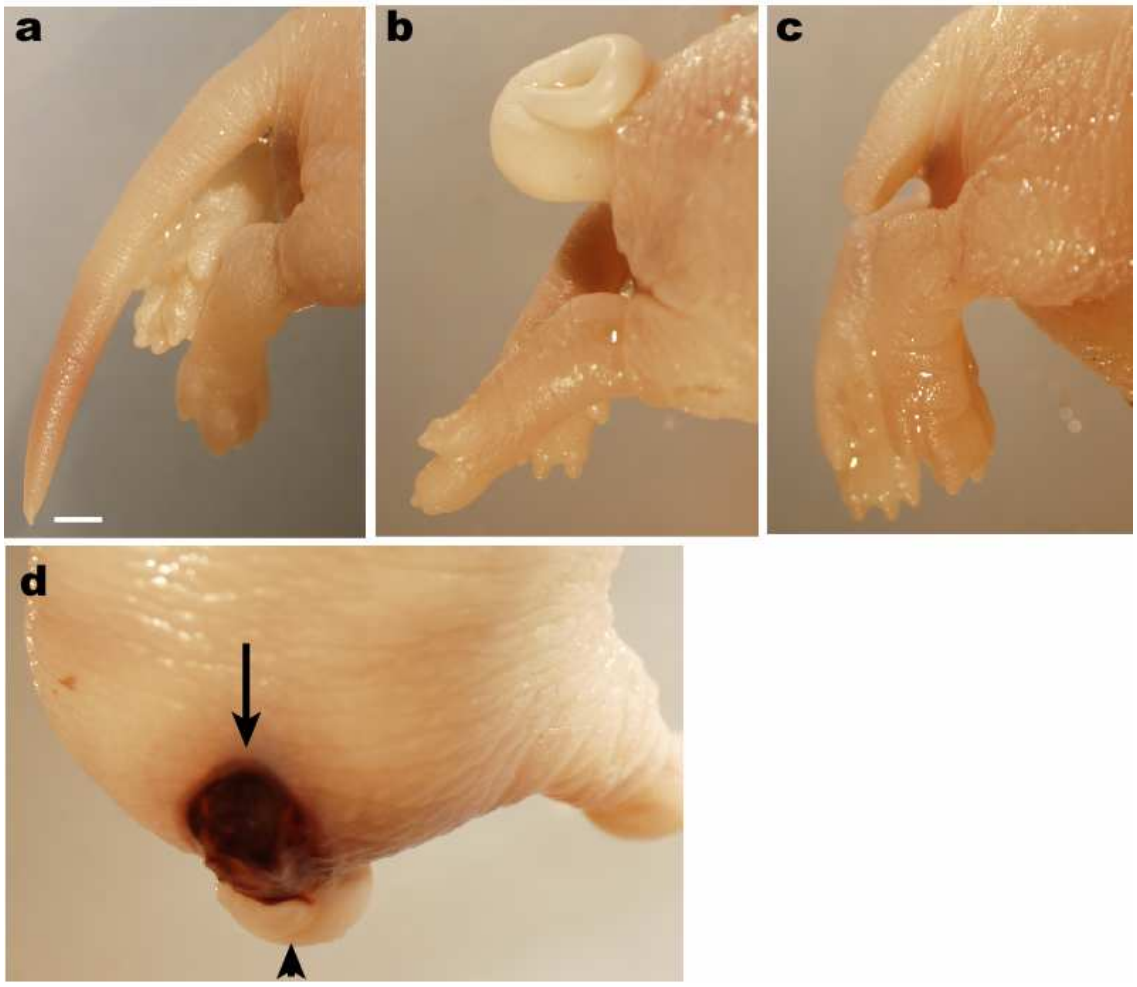

Supplementary Figure 5 Phenotypes from *Wnt3a* $^{vt/vt}$ X *Vangl2* $^{Lp/+}$ *Wnt3a* $^{vt/+}$ cross. a, Neonate with normal tail. **b**, Neonate with curled *Loop-Tail* phenotype typical of *Vangl2* $^{Lp/+}$ (see also Figure 5b). **c,** Neonate with short tail phenotype characteristic of *Wnt3a* $^{vt/vt}$. **d**, Synthetic *Wnt3a* $^{vt/vt}$; *Vangl2* $^{Lp/+}$ phenotype showing spina bifida (arrow) as well as a short, curled tail (arrowhead). Scale bar: 1mm

Chapter 4, Additional Data:

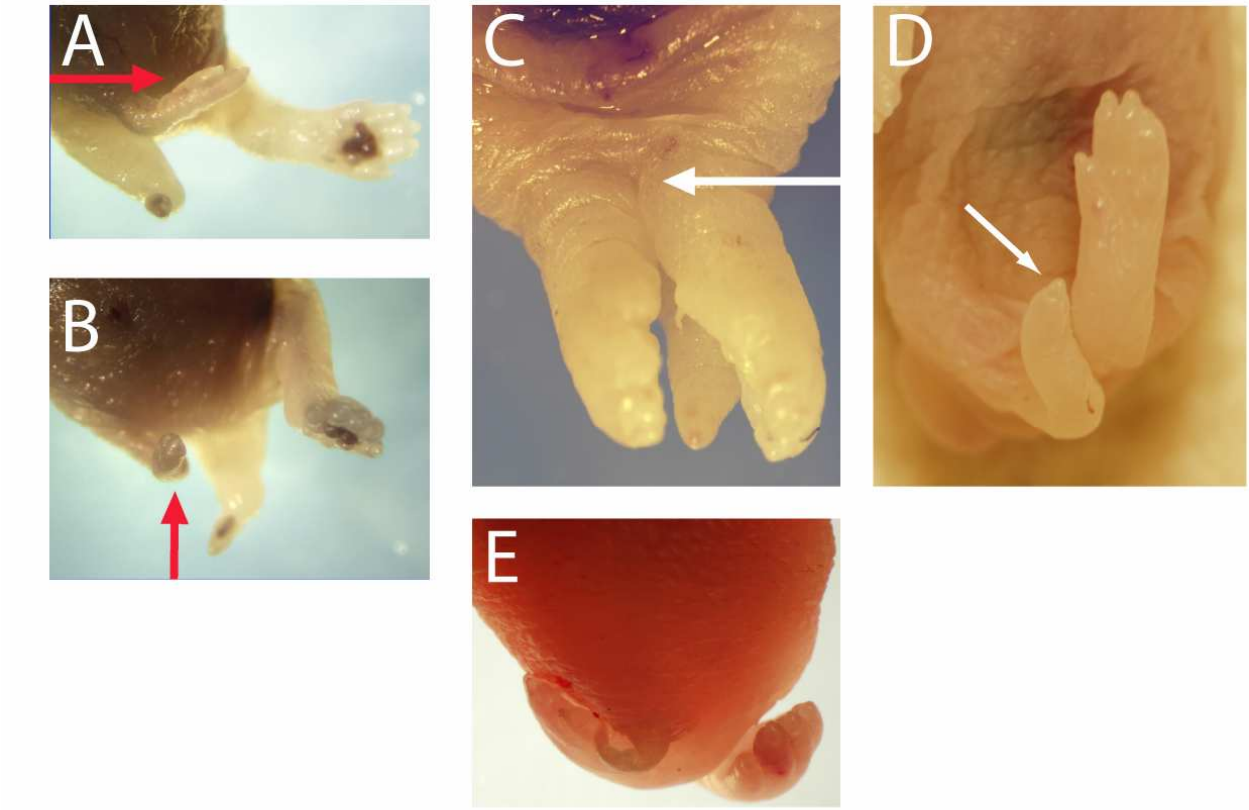

Chapter 4, Additional Data, Fig. 1: Unusual hindlimb defects observed in neonatal *Dact1* -/- mice.

A and B, lateral (A) and ventral (B) views of a neonate showing a unilaterally affected hindlimb including only two toes (red arrows).

C, fused hindlimbs (arrow), a trait sometimes associated with defects in PCP signaling in the embryo.

D, unilaterally affected hindlimb ending in a single digit distally (arrow).

E, crossed hindlimbs, a trait also sometimes associated with defects in PCP signaling in the embryo.

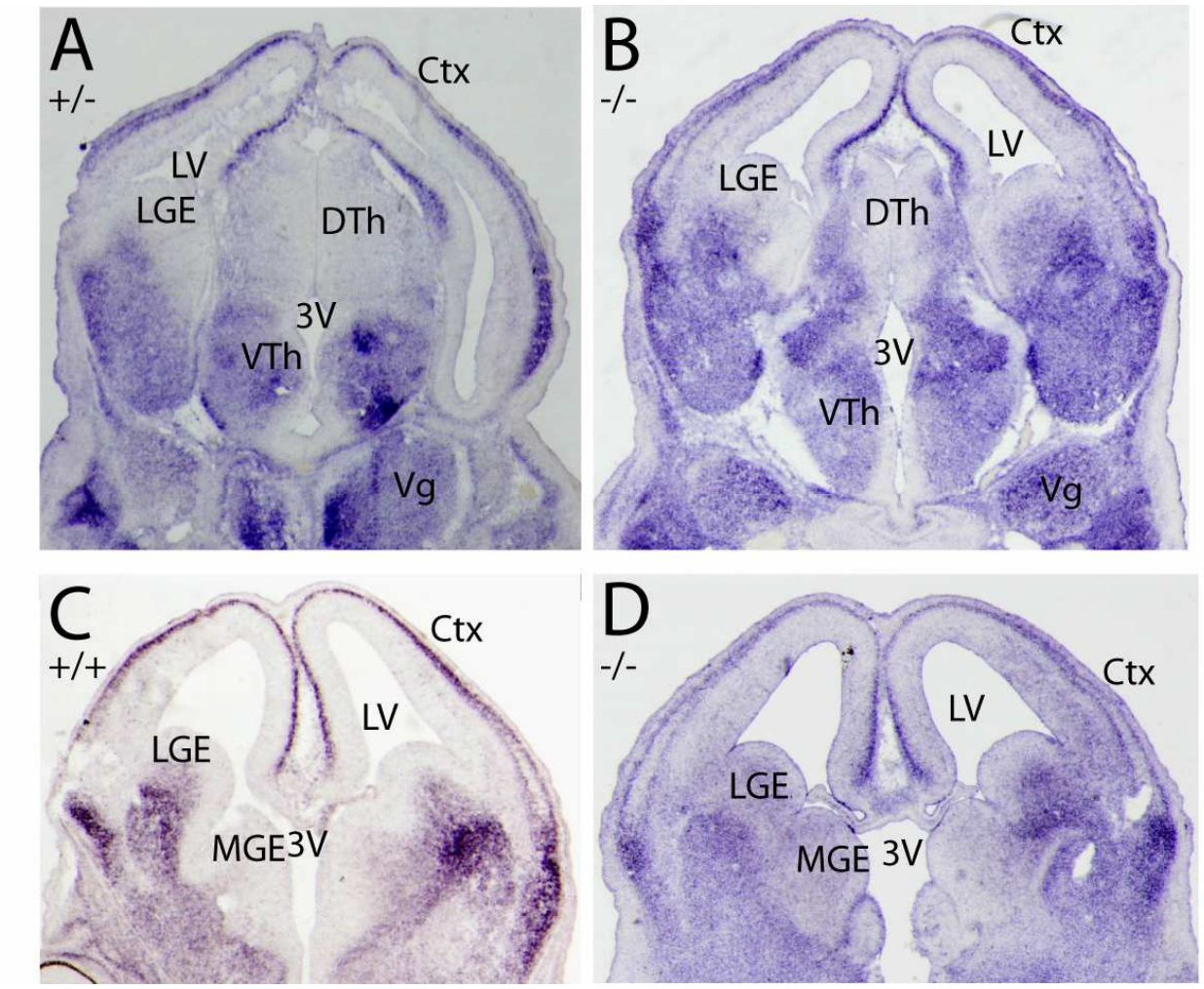

Chapter 4, Additional Data, Fig. 2: Grossly normal structure of *Dact1* expressing brain regions at E14 in *Dact1* -/- embryos.

Images are coronal 20μm thick cryosections of E14 embryonic mouse brains, labeled by in situ hybridization for *Dact1* mRNA. Note that in the *Dact1* -/- embryos, although Dact1 protein is absent, *Dact1* mRNA species are present (see Supplementary Fig. 1) which hybridize with the *Dact1* "C" mRNA probe described in methods of Chapters 2, 3, and 4, and which was used in this experiment.

A and B, equivalent level sections of *Dact1* +/- (A) and *Dact1* -/- (B) embryonic brains.

C and D, equivalent level sections of *Dact1* +/+ (C) and *Dact1* -/- (D) embryonic brains.

Abbreviations: Ctx, cerebral cortex. LV, lateral ventricle. 3V, third ventricle. LGE, lateral ganglionic eminence. MGE, medial ganglionic eminence. DTh, dorsal thalamus. VTh, ventral thalamus. Vg, trigeminal (CN V) ganglion.

Note that locations of cells expressing *Dact1* mRNA are unaltered in *Dact1* -/- embryonic brains.

Chapter 4, Additional Data, Table 1: *Lunatic fringe* cycle phases observed in *Dact1* -/- embryos and their littermates at E9.

Lunatic fringe cycle phase (N):	Phase I	Phase II	Phase III
Dact1 +/+	7	8	13
Dact1 +/-	18	8	25
Dact1 -/-	8	4	10

N.B.: *Lunatic fringe* cycle phases are by convention numbered in roman numerals (see Chapter 3 and its refs. Dale et al., 2003, Aulehla et al., 2003). The normal distribution ratio of Phases I:II:III was defined by Dale et al. (2003) as 1:1:2 in chick, and this ratio was confirmed to be conserved in mouse by Aulehla et al. (2003) and by Rowena Suriben and myself (Chapter 3). The data shown here are consistent with subtle alterations of *Lunatic fringe* cycling in *Dact1* +/- and -/- mutants.

Chapter 4, Additional Data, Fig. 3: *Lunatic fringe* cycle phases observed in *Dact1* -/- E9 embryos.

Chapter 4, Additional Data, Fig. 3: *Lunatic fringe* cycle phases observed in *Dact1* -/- E9 embryos.

This figure shows dorsal and lateral views of caudal portions of E9 embryos containing presomitic mesoderm (PSM) labeled by WISH for *Lunatic fringe* mRNA, and showing *Lunatic fringe* cycle phase patterns. All the embryos shown here are *Dact1* -/- embryos used in the experiment whose results are tabulated in Additional Data, Table 1.

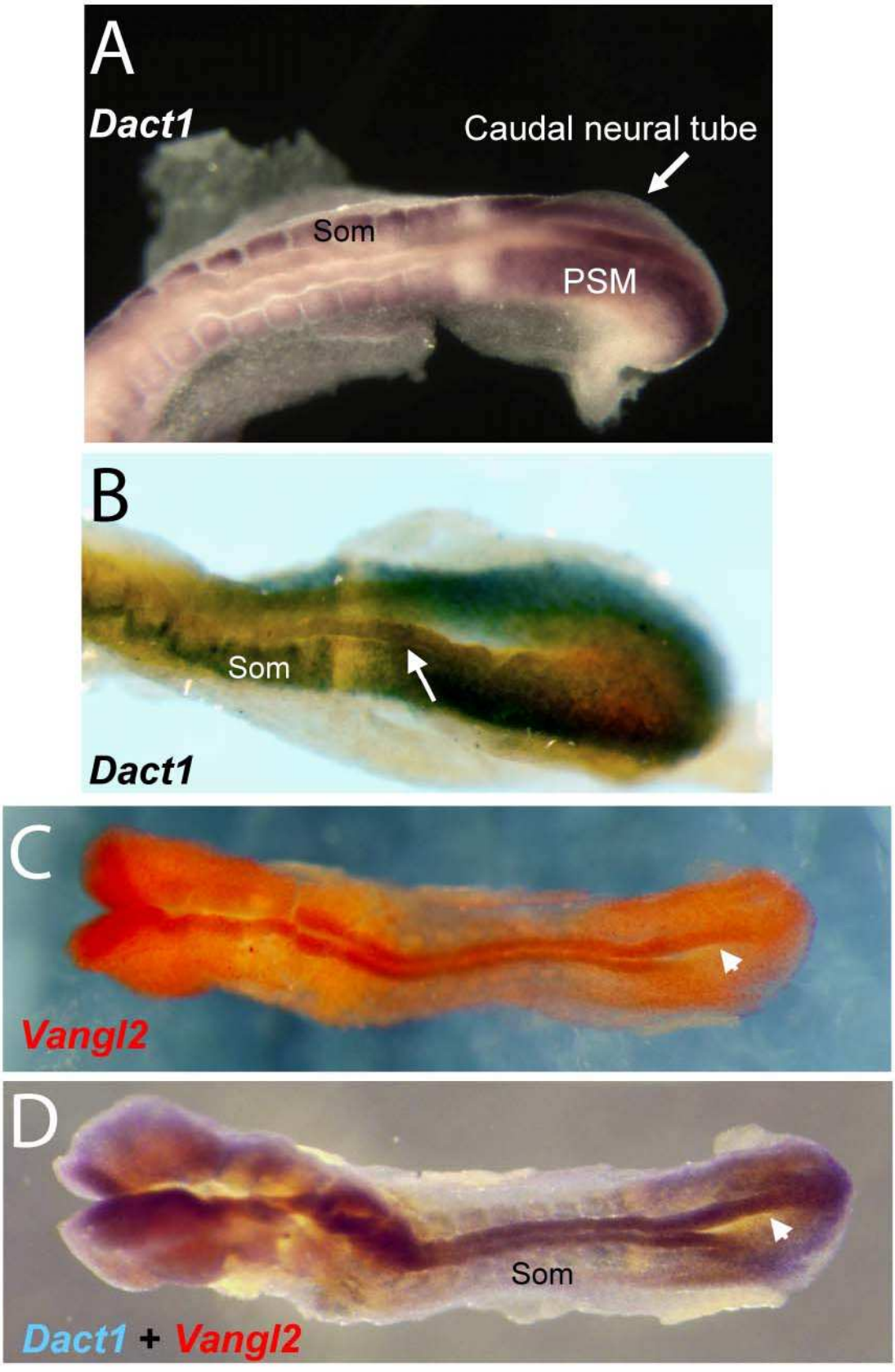
A
Dact1
Caudal neural tube
Som
PSM
B
Som
Dact1
C
Vangl2
D
Som
Dact1 + Vangl2

Chapter 4, Additional Data, Fig. 4: Coexpression of *Dact1* and *Vangl2* in caudal embryos at E8-E8.5 (WISH).

A, B, E8.5 mouse embryos labeled for *Dact1* by WISH. *Dact1* mRNA signal is visible in the presomitic mesoderm (PSM) and somites (Som), but also in the caudal portion of the neural tube (arrow), which is still open in this embryo. *Dact1* mRNA signal is not visible in the more rostral closed neural tube.

C, D, E8.0-8.5 (10 somite) embryo labeled by WISH, initially for *Vangl2* mRNA using Vector Red reagent (C, also see Chapter 3, methods) and subsequently labeled for *Dact1* mRNA using Vector Blue reagent (D, also see Chapter 3, methods). The same individual embryo is shown in both images C and D. Coexpression of *Dact1* and *Vangl2* in D is evident in the areas which are violet in color, due to the overlapping red signal from *Vangl2* and blue signal from *Dact1*. *Dact1*, but not *Vangl2*, is expressed in the somites (Som), which show the light blue colored stain in D. In contrast, the caudal neural tube (arrowheads) is stained in red in C and violet in D, hence it is an area of coexpression of the two genes.

Chapter 5:

Discussion and Conclusions.

1. **Fundamentals of the studies undertaken.**
2. **The Dvl's choice: the mystery of Dishevelled and Wnt pathway selectivity.**
3. **The *Dact1* null phenotypes: direct and indirect effects of the mutation.**
4. **Dact1 effects on Wnt signaling modalities.**
5. **A "mutual antagonism" hypothesis coupling gastrulation and neurulation.**
6. **Why no ectopic neural tubes?**
7. **Relevance of the studies for neuroscience.**
8. **Conclusion.**

Discussion and Conclusions

Fundamentals of the studies undertaken.

I have characterized the *Dact* gene family in the development of the mouse. The *Dact* gene family was originally described in *Xenopus laevis* (Cheyette et al., 2002; Gloy et al., 2002). The identification of mouse and human *Dact1* was part of one of the original studies, that by my mentor, Benjamin Cheyette, and his colleagues (Cheyette et al., 2002). An extensive characterization of the gene family was yet to be undertaken. The original studies identified two highly similar, but distinct, Dact1 homologs in *Xenopus laevis,* named Dapper and Frodo by the authors of these studies (Cheyette et al., 2002; Gloy et al., 2002). *Xenopus laevis* Dapper and Frodo proteins are roughly 90% identical to each other at the amino acid level. They were both identified by their binding to Dishevelled proteins, which are functionally at a central point in the activation of

multiple signaling pathways downstream of Wnt/Frizzled interactions (Wallingford and Habas, 2005 for review). The activity of all, or nearly all, Wnt signaling pathways is dependent on Dishevelled proteins.

Subsequently, *Dact* family genes have been identified from multiple species. In particular, *Danio rerio* (zebrafish) *Dact1* and *Dact2* genes were identified, which are homologs of mouse and human *Dact1* and *Dact2* genes (Gillhouse et al., 2004; Waxman et al., 2004). *Danio rerio* (zebrafish) apparently has at least two other *Dact* family genes, based on overlapping sequences in genomic DNA databases (B. Cheyette, unpublished). Based on homologous sequences in mouse and human genomic DNA databases, Benjamin Cheyette was also able to identify *Dact3*, of which I have characterized the developmental mRNA expression in the mouse, along with *Dact1* and *Dact2* (Fisher et al., 2006 and Chapter 2). So far no *Dact* family homologs have been described in any invertebrate species. The *Dact* gene family appears to be distantly evolutionarily related to *Sec8* (B. Cheyette, unpublished observation) and to *Dystrophin* and *Utrophin* molecules (Gloy et al., 2002).

I have designed mRNA probes for mouse *Dact1*, *Dact2*, and *Dact3* (Fisher et al., 2006 and Chapter 2). Multiple non-overlapping antisense probes for each gene were tested on whole mount embryos, floating sections of embryos, and floating sections of adult mouse brains. Identical expression patterns were confirmed for each probe employed in my subsequent studies. Sense probes were also used as negative controls (Fisher et al., 2006, Supplemental Data included in Chapter 2). These safeguards were

necessary because the expression patterns for these genes had not previously been described in the mouse.

The most strikingly distinct expression patterns I observed in mouse embryonic development were for *Dact1* and *Dact2*. Expression of *Dact1* mRNA was observed in the embryonic tail bud, presomitic mesoderm, and caudal somites from E8 to E10, and also in the neural crest and its derivatives, particularly the branchial arches (Fisher et al., 2006; also see Hunter et al., 2006; Suriben et al., 2006). Later, *Dact1* mRNA was observed in neurons of the embryonic CNS, and in a columnar, striated pattern in CNS neuroepithelia (Chapter 2, especially additional data). *Dact2* mRNA, in contrast, was nearly absent from the brain, but highly expressed in spinal cord grey matter, PNS ganglia, salivary glands, thymus, and the ductal system of the kidneys (Chapter 2: Fisher et al., 2006). *Dact3* expression overlapped substantially with that for one or both of the other two *Dact* genes. *Dact3* was often more diffusely expressed as compared with *Dact1* or *Dact2* in tissues where *Dact1* or *Dact2* was expressed in specific cell populations. This was particularly evident in the embryonic CNS, where *Dact1* was highly expressed in neurons and populations of cells in neuroepithelia, while in contrast *Dact3* was expressed diffusely throughout the CNS (Chapter 2). This observation leads to the hypothesis that Dact3 may act as a "backup Dact", for Dact1 and/or Dact2. This would mean that a nearly ubiquitous, low level expression of *Dact3* might compensate for loss of *Dact1* or *Dact2* in many tissues. My colleague Saul Kivimäe has constructed *Dact3* null mice, and is breeding *Dact1*/*Dact3* double null mice, which grossly resemble *Dact1* nulls neonatally (unpublished observation). It will be highly interesting to observe

whether these mice exhibit phenotypes, particularly in the brain, that have been hypothesized for, but not observed in, *Dact1* null mice.

In early mouse embryos, *Dact1* is predominantly expressed in the embryonic tail bud, presomitic mesoderm (PSM), and caudal somites, from E8 to E10. Since a number of genes had been shown to be expressed cyclically in the PSM during somitogenesis, including the Wnt/β-catenin signaling inhibitor *Axin2* (Aulehla et al., 2003), it was logical to inquire whether *Dact1* exhibited a similar cyclic expression in somitogenesis. I confirmed that *Dact1* expression in the PSM is variable and exhibits phase patterns with an approximate resemblance to those for *Axin2*. My collaborator Rowena Suriben and I showed that *Dact1* is expressed in phase with *Axin2*, in what was characterized by Olivier Pourquie and colleagues as the "Wnt cluster" of genes: genes that are predominantly Wnt signaling effectors and are expressed in phase with *Axin2* in the somite segmentation cycle (Dequeant et al., 2006). The results of the expression study by Rowena Suriben and me were published in *Developmental Dynamics* (Suriben et al., 2006).

Along with, and following, my characterization of *Dact* family gene expression in mouse development, I characterized the phenotypes of *Dact1* null mice. *Dact1* null mice die neonatally. I characterized the skeletal phenotypes of the *Dact1* null neonates, and their gross anatomy. *Dact1* null neonates have short, kinked, or absent tails. Most of them also have undeveloped perinea, lacking external genitalia and external openings for digestive and urogenital systems; the finding of hydronephrosis in the kidneys marks excretory failure as a likely cause of neonatal mortality. The skeletons of *Dact1* null

neonates show truncation at levels in the lumbar regions or more caudal, and in some cases vertebral disorganization extending 2-3 vertebral levels rostral from the truncation, but rarely farther rostral than that (see Intro. Fig. 2 and Chapter 4). There were not rib defects such as the rib fusions observed in *Dvl2* null mice (Hamblet et al., 2003) or *Sfrp1*/*Sfrp2* double nulls (Satoh et al., 2006).

There were two subsequent evident questions concerning the etiology of the *Dact1* null phenotypes. First, what is the etiology of the *Dact1* null phenotypes, embryologically. This was the subject of further study by my collaborator Rowena Suriben, and will presumably be a centerpiece of her doctoral thesis, while my own contribution to the *Dact1* null embryology amounted to ancillary assistance to her work. The other major question was which molecular signaling pathways were altered in *Dact1* null embryos. I focused on Wnt signaling pathways, since these were the pathways affected by overexpression and antisense morpholino studies with the previously described *Xenopus Dapper* and *Frodo*, which are homologs of mammalian *Dact1*, and similar studies with the zebrafish homolog as well (Cheyette et al., 2002; Gloy et al., 2002; Waxman et al., 2004). These studies had led to contradictory conclusions: Cheyette et al. (2002) concluded that *Xenopus* Dapper inhibited both Wnt/β-catenin and Wnt/JNK (possibly linked to PCP) pathways. In contrast, Gloy et al (2002) concluded that *Xenopus* Frodo synergized with Dishevelled as a Wnt/β-catenin agonist. A later study by the same group concluded that *Xenopus* Dapper and Frodo were both Wnt/β-catenin agonists at low concentrations, and antagonists at higher concentrations (Hikasa and Sokol, 2004). Meanwhile, Waxman et al. (2004) concluded that the zebrafish

homolog of Dact1 was a Wnt/β-catenin agonist, while the zebrafish homolog of Dact2 affected convergent extension. The roles of Dact proteins in Wnt signaling were clearly either multifarious or ambiguous.

I found that the tailbuds of *Dact1* null embryos showed reduced Wnt/β-catenin signaling, both by *LacZ* whole mount in situ hybridization using the BATGal Wnt/β-catenin reporter mouse (Maretto et al., 2003), and by ELISA for soluble β-catenin. The reductions were modest: in the range of 50% or less, in comparison with wild-type littermates.

I also crossed the *Dact1* null mouse with the *Vangl2* point mutant mouse *Loop-Tail*, which is a loss-of-function mutant in the PCP pathway, to test for genetic epistasis. *Loop-Tail* heterozygotes are characterized by curled tails, albeit of normal length, while *Loop-Tail* homozygotes exhibit craniorachischisis (Kibar et al., 2001a; Murdoch et al., 2001). *Loop-Tail* homozygotes also exhibit failures of convergent extension in notochord formation (Ybot-Gonzalez et al., 2007), and have disorganized cochlear sensory epithelia, which are a structure exhibiting PCP characteristics similar to those studied in *Drosophila* (Montcouquiol et al., 2003, 2006).

Since *Dact1* null neonates exhibit spina bifida at a rate of about 15% (Chapter 4, Supplementary Table 3), I reasoned that this rate would increase with the addition of *Loop-Tail* heterozygosity to their genetic makeup. Spina bifida is associated with failures in convergent extension, and is a hallmark of PCP pathway failure in both mice (reviews:

Torban et al., 2004; Doudney and Stanier, 2005) and humans (Doudney et al., 2005; Kibar et al., 2007a, b). A heterozygous *Loop-Tail* allele had already been shown to lead to cranorachischisis and cochlear disorganization in *Dvl2* null mice, which otherwise lack these phenotypes (Wang et al., 2005). Since Dishevelled proteins are known to be required for transduction of the PCP pathway, as well as of other Wnt signaling pathways, and since Dact proteins have been hypothesized to act as synergistic partners of Dishevelled proteins (Gloy et al., 2002; Brott and Sokol, 2005), it seemed likely that the *Loop-Tail* mutation might interact synergistically with the *Dact1* null mutation, as it had with the *Dvl2* null mutation. In contrast to my expectation of a similar result for *Dact1* as for *Dvl2*, in fact the opposite result was obtained. *Loop-Tail* heterozygosity rescued the *Dact1* null mice altogether. These mice were viable and most often fertile, except for a subset of the females which exhibited vaginal imperforacy, a frequent phenotype among *Loop-Tail* heterozygotes. Additionally, approximately 90% of the *Dact1* null mice rescued by *Loop-Tail* heterozygosity had long, straight tails, implying the *Loop-Tail* heterozygous phenotype was rescued as well. The mutual rescue of *Dact1* loss and *Loop-Tail* heterozygosity (a semidominant phenotype) implies that Dact1 and Vangl2 proteins antagonize one another in PCP signaling. This sort of effect has not previously been described in the mouse. Although *Wnt5a* and *Sfrp1*/*Sfrp2* null mutations, as well as the *Dvl2* null, have been shown to synergize with *Loop-Tail* heterozygosity to produce neural tube defects in mice (Wang et al., 2005; Qian et al., 2007; Satoh et al., 2008), a mutation rescuing a PCP loss-of-function mutant has not yet been described in the mouse (such rescues have been described in Drosophila: see Seifert and Mlodzik, 2007; Lawrence et al., 2007 for reviews).

In conclusion to my study of the *Dact1* null mice, I hypothesize that Dact1 acts to promote Wnt/β-catenin signaling at the expense of PCP signaling in the caudal ectoderm of the mouse embryo, and that Dact proteins are likely to have similar functions in other systems.

The Dvl's choice: the mystery of Dishevelled and Wnt pathway selectivity.

Dishevelled proteins are required for divergent Wnt signaling pathways, including Wnt/β-catenin and PCP. It has not, however, been evident how distinct Wnt signaling pathways are selected for activation within the cell by Dishevelled. Different domains of Dishevelled proteins are required for the activation of different downstream pathways: the DIX domain is required for the Wnt/β-catenin pathway, the DEP domain is required for PCP, and the PDZ domain, which binds to Frizzled receptors (Wong et al., 2003), is presumably required for both these pathways and others as well (see Wallingford and Habas, 2005 for review). Intriguingly, the *Xenopus* homologs of Dact1 were originally identified from their binding to the PDZ domain as well (Cheyette et al., 2002; Gloy et al., 2002), although subsequently it was found that Dact1 may bind to the DEP domain of Dishevelled as well, via a different region of Dact1 from that which binds to the PDZ domain (Zhang et al., 2006).

The selection of the downstream Dishevelled-activated pathway presumably depends on the presence of distinct Dishevelled interactors, which by this process become actors in the drama of intracellular signaling. The subcellular localization of the Dishevelled protein is highly important. Plasma membrane association of Dvl protein is required for convergent extension in *Xenopus* embryos, while cytoplasmic and nuclear Dvl are associated with Wnt/β-catenin signaling (Itoh et al., 2005; Park et al., 2005). It has also been shown that the DIX domain, required for Wnt/β-catenin signaling, targets Dvl to actin stress fibres and vesicular membranes (Capelluto et al., 2002); and that Dvl protein is associated with large, intracellular multiprotein complexes at these sites (Schwarz-Romond et al., 2005, 2007a). The Dvl and Axin DIX domains mediate concatameric heteropolymerization in large, dynamic, multiprotein arrays of a helical filamentous structure, which are associated with active Wnt/β-catenin signaling (Schwarz-Romond et al., 2007b). The formation of these Dvl-Axin concatamers may sequester Axin molecules and thereby prevent their joining the formation of β-catenin destruction complexes. With enough Dvl-Axin concatamerization, the equilibrium of Axin heteromerization might be shifted to favor the accumulation of cytoplasmic β-catenin.

Dishevelled, however, is a cytoplasmic protein that can integrate with PCP complexes at the plasma membrane as well as Dvl-Axin heteromers intracellularly. What is to help the Dvl make its choice? (Speak of the Dvl!). It has been shown that Lrp5 or Lrp6 is required in a complex together with Fz and Wnt, in order to activate Wnt/β-

catenin signaling (Schweizer and Varmus, 2003; Cong et al., 2004; Mikels and Nusse, 2006). The mechanism by which Lrp5 or Lrp6 specifies Wnt/β-catenin signaling is still unclear, however. A partial mechanism has been described whereby Lrp6 binds Axin, and this recruits GSK-3, which in turn phosphoryplates Lrp6, thereby initiating the "canonical" Wnt signaling cascade (Zeng et al., 2005; Zeng et al., 2008). While this explains how the "canonical" Wnt signaling cascade is initiated, it does not show how its activation occurs in preference over "non-canonical" Wnt signaling pathways, which are also activated by the complex of Wnt, Fz, and Dvl.

The results of my *Dact1*/*Loop-Tail* genetic experiment suggest that a function of Dact1 may be to help the Dvl choose. Absence of Dact1 leads to diminution of Wnt/β-catenin signaling, together with a partial rescue of a PCP loss-of-function in the form of the *Vangl2 Loop-Tail* heterozygous mutation. *Loop-Tail* homozygotes, in contrast to heterozygotes, are not rescued from craniorachischisis, perhaps because there is not enough intact PCP signaling in the *Loop-Tail* homozygous embryo even with the compensating loss of Dact1.

The implication is that Dact1 functions as a PCP antagonist and simultaneously as a Wnt/β-catenin agonist. Since it binds to Dvl, which is an agonist of both pathways, it may act by directing Dvl into complexes that promote Wnt/β-catenin signaling, rather than those which mediate PCP signaling. Alternatively, it may directly inhibit signaling by the core PCP complex, and the promotion of Wnt/β-catenin signaling may be an indirect effect of this inhibition. This hypothesis is favored by the evidence that Dact1

binds to Vangl2 (Chapter 4), while competition between Dact1 and Vangl2 for Dvl has yet to be demonstrated. Indeed, the three proteins can bind to one another in a ternary complex (Chapter 4 and S. Kivimäe and B. Cheyette, unpublished observation). If there is competition, it may be at the level of the interaction of different domains within this ternary complex. It is probably not only at the level of the molecules' ability to bind to and enter into the complex.

The *Dact1* null phenotypes: direct and indirect effects of the mutation.

Dact1 null neonates exhibit a constellation of phenotypes, most of which can be described as caudal truncations. Mesodermal and endodermal derivatives are caudally truncated. In E8-10 embryos, *Dact1* is predominantly expressed in mesodermal derivatives, particularly the PSM and caudal somites. The rescue of *Dact1* null phenotypes in their entirety by *Vangl2 Loop-Tail* heterozygosity, however, suggests that the primary effects of Dact1 loss occur in the ectoderm. Vangl2 protein, and the mRNA encoding it, are predominantly expressed in the neural tube (Chapter 4, also see Kibar et al., 2001a; Murdoch et al., 2001; Torban et al., 2007), with expression also in its precursor, the unfolded neural plate, and the ectoderm of the primitive streak region which is contiguous with the neural plate without any separation by a structural landmark (reviews: Schoenwolf, 1991; Colas and Schoenwolf, 2001). Vangl2 is also present in the

embryonic gut epithelium, i.e. endoderm (Chapter 4). If there is expression in the embryonic mesoderm, however, it is at very low levels (Torban et al., 2007). In contrast, *Dact1* is coexpressed with *Vangl2* in the caudal ectoderm (Chapter 4). Therefore, this is where the primary phenotypic effect of *Dact1* loss most likely occurs.

Given this localization for the primary phenotype of the *Dact1* null, the *Dact1* null phenotypes are most likely consequences of defective gastrulation. The effect on gastrulation is not severe, however. It seems to progress normally from its beginning until about E8.0, when the brachial level somites are formed. Interestingly, this is the point at which somite development is arrested in *T, Wnt3a, Tbx6*, and *pMesogenin1* nulls (Herrmann et al., 1990; Takada et al., 1994; Chapman and Papaioannou, 1998; Yoon and Wold, 2001; Yoon et al., 2001), and *Lef1/Tcf1* double nulls (Galceran et al., 1999). The typical level of truncation in *Dact1* nulls is much lower, however, and similar to what is seen in the *Wnt3a* hypomorph *Vestigial tail*, or in compound heterozygotes of *Wnt3a* null and *Vestigial tail* alleles (*Wnt3a* $^{Neo/Vt}$: Greco et al, 1996). So the *Dact1* null is much less severe than, for example, the *Wnt3a* null.

The *Wnt3a* null phenotype is also thought to be substantially due to gastrulation failure: mesoderm is not produced and ectopic neural tubes form caudally instead (Takada et al., 1994; Yoshikawa et al., 1997). Gastrulation and consequent mesoderm generation only fail at lower cervical to upper thoracic levels in *Wnt3a* nulls, because the Wnt requirement in gastrulation prior to that is supplied by the closely homologous *Wnt3* (Liu et al., 1999; Barrow et al., 2007).

This is an insufficient explanation of the *Wnt3a* null, however. *Wnt3a* nulls form a substantial amount of caudal mesoderm; however, it fails to differentiate into somites, lacks β-catenin dependent transcription, and expression of mesoderm inducers such as *pMesogenin1* and *Ripply2* (Yamaguchi et al., 1999; Nakaya et al., 2005; Biris et al., 2007). In view of this information, it is fair to say that the phenotypes of the *Wnt3a* null are as much results of failure in cell fate determination as in gastrulation. The ectopic neural tube formation may actually result from a default cell fate, similar to the default neural fate that has been documented in the *Drosophila* embryo (Bourouis et al., 1989; Castro et al., 2005). A cell fate failure hypothesis for the *Wnt3a* null mouse is also more in keeping with conventional thinking concerning the roles of "canonical" and "non-canonical" Wnts. The "non-canonical" Wnts, for example mouse Wnt5a, are thought to effect cell movements: indeed, Wnt5a has been shown to act through the PCP pathway in concert with Vangl2 (Qian et al., 2007). The "canonical" Wnts, in contrast, are thought primarily to act via the Wnt/β-catenin pathway to affect transcription, thereby most often affecting cell fate or cell division. For example, overexpression of *Wnt1* leads mouse cranial neural crest cells to adopt a sensory neuron fate in preference over other fates (Lee et al., 2004); while loss of *Wnt1* and *Wnt3a* ablates generation of multiple cranial nerve ganglia (Ikeya et al., 1997).

The *Dact1* null mouse, in contrast to the *Wnt3a* null mouse, may predominantly reflect a failure of gastrulation movements. *Dact1* null embryos often show unusual clusterings of cells around the primitive streak and in the folding neuroectoderm (R.

Suriben and B. Cheyette, unpublished observation). They also show the formation of masses of cells in the caudoventral tail bud region (Chapter 4, Figure 3) that are not seen in wild-type littermates. These observations suggest cell movements and histogenic cell organization are partly impaired in the caudal embryo. My colleague and collaborator Rowena Suriben is currently studying further the cell movements in the caudal *Dact1* null embryo.

A significant unresolved question concerning the *Dact1* null phenotypes is; why are there visceral phenotypes as well as skeletal ones? The caudal truncation of the digestive and urogenital systems may be a result of caudal gastrulation failure, since endoderm is generated at gastrulation as well as mesoderm. Alternatively, it may reflect a failure of proper induction of the endoderm by the mesoderm: a non-cell-autonomous phenotype. Intriguingly, *Tcf1/Tcf4* double null embryos show anterior transformations of the caudal digestive tract, as well as caudal truncations and ectopic neural tubes similar to *Wnt3a* mutants (Gregorieff et al., 2004). Clearly, Wnt signaling can affect the fate of the caudal digestive tract, although whether it might do so non-cell-autonomously is unclear. Also interestingly, some *Dact1/Dvl1* double null neonates have digestive tract truncations more rostral than those in *Dact1* null mice (at the duodenum, for example), while their skeletal truncations resemble those of *Dact1* nulls.

The phenotype of renal agenesis sometimes observed in *Dact1* null mice is probably a direct, cell-autonomous effect on Wnt signaling, separate from the caudal ectoderm. Kidney tubules are induced to invade the metanephric mesenchyme by Wnt4

and Wnt9b: in absence of this, the metanephric (definitive) kidney never develops (Stark et al., 1994; Kispert et al., 1998; Park et al., 2007). This involves redistribution of Dvls and other Wnt signaling components in the tubule precursor cells (Torres and Nelson, 2000). So it is not surprising if a Dact molecule is involved in this process as well.

Dact1 effects on Wnt signaling modalities.

The phenotypes of the *Dact1* null mutation are quite eloquent, concerning the signaling modalities that are affected, particularly by analogy with other Wnt signaling related mutant mice. The combination of caudal truncation and caudal vertebral disorganization closely resembles the phenotype of *Lrp6* nulls (Pinson et al., 2000; Kelly et al., 2004). As Lrp proteins mediate "canonical" Wnt/β-catenin signaling, these can be considered "classic canonical Wnt phenotypes". The other published mutants whose skeletons most closely resemble those of *Dact1* null mice are the *Wnt3a* hypomorphic mutant *Vestigial tail*, *Wnt3a* $^{Vt/Vt}$, and the compound heterozygote, *Wnt3a* $^{Neo/Vt}$ (Greco et al., 1996). Considering that the caudal phenotype of *Vestigial tail*, *Wnt3a* $^{Vt/Vt}$, was rescued by the β-catenin-Lef1 fusion transgene, CatCLef (Galceran et al., 2001), this could be considered a "pure", "canonical" Wnt/β-catenin phenotype. Ideally, such a rescue experiment should be done with the *Dact1* null as well. At first glance, however, the *Dact1* null skeletal phenotype appears also to be a "classic canonical Wnt phenotype", at least by analogy with *Vestigial tail* and with the *Lrp6* null.

Then what of the rescue of the *Dact1* null by *Loop-Tail* heterozygosity (*Vangl2* $^{Lp/+}$)? If the *Dact1* null skeletal phenotype is a "classic canonical Wnt phenotype", then how can it be rescued by a PCP mutant? Speaking frankly, when I first observed this result, my immediate thought was "It's not: the result is wrong". It is hard to argue with numbers, however. In the original *Dact1* $^{+/-}$ *X Dact1* $^{+/-}$, *Vangl2* $^{Lp/+}$ genetic cross experiment, I observed 100% rescue of the *Dact1* caudal phenotype (including visceral phenotypes), and 90% rescue of the *Loop-Tail* heterozygous (*Vangl2* $^{Lp/+}$) phenotype (Chapter 4, Figure 5). Even Dact1 heterozygosity gave a small increase (an increment of about 20%) in the non-penetrance of the *Loop-Tail* heterozygous (*Vangl2* $^{Lp/+}$) phenotype (Chapter 4, Figure 5). A possibly disappointing result in this experiment was that 40% of the *Dact1* null pups born that were completely wild-type at the *Vangl2* locus (*Dact1* $^{-/-}$, *Vangl2* $^{+/+}$) were also normal: only 60% penetrance of the *Dact1* null tail truncation, which was 90% penetrant on the N10 C57bl/6 background (129 SvEv backcrossed 10 generations to C57bl/6: Chapter 4, Compare Table 3 with Figure 5e). The penetrance at less backcrossed (129:C57bl/6) combinations initially studied was also in the vicinity of 90%. The background strain of the *Loop-Tail* mutant is A/J. In my experiment, it had been crossed twice to N10 C57bl/6: once to generate the *Dact1* $^{+/-}$, *Vangl2* $^{Lp/+}$ double heterozygotes, and a second time when these were crossed to N10 C57bl/6 *Dact1* heterozygotes (*Dact1* $^{+/-}$). So the experimental pups were effectively ¾ C57bl/6, ¼ A/J. This ¼ A/J contribution was evidently sufficient to cause a background rescue of 40%, or incrementally four times more than in N10 C57bl/6. Alternatively, one can consider the

Dact1 null phenotype to be only two-thirds as penetrant on the ¾ C57bl/6, ¼ A/J background as on N10 C57bl/6.

This caveat about background rescue is prompting two more experiments which I have begun but not yet completed. One is a repeat of the rescue experiment using N4 backcrossed *Dact1* $^{+/-}$, *Vangl2* $^{Lp/+}$ double heterozygotes (1/16 A/J, 15/16 C57bl/6: the experimental pups will be 31/32 C57bl/6, only 1/32 A/J). This experiment, of course, might not give a different result from the previous one as regards background rescue. If there is another PCP-antagonistic allele in the A/J background that is closely linked to the *Vangl2* locus, this further backcrossing might not make a substantial difference in the rate of background rescue. If that is the case, it might make for an exciting gene discovery project for someone else in the near future, but it won't change the results of my experiment. The other experiment I have started to control for the background rescue effect is to use a separate *Loop-Tail* allele, the ENU-induced *Lp1MJus* allele, which gives a similar phenotype to the original *Loop-Tail* allele (*Vangl2* ^{Lp}), although it represents a different point mutation in the cytoplasmic tail of Vangl2 (Kibar et al, 2001a, b). The background strain for *Lp1MJus* is C3H/R1. There is no reason to suspect it would carry a PCP-antagonistic allele specific to the A/J background. It has, however, been reported that the penetrance of the *Loop-Tail* heterozygous is somewhat less for *Vangl2* $^{Lp1mJus/+}$ than for *Vangl2* $^{Lp/+}$ (Kibar et al, 2001b). I think it is nonetheless a reasonable positive control experiment for the rescue of the *Dact1* null by Vangl2 loss-of-function.

If we conclude the rescue of the *Dact1* null by Vangl2 loss-of-function is real, which seems likely from the current data, then we are left with the dilemma of deciphering how this can happen. A "canonical" Wnt/β-catenin loss-of-function phenotype is rescued by a PCP loss-of-function phenotype. The simplest way to explain this is if the two pathways are coupled by mutual antagonism. The first evidence for PCP antagonism of the Wnt/β-catenin pathway was the observation that the "non-canonical" Wnt5a could block transcriptional activation by the "canonical" Wnt1 in *Xenopus* embryos (Torres et al., 1996). This antagonism was shown to occur upstream of GSK-3 and β-catenin, whose effects on target gene expression were not affected by Wnt5a. The hypothetical model of mutual antagonism stipulates that the antagonism is (or can be) bidirectional. The mutual rescue of *Dact1* null and *Loop-Tail* heterozygous phenotypes is evidence that this model is, at least in some circumstances, true.

The caudal ectoderm of the mouse embryo (a.k.a. the neural plate) is apparently a tissue where mutual antagonism between the PCP and Wnt/β-catenin pathways occurs. Dact1 and Vangl2 seem to be two important molecules among those mediating this mutual antagonism. The evidence that PCP antagonism of the Wnt/β-catenin pathway occurred upstream of GSK-3 and β-catenin in *Xenopus* gastrulation (Torres et al., 1996), makes a Dact1-Vangl2 interaction an attractive locus in the two pathways for this antagonism to occur. Dact1 and Vangl2 proteins can bind to one another, or be joined in a ternary complex including Dvl (Chapter 4, esp. Figure 6). The "seesaw" between PCP and Wnt/β-catenin pathways (Chapter 4, Figure 7) may be mediated by Dact1 and Vangl2

proteins. A hypothesis where Dact1 and Vangl2 proteins are engaged in a tug-of-war for Dvl is attractive, although so far there is no evidence for this particular model.

A "mutual antagonism" hypothesis coupling gastrulation and neurulation.

What would be the consequences of mutual antagonism between the PCP and Wnt/β-catenin pathways in vivo? Using mouse genetics, we are able to study this phenomenon of competing Wnt signaling pathways, in gastrulation and neurulation. Mutations in multiple PCP proteins cause defects in neurulation (Torban et al., 2004), while mice with "canonical" Wnt/β-catenin pathway loss-of-function mutations often exhibit caudal truncations, which may be partly due to late gastrulation defects. In fairness, it is not exactly clear to what extent these "canonical" Wnt/β-catenin pathway loss-of-function phenotypes are due to gastrulation failure (as opposed to defects in cell fate and tissue differentiation, as I have described earlier in this chapter). The evidence is that Wnt/β-catenin signaling affects a decision-point between a mesodermal fate and a neural tube fate (hence the ectopic neural tubes in *Wnt3a* mutants and others), and that Wnt/β-catenin signaling is antagonized by PCP signaling in the neural plate / caudal ectoderm prior to neurulation (from my study). This suggests a model where Wnt/β-catenin signaling in the caudal ectoderm promotes gastrulation and adoption of a

mesodermal fate, while PCP signaling promotes maintenance of a neural fate and cell movements mediating neural tube closure.

A useful tool for investigating this model is the Wnt reporter mouse, BATGal, which expresses *LacZ* under a TCF-inducible promoter (Maretto et al., 2003). While *LacZ* encoded β-galactosidase protein may be too stable for examination of signaling in a rapidly-changing embryo, I have utilized *LacZ* in situ hybridization as an alternative to study more acute changes (Chapter 4, Figure 4). It would be interesting to see if BATGal transcriptional activity in the caudal ectoderm is highest in the vicinity of the primitive streak, and diminishes with greater distance from it. Such a finding would support the hypothesized model. It is observable that once the neural tube is closed, BATGal *LacZ* mRNA is highest dorsally within it (observable in Chapter 4, Figure 4), coincident with the expression of *Wnt1, Wnt3,* and *Wnt3a* in the dorsal neural tube (Megason and McMahon, 2002; Robertson et al., 2004). The dynamics of BATGal transcription within the neural plate, or during gastrulation, have yet to be described.

In contrast, the hypothesis that Wnt/β-catenin signaling opposes the normal dynamics of neurulation could be addressed by embryo culture experiments (perhaps in chick?). A local elevation of Wnt/β-catenin signaling could create a local defect in neurulation, and consequently, in neural tube structure. Locally overexpressing a "canonical" Wnt should have such an effect. Overexpessing Dvl locally might also. If the mutual antagonism occurs at the level of Dact and Dvl, however, overexpressing β-

catenin might not have such an effect, since it is downstream. The hypothesis generates these predictions which are clearly testable.

Why no ectopic neural tubes?

One of the most striking features among Wnt/β-catenin pathway loss-of-function mouse mutants is the presence of ectopic neural tubes. These are present not only in mice lacking *Wnt3a* or its downstream effectors, but also in the *Wnt3a* expression hypomorph *Vestigial tail*, *Wnt3a* $^{Vt/Vt}$ (Yoshikawa et al., 1997; Shum et al., 1999). Ectopic neural tubes have never been observed in *Dact1* null mice, however. In contrast, *Dact1* null mice seem in some ways more severe phenotypically than *Vestigial tail* mutants. Both *Vestigial tail*, *Wnt3a* $^{Vt/Vt}$, and the compound heterozygote, *Wnt3a* $^{Neo/Vt}$, have external genitals and anuses, notably lacking in *Dact1* nulls. These differences likely reflect differences in the signaling modalities affected.

Dact1 seems to be a direct antagonist of PCP signaling (or to mediate this antagonism in concert with other proteins), through its binding to Vangl2. Therefore loss of Dact1 enhances PCP signaling (see Chapter 4, Figure 7). Wnt3a, in contrast, might antagonize PCP signaling more indirectly, through Dact1. So the *Dact1* null might well have a greater alteration of PCP signaling than *Wnt3a* mutants. Wnt/β-catenin signaling, in contrast, might be affected in the *Dact1* null less severely but more broadly, since signaling downstream of multiple Wnts, rather than only one, would be affected. In

Dact1 null embryos there might still be sufficient Wnt/β-catenin signaling locally to prevent poorly differentiated mesodermal cells from adopting a default neural fate outright. At this point, this is pure speculation, although it might be addressed experimentally using BATGal mice. Alternatively, the failure of ectopic neural tubes to form in *Dact1* null embryos may be because excess PCP signaling actually paralyzes the cells that would otherwise for these structures. The idea would be that a normal level of PCP signaling is required for neural tube closure, but an excess, in conjunction with cells being more predisposed to a neural fate than a mesodermal one (due to a loss of Wnt/β-catenin signaling), causes the formation of ectopic neural tubes from the primitive streak ectoderm. This would be the situation in *Wnt3a* $^{Vt/Vt}$ and *Wnt3a* $^{Neo/Vt}$ embryos. An even greater elevation of PCP signaling, as in *Dact1* null embryos, might paralyze the primitive streak ectoderm cells to a degree that the ectopic neural tubes could never form, and normal neurulation and gastrulation would be impaired as well. This hypothesis is supported by the findings of spina bifida (Chapter 4, Figure 1) and abnormal neural plate structure (Chapter 4, Figure 3) in *Dact1* nulls.

A necessary corollary hypothesis would be that an excess of PCP signaling has similar effects to a loss of PCP signaling. The combination of spina bifida in *Dact1* nulls, together with their mutual rescue with *Loop-Tail* heterozygotes, suggests this. PCP polarizes cells and maintains them in a polarized state, with respect to each other or with respect to an extracellular ligand present in a gradient. An example of this was recently published, in which Wnt5a was required to polarize mesenchymal cells to a gradient of CXCL12 in vitro (Witze et al., 2008). With an excess of PCP signaling, however, the

cell might not be able to polarize itself in response to the extracellular ligand. Another way to think of this is in terms of intracellular microdomains. When a cell in the caudal ectoderm is polarized, for example, one side must be oriented toward the primitive streak (ventromedially) and the other away from it (dorsolaterally). But if both sides of the cell are receiving a high level of signal appropriate to only one side, the cell may lose its normal polarity.

A problem with these hypotheses is that PCP signaling, unlike Wnt/β-catenin signaling, cannot be quantified straightforwardly in vivo. Until a reliable method is developed for quantifying PCP signaling within cells, or most likely, within microdomains of cells, hypotheses concerning relative or quantitative levels of PCP signaling, will be very difficult to test.

Relevance of the studies for neuroscience.

Having studied neuroscience as a major field, it is appropriate that I include some commentary on the relevance (or lack thereof?) of the studies I have undertaken to this field. I can say straightforwardly that I have made two potentially significant contributions:

1. The development of a hypothesis concerning Dact protein function and mutual antagonism between Wnt/β-catenin and PCP signaling pathways. While this

hypothesis results from data concerning the caudal ectoderm of neurulation-stage embryos, it is likely to be applicable to other tissues as well. Dact1 and Vangl2 can antagonize one another, and these proteins are expressed in multiple tissues, most prominently the embryonic brain (Fisher et al., 2006; Tissir and Goffinet, 2006; Torban et al., 2007). There are also additional homologs of Dact1 (Dact2 and Dact3 in mammals) and Vangl2 (Vangl1, which synergizes with Vangl2 in mouse neurulation, and has also been found to be mutated in human cases of spina bifida: Doudney et al., 2005; Kibar et al., 2007a, b; Torban et al., 2008). So the potential for signaling pathway antagonism like that observed for Dact1 and Vangl2 in the embryonic ectoderm is truly widespread.

2. Characterization of the gene expression of the *Dact* family in mouse development. This data is presented in Chapter 2 and is published in *Developmental Dynamics* as the paper Fisher et al. (2006). It is notable that *Dact1* is highly expressed in the embryonic brain, predominantly if not exclusively in postmitotic neurons, while all three *Dact* genes are expressed in the adult brain.

It is notable that while all three *Dact* genes are expressed in the embryonic nervous system, their expression patterns there are markedly distinct. *Dact1* is expressed in postmitotic neurons once they appear, starting with motor neurons, the earliest CNS neurons generated. The embryonic spinal cord expresses all three *Dact* genes. The embryonic PNS ganglia express *Dact2* and/or *Dact3*, but generally not *Dact1*. Embryonic brain neurons instead express predominantly *Dact1*, while *Dact3* is expressed

diffusely throughout the embryonic brain, where *Dact2* is expressed at very low levels if at all. These observations are likely to be useful for future genetic studies of nervous system development in the mouse.

Unlike in utero, adult mouse brains express all three *Dact* genes, predominantly in similar patterns, namely in neurons of the cerebral cortex, hippocampus, and olfactory bulb. The exception to this similarity is the cerebellum, where *Dact1* is predominantly expressed in granule cells, while *Dact2* and *Dact3* are predominantly expressed in Purkinje cells. I have performed in situs on the three *Dact* genes in postnatal cerebellar development to try to identify the onset of these distinct patterns (Chapter 2, additional data).

A very interesting observation with relevance to brain development and to the Dact1-Vangl2 mutual antagonism I have identified in the early embryonic ectoderm, is that *Vangl1* is not expressed in almost the entire neonatal and postnatal mouse brain (Tissir and Goffinet, 2006: in the embryonic brain both *Vangl1* and *Vangl2* are expressed, in similar patterns). This leads me to suspect that *Loop-Tail* heterozygous mice, *Vangl2* $^{Lp/+}$, will show substantial defects in postnatal brain development due to deficient PCP signaling. A great deal of nervous system development is activity-dependent and occurs postnatally. The formation of dendritic arbors, synaptogenesis, and synapse selection are examples of phenomena that occur almost entirely postnatally in the mammalian brain. Some connectivity maps within the CNS are also activity-dependent and therefore develop postnatally. The ocular dominance columns in the lateral geniculate nucleus of

many mammals are an example of this. That such a process might be regulated by PCP or other Wnt-directed signaling would not be surprising. Indeed, the similar, but earlier and non-activity dependent phenomenon of retinotectal map development in the chick embryo has been shown to be regulated by Wnt3/Ryk signaling (Schmitt et al., 2006). Depending on the extent to which postnatal brain wiring requires a threshold level of PCP signaling, the *Loop-Tail* heterozygous mice, *Vangl2* $^{Lp/+}$, may show substantial defects. *Loop-Tail* homozygous mice, *Vangl2* $^{Lp/Lp}$, which logically would have more impaired PCP signaling than the heterozygotes, do not survive to birth. An elegant experiment could be imagined, however, in which embryonic *Loop-Tail* homozygous neuronal precursors were transplanted into a wild-type mouse brain, and the development of the transplanted cells and their descendants, *Loop-Tail* homozygous versus wild-type, could be studied.

Conclusion.

I have undertaken studies which have substantially characterized the expression of the *Dact* gene family in mouse development, and, through the study of the *Dact1* null mouse, contributed hypotheses concerning both the role of Dact1 in Wnt signaling and mutual antagonism between Wnt/β-catenin and PCP signaling pathways. I hope the results of these studies will be useful to the authors of future studies of Wnt and PCP signaling. Likewise I hope that this thesis will be considered worthy of the effort

undertaken. My hypotheses may be correct or incorrect, but hopefully they will be of sufficient interest to the scientific community to be tested further. I think it is a reasonable expectation that the mechanisms I have hypothesized, particularly as regards the mutual antagonism between Wnt/β-catenin and PCP signaling pathways, will translate to other systems besides that in which they were originally observed (in this case, the early mouse embryo).

Finally, I would like to thank once again my mentor, Dr. Benjamin Cheyette, and all the members of the Cheyette laboratory during the time in which this work was accomplished. I will always be grateful for the opportunities I have had to work and learn there. I have had the pleasure of working with some excellent colleagues, in particular Rowena Suriben, who was my co-author on all the studies from the Cheyette laboratory which we have submitted for publication. Our collaboration has been very pleasant from start to finish, and is expected to contribute the majority of the work subsumed in both our doctoral theses. While our life as doctoral students is ending, our lives as students of developmental and medical biology have years ahead, hopefully many. In this sense it is my great hope that my submission of this thesis is not an endpoint so much as it is, more importantly, only the end of a beginning.

Discussion and Conclusions: References.

Aulehla,A., Wehrle,C., Brand-Saberi,B., Kemler,R., Gossler,A., Kanzler,B., and Herrmann,B.G. (2003). Wnt3A plays a major role in the segmentation clock controlling somitogenesis. Developmental Cell *4*, 395-406.

Aulehla,A., Wiegraebe,W., Baubet,V., Wahl,M.B., Deng,C., Taketo,M., Lewandoski,M., and Pourquie,O. (2008). A beta-catenin gradient links the clock and wavefront systems in mouse embryo segmentation. Nat. Cell Biol. *10*, 186-193.

Barrow,J.R., Howell,W.D., Rule,M., Hayashi,S., Thomas,K.R., Capecchi,M.R., and McMahon,A.R. (2007). Wnt3 signaling in the epiblast is required for proper orientation of the anteroposterior axis. Developmental Biology *312*, 312-320.

Biris,K.K., Dunty,W.C., and Yamaguchi,T.P. (2007). Mouse Ripply2 is downstream of Wnt3a and is dynamically expressed during somitogenesis. Developmental Dynamics *236*, 3167-3172.

Bourouis,M., Heitzler,P., Elmessal,M., and Simpson,P. (1989). Mutant Drosophila Embryos in Which All Cells Adopt A Neural Fate. Nature *341*, 442-444.

Brott,B.K. and Sokol,S.Y. (2005). Frodo proteins: modulators of Wnt signaling in vertebrate development. Differentiation *73*, 323-329.

Capelluto,D.G.S., Kutateladze,T.G., Habas,R., Finkielstein,C.V., He,X., and Overduin,M. (2002). The DIX domain targets dishevelled to actin stress fibres and vesicular membranes. Nature *419*, 726-729.

Castro,B., Barolo,S., Bailey,A.M., and Posakony,J.W. (2005). Lateral inhibition in proneural clusters: cis-regulatory logic and default repression by Suppressor of Hairless. Development *132*, 3333-3344.

Chapman,D.L. and Papaioannou,V.E. (1998). Three neural tubes in mouse embryos with mutations in the T-box gene Tbx6. Nature *391*, 695-697.

Cheyette,B.N.R., Waxman,J.S., Miller,J.R., Takemaru,K.I., Sheldahl,L.C., Khlebtsova,N., Fox,E.P., Earnest,T., and Moon,R.T. (2002). Dapper, a Dishevelled-associated antagonist of beta-catenin and JNK signaling, is required for notochord formation. Developmental Cell *2*, 449-461.

Colas,J.F. and Schoenwolf,G.C. (2001). Towards a cellular and molecular understanding of neurulation. Developmental Dynamics *221*, 117-145.

Cong,F., Schweizer,L., and Varmus,H. (2004). Wnt signals across the plasma membrane to activate the beta-catenin pathway by forming oligomers containing its receptors, frizzled and LRP. Development *131*, 5103-5115.

Dequeant,M.L., Glynn,E., Gaudenz,K., Wahl,M., Chen,J., Mushegian,A., and Pourquie,O. (2006). A complex oscillating network of signaling genes underlies the mouse segmentation clock. Science *314*, 1595-1598.

Doudney,K., Moore,G.E., Stanier,P., Ybot-Gonzalez,P., Paternotte,C., Greene,N.D.E., Copp,A.J., and Stevenson,R.E. (2005). Analysis of the planar cell polarity gene VANGL2 and its co-expressed paralogue VANGL1 in neural tube defect patients. American Journal of Medical Genetics Part A *136A*, 90-92.

Doudney,K. and Stanier,P. (2005). Epithelial cell polarity genes are required for neural tube closure. American Journal of Medical Genetics Part C-Seminars in Medical Genetics *135C*, 42-47.

Fisher,D.A., Kivimae,S., Hoshino,J., Suriben,R., Martin,P.M., Baxter,N., and Cheyette,B.N.R. (2006). Three Dact gene family members are expressed during embryonic development and in the adult brains of mice. Developmental Dynamics *235*, 2620-2630.

Galceran,J., Farinas,I., Depew,M.J., Clevers,H., and Grosschedl,R. (1999). Wnt3a(-/-)-like phenotype and limb deficiency in Lef1(-/-)Tcf1(-/-) mice. Genes & Development *13*, 709-717.

Galceran,J., Sustmann,C., Hsu,S.C., Folberth,S., and Grosschedl,R. (2004). LEF1-mediated regulation of Delta-like1 links Wnt and Notch signaling in somitogenesis. Genes & Development *18*, 2718-2723.

Gillhouse,M., Nyholm,M.W., Hikasa,H., Sokol,S.Y., and Grinblat,Y. (2004). Two Frodo/Dapper homologs are expressed in the developing brain and mesoderm of zebrafish. Developmental Dynamics *230*, 403-409.

Gloy,J., Hikasa,H., and Sokol,S.Y. (2002). Frodo interacts with Dishevelled to transduce Wnt signals. Nature Cell Biology *4*, 351-357.

Greco,T.L., Takada,S., Newhouse,M.M., McMahon,T.A., McMahon,A.P., and Camper,S.A. (1996). Analysis of the vestigial tail mutation demonstrates that Wnt-3a gene dosage regulates mouse axial development. Genes & Development *10*, 313-324.

Gregorieff,A., Grosschedl,R., and Clevers,H. (2004). Hindgut defects and transformation of the gastrointestinal tract in Tcf4(-/-)/Tcf1(-/-) embryos. Embo Journal *23*, 1825-1833.

Hamblet,N.S., Lijam,N., Ruiz-Lozano,P., Wang,J.B., Yang,Y.S., Luo,Z.G., Mei,L., Chien,K.R., Sussman,D.J., and Wynshaw-Boris,A. (2002). Dishevelled 2 is essential for cardiac outflow tract development, somite segmentation and neural tube closure. Development *129*, 5827-5838.

Herrmann,B.G., Labeit,S., Poustka,A., King,T.R., and Lehrach,H. (1990). Cloning of the T-Gene Required in Mesoderm Formation in the Mouse. Nature *343*, 617-622.

Hikasa,H. and Sokol,S.Y. (2004). The involvement of Frodo in TCF-dependent signaling and neural tissue development. Development *131*, 4725-4734.

Ikeya,M., Lee,S.M.K., Johnson,J.E., McMahon,A.P., and Takada,S. (1997). Wnt signalling required for expansion of neural crest and CNS progenitors. Nature *389*, 966-970.

Itoh,K., Brott,B., Ratcliffe,M., and Sokol,S. (2002). Nuclear localization of disheveled is required for Wnt/beta-catenin signal transduction. Developmental Biology *247*, 522.

Kelly,O.G., Pinson,K.I., and Skarnes,W.C. (2004). The Wnt co-receptors Lrp5 and Lrp6 are essential for gastrulation in mice. Development *131*, 2803-2815.

Kibar,Z., Vogan,K.J., Groulx,N., Justice,M.J., Underhill,D.A., and Gros,P. (2001). Ltap, a mammalian homolog of Drosophila Strabismus/Van Gogh, is altered in the mouse neural tube mutant Loop-tail. Nature Genetics *28*, 251-255.

Kibar,Z., Underhill,D.A., Canonne-Hergaux,F., Gauthier,S., Justice,M.J., and Gross,P. (2001). Identification of a new chemically induced allele (Lp(m1Jus)) at the loop-tail locus: Morphology, histology, and genetic mapping. Genomics *72*, 331-337.

Kibar,Z., Capra,V., and Gros,P. (2007). Toward understanding the genetic basis of neural tube defects. Clinical Genetics *71*, 295-310.

Kibar,Z., Torban,E., McDearmid,J.R., Reynolds,A., Berghout,J., Mathieu,M., Kirillova,I., De Marco,P., Merello,E., Hayes,J.M., Wallingford,J.B., Drapeau,P., Capra,V., and Gros,P. (2007). Mutations in VANGL1 associated with neural-tube defects. New England Journal of Medicine *356*, 1432-1437.

Kispert,A., Vainio,S., and McMahon,A.P. (1998). Wnt-4 is a mesenchymal signal for epithelial transformation of metanephric mesenchyme in the developing kidney. Development *125*, 4225-4234.

Lawrence,P.A., Struhl,G., and Casal,J. (2007). Planar cell polarity: one or two pathways? Nature Reviews Genetics *8*, 555-563.

Lee,H.Y., Kleber,M., Hari,L., Brault,V., Suter,U., Taketo,M.M., Kemler,R., and Sommer,L. (2004). Instructive role of Wnt/beta-catenin in sensory fate specification in neural crest stem cells. Science *303*, 1020-1023.

Liu,P.T., Wakamiya,M., Shea,M.J., Albrecht,U., Behringer,R.R., and Bradley,A. (1999). Requirement for Wnt3 in vertebrate axis formation. Nature Genetics *22*, 361-365.

Maretto,S., Cordenonsi,M., Dupont,S., Braghetta,P., Broccoli,V., Hassan,A.B., Volpin,D., Bressan,G.M., and Piccolo,S. (2003). Mapping Wnt/beta-catenin signaling

during mouse development and in colorectal tumors. Proceedings of the National Academy of Sciences of the United States of America *100*, 3299-3304.

Megason,S.G. and McMahon,A.P. (2002). A mitogen gradient of dorsal midline Wnts organizes growth in the CNS. Development *129* , 2087-2098.

Mikels,A.J. and Nusse,R. (2006). Purified Wnt5a protein activates or inhibits beta-catenin-TCF signaling depending on receptor context. Plos Biology *4*, 570-582.

Montcouquiol,M., Rachel,R.A., Lanford,P.J., Copeland,N.G., Jenkins,N.A., and Kelley,M.W. (2003). Identification of Vangl2 and Scrb1 as planar polarity genes in mammals. Nature *423*, 173-177.

Montcouquiol,M., Sans,N., Huss,D., Kach,J., Dickman,J.D., Forge,A., Rachel,R.A., Copeland,N.G., Jenkins,N.A., Bogani,D., Murdoch,J., Warchol,M.E., Wenthold,R.J., and Kelley,M.W. (2006). Asymmetric localization of Vangl2 and Fz3 indicate novel mechanisms for planar cell polarity in mammals. Journal of Neuroscience *26*, 5265-5275.

Murdoch,J.N., Doudney,K., Paternotte,C., Copp,A.J., and Stanier,P. (2001). Severe neural tube defects in the loop-tail mouse result from mutation of Lpp1, a novel gene involved in floor plate specification. Human Molecular Genetics *10*, 2593-2601.

Nakaya,M.A., Biris,K., Tsukiyama,T., Jaime,S., Rawls,J.A., and Yamaguchi,T.P. (2005). Wnt3a links left-right determination with segmentation and anteroposterior axis elongation. Development *132*, 5425-5436.

Park,J.S., Valerius,M.T., and McMahon,A.P. (2007). Wnt/beta-catenin signaling regulates nephron induction during mouse kidney development. Development *134*, 2533-2539.

Park,T.J., Gray,R.S., Sato,A., Habas,R., and Wallingford,J.B. (2005). Subcellular localization and signaling properties of dishevelled in developing vertebrate embryos. Current Biology *15*, 1039-1044.

Pinson,K.I., Brennan,J., Monkley,S., Avery,B.J., and Skarnes,W.C. (2000). An LDL-receptor-related protein mediates Wnt signalling in mice. Nature *407*, 535-538.

Qian,D., Jones,C., Rzadzinska,A., Mark,S., Zhang,X.H., Steel,K.P., Dai,X., and Chen,P. (2007). Wnt5a functions in planar cell polarity regulation in mice. Developmental Biology *306*, 121-133.

Robertson,C.P., Braun,M.M., and Roelink,H. (2004). Sonic hedgehog patterning in chick neural plate is antagonized by a Wnt3-like signal. Developmental Dynamics *229*, 510-519.

Satoh,W., Gotoh,T., Tsunematsu,Y., Aizawa,S., and Shimono,A. (2006). Sfrp1 and Sfrp2 regulate anteroposterior axis elongation and somite segmentation during mouse embryogenesis. Development *133*, 989-999.

Satoh,W., Matsuyama,M., Takemura,H., Aizawa,S., and Shimono,A. (2008). Sfrp1, Sfrp2, and Sfrp5 regulate the Wnt/beta-catenin and the planar cell polarity pathways during early trunk formation in mouse. Genesis *46*, 92-103.

Schmitt,A.M., Shi,J., Wolf,A.M., Lu,C.C., King,L.A., and Zou,Y.M. (2006). Wnt-Ryk signalling mediates medial-lateral retinotectal topographic mapping. Nature *439*, 31-37.

Schoenwolf,G.C. (1991). Cell Movements Driving Neurulation in Avian Embryos. Development 157-168.

Schwarz-Romond,T., Merrifield,C., Nichols,B.J., and Bienz,M. (2005). The Wnt signalling effector Dishevelled form dynamic protein assemblies rather than stabile associations with cytoplasmic vesicles. Journal of Cell Science *118*, 5269-5277.

Schwarz-Romond,T., Metcalfe,C., and Bienz,M. (2007a). Dynamic recruitment of axin by Dishevelled protein assemblies. Journal of Cell Science *120*, 2402-2412.

Schwarz-Romond,T., Fiedler,M., Shibata,N., Butler,P.J.G., Kikuchi,A., Higuchi,Y., and Bienz,M. (2007b). The DIX domain of Dishevelled confers Wnt signaling by dynamic polymerization. Nature Structural & Molecular Biology *14*, 484-492.

Schweizer,L. and Varmus,H. (2003). Wnt/Wingless signaling through beta-catenin requires the function of both LRP/Arrow and frizzled classes of receptors. Bmc Cell Biology *4*.

Seifert,J.R.K. and Mlodzik,M. (2007). Frizzled/PCP signalling: a conserved mechanism regulating cell polarity and directed motility. Nature Reviews Genetics *8*, 126-138.

Shum,A.S.W., Poon,L.L.M., Tang,W.W.T., Koide,T., Chan,B.W.H., Leung,Y.C.G., Shiroishi,T., and Copp,A.J. (1999). Retinoic acid induces down-regulation of Wnt-3a, apoptosis and diversion of tail bud cells to a neural fate in the mouse embryo. Mechanisms of Development *84*, 17-30.

Stark,K., Vainio,S., Vassileva,G., and McMahon,A.P. (1994). Epithelial Transformation of Metanephric Mesenchyme in the Developing Kidney Regulated by Wnt-4. Nature *372*, 679-683.

Suriben,R., Fisher,D.A., and Cheyette,B.N.R. (2006). Dact1 presomitic mesoderm expression oscillates in phase with Axin2 in the somitogenesis clock of mice. Developmental Dynamics *235*, 3177-3183.

Takada,S., Stark,K.L., Shea,M.J., Vassileva,G., Mcmahon,J.A., and McMahon,A.P. (1994). Wnt-3A Regulates Somite and Tailbud Formation in the Mouse Embryo. Genes & Development *8*, 174-189.

Tissir,F. and Goffinet,A.M. (2006). Expression of planar cell polarity genes during development of the mouse CNS. European Journal of Neuroscience *23*, 597-607.

Torban,E., Kor,C., and Gros,P. (2004). Van Gogh-like2 (Strabismus) and its role in planar cell polarity and convergent extension in vertebrates. Trends in Genetics *20*, 570-577.

Torban,E., Wang,H.J., Patenaude,A.M., Riccomagno,M., Daniels,E., Epstein,D., and Gros,P. (2007). Tissue, cellular and sub-cellular localization of the Vangl2 protein during embryonic development: Effect of the Lp mutation. Gene Expression Patterns *7*, 346-354.

Torres,M.A., YangSnyder,J.A., Purcell,S.M., DeMarais,A.A., Mcgrew,L.L., and Moon,R.T. (1996). Activities of the Wnt-1 class of secreted signaling factors are antagonized by the Wnt-5A class and by a dominant negative cadherin in early Xenopus development. Journal of Cell Biology *133*, 1123-1137.

Torres,M.A. and Nelson,W.J. (2000). Colocalization and redistribution of dishevelled and actin during Wnt-induced mesenchymal morphogenesis. Journal of Cell Biology *149*, 1433-1442.

Wallingford,J.B. and Habas,R. (2005). The developmental biology of Dishevelled: an enilgmatic protein governing cell fate and cell polarity. Development *132*, 4421-4436.

Wang,J.B., Hamblet,N.S., Mark,S., Dickinson,M.E., Brinkman,B.C., Segil,N., Fraser,S.E., Chen,P., Wallingford,J.B., and Wynshaw-Boris,A. (2006). Dishevelled genes mediate a conserved mammalian PCP pathway to regulate convergent extension during neurulation. Development *133*, 1767-1778.

Waxman,J.S., Hocking,A.M., Stoick,C.L., and Moon,R.T. (2004). Zebrafish Dapper1 and Dapper2 play distinct roles in Wnt-mediated developmental processes. Development *131*, 5909-5921.

Witze,E.S., Litman,E.S., Argast,G.M., Moon,R.T., and Ahn,N.G. (2008). Wnt5a control of cell polarity and directional movement by polarized redistribution of adhesion receptors. Science *320*, 365-369.

Wong,H.C., Bourdelas,A., Krauss,A., Lee,H.J., Shao,Y.M., Wu,D.Q., Mlodzik,M., Shi,D.L., and Zheng,J. (2003). Direct binding of the PDZ domain of Dishevelled to a conserved internal sequence in the C-terminal region of frizzled. Molecular Cell *12*, 1251-1260.

Yamaguchi,T.P., Bradley,A., McMahon,A.P., and Jones,S. (1999). A Wnt5a pathway underlies outgrowth of multiple structures in the vertebrate embryo. Development *126*, 1211-1223.

Ybot-Gonzalez,P., Savery,D., Gerrelli,D., Signore,M., Mitchell,C.E., Faux,C.H., Greene,N.D.E., and Copp,A.J. (2007). Convergent extension, planar-cell-polarity signalling and initiation of mouse neural tube closure. Development *134*, 789-799.

Yoon,J.K., Moon,R.T., and Wold,B. (2000). The bHLH class protein pMesogenin1 can specify paraxial mesoderm phenotypes. Developmental Biology *222*, 376-391.

Yoon,J.K. and Wold,B. (2000). The bHLH regulator pMesogenin1 is required for maturation and segmentation of paraxial mesoderm. Genes & Development *14*, 3204-3214.

Yoshikawa,Y., Fujimori,T., McMahon,A.P., and Takada,S. (1997). Evidence that absence of Wnt-3a signaling promotes neuralization instead of paraxial mesoderm development in the mouse. Developmental Biology *183*, 234-242.

Zeng,X., Tamai,K., Doble,B., Li,S.T., Huang,H., Habas,R., Okamura,H., Woodgett,J., and He,X. (2005). A dual-kinase mechanism for Wnt co-receptor phosphorylation and activation. Nature *438*, 873-877.

Zeng,X., Huang,H., Tamai,K., Zhang,X.J., Harada,Y., Yokota,C., Almeida,K., Wang,J., Doble,B., Woodgett,J., Wynshaw-Boris,A., Hsieh,J.C., and He,X. (2008). Initiation of Wnt signaling: control of Wnt coreceptor Lrp6 phosphorylation/activation via frizzled, dishevelled and axin functions. Development *135*, 367-375.

Zhang,L., Gao,X., Wen,J., Ning,Y.H., and Chen,Y.G. (2006). Dapper 1 antagonizes Wnt signaling by promoting dishevelled degradation. Journal of Biological Chemistry *281*, 8607-8612.